MONASH University

Separation and Identification Strategies for Lipids and Volatiles Analysis in Natural Oils

Habtewold Deti Waktola
(B. Pharm, MSC)

A thesis submitted for the degree of Doctor of Philosophy at

Monash University

Faculty of Science

School of Chemistry

2020

Copyright notice and permissions

I certify that I have made all reasonable efforts to secure copyright permissions for third-party content included in this thesis and have not knowingly added copyright content to my work without the owner's permission.

Chapter 3: Reprinted with the permission from *Analytical and Bioanalytical Chemistry*. H.D. Waktola, C. Kulsing, Y. Nolvachai, C.M. Rezende, H.R. Bizzo, P.J. Marriott, Gas chromatography–mass spectrometry of sapucainha oil (*Carpotroche brasiliensis*) triacylglycerols comprising straight chain and cyclic fatty acids, 411 (2019) 1479–1489. Copyright 2019 with permission from Springer Nature.

Chapter 4: Reprinted with the permission from *Journal of Chromatography A*. H.D. Waktola, C. Kulsing, Y. Nolvachai, P.J. Marriott, High temperature multidimensional gas chromatographic approach for improved separation of triacylglycerols in olive oil, 1549 (2018) 77–84. Copyright 2018 with permission from Elsevier.

Chapter 5: Reprinted with the permission from *Journal of Chromatography A*. H.D. Waktola, Y. Nolvachai, P.J. Marriott, Multidimensional gas chromatographic–mass spectrometric method for separation and identification of triacylglycerols in olive oil, 1629 (2020) 461474. Copyright 2020 with permission from Elsevier.

This page intentionally left blank

Contents

I. Abstract

The analysis of chemical compounds such as fatty acids (FAs), triacylglycerols (TAGs), volatile organic compounds (VOCs), etc. in food oil samples are important for characterisation, authentication and traceability of the oil samples. In food analysis the quantification and characterisation of the molecular species of FAs and TAGs are important for authentication of particular oil or fat products, for nutritional profiling, as well as food quality control. For instance, TAG analysis is used to detect adulteration of extra virgin olive oil which may arise through addition of seed oils. The analysis of FAs and VOCs in extra virgin olive oil (EVOO) also has a particular role in the authentication as well as differentiation of varieties of oil samples.

TAGs are the main constituents of natural oils and fats, the number of which is a function of the number of FAs present in the TAG components, and the specificity of the enzymes involved in their synthesis. The number of TAGs that can be uniquely detected in a given lipid sample depends on the degree of separation achieved for the chromatographic stage, and the mode of detection and/or identification used. TAGs separation and identification in natural oil or fat samples are complicated by the fact that a large number of them have similar chemical and physical properties, or more correctly, have insufficient differences in their properties to allow for adequate separation selectivity. TAGs separation is often carried out using high temperature gas chromatography (HTGC). Their separation usually is based primarily on their carbon number (CN) and then their degree of unsaturation, analysed on mid-polar or polar columns. However, separation of TAGs with the same CN and similar degree of unsaturation is incomplete and hence they often co-elute. Peak identification is based on elution data of individual standard TAG compounds, or interpretation of mass spectra, using GC–MS. In many cases, both standard TAGs and mass spectrum library information are not available. In these instances, identification can be performed based on diagnostic fragment ions in the mass spectrum, generated through loss of, or from, fatty acid residue(s) comprising the TAG molecules.

Based on these comments, this thesis will address various approaches to improved resolution for analysis of TAGs, supported by FA analysis. Results and experimental development are described in 4 Chapters.

In Chapter 3, the analysis of a plant oil, sapucainha oil, that comprises of cyclic and straight chain FAs and their TAGs, using HTGC–EIMS was investigated as an introduction to HTGC methodology and MS interpretation, against which future higher dimensionality methods can be assessed. Overlapping TAGs were deconvoluted based on mass fingerprint data. FAs and TAGs were identified based on characteristic fragment ions, in the absence of standard FAs and TAGs as well as mass spectral library. In subsequent Chapter 4, TAGs separation in olive oil samples was investigated and improved using a multidimensional gas chromatographic (MDGC) approach, with FID detection. Using a 'heart-cut' (H/C) MDGC method overlapped regions of TAGs in a first dimension (^{1}D) column were H/C sampled and transferred to a second dimension (^{2}D) column for further separation, which revealed substantially more TAG components present in the oil sample by separating each H/C zones of ^{1}D into multiple TAG peaks on the ^{2}D. This provided confirmation of the relevance of the MDGC approach, and subsequently prompted further evaluation of the individual TAGs thus revealed in the samples. Chapter 5 provided the evidence of molecular speciation by further study of MDGC but now using MS as detection mode, making possible the identification of separated TAGs based on characteristic mass fragment ions. The knowledge provided by MS interpretation in Chapter 3 aided classification of individual TAG. Finally, Chapter 6 examined the differentiation of EVOO varieties based on the analysis of both VOCs and FAs compositions. Principal component analysis was used to display and interpret data for original single variety EVOO, some signature EVOO mixtures produced by a commercial EVOO supplier on the basis of sensory analysis to generate reproducible year-to-year profiles, and a suite of lab-mixtures of single EVOO varieties to simulate the signature mixtures. It was found that determination of FAs composition in mixed EVOO varieties was used as a reliable tool to reveal the proportion of single varieties in the mixed EVOO varieties, whereas VOC was not so rugged an approach.

Overall, a first account on the analysis of TAGs derived from mixed straight chain and cyclic FAs using GC–EIMS based on peak deconvolution was demonstrated. The use of a tandem column strategy for the analysis of TAGs was able to resolve more components than the usual single column. Future studies that may include different types of columns and configurations may even result in better separations of TAGs. The application can also be expanded to different types of lipid matrices. Extending the MDGC approach to comprehensive two-dimensional gas chromatography (GC×GC) would be a desirable study.

II. Publications during enrolment

Publication submitted

- M.F.S. Mota, H.D. Waktola, Y. Nolvachai, P.J. Marriott, Gas chromatography – mass spectrometry for characterisation, assessment of quality and authentication of seed and vegetable oils, submitted to TrAC - Trends in Analytical Chemistry.

Publications published

2018

- H.D. Waktola, C. Kulsing, Y. Nolvachai, P.J. Marriott, High temperature multidimensional gas chromatographic approach for improved separation of triacylglycerols in olive oil, Journal of chromatography A 1549 (2018) 77–84.

2019

- H.D. Waktola, C. Kulsing, Y. Nolvachai, C.M. Rezende, H.R. Bizzo, P.J. Marriott, Gas chromatography–mass spectrometry of sapucainha oil (*Carpotroche brasiliensis*) triacylglycerols comprising straight chain and cyclic fatty acids, Analytical and Bioanalytical Chemistry 411 (2019) 1479–1489.

2020

- J.S. Zavahir, J.S.P. Smith, S. Blundell, H.D. Waktola, Y. Nolvachai, B.R. Wood, P.J. Marriott, Relationships in gas chromatography—Fourier transform infrared spectroscopy—comprehensive and multilinear analysis, Separations 7 (2020) 27.
- H.D. Waktola, A.X. Zeng, S-T. Chin, P.J. Marriott, Advanced gas chromatography and mass spectrometry technologies for fatty acids and triacylglycerols analysis, TrAC - Trends in Analytical Chemistry 129 (2020) 115957.
- H.D. Waktola, Y. Nolvachai, P.J. Marriott, Multidimensional gas chromatographic–mass spectrometric method for separation and identification of triacylglycerols in olive oil, Journal of chromatography A 1629 (2020) 461474.

III. Selected conference presentations

November 2018

Poster presentation 2nd international conference on food analysis (ICFA 2018), Melbourne, Australia

Title: High temperature multidimensional gas chromatographic approach for improved separation of triacylglycerols in olive oil

May 2018

Poster presentation on 42nd international symposium on capillary chromatography and 15th GC×GC symposium, Riva del Garda, Italy

Title: Analysis of triacylglycerols derived from straight chain and cyclic fatty acids using GC–(EI) MS in Sapucainha oil (*Carpotroche brasiliensis*)

July 2017

Oral presentation on Royal Australian Chemical Institute centenary congress 2017 (RACI 100), Melbourne, Australia

Title: High-temperature multidimensional gas chromatographic separation of triacylglycerols in olive oil

November 2016

Poster presentation on Australian centre for research on separation sciences (ACROSS) conference, Hobart, Tasmania, Australia

Title: Optimising the relationship between chromatographic efficiency and retention times in temperature-programmed GC

IV. Thesis including published works declaration

I hereby declare that this thesis contains no material which has been accepted for the award of any other degree or diploma at any university or equivalent institution and that, to the best of my knowledge and belief, this thesis contains no material previously published or written by another person, except where due reference is made in the text of the thesis.

This thesis includes 3 original papers published in peer reviewed journals and no submitted publications. The core theme of the thesis is to develop a separation and identification strategies for lipids such as fatty acids and triacylglycerols and also differentiate extra virgin olive oil based on fatty acid and volatile compounds composition. The ideas, development and writing up of all the papers in the thesis were the principal responsibility of myself, the student, working within the School of Chemistry, Faculty of Science under the supervision of Professor Philip J. Marriott (Main supervisor) and Professor Bayden R. Wood (Associate supervisor).

The inclusion of co-authors reflects the fact that the work came from active collaboration between researchers and acknowledges input into team-based research.

In the case of *Chapter 3-6* my contribution to the work involved the following:

Thesis Chapter	**Publication Title**	**Status** *(published, in press, accepted or returned for revision, submitted)*	**Nature and % of student contribution**	**Co-author name(s) Nature and % of Co-author's contribution***	**Co-author(s), Monash student Y/N***
3	Gas chromatography–mass spectrometry of sapucainha oil (*Carpotroche brasiliensis*) triacylglycerols comprising straight chain and cyclic fatty acids	Published	78 % - proposed idea, developed and validated methods, analysed and interpreted all data, prepared fully drafted manuscript	1. Chadin Kulsing – technical assistance. 5% 2. Yada Nolvachai – technical assistance. 5% 3. Claudia M. Rezende – editorial assistance. 1% 4. Humberto R. Bizzo – editorial assistance. 1% 5. Philip J. Marriott- supervision, assisted interpretation of results, editorial assistance. 10%	1. No 2. No 3. No 4. No 5. No
4	High temperature multidimensional gas chromatographic approach for improved separation of triacylglycerols in olive oil	Published	75 % - proposed idea, developed and validated methods, analysed and interpreted all data, prepared fully drafted manuscript	1. Chadin Kulsing – assisted interpretation of result, technical assistance. 10% 2. Yada Nolvachai – technical assistance. 5% 3. Philip J. Marriott – supervision, assisted interpretation of results, editorial assistance. 10%	1. No 2. No 3. No
5	Multidimensional gas chromatographic–mass spectrometric method for separation and identification of triacylglycerols in olive oil	Published	80 % - proposed idea, developed and validated methods, analysed and interpreted all data, prepared fully drafted manuscript	1. Yada Nolvachai – technical assistance, editorial assistance. 10% 2. Philip J. Marriott - supervision, assisted interpretation of results, editorial assistance. 10%	1. No 2. No

6	Extra virgin olive oil signature flavour mix differentiation based on analysis of volatile organic compounds and fatty acids	Not Submitted (Prepared for submission)	80 % - proposed idea, developed and validated methods, analysed and interpreted all data, prepared fully drafted manuscript	1. Yada Nolvachai – technical assistance, editorial assistance. 4% 2. Claudia Guillaume – editorial assistance. 1% 3. Bayden R. Wood – supervison, editorial assistance. 5%. 4. Philip J. Marriott - supervision, assisted interpretation of results, editorial assistance. 10%	1. No 2. No 3. No 4. No

I have not renumbered sections of published papers in order to generate a consistent presentation within the thesis.

Student name: Habtewold Deti Waktola **Signature:** **Date: 14 December, 2020**

The undersigned hereby certify that the above declaration correctly reflects the nature and extent of the student's and co-authors' contributions to this work.

Main supervisor name: Philip J. Marriott **Signature:** **Date: 14 December, 2020**

V. Acknowledgements

For most, I would like to express my deepest gratitude for my supervisor professor Philip J. Marriott for his continuous guidance and support throughout my PhD study and research. His guidance helped me from the inception of the research project to the execution of the experimental works, publications and the write up of the thesis. I could not have imagined having a better supervisor and mentor for my PhD study. It was a great privilege and honour to work under his supervision and guidance. I would also like to express my gratitude to my co-supervisor Professor Bayden R. Wood for his supervision and support during my study. My sincere thanks also go to my panels Professor Alan Chaffee and Professor Perran Cook for their feedbacks and supports during my milestone presentations. Special thanks to Anna Severin for her assistance on administration matters. I am grateful for the supports and scholarships I received from School of chemistry, Faculty of Science and Monash Graduate Education.

My sincere thanks go also to Modern Olives (Lara, Victoria) for providing me with extra virgin olive oil samples used in the research project. I would like to thank also Australian Research Council (ARC) and PerkinElmer for the research grant that supported the research works included in the thesis.

I would like to express my sincere gratitude to Dr. Yada Nolvachai and Dr. Chadin Kulsing for the guidance and support they gave me during my laboratory experiments as well as in managing experimental results. Special thanks also to Shezmin Ismail for encouragements and feedbacks on research works as well as her friendship. I thank my fellow graduate research students and visitors I met in Marriott research group: Sharif, Jalal, Giselle, Dandan, Aprilia, Jamieson, Raj, Mala, Zahra, Michelle, Riley, Maria, Fabio and Ademario for discussions and for all the fun we have had during the PhD time. Thanks to Kim Shepherd for support on administrative matters.

I have no valuable words to thank my wife Tigist Leta for her support, patience and understanding, and also for taking care of our daughter Nadhii. I would like to extend my sincere gratitude also to everyone in the family, my father, mother, sisters and brothers for supporting and encouraging me throughout my study.

Vi. List of abbreviations and parameters

^{1}D	First dimension
1D	One-dimensional
$^{1}t_{R}$	First dimension retention time
^{2}D	Second dimension
2D	Two-dimensional
$^{2}t_{R}$	Second dimension retention time
Ag^{+}-HPLC	Silver ion high performance liquid chromatography
CGC	Capillary gas chromatography
CN	Carbon number
CT	Cryofocusing trap
DAG	Diacylglycerol
d_f	Film thickness
DS	Deans switch
DVB/CAR/PDMS	Divinylbenzene/Carboxen/polydimethylsiloxane
ECN	Equivalent carbon number
EI	Electron ionisation
EVOO	Extra virgin olive oil
FA	Fatty acid
FAME	Fatty acid methyl ester
FID	Flame ionisation detector
GC	Gas chromatography
GC×GC	Comprehensive two-dimensional gas chromatography
H/C	'Heart-cut'
HPLC	High performance liquid chromatography
HS	Head space
HTGC	High temperature gas chromatography
I.D.	Internal diameter
IE	Ionisation energy
IOC	International olive council
LC	Liquid chromatography
LC×GC	Comprehensive two-dimensional liquid chromatography × gas chromatography
LC×LC	Comprehensive two-dimensional liquid chromatography
m/z	Mass-to-charge ratio
MAG	Monoacylglycerol
MD	Multidimensional
MDGC	Multidimensional gas chromatography
MS	Mass spectrometry
MUFA	Monounsaturated fatty acid
NARP	Non-aqueous reversed phase
NIST	National Institute of Standards and Technology
NP	Normal-phase
PCA	Principal component analysis
PDMS	Polydimethylsiloxane
PUFA	Polyunsaturated fatty acid
QMS	Quadrupole mass spectrometry
RP	Reversed-phase
SFA	Saturated fatty acid
SFC	Supercritical fluid chromatography
SIM	Selected ion monitoring
SPME	Solid phase microextraction
T	Temperature
TAG	Triacylglycerol
TLC	Thin layer chromatography
TOFMS	Time-of-flight mass spectrometry
VOC	Volatile organic compound
VUV	Vacuum ultraviolet spectroscopy

This page intentionally left blank

Chapter 1

Introduction

Contents

1.1. Fatty acids, triacylglycerols and olive oil

1.1.1. Fatty acids (FAs)

Fatty acids originating from plant, animal and microbes, usually present as glycerol derivatives, generally vary in chain length and contain an even number of carbon atoms with a terminal carboxyl functional group and may contain double bonds of the *cis* configuration in specific positions in relation to this. This is due to the biosynthetic pathway that passes through acetyl-CoA [1]. Odd numbered and branched chain FAs can be synthesised by bacteria and other organisms, with 15 or 17 carbon atom FAs found in ruminants' milk being produced by bacteria in rumen [2]. Cyclic FAs occur in plants, especially certain seed oils, and microorganisms. They rarely occur in animal tissue. During food processing they can be formed from conventional unsaturated FAs as artefacts [3].

Most natural lipids contain an abundant amount of straight chain FAs, with those FAs of 14, 16 and 18 carbon number being the most abundant. They are composed of saturated FAs (SFAs), and monounsaturated FAs (MUFAs) and polyunsaturated FAs (PUFAs) with *cis*-configuration [4]. The double bonds in PUFA are separated by a single methylene group. **Figure 1.1** shows the general formulas and examples for straight chain SFAs, MUFAs, and PUFAs. FAs are named systematically based on the respective hydrocarbon nomenclature with the same number of carbon atoms, omitting the 'e' and appending 'oic' for SFAs and 'enoic'/'dienoic'/'trienoic' for unsaturated FAs. FAs are designated in shorthand nomenclature as A:B(n-x), where A is the number of carbon atoms, B is the number of double bonds, n is the chain length of the FA and x is the position of the first double bond counted from the methyl end of the fatty acid chain. Thus, 18:2(n-6) indicates an 18 carbon FA with 2 double bonds and 6 carbons from the methylene end to the first double bond. They are also often referred by their trivial names usually for known sources of the oil (e.g. palmitic, oleic, linoleic and α-linolenic are for 16:0, 18:1(n-9), 18:2(n-6) and 18:3(n-3) respectively) (**Table 1.1**). The two most

recognised families of PUFAs are called n-6 (ω6) and n-3 (ω3). PUFAs are derived biosynthetically from 18:2(n-6) and 18:3(n-3) (in some literature, these are also expressed as 18:2ω6 and 18:3ω3) respectively [4].

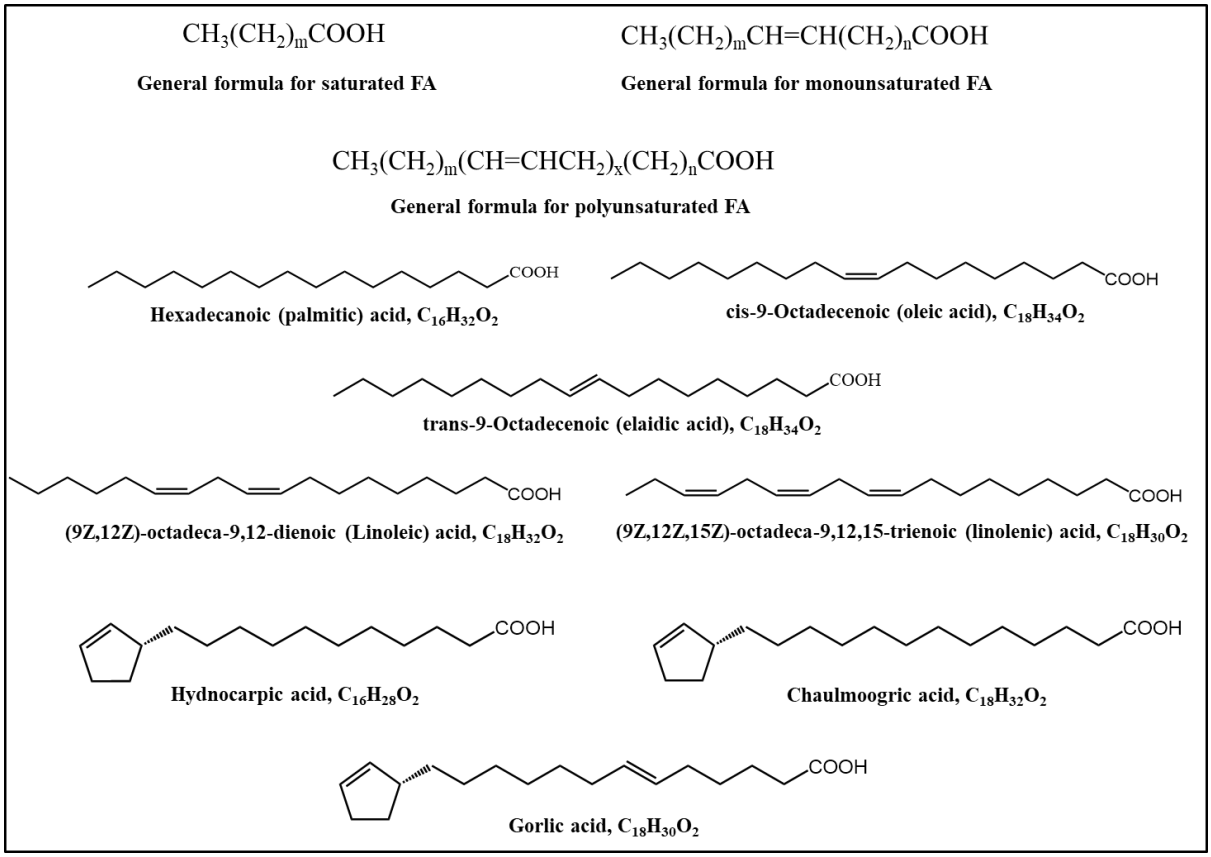

Figure 1.1. General formulas and examples for straight chain saturated, monounsaturated, polyunsaturated FAs and *cis*/*trans* isomers, and examples for cyclopentenyl FAs.

Naturally occurring cyclic FAs belong to two families. The first family of cyclic FAs comprises the cyclopentenyl FAs. The major cyclopentenyl FAs are hydnocarpic (C16:1cyc), chaulmoogric (C18:1cyc) and gorlic (C18:2cyc) acids, structures shown in **Figure 1.1**. They are found in seed oils of *Hydnocarpus* species and other genera of the *Flacourtiacea* family [5]. One example is sapucainha oil (*Carpotroche brasiliensis* Endl.) which was used for the treatment of leprosy until the development of sulpha drugs. In addition to gorlic, chaulmoogric and hydnocarpic FAs, sapucainha oil contains also straight chain FAs such as palmitic and

oleic acids [6]. Cyclopropane and cyclopropene FAs are another family of cyclic FAs that are found in a number of seed oils. Cyclopropane FA has been found in a wide range of bacterial species [5].

Table 1.1. Nomenclature and designations of some of the more common fatty acids.

Systematic Name	**Trivial Name**	**Shorthand Designation**	**Letter abbreviations**
Dodecanoic	Lauric	12:0	La
Tetradecanoic	Myristic	14:0	M
Hexadecanoic	Palmitic	16:0	P
9-Hexadecenoic	Palmitoleic	16:1(n-7)	Po
Heptadecanoic	Margaric	17:0	Mg
Octadecanoic	Stearic	18:0	S
9-Octadecenoic	Oleic	18:1(n-9)	O
9,12-Octadecadienoic	Linoleic	18:2(n–6)	L
9,12,15-Octadecatrienoic	α-Linolenic	18:3(n–3)	Ln
6,9,12-Octadecatrienoic	γ-Linolenic	18:3(n–6)	G
Eicosanoic	Arachidic	20:0	A
5,8,11,14,17-Eicosapentaenoic	EPA	20:5(n-3)	-
Docosanoic	Behenic	22:0	Be
4,7,10,13,16,19-Docosahexaenoic	DHA	22:6(n-3)	-
Tetracosanoic	Lignoceric	24:0	Lg

1.1.2. Triacylglycerols (TAGs) (synonyms – triglycerides, triacylglycerides)

Triacylglycerols are compounds that are formed when all the three hydroxyl positions of glycerol are esterified with FAs (**Figure 1.2**), such as straight chain and cyclic FAs. They are main components of oils and fats of plant and animal origin. Based on the number of FAs present and the specificity of the enzyme involved in the synthesis of the particular fat or oil,

the number of different TAGs that can be found is both relatively large, and variable in abundance [1].

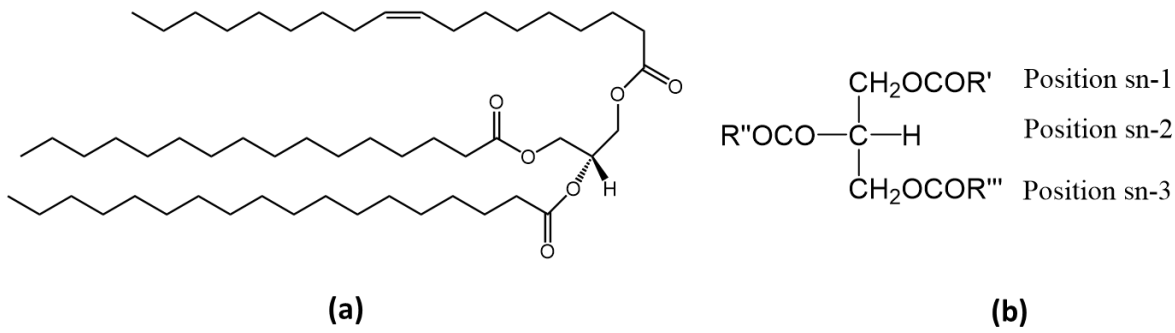

Figure 1.2. (a) *sn*-1-Palmitoyl-2-stearoyl-3-oleoyl-*sn*-glycerol/1-hexadecanoyl-2-octadecanoyl-3-(9Z-octadecenoyl)-*sn*-glycerol (b) triacyl-*sn*-glycerol

When FA substituents on the glycerol at position 1 and 3 are different a chiral carbon is created at position 2. Stereospecific numbering (*sn*) system is employed in order to differentiate between the two terminal carbons [7]. Then the TAG is specified as triacyl-*sn*-glycerol, for example, *sn*-1-palmitoyl-2-stearoyl-3-oleoyl-*sn*-glycerol has palmitic acid at position 1, stearic acid at position 2 and oleic acid at position 3 (**Figure 1.2**). TAGs are often described by a combination of three letters representing the FAs from which they are composed. For instance, OOO, POL and OLLn represents TAGs composed of various arrangements of oleic (O), palmitic (P), linoleic (L) and linolenic (Ln) acids. The common letter abbreviations for FAs is shown in **Table 1.1**.

1.1.3. Olive oil

Olive oil is a vegetable oil obtained from the fruit of the olive tree which was formerly confined almost entirely to the Mediterranean countries (Spain, Italy, Greece, Tunisia, Morocco, Syria and Turkey). Moreover, new olive plantations are being developed worldwide, including in Australia and California. For Mediterranean communities, being historically the main producers and consumers of olive oil**,** evidence suggests they are less prone to various

chronic diseases such as coronary heart disease. Several constituents of olive oil including FAs have been demonstrated to have a protective effect towards these chronic diseases [8, 9]. Newly pressed extra virgin olive oil was reported to contain a compound called oleocanthal which has anti-inflammatory activity with a potency and profile similar to ibuprofen [10].

The chemical composition of olive oil can be divided into two fractions. The first fraction containing major compounds (98 - 99% of total weight) include free FAs or esterified FAs with glycerol to form TAGs, diacylglycerols (DAGs) and monoacylglycerols (MAGs). The second fraction containing minor compounds (1 - 2%), formed by micro-components include sterols, waxes, fat soluble vitamins, aliphatic alcohols, carotenoids, chlorophylls, hydrocarbons, etc [11-13]. The minor components are responsible for the unique flavour and oxidative stability of olive oil. Both fractions have important roles in the characterisation, authentication and traceability [12, 14-17], and as well as determination of the quality and purity of olive oil [18, 19]. The chemical composition of olive oil varies based on many factors including the stage of ripening of the olives, variety, environmental and processing factors.

Unrefined olive oil is composed of many different FAs, which are mainly present in the form of TAGs. Olive oil is characterised by high levels of palmitic acid, oleic acid and linoleic acid, with oleic acid being present in the highest amount. Olive oil also contains trace amounts of myristic, palmitoleic, margaric, heptadecenoic, linolenic, arachidic, benhenic, and lignoceric acid [12]. Oleic acid content increases with ripening of the olives whereas palmitic and linoleic acids tend to decrease as fruit ripening progresses. Ripening of olives is reported to result in an increase of the amount of MUFAs and a decrease of total PUFAs [20]. There is also a variation in FA profile of olive oils, i.e. the ratio of unsaturated versus saturated FAs composition based on the source (cultivars) of the olives [12, 21, 22]. FA composition may also vary based on the type of processing (extraction) technique that is used to prepare the olive oil from its fruit [22]. The variations in TAG content of olive oil, which is related to the variations in FA content,

based on ripening of olives and its varieties was also reported. Kosma et al. [17] reported that the most affected TAGs and FAs by ripening were triolein (OOO), 1,2-linoleoyl-3-oleoyl-glycerol (OLL), 1,2-dioleoyl-3-linoleoyl-glycerol (LOO), and 1,2-dioleoyl-3-palmitoyl-glycerol (POO) TAGs and 18:1(n-9), 18:2(n-6), and 16:0 FAs. Their amounts were varied based on the maturity index of the olives and its varieties.

Volatile organic compounds (VOCs) in olive oil are responsible for its unique and delicate flavour. The VOCs in olive oil were identified as aldehydes, alcohols, ketones, esters, hydrocarbons, furans and others. The compounds are related to the sensory quality of olive oil [23]. The typical fruity and green aroma of the high-quality extra virgin olive oil (EVOO) is related to the six carbon (C6) and five carbon (C5) compounds, which are the main fractions of the VOCs, with the C6 linear unsaturated and saturated aldehydes representing the most important fractions. Hexanal, trans-2-hexenal, hexan-1-ol and 3-methylbutan-1-ol are among the major compounds found in most virgin olive oils [23, 24]. The VOCs are produced through enzymatic process. The C6 and C5 compounds are produced through the lipoxygenase (LOX) pathway from PUFAs, linoleic and linolenic acids, during olive fruit milling and paste malaxation steps and their concentration depends on the level and activities of enzymes involved [23, 24]. The C6 aldehydes reduce to C6 alcohols by alcohol dehydrogenase, and transform to C6 esters by alcohol acyl transferase. The LOX cascade produces also compounds from other chemical classes, such as hydrocarbons, terpenes, benzenoids, etc. [24].

The VOCs concentration in olive oil depends on several factors such as varietal origin, geographical location and growing conditions, harvest date, processing technology as well as finalisation and storage conditions [24-27]. It is important to note that a volatile compound with high concentration is not necessarily a major contributor to odour [28]. Post-harvest handling of the olive fruits and storage conditions of oils until it reaches consumers result in different volatile profiles [24].

Therefore, the authenticity or quality of olive oil depends upon its chemical composition which should be monitored using appropriate analytical methods. Moreover, one can assume that there are commercial fraudulent activities involving substitution of substandard olive oil or non-olive oils for the authentic product. Thus, the European Union regulates olive oil quality and authenticity through different regulations. The physical, chemical and organoleptic characteristics of olive oil are regulated by Commission Regulation (EEC) No 2568 /91. The European Union also recognises and supports differentiation of quality products of olive oil on a regional basis through specific regulation (EU Regulations 2081/1992 and 510/2006). Conte *et al*. [29] reviewed the current EU legislation, standards, relevant methods of analyses and their drawbacks, and proposed possible solutions to safeguard the consumer and protect the olive oil market.

Most often olive oil analysis follows International Olive Council (IOC) adopted testing methods. The methods are categorised as chemical analysis of olive oil and olive-pomace oils, methods for oil mixtures determination, and organoleptic assessment methods. Among chemical analysis tests listed by the council, the analysis of sterols, triterpenes, waxes, fatty acid methyl esters (FAMEs), TAGs and stigmastadienes in olive oil are carried out by capillary gas chromatography (GC). The determination of the content of waxes, chlorophyll, FAMEs and FA ethyl esters are used to distinguish between olive oil and olive-pomace oil, and as a quality parameter for extra virgin olive oils. This makes possible the detection of fraudulent mixtures of extra virgin olive oils with lower quality oils. The determination of stigmastadienes is important to detect the presence of refined vegetable oils (olive, olive-pomace, sunflower, soybean, palm, etc.) in virgin olive oil since refined oils contain stigmastadienes and virgin oils do not [30]. In Australia the Australian Olive Oil Association (AOOA) is the responsible body in assisting IOC in monitoring and regular random testing of major brands of olive oil sold in Australia and is the primary source of information relating to the quality standards.

In Australia the biggest olive farmer and extra virgin olive oil producer is located in Victoria, owned by Boundary Bend Limited Company. Boundary Bend owns Australia's two leading locally grown-olive oil brands. Its first brand, Cobram Estate came to market in 2007 and later Boundary Bend bought the second brand Red Island in 2012, which together make them the biggest producers of olive oil in Australia (produced 13.6 million litres in 2013). Boundary Bend also owns Modern Olives, which provides a laboratory service for testing olive oils, but is also responsible for ensuring the quality of the Boundary Bend produced oils, maintains testing procedures set by the International Olive Council, and instructs the blending of various oils produced by Boundary Bend to ensure reproducible quality of their premium products. The company is also a manufacturer of olive harvesters, owners of Australia's largest olive tree nursery and olive oil bottling and storage facility. Under the brand Cobram Estate, they produce extra virgin olive oil categorised under: limited edition (includes first harvest, reserve Hojblanca and reserve Picual), superior (Première) and infused (includes chilli, lemon, garlic, roasted onion or mixed herb infused). The company bought 9 acre of industrial property in Woodland, California in 2014 for construction of a facility for oil milling, bottling facility, olive oil laboratory and an administrative office [31]. Following a visit to this organisation and laboratory at Lara, Victoria, and general discussion on their testing methods, and growing olives, processing and product authentication, samples of olive oil used in this project were kindly provided.

1.2. Literature review

1.2.1. Gas chromatographic analysis of FAs

FAs derived from oil samples are mainly determined by using gas chromatography (GC) following their conversion to volatile derivatives, mainly to the fatty acid methyl ester (FAME). There are various methods of FA esterification methods with their own pros and cons. Acid

catalysed esterification and transesterification and the base catalysed transesterification are widely applicable methods of derivatisation for FAMEs [32].

In acid catalysed esterification and transesterification free FAs are esterified and lipid-bound FAs, such as FA residues in TAGs, are transesterified by heating them in the presence of acidic catalyst with excess of anhydrous methanol. The commonly used reagents for acid-catalysed transesterification are hydrochloric (HCl) or sulfuric (H_2SO_4) acid in methanol, and boron trifluoride (BF_3) in methanol. Both acid-catalysed and BF_3-catalysed reactions require heating. In HCl catalysed derivatisation complete transesterification with 5% methanolic HCl occur by heating the sample with the reagent under reflux for about 2 h. H_2SO_4 is also used in the same way for transesterification of lipid samples. Since H_2SO_4 is a strong oxidising agent it is not recommended for the analysis of PUFAs. BF_3 in methanol (12–14%, w/v), a Lewis acid, has been widely used for transesterification of all types of lipids and esterification of free FAs. The reagent has limited stability and the use of old or concentrated solution results in production of artefacts and loss of PUFAs by addition of methanol across the double bonds. In the presence of basic catalyst, lipid-bound FAs are transesterified rapidly in anhydrous methanol. Sodium or potassium methoxide, and potassium hydroxide in anhydrous methanol were used for basic transesterification. Base-catalysed transesterification has the advantages of simplicity, no double bond isomerisation, and short derivatisation time. Using basic transesterification free FAs are not esterified but complete transesterification can be achieved for glycerolipids in a few minutes at room temperature. The basic transesterification has also less risk of decomposition of PUFAs. Both acid and base catalysed transesterifications require the use of additional solvent such as toluene to effect solution of non-polar lipids such as cholesterol esters or TAGs [32-34].

From early in the development of GC, this technique has been used as a preferred method to analyse FAs, first by packed GC, and now using various commercially available

fused-silica capillary columns [32]. Traditionally GC–FID is a commonly employed technique used to analyse FAs in various samples. The *cis*- and *trans*- FA composition of refined olive oil and other seed oils have been previously determined by using GC–FID. The identification of FAs was based on the comparison of their retention times versus pure standards analysed under the same condition [35]. FAMEs are often studied also using GC–MS, which is a powerful technique for separation, identification and quantification of FAs [36]. A typical study reported determination of olive oil FA profile using GC–MS where both retention time data and mass spectra were used to identify the FAs [37]. One-dimensional GC (1D GC) analysis of FAMEs from complex samples leads to co-elution of isomers. The *cis*- and *trans*-isomers of FAs are often eluted as overlapped components [38]. In accordance with the above statement, several studies performed on olive oil FA profiling reported their result either as the sum or percentage value of the total amount of FAME of a given carbon numbers regardless of the type of isomers it constitutes [12, 20, 35, 39]. The study of olive oil FA composition is most commonly done using 1D GC following mainly EU regulations.

In GC the degree of separation of FAs in complex samples depend on the type/polarity of the column being used. In general, polar stationary phases were used for separation of FAs in complex mixtures [40]. On polar columns FAs separates based on their degree of unsaturation and position of the double bonds, with greater degree of unsaturation eluting later. The separation of *cis*- and *trans*- isomers found in complex lipid matrices may require polar stationary phase columns with longer lengths [41].

The introduction of capillary columns with various polarity such as ionic liquid columns increased the capability of GC in separation of FA mixture [42]. The most polar ionic liquid column, SLB-IL111, provided enhanced separation as well as alternative separation patterns of FAs in most complex lipid mixtures as compared to the commonly employed cyanopropylsiloxane column or polyethyleneglycol [43]. High speed GC analysis was

achieved using micro-bore capillary columns [44]. Mondello *et al*. [45] developed a fast GC method for the analysis of FAs in complex lipid matrices.

Confirmation of FA identity requires exclusion of matrix compounds, employing several elution conditions, using suitable authentic standards and stable retention times for each set of conditions. Retention time can be used to a first approximation to determine FAME by using the retention time related to reference standards known as the retention index. A variation on the FAMEs retention index system is expressed as equivalent chain length (ECL), which is calculated based on a homologous series of saturated straight chain FAMEs. Using MS as a detector, there is a possibility to support 'tentative' identity of FAs based on their ion fragments. Nonetheless, many FA isomers of a given carbon number are known to give similar or identical mass spectra. In addition, target sample might constitute matrix, where other target FAs due to peak overlap cause interference with a FA whose identification is sought, leading to poor identification of the mass spectrometry ions attributed to FA of interest. Thus, in the analysis of FAs in complex lipid samples the exclusion of matrix interferences, and/or an increased separation to the individual FAs is indispensable.

Recently a GC coupled to vacuum ultraviolet spectroscopy (GC–VUV) technique was developed and used in FA analysis. Characterised as a universal detector VUV (in the range of 120-240 nm) can differentiate molecular structure of analytes such as degree of unsaturation and presence of conjugation. It has high sensitivity, specificity and fast data acquisition rate, and overlapped signals can be deconvoluted using software [46-48]. The difference in gas phase molecular absorption profiles between unsaturated FAMEs and saturated FAMEs as well as *cis-*/*trans*- isomers was demonstrated using GC–VUV [47]. The analysis of bacterial FAMEs using GC–VUV resulted in a unique FAMEs profiles for each bacteria investigated mainly composed of hydroxy, cyclopropane, branched, saturated, and unsaturated FAMEs [49].

Additional resolution was obtained for mixtures containing *cis-/trans-* isomers of FAs using IL columns with VUV detection [50].

1.2.2. Gas chromatographic analysis of TAGs

The analytical techniques mainly employed in the analysis of TAGs in vegetable oils are high performance liquid chromatography (HPLC), high temperature gas chromatography (HTGC), supercritical fluid chromatography (SFC) and thin layer chromatography (TLC) [51]. Given their automation and coupling with different detection and identification techniques such as mass spectrometry (MS), HPLC and GC are the commonly employed techniques for analysis of TAGs.

Since its inception GC has played a leading role in the analysis of oil and fat samples. The use of GC to study TAGs spans from the earliest time when glass or stainless-steel packed columns were used, to the recent times of capillary column technology [52]. The advantages of capillary columns include shorter analysis time, better separation efficiency, greater peak capacity and reproducibility of retention data over a packed column. Being a universal detector with linear response FID can be considered as a preferable technique for TAGs analysis while HTGC−MS is often used to generate MS fingerprint fragments and molecular ions of TAGs for identification purpose [53].

Capillary columns with stationary phases based on polysiloxane with methyl, phenyl and cyanopropyl groups were employed for TAG analysis. The polarity of the columns used may vary from non-polar (100% dimethyl polysiloxane phase) to the moderately polar phase (65% diphenyl dimethyl polysiloxane) [54]. On non-polar columns TAGs elute based on their increasing carbon number (CN) or molecular mass whereas on the commonly employed medium polarity and polar stationary phases elution occurs according to both molecular mass and degree of unsaturation in the fatty acyl groups on the TAG molecules. On medium polarity

and polar columns, retention times of TAGs with the same CN but different degree of unsaturation increase with increasing number of double bonds [55].

Structurally, TAGs differ based on chemical variations on the acyl group (such as degree of unsaturation, presence of cyclic structure or branched chain), variation of the acyl group position on the glycerol backbone and its total CN. Depending on the efficiency of the chromatographic step TAGs with the same CN often co-elute and their separation can be quit challenging. In capillary GC, TAG separation is even more challenging due to the availability of limited number of columns with high temperature limit phases compared to the high elution temperature of TAGs (mostly >300 °C).

Given the little differences between many TAG species present in oil samples no single technique has the ability to offer complete TAG profiling. Andrikopoulos et al. [51] reviewed chromatographic and spectroscopic methods of TAGs detection, identification and quantification in edible vegetable oils and revealed that most of the studies reported different number and species of TAGs present in a given oil sample analysed using CGC or HPLC techniques, with most reported peaks detected in the analysis to contain a combination of co-eluted TAGs. A study using CGC−FID to analyse virgin olive oil reported 16 TAG species detected compared to a total sum of 39 TAG species reported by different studies [51, 56]. Another study that used HTGC−MS to analyse olive oil was able to detect and identify only 8 TAG species due to poor resolution [57]. Thus, there is a need for a more advanced technique that may improve the separation of TAG components in lipid samples. The application of advanced multidimensional techniques presents an opportunity for TAGs separation, since it is relatively little studied, but the value of these approaches for analysis of FA is a signpost to future developments.

The analysis of intact TAGs may be considered preferred over their FA derivatives due to uncertainty as to which original TAGs they are derived from [58]. Also authentication of

different fats and oils is often based on the analysis of TAG composition [56]. Oils from different sources differ in their TAG composition attributed to the specificity of enzymes involved in their synthesis [59]. The blending of olive oil with other edible oils was identified and quantified using HTGC–MS and chemometric tools through fingerprinting of TAG components [18]. The degree of separation and identification of TAG components greatly determines the use of TAG composition as a tool for determination of the origin, authenticity, or to detect adulteration or fraud. In this regard 1D GC has a demonstrated application for this separation. The use of HTGC over a period of 10 years to analyse various vegetable and food samples was reviewed elsewhere [54].

1.2.3. Gas chromatography–mass spectrometric analysis of TAGs

The role of GC is to separate TAG molecules as much as possible into individual TAG components. The MS provides mass spectrum information that helps in identifying the TAG components. The usefulness of the information obtained from the MS is highly dependent on the degree of separation achieved by GC. It could be very difficult to interpret MS information obtained from unresolved TAG components due to the similarity of mass fragments generated from different fatty acyl groups. Deconvolution methods for GC–MS techniques offers some measure of improved identification of overlapping compounds.

Mass spectrometry generates ions which provide information on molecular mass, the composition and structure of fatty acyl residues and some measure of stereospecificity (FAs sn-1/3 or sn-2 positions on the glycerol molecule) [60]. The MS enables the identification of TAG structures based on information about molecular mass and characteristic fragment ions, without the use of standards. Note that standards of TAG can be difficult to obtain.

GC–MS that utilises electron ionisation (EI) is the most widely used technique to analyse TAGs. Electron energy of 70 eV is used to generate standard EI mass spectra. The EI mass spectra of TAGs contains fragment ions, which are important for their structural

elucidation, such as $[M–RCO_2]^+$, $[M–RCO_2H]^+$, $[M–RCO_2CH_2]^+$, $[RCO+128]^+$, $[RCO+74]^+$ and RCO^+, where R = aliphatic hydrocarbon chain [60, 61]. These fragments are also useful for identification of molecular species of the TAGs [62]. The abundance of the fragment ions can be affected by chain length of the fatty acid residues, position of the fatty acids on the TAG molecule and unsaturation [63]. The abundance of $[M\text{-}RCO_2CH_2]^+$ was used to discriminate between FAs at position sn-1/3 and position sn-2 [64]. The drawback for using EI mass spectra is the low abundance of $M^{+\bullet}$ or $[M\text{-}18]^+$, which provide molecular weight information. Ruiz-Samblás et al. [57] developed HTGC–EIMS method, in a selected ion monitoring (SIM) mode, to analyse triacylglycerol composition of olive oil. Peak assignment was carried out based on locating the characteristic fragment ions having the same retention time on SIM profile such as $[M–RCO_2]^+$, $[RCO+128]^+$ and $[RCO+74]^+$. It has a disadvantage of difficulty in peak assignment since most fatty acyl residues have common fragment ions in their MS spectra.

1.2.4. High-performance liquid chromatographic analysis of TAGs

In HPLC separation occurs as a result of selective interaction of solutes, in this case TAGs, with a stationary phase packed in a column and liquid mobile phase that passes through the column. Solutes separate as they move along the column with the mobile phase based on their affinity for the stationary phase. Generally, there are two modes of HPLC, normal phase HPLC (NP-HPLC) and reversed-phase HPLC (RP-HPLC). In NP-HPLC solutes reversibly adsorb to a polar stationary phase whereas in RP-HPLC the solutes partition between a lower polarity stationary phase, which is a liquid coated or bonded to a solid support, and a polar liquid mobile phase. In RP-HPLC the stationary phase commonly employed is octadecylsilyl (C_{18}) modified silica [52]. The mobile phase used is selected based on the nature of the stationary phase such that it has a different polarity with respect to the stationary phase. For instance, polar solvent is used in RP-HPLC with respect to the non-polar stationary phase.

HPLC is a commonly used technique for the analysis of TAGs. Given its greater resolving power non-aqueous RP-HPLC (NARP-HPLC) is the more commonly employed technique than NP-HPLC. In RP-HPLC TAGs separate based on the chain lengths of FA residues on the TAG molecule and their degree of unsaturation. This was expressed by equivalent carbon number (ECN), which was defined as ECN = CN – 2DB, where CN is the total carbon numbers in the fatty acyl chains and DB is the total number of double bonds in the fatty acyl chains. Thus, TAGs are eluted in RP-HPLC based on their increasing ECN. Holčapek et al. [65] developed a RP-HPLC coupled to atmospheric pressure chemical ionisation MS (APCI–MS) method to achieve the identification of the highest possible number of TAGs in plant oils. TAGs with the same ECN, called critical pairs, and regioisomers often co-elute in RP-HPLC [2, 51]. Different studies applied NARP-HPLC with APCI–MS to determine TAG regioisomers in fats and oils only based on the basis of the difference in relative abundances of the fragment ions produced by preferred losses of the fatty acid from the sn-1/3 position compared to the sn-2 position on the TAG molecules [66, 67].

The other commonly employed technique for TAGs separation is silver ion HPLC (Ag^+-HPLC). In Ag^+-HPLC TAGs separation is based on reversable complexation formed between Ag^+ and the double bonds in the unsaturated fatty acyl chains. The commercially available column used for Ag^+-HPLC contains a stationary phase in which a strong cation exchanger, phenylsulfonic acid groups, is chemically bonded to silica and loaded with silver ion. Separation of TAGs in Ag^+-HPLC depends on the number, position and configuration of the double bonds, on the distribution of double bonds among the acyl groups of the same TAG molecule, and on the sn-positions of the FAs [2, 68]. Ag^+-HPLC is often used for regioisomeric analysis [69]. Lísa et al. [70] developed a method for regioisomeric characterisation of TAGs using Ag^+-HPLC–MS and synthetic standard TAGs, which is produced through randomisation of the FAs distribution on the TAGs. The method was applied for characterisation of plant oils

and animal fats with respect to regioisomeric TAGs and found that the preference of sn-2 occupation in plants oil was mainly unsaturated FAs whereas it was mainly saturated FAs in animal fats. However, regioisomeric TAGs with a large number of double bonds, for instance L/Ln/Ln and Ln/L/Ln, separate incompletely or with considerable difficulty. In Ag^{+}-HPLC the choice of the mobile phase composition is crucial in TAGs separation. A binary gradient of solvents may be sufficient to separate TAGs in less complex samples containing small proportions of dienoic FAs whereas for more complex samples containing a higher proportion of linoleic or linolenic acid a ternary gradient system is required [68, 71].

Other useful techniques worth mentioning is the use of supercritical fluid chromatography (SFC) for TAGs separation. SFC is a type of chromatography in which a gas compressed above its critical temperature and pressure is used as a mobile phase to elute analytes through the chromatographic column. Both packed and capillary columns were used to analyse TAGs with SFC [72, 73], although in recent times, packed columns are now featured. SFC has the advantage of short time of analysis attributed to the high diffusivity and low viscosity of the supercritical fluid, usually CO_2. A SFC–MS was used to separate soybean TAGs within 8 min [74]. Lee et al. [75] demonstrated the use of SFC coupled to tandem MS to profile regioisomeric TAGs in edible oils, where 70 TAG molecules, including 20 pairs of isomers, were identified in palm and canola oils.

1.2.5. Gas chromatographic analysis of volatile organic compounds (VOCs) in olive oil

Olive oil quality is assessed through either chemical analysis or sensory evaluation or both. VOCs are the main components that are being assessed. Chemical evaluation of VOCs in olive oil require techniques with an enrichment method. One such method is the novel technique called head-space solid phase microextraction (HS SPME). SPME consists of a fibre coated with stationary phase onto which VOCs are adsorbed based on their affinity for the coating material. A wide variety of coated fibres with different degree of polarity are

commercially available for analysing VOCs in different samples [24]. For the characterisation of olive oil VOCs HS SPME is a preferable technique compared to other techniques such as headspace sorptive extraction (HSSE; also referred to as stir-bar extraction) and direct thermal desorption (DTD) due to its operational simplicity, repeatability, and low cost, and hence may be usefully employed for routine quality control [76]. However, the durability of the SPME fibres is an issue. The two commonly employed SPME fibres in the analysis of VOCs in olive oil were 100 µm polydimethylsiloxane (PDMS) [14, 77, 78] and 50/30 µm divinylbenzene/Carboxen©/polydimethylsiloxane (DVB/CAR/PDMS) [15, 16, 77, 79-81]. **Table 1.2** shows the application of HS SPME and GC in the analysis of VOCs in olive oil. Capillary columns with stationary phases of 5% dimethyl polysiloxane and Wax were employed for the analysis of the VOCs.

Table 1.2. Selected application of HS SPME GC–MS in the analysis of VOCs in olive oil.

Study purpose	SPME fibre used	Column	Data processing	Ref.
Differentiation of virgin olive oils according to variety and geographical origin	DVB/CAR/PDMS	VF-WAX (30 m×0.25 mm×0.25 µm)	ANOVA, PCA, SLDA	[16]
Volatile profiles of olive oil in different heating conditions	100 µm PDMS	TG-5MS (30 m×0.25 mm×0.25 µm)	ANOVA	[77]
Differentiation of EVOOs according to cultivar	50/30 µm DVB/CAR/PDMS	DB-5MS (60 m × 0.32 mm × 1 µm)	MANOVA, LDA	[79]
Sesquiterpene fingerprinting for traceability of olive oil	100 µm PDMS	SPB-5 (30 m × 0.25 mm × 0.25 µm)	-	[14]
Comparison of volatile profile of virgin olive oils from two countries	DVB/CAR/PDMS	HP-5ms (30 m×0.25 mm×0.25 µm)	-	[82]
Characterization and classification of olive oils according to cultivar and geographical origin	50/30 µm DVB/CAR/PDMS	DB-5MS (60 m×0.32 mm×1 µm)	ANOVA, LDA, PCA	[80]
Varietal and processing effects on the volatile profile of olive oils	100 µm PDMS	DB-5 (30 m×0.25 mm×0.25 µm) ZB-5 (30 m×0.25 mm×0.25 µm)	HCA	[78]
Traceability of olive oil based on volatiles pattern	50/30 µm DVB/CAR/PDMS	HP-INNOWax (30 m×0.25 mm×0.25 µm)	LDA, ANN-MLP	[15]
Quantification of the volatile profile of virgin olive oil for supporting the panel test in their classification	50/30 µm DVB/CAR/PDMS	HP-INNOWax (50 m×0.2 mm×0.4 µm)	PCA, LDA	[83]
Natural variation (genetic variability) of VOCs in virgin olive oil	50/30 µm DVB/CAR/PDMS	DB-WAX (60 m×0.25 mm×0.25 µm)	FA, PCA	[26]
Investigation of changes in VOCs of olive oil in terms of cultivar, harvest year, and geographic regions	50/30 µm DVB/CAR/PDMS	HP-1 (50 m×0.2 mm×0.55 µm)	PCA	[25]

ANN-MLP - artificial neural networks with multilayer perceptrons, ANOVA – one-way analysis of variance, CA – cluster analysis, EVOO – extra virgin olive oil, FA – factor analysis, HCA - hierarchical cluster analysis, LDA – linear discriminant analysis, MANOVA – multivariate analysis of variance, PCA – principal component analysis, PDMS – polydimethylsiloxane, DVB/CAR/PDMS – divinylbenzene/carboxen/polydimethylsiloxane, SLDA – stepwise linear discriminant analysis, "-" – not specified

One-dimensional GC and comprehensive two-dimensional gas chromatography (GC×GC) techniques were used to analyse VOCs in olive oil [16, 78, 79, 84]. HS SPME GC–MS is the main technique used for separation, detection and identification of VOCs in olive oil [85]. 1D GC is used to analyse VOCs in olive oil where the focus is on major compounds that are used to differentiate between olive oils of different varieties. The limitation on major components is because 1D GC has a limited capacity in resolving the complex VOC mixtures or detecting the minor compounds that are found in olive oil. In contrast GC×GC can resolve components unresolved in 1D GC and also can increase the detection of many minor compounds that are undetected in the usual 1D GC analysis [16]. The application of GC×GC in the analysis of olive oil VOCs is discussed in more details in Section 1.2.8.

The major VOCs that were found in olive oils were alcohols, aldehydes, ketones, esters, acids and terpenes [81]. The carbon six (C6) aldehydes and alcohols are the most abundant VOCs, which favourably contribute to the aroma of olive oil. They are produced through lipoxygenase (LOX) pathway. Carbon five (C5) aldehyde and alcohols are also positive flavour contributors to olive oil [80, 82].

The VOCs are mostly identified by comparing their mass spectrum data and retention times to those in the selected MS library [16, 80]. They may also be identified through comparison of their retention indices and mass spectra with those of authentic samples [78] or pure standards [16]. Chemometric techniques were used to analyse data from VOCs analysis (**Table 1.2**). The analysis of VOCs in olive oils is mainly for fingerprinting or classification of olive oil according to cultivar and geographical origin (**Table 1.2**) [79, 80, 84]. Quantification is made by expressing the amounts of the VOCs relative to an added internal standard based on the area ratio of the analyte compound and the internal standard [81, 85]. Quantification using SPME extraction can be subjected to misinterpretation because the amount of a compound extracted by the SPME fibre may not necessarily reflect the concentration of that

compound in the oil. It may only reflect the concentration of the compound in the head-space based on its affinity for the fibre used. This is because the concentration of the compound in the head-space is dependent on its volatility and the amount of the compound extracted by the fibre depends on its affinity for the fibre coatings. During SPME extraction analytes or VOCs undergo a series of transport process from the liquid sample to the head space, and eventually to the fibre, until the system reaches equilibrium. Different analytes have different equilibration time based on their partition coefficient [86].

1.2.6. Multidimensional gas chromatography

The introduction of multidimensional gas chromatography (MDGC) techniques has offered a solution to solve separation problems due to its greater resolving power and increased peak capacity than a single dimensional chromatography method [87]. Two approaches of the technique exist (1) a target portion of a chromatographic effluent from a first column is subjected to a second column separation (called 'heart cut' MDGC – H/C MDGC) (2) a two-column separation is applied to the entire sample (called comprehensive two-dimensional gas chromatography – GC×GC). The H/C MDGC method, which samples small segments of the first dimension (^{1}D) column effluent and subjects it to a conventional dimension second dimension (^{2}D) column, gives an improved separation of selected overlapped regions of the ^{1}D column. By contrast, the unique separation power of GC×GC due to its enhanced resolution, increased sensitivity and peak capacity over one-dimensional GC (1D GC) together with its ability to generate a unique two-dimensional (2D) chromatogram (2D chemical map) for the total chromatogram has made its application to analysis of complex samples more attractive [88]. It is applied to a wide range of samples from almost all fields of study suited to GC analysis, including analysis of FAMEs and VOCs in olive oil. The application of GC×GC and H/C MDGC to the analysis of various samples have been demonstrated in different research

studies in our research group (Marriott group) previously. The experience obtained in H/C MDGC studies were utilised in the research studies included in this thesis.

1.2.6.1. 'Heart-cut' multidimensional gas chromatography (H/C MDGC)

In complex sample analysis using 1D GC, peak overlapping leads to problematic or ambiguous component identification. The problem can be solved through coupling of two independent or nearly independent separation steps using multidimensional chromatography [89]. One such technique is H/C MDGC. 'Heart-cutting' (H/C) is defined as 'transfer of one or more selected groups of compounds eluted from a gas chromatographic column onto a second column' [90]. Target groups of compounds with poor resolution or that are unresolved in the ^{1}D column are selectively transferred to the ^{2}D column having different selectivity. The precise control and transfer of compounds from the ^{1}D to the ^{2}D column is an important step in H/C MDGC. Commonly an online H/C transfer is employed. The transfer or H/C is achieved generally in two different approaches (1) by using a switching valve or (2) by using pneumatic flow switching device (Deans switch). The Deans switch developed in 1968 [90] by Deans is the most widely used device in H/C MDGC due to its simplicity and flexibility in controlling pressure and flow. Switching valves may have some drawbacks including memory effects due to analyte stability and adsorption [91] and broadened peaks attributed to high dead volume of the valve [88], although passivated devices are now available.

The H/C fractions are generally sufficiently small to avoid excessive sampling, that can lead to overlapping of peaks in the second column. Further, the introduction of a cryotrap at the inlet section of the second column helps in trapping and refocusing of the H/C fraction. The refocusing can effectively minimise peak broadening and maximise separation in the second column.

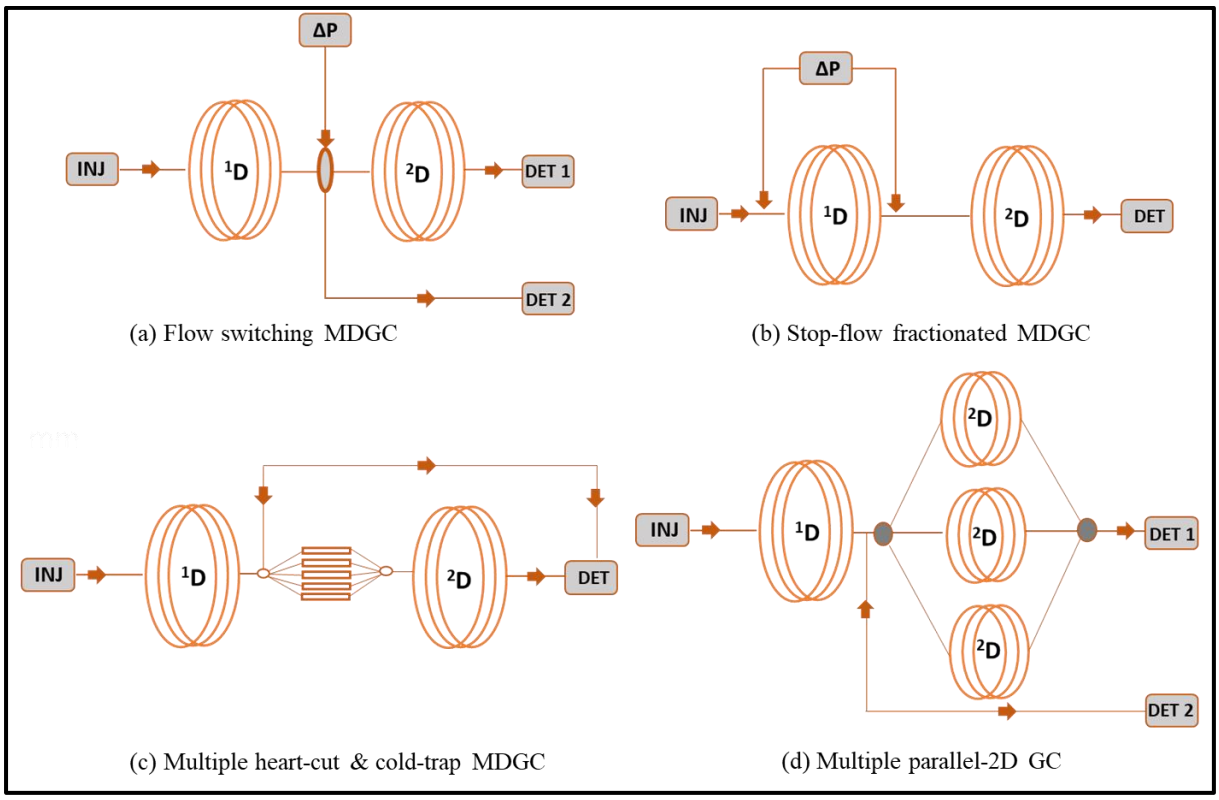

Figure 1.3. MDGC configurations used in most studies. ^{1}D – conventional first-dimension column, ^{2}D – conventional second-dimension column, ΔP – pneumatic control, INJ – injector and DET – universal, specific or mass-selective detector or infrared spectroscopy. Adapted from Ref. [88] with permission.

There are different configurations of MDGC techniques. **Figure 1.3a** shows a system in which a H/C switching device is used to switch one or more ^{1}D column effluent zones to a ^{2}D column [88, 92]. A Deans switch is the most commonly employed device used in such configurations. In-situ fractionation technique in which controlled fractions of effluent from ^{1}D column based on a stop-flow approach are transferred sequentially to the ^{2}D column was introduced by Goode (**Figure 1.3b**) [93]. A MDGC system with multiple parallel cryogenic traps was also introduced and used in many analysis (**Figure 1.3c**) [94-97]. Parallel ^{2}D column MDGC, in which a precolumn is linked to a set of parallel columns having different stationary phases was developed (**Figure 1.3d**) [98, 99]. The ^{2}D columns are all connected to a single

detector which make possible the collection of retention information on multiple stationary phases. Other configuration such as multiple oven arrangements were also used [100].

The purpose of H/C MDGC is to improve the separation of limited unresolved regions of 1D GC analysis. If the whole region in the sample analysis requires further separation using MDGC techniques, the alternative method is to use GC×GC.

1.2.6.2. Comprehensive two-dimensional gas chromatography (GC×GC)

According to Giddings [101] a two-dimensional separation is a technique that subjects a sample to two independent displacement processes. The displacement processes now define components in a 2D space where there is more 'space' for resolution than the 1D separation system. Liu and Phillips [102] in 1991 described and conducted an experiment for the first time using GC×GC and generated sequential fast ^{2}D chromatograms of separated components over the whole analysis. This can be reconstructed as a '2D separation space', with axes of ^{1}D retention and ^{2}D retention. The 2D GC technique requires two columns of different selectivity in combination with a device to selectively transfer a portion of chromatographic effluent from ^{1}D into ^{2}D column [103]. The interface between the two columns is a crucial component for GC×GC. It is termed a modulator. Unlike H/C MDGC, GC×GC subjects the entire eluate from the ^{1}D column to separation on the ^{2}D column, and in the process all information gained during the ^{1}D separation will be reserved. This results in increased peak capacity, for instance if n_1 and n_2 are peak capacities of ^{1}D and ^{2}D separation respectively, then the peak capacity of the GC×GC will be approximately $n_1 \times n_2$ [104].

Modulators are broadly classified based on their operational characteristics as thermal modulators and pneumatic modulators [105]. Liu and Phillips [102] used a dual-stage thermal-desorption (TD) modulator in their experiments. Subsequently, various cryogenic modulators [106, 107], and valve-based and flow modulators [108] have been developed with different functionality, as reviewed elsewhere [105, 109, 110].

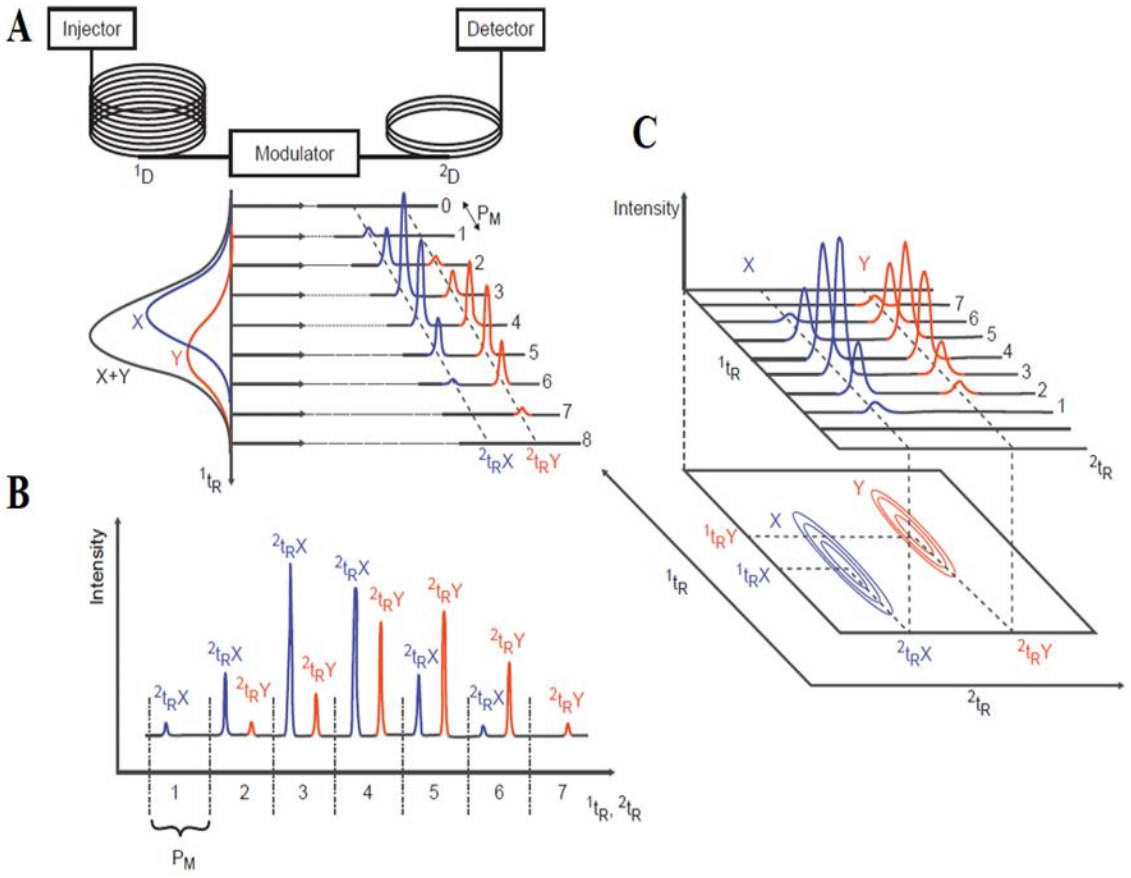

Figure 1.4. Basic setup of a GC×GC and peak processing method. (A) Two overlapped analytes of X and Y at ^{1}D with apparent retention ($^{1}t_{R}$) with narrow bands of the analytes entering ^{2}D with retention defined as $^{2}t_{R}$X and $^{2}t_{R}$Y based on the modulation period (P_{M}). (B) A raw data signal of the entire separation process. (C) The construction of a 2D contour plot from the collected data in (B). Adapted from Ref. [111] with permission.

The modulator continuously samples, re-focuses narrow adjacent fractions of ^{1}D effluent, and re-injects each fraction onto the ^{2}D column. The time required to complete one cycle of the process (modulation) is called the modulation period (P_{M}), and usually ranges 1–8 s [105]. To preserve the ^{1}D separation the process should be rapid and also the ^{2}D separation should be finished, in a time shorter than P_{M}, before the next introduction of the subsequent fraction of ^{1}D to avoid wrap-around [112, 113]. **Figure 1.4A-C** shows the basic setup of a GC×GC system, peak processing and data handling. The P_{M} setting depends on the peak width

of the ^{1}D peak ($^{1}w_b$); if $^{1}w_b > P_M$, the ^{1}D peak is sliced into a series of pulsed peaks on ^{2}D. The modulation ratio (M_R) determines the number of times that a given peak is sampled or modulated. The M_R is proposed to be the ratio of 4 times the ^{1}D peak standard deviation (4σ = peak base width; $^{1}w_b$) divided by P_M. The recommended M_R values for quantification and screening are 3 and 1.5 respectively [88]. From GC×GC analysis a large series of high-speed ^{2}D chromatograms is obtained. They are usually 'stacked side by side' using a suitable computer program to form a '2D chromatogram' with one dimension representing the ^{1}D retention time and the second representing the ^{2}D retention time (**Figure 1.4C**). The chromatogram can be visualised in different forms such as 2D colour plot, contour plot or 3D plot, where peak response is the 3rd dimension for the latter presentation.

1.2.7. Multidimensional chromatographic analysis of TAGs

1.2.7.1. H/C MDGC and GC×GC analysis of TAGs

Few reports of GC×GC applications for the separation of TAGs have been noted. A study on the separation of low volatility compounds and TAGs using GC×GC from extracted coffee bean samples was reported by Novaes *et al.* [114]. The study reported poorly separated TAG peaks due to major peaks broadening, which masked trace TAG peaks. Wraparound phenomena and some 'streaking' of the major components were also reported, for which diluting the sample solution and increasing the final elution temperature to 370 °C were used as a solution. To my knowledge there was no H/C MDGC studies on TAGs analysis reported thus far other than those included in this thesis.

1.2.7.2. LC×GC analysis of TAGs

Hyphenation of LC and GC gives the combined advantages from the capabilities of the two individual systems. LC gives moderate sample separation capacity with alternative separation mechanisms, whilst GC has high separation efficiency and capacity, different

separation factors arising from different column polarity, and can be coupled to various detection devices [115]. Due to the high molecular masses of TAGs, except for TAGs derived from short acyl groups, HTGC offer limited resolution for most lipids. In comparison a well-tuned LC method has good selectivity for TAGs of different mass and unsaturation, and has the ability to resolve TAGs of different degree of unsaturation and CN. Combining LC with GC analyses offers some degree of orthogonality of separation, due to their quite different separation mechanisms.

Janssen *et al.* [116] demonstrated the use of LC×GC for the separation of TAGs in edible fats and oils. The entire complex sample was characterised by transferring narrow time fractions of the ^{1}D LC run to a ^{2}D GC column to achieve higher overall resolution. Fractions from LC were collected at time intervals of 0.5 or 1 min, which is $<{}^{1}w_b$ (peak width at baseline on the first column), and injected into GC for further separation. Using the highest possible programming rate of the instrument and a short column, a typical AgLC×GC analysis (of 35 fractions) took a total analysis time of about 11 h per sample. TAGs were separated using normal phase LC based on polarity, and further separated on approximate basis of boiling point using GC, with FID detection, by an independent ^{2}D separation. Automated on-line comprehensive two-dimensional LC×GC and LC×GC–TOFMS instrument design was reported by Koning *et al.* [117]. The system was demonstrated to be useful through the analysis of FAMEs and TAGs in edible fat and oils. More information was obtained using the comprehensive system as compared to the individual separation modes. The use of silver-phase LC improved the separation of TAGs by separating individual components based on two independent parameters of CN and number of double bonds, and component identification was improved through hyphenation of the GC stage with TOFMS.

1.2.7.3. Two-dimensional LC analysis of TAGs

The combination of two independent separation techniques, for instance NARP-HPLC and Ag^+-HPLC, is useful for the separation of critical pairs and isomers. In two-dimensional liquid chromatography (2D LC) TAGs are subjected to two different retention mechanisms. 2D LC has two different modes of approaches, namely on-line and off-line modes. Off-line approach requires collection of fractions from the ^{1}D and re-injecting to the ^{2}D for further separation, which is often time consuming and laborious. The combination of NARP-HPLC and Ag^+-HPLC both in on-line and off-line mode were used to separate TAGs. Hu et al. [118] used an off-line system coupling NARP-HPLC and Ag^+-HPLC with APCI–MS to investigate peanut oil TAGs. The on-line 2D LC approach is fast and automated but has a drawback of complexity of the system and incompatibility of the two different eluents required for each LC stage. Beccaria et al. [119] applied comprehensive stop flow Ag^+-LC×NARP-LC and off-line Ag^+-LC×NARP-LC approaches, to analyse TAGs in fish oil and compared the two approaches in terms of peak capacity. It was found that the off-line approach has a better separation, hence higher peak capacity than the comprehensive approach allowing the identification and semi-quantification of more than 250 TAGs.

1.2.8. GC×GC analysis of VOCs in olive oil

One-dimensional GC is widely used for the analysis of VOCs in several matrices, including olive oil as stated above. Many times, 1D GC produces chromatograms with many unresolved peaks resulting in information loss and difficulty on identification. In addition, minor compounds may not be detected, especially when overlapped by major components. However, GC×GC can solve these problems. Lukić et al. [16] studied the VOCs in EVOO using both GC–TOFMS and GC×GC–TOFMS after HS SPME extraction. The study reported that <30 compounds were detected and identified using 1D GC method whereas up to 1000

compounds were detected and about 256 compounds were (tentatively) identified using the GC×GC method. In a similar study, a targeted analysis of VOCs in EVOO using GC×GC–MS, about 119 compounds were identified [84].

For the purpose of identification MS was used as a detector in all GC×GC analysis of VOCs (**Table 1.3**). VOCs were mainly identified based on linear retention index matching and MS spectra. MS spectra were compared with that of a pure standard substance, where available, and with library of mass spectra, commonly with NIST library [16, 84, 120]. Note that in the absence of authentic standards. The column configuration mainly employed in the VOCs analysis were either *polar*×*mid-polar*, such as wax column in the ^{1}D and a BPX50 column as ^{2}D or *apolar*×*polar*, such as BPX5 column as ^{1}D and wax column as ^{2}D (**Table 1.3**). The data obtained from VOCs analysis in EVOO when a large cohort of samples and their inter-relationship is of interest, are usually processed using multivariate analysis techniques such as principal component analysis (PCA), partial least square discriminant analysis (PLS-DA) and other methods [120, 121].

The purpose of studying VOCs in EVOO includes profiling, differentiation of cultivar and/or geographical origin, pattern recognition, investigating traceability and sensory quality of EVOO (**Table 1.3**).

Table 1.3. Selected applications of GC×GC−MS in the analysis of VOCs in olive oil.

Study purpose	Modulator	Column	Data processing	Ref.
Differentiation of virgin olive oil according to variety and geographical origin	Non-moving quadjet dual-stage thermal modulator	^{1}D: VF-WAX (30 m×0.25 mm×0.25 µm) ^{2}D: Rxi-17Sil MS (1.50 m×0.15 mm×0.15 µm)	ANOVA, PCA, SLDA	[16]
Combined untargeted and targeted fingerprinting for volatiles and ripening indicators in olive oil	Two-stage KT 2004 loop-type thermal modulator	^{1}D: SolGel-WAX (30 m×0.25 mm×0.25 mm) ^{2}D: OV-1701 (1 m×0.1 mm×0.10 µm)	PCA	[84]
Fingerprint pattern recognition in olive oil produced by two different techniques in olive varieties	Longitudinally modulated cryogenic system	^{1}D: BPX5 (30 m×0.25mm×0.25µm ^{2}D: BPX20 (1.5 m×0.1mm×0.1µm	ANOVA, PCA	[121]
Untargeted and targeted fingerprinting of EVOO volatiles	Two-stage KT 2004 loop type thermal modulator	^{1}D: SolGel-WAX (30 m×0.25 mm×0.25 µm) ^{2}D: OV1701 (1 m×0.1 mm×0.10 µm)	PCA	[122]
Defining a chemical blue print of virgin olive oil volatiles to be correlated to the product sensory quality	*Set up 1: apolar×polar* A loop-type single-jet prototype developed at the University of Udine, was adopted as a cryogenic modulator *Set up 2: polar×apolar* Two-stage KT 2004 loop thermal modulator	*Set up 1: apolar×polar* ^{1}D Rxi-5ms (30 m×0.25 mm×0.50 µm) ^{2}D: SUPELCOWAX10 (1.2 m×0.1 mm×0.10 µm) *Set up 2: polar×apolar* ^{1}D: SolGel–WAX (30 m×0.25 mm×0.25 µm) ^{2}D: OV-1701 (1 m×0.1 mm×0.10 µm)	PCA, PLS-DA, OPLS-DA	[120]
Traceability of olive oil based on volatiles pattern	Cryogenic modulator	^{1}D: HP-INNOWax (30 m×0.25 mm×0.25 µm) ^{2}D: BPX50 (1.25 m×0.1 mm×0.1 µm)	PCA, LDA, ANN	[15]

ANOVA – one-way analysis of variance, ANN – artificial neural networks, EVOO – extra virgin olive oil, LDA – linear discriminant analysis, PCA – principal component analysis, PLS-DA – partial least square discriminant analysis, OPLS-DA – orthogonal partial least square discriminant analysis, SLDA – stepwise linear discriminant analysis

1.3. Scope of the thesis

The thesis describes different strategies that can be utilised in the analysis of FAs, TAGs and VOCs in oil samples. It details the identification of FA and TAG components in plant oil sample using mass spectrum fingerprinting. It also describes the development of an MDGC method for the separation and identification of TAGs in olive oil, that can be extended to the analysis of other lipid matrices. The thesis covers also the differentiation of EVOO varieties based on the analysis of FAs and VOCs.

Chapter 1 presents the thesis introduction and literature review of relevant prior research studies. A brief background on FAs, TAGs and olive oil was followed by a literature review which details on different approaches of analysis of FAs, TAGs and VOCs in oil samples, and recent developments in the field. **Chapter 2** describes the methodologies used in the studies included in the thesis.

The thesis project begins with **Chapter 3**, which details a GC–EIMS method of analysis of FAs and TAGs in sapucainha oil. The GC–EIMS method demonstrates the identification of TAG components in sapucainha oil based on FAs composition, mass spectral fingerprinting, and peak deconvolution, in the absence of standard TAGs and mass spectrum library information. It describes the possible TAG composition of sapucainha oil which mostly co-elutes.

Based on this first study, MDGC-FID and MDGC-MS methods were then applied to EVOO. **Chapter 4** focuses on the development of H/C MDGC for improved separation of TAGs in olive oil. The H/C MDGC strategy demonstrates a significantly improved separation of co-eluted TAG components through the use of a relatively short ^{1}D and ^{2}D columns under suitable flow and elevated temperature conditions. Identification of separated TAGs in TAG analysis is an important step. Thus, as a continuation to this C**hapter 5** demonstrates the use

of MDGC–MS approach for the separation and identification of TAG components using MS as ^{2}D detector.

Chapter 6 demonstrates the differentiation of EVOO varieties based on the analysis of FAs and VOCs. The method applies chemometric approaches to reveal the varietal differences. SPME was used for VOCs, and a 1D GC-FID method for FAME in the oils.

Chapter 7 details the overall conclusion drawn out of the studies conducted and presented in the thesis and outlines the future directions for strategies that should be followed in future for the analysis of FAs, TAGs and VOCs in oil samples and similar matrices.

1.4. References

[1] F. Marini, Triacylglycerols: characterization and determination, In, Encyclopedia of food and health, Academic Press, Oxford, 2016, pp. 345-350.

[2] T. Řezanka, K. Pádrová, K. Sigler, Regioisomeric and enantiomeric analysis of triacylglycerols, Anal. Biochem. 524 (2017) 3-12.

[3] O. Berdeaux, P.C. Dutta, M.C. Dobarganes, J.L. Sébédio, Analytical methods for quantification of modified fatty acids and sterols formed as a result of processing, Food Anal. Methods 2 (2009) 30-40.

[4] W.W. Christie, X. Han, Chapter 1: Lipids: their structures and occurrence, In: W.W. Christie, X. Han (Eds.), Lipid Analysis: Isolation, Separation, Identification and Lipidomic Analysis, Fourth edition, Woodhead Publishing Limited, Cambridge, UK, 2010, pp. 3-19.

[5] J.L. Sebedio, A. Grandgirard, Cyclic fatty acids: Natural sources, formation during heat treatment, synthesis and biological properties, Prog. Lipid Res. 28 (1989) 303-336.

[6] H.I. Cole, H.T. Cardoso, Analysis of chaulmoogra oils. I. Carpotroche brasiliensis (sapucainha) oil, J. Am. Chem. Soc. 60 (1938) 614-617.

[7] F.J. Hidalgo, R. Zamora, Triacylglycerols: Structures and properties, In: B. Caballero, P.M. Finglas, F. Toldrá (Eds.), Encyclopedia of Food and Health, Academic Press, Oxford, 2016, pp. 351-356.

[8] C.L. Huang, B.E. Sumpio, Olive oil, the mediterranean diet, and cardiovascular health, J. Am. Coll. Surg. 207 (2008) 407-416.

[9] M. Jacomelli, V. Pitozzi, M. Zaid, M. Larrosa, G. Tonini, A. Martini, S. Urbani, A. Taticchi, M. Servili, P. Dolara, L. Giovannelli, Dietary extra-virgin olive oil rich in phenolic antioxidants and the aging process: long-term effects in the rat, J. Nutr. Biochem. 21 (2010) 290-296.

[10] G.K. Beauchamp, R.S.J. Keast, D. Morel, J. Lin, J. Pika, Q. Han, C.H. Lee, A.B. Smith, P.A.S. Breslin, Ibuprofen-like activity in extra-virgin olive oil, Nature 437 (2005) 45-46.

[11] D.L. García-González, R. Aparicio-Ruiz, R. Aparicio, Virgin olive oil - chemical implications on quality and health, Eur. J. Lipid Sci. Technol. 110 (2008) 602-607.

[12] T.H. Borges, J.A. Pereira, C. Cabrera-Vique, L. Lara, A.F. Oliveira, I. Seiquer, Characterization of Arbequina virgin olive oils produced in different regions of Brazil and Spain: Physicochemical properties, oxidative stability and fatty acid profile, Food Chem. 215 (2017) 454-462.

[13] G. Lercker, M.T. Rodriguez-Estrada, Chromatographic analysis of unsaponifiable compounds of olive oils and fat-containing foods, J. Chromatogr. A 881 (2000) 105-129.

[14] A. Damascelli, F. Palmisano, Sesquiterpene fingerprinting by headspace SPME-GC-MS: preliminary study for a simple and powerful analytical tool for traceability of olive oils, Food Anal. Methods 6 (2013) 900-905.

[15] T. Cajka, K. Riddellova, E. Klimankova, M. Cerna, F. Pudil, J. Hajslova, Traceability of olive oil based on volatiles pattern and multivariate analysis, Food Chem. 121 (2010) 282-289.

[16] I. Lukić, S. Carlin, I. Horvat, U. Vrhovsek, Combined targeted and untargeted profiling of volatile aroma compounds with comprehensive two-dimensional gas chromatography for differentiation of virgin olive oils according to variety and geographical origin, Food Chem. 270 (2019) 403-414.

[17] M. Guissous, Y. Le Dréau, H. Boulkhroune, T. Madani, J. Artaud, Chemometric characterization of eight monovarietal algerian virgin olive oils, J. Am. Oil Chem. Soc. 95 (2018) 267-281.

[18] C. Ruiz-Samblás, F. Marini, L. Cuadros-Rodríguez, A. González-Casado, Quantification of blending of olive oils and edible vegetable oils by triacylglycerol fingerprint gas chromatography and chemometric tools, J. Chromatogr. B: Anal. Technol. Biomed. Life Sci. 910 (2012) 71-77.

[19] M. Fasciotti, A.D. Pereira Netto, Optimization and application of methods of triacylglycerol evaluation for characterization of olive oil adulteration by soybean oil with HPLC–APCI-MS–MS, Talanta 81 (2010) 1116-1125.

[20] M. Fuentes de Mendoza, C. De Miguel Gordillo, J. Marín Expóxito, J. Sánchez Casas, M. Martínez Cano, D. Martín Vertedor, M.N. Franco Baltasar, Chemical composition of virgin olive oils according to the ripening in olives, Food Chem. 141 (2013) 2575-2581.

[21] B.P. Chapagain, Z. Wiesman, MALDI-TOF/MS fingerprinting of triacylglycerols (TAGs) in olive oils produced in the Israeli Negev desert, J. Agric. Food Chem. 57 (2009) 1135-1142.

[22] M. Issaoui, S. Dabbou, F. Brahmi, K.B. Hassine, M.H. Ellouze, M. Hammami, Effect of extraction systems and cultivar on the quality of virgin olive oils, Int. J. Food Sci. Technol. 44 (2009) 1713-1720.

[23] A.K. Kiritsakis, Flavor components of olive oil - A review, J. Am. Oil Chem. Soc. 75 (1998) 673-681.

[24] F. Angerosa, M. Servili, R. Selvaggini, A. Taticchi, S. Esposto, G. Montedoro, Volatile compounds in virgin olive oil: Occurrence and their relationship with the quality, J. Chromatogr. A 1054 (2004) 17-31.

[25] Ş.Ş. Oğraş, G. Kaban, M. Kaya, Volatile compounds of olive oils from different geographic regions in Turkey, Int. J. Food Prop. 21 (2018) 1833-1843.

[26] C. Sanz, A. Belaj, A. Sánchez-Ortiz, A.G. Pérez, Natural variation of volatile compounds in virgin olive oil analyzed by HS-SPME/GC-MS-FID, Separations 5 (2018) 24.

[27] A. Amanpour, H. Kelebek, S. Selli, Characterization of aroma, aroma-active compounds and fatty acids profiles of cv. Nizip Yaglik oils as affected by three maturity periods of olives, J. Sci. Food Agric. 99 (2019) 726-740.

[28] J. Reiners, W. Grosch, Odorants of virgin olive oils with different flavor profiles, J. Agric. Food Chem. 46 (1998) 2754-2763.

[29] L. Conte, A. Bendini, E. Valli, P. Lucci, S. Moret, A. Maquet, F. Lacoste, P. Brereton, D.L. García-González, W. Moreda, T. Gallina Toschi, Olive oil quality and authenticity: A review of current EU legislation, standards, relevant methods of analyses, their drawbacks and recommendations for the future, Trends Food Sci. Technol. 105 (2020) 483-493.

[30] International Olive Council, Method for the determination of stigmastadienes in vegetable oils, in, Decision No DEC-III-1/106-VI/2017, Method COI/T.20/Doc. No 11/Rev. 3 – 2017, 2017, pp. 1-12.

[31] Boundary Bend Limited, http://www.boundarybend.com/about/, in, accessed March, 2020.

[32] K. Eder, Gas chromatographic analysis of fatty acid methyl esters, J. Chromatogr. B: Biomed. Sci. Appl. 671 (1995) 113-131.

[33] W.W. Christie, X. Han, Chapter 7: Preparation of derivatives of fatty acids, In: W.W. Christie, X. Han (Eds.), Lipid Analysis: Isolation, Separation, Identification and Lipidomic Analysis, Fourth edition, Woodhead Publishing Limited, Cambridge, UK, 2010, pp. 145-158.

[34] H.H. Chiu, C.H. Kuo, Gas chromatography-mass spectrometry-based analytical strategies for fatty acid analysis in biological samples, J. Food Drug Anal. 28 (2020) 60-73.

[35] A. Zribi, H. Jabeur, F. Aladedunye, A. Rebai, B. Matthäus, M. Bouaziz, Monitoring of quality and stability characteristics and fatty acid compositions of refined olive and seed oils during repeated pan- and deep-frying using GC, FT-NIRS, and chemometrics, J. Agric. Food Chem. 62 (2014) 10357-10367.

[36] L.D. Roberts, G. McCombie, C.M. Titman, J.L. Griffin, A matter of fat: An introduction to lipidomic profiling methods, J. Chromatogr. B: Anal. Technol. Biomed. Life Sci. 871 (2008) 174-181.

[37] F.-f. Ai, J. Bin, Z.-m. Zhang, J.-h. Huang, J.-b. Wang, Y.-z. Liang, L. Yu, Z.-y. Yang, Application of random forests to select premium quality vegetable oils by their fatty acid composition, Food Chem. 143 (2014) 472-478.

[38] A.X. Zeng, S.-T. Chin, P.J. Marriott, Integrated multidimensional and comprehensive 2D GC analysis of fatty acid methyl esters, J. Sep. Sci. 36 (2013) 878-885.

[39] C.A. Ballus, A.D. Meinhart, F.A. de Souza Campos Jr, L.F.d.O. da Silva, A.F. de Oliveira, H.T. Godoy, A quantitative study on the phenolic compound, tocopherol and fatty acid contents of monovarietal virgin olive oils produced in the southeast region of Brazil, Food Res. Int. 62 (2014) 74-83.

[40] B. Bicalho, F. David, K. Rumplel, E. Kindt, P. Sandra, Creating a fatty acid methyl ester database for lipid profiling in a single drop of human blood using high resolution capillary gas chromatography and mass spectrometry, J. Chromatogr. A 1211 (2008) 120-128.

[41] J.K.G. Kramer, C.B. Blackadar, J. Zhou, Evaluation of two GC columns (60-m SUPELCOWAX 10 and 100-m CP Sil 88) for analysis of milkfat with emphasis on CLA, 18:1, 18:2 and 18:3 isomers, and short- and long-chain FA, Lipids 37 (2002) 823-835.

[42] P. Delmonte, A.-R. Fardin Kia, J.K.G. Kramer, M.M. Mossoba, L. Sidisky, J.I. Rader, Separation characteristics of fatty acid methyl esters using SLB-IL111, a new ionic liquid coated capillary gas chromatographic column, J. Chromatogr. A 1218 (2011) 545-554.

[43] P. Delmonte, A.R. Fardin-Kia, J.K.G. Kramer, M.M. Mossoba, L. Sidisky, C. Tyburczy, J.I. Rader, Evaluation of highly polar ionic liquid gas chromatographic column for the determination of the fatty acids in milk fat, J. Chromatogr. A 1233 (2012) 137-146.

[44] K. Maštovská, S.J. Lehotay, Practical approaches to fast gas chromatography-mass spectrometry, J. Chromatogr. A 1000 (2003) 153-180.

[45] L. Mondello, A. Casilli, P.Q. Tranchida, R. Costa, B. Chiofalo, P. Dugo, G. Dugo, Evaluation of fast gas chromatography and gas chromatography–mass spectrometry in the analysis of lipids, J. Chromatogr. A 1035 (2004) 237-247.

[46] I.C. Santos, K.A. Schug, Recent advances and applications of gas chromatography vacuum ultraviolet spectroscopy, J. Sep. Sci. 40 (2017) 138-151.

[47] H. Fan, J. Smuts, L. Bai, P. Walsh, D.W. Armstrong, K.A. Schug, Gas chromatography-vacuum ultraviolet spectroscopy for analysis of fatty acid methyl esters, Food Chem. 194 (2016) 265-271.

[48] K.A. Schug, I. Sawicki, D.D. Carlton, H. Fan, H.M. McNair, J.P. Nimmo, P. Kroll, J. Smuts, P. Walsh, D. Harrison, Vacuum ultraviolet detector for gas chromatography, Anal. Chem. 86 (2014) 8329-8335.

[49] I.C. Santos, J. Smuts, W.S. Choi, Y. Kim, S.B. Kim, K.A. Schug, Analysis of bacterial FAMEs using gas chromatography – vacuum ultraviolet spectroscopy for the identification and discrimination of bacteria, Talanta 182 (2018) 536-543.

[50] C.A. Weatherly, Y. Zhang, J.P. Smuts, H. Fan, C. Xu, K.A. Schug, J.C. Lang, D.W. Armstrong, Analysis of long-chain unsaturated fatty acids by ionic liquid gas chromatography, J. Agric. Food Chem. 64 (2016) 1422-1432.

[51] N.K. Andrikopoulos, Triglyceride species compositions of common edible vegetable oils and methods used for their identification and quantification, Food Rev. Int. 18 (2002) 71-102.

[52] M. Buchgraber, F. Ulberth, H. Emons, E. Anklam, Triacylglycerol profiling by using chromatographic techniques, Eur. J. Lipid Sci. Technol. 106 (2004) 621-648.

[53] P.A. Sutton, S.J. Rowland, High temperature gas chromatography–time-of-flight-mass spectrometry (HTGC–ToF-MS) for high-boiling compounds, J. Chromatogr. A 1243 (2012) 69-80.

[54] C. Ruiz-Samblás, A. González-Casado, L. Cuadros-Rodríguez, Triacylglycerols determination by high-temperature gas chromatography in the analysis of vegetable oils and foods: A review of the past 10 years, Crit. Rev. Food Sci. Nutr. 55 (2015) 1618-1631.

[55] B.X. Mayer, E. Lorbeer, Triacylglycerol mixture for testing capillary columns for high-temperature gas chromatography, J. Chromatogr. A 758 (1997) 235-242.

[56] N.K. Andrikopoulos, I.G. Giannakis, V. Tzamtzis, Analysis of olive oil and seed oil triglycerides by capillary gas chromatography as a tool for the detection of the adulteration of olive oil, J. Chromatogr. Sci. 39 (2001) 137-145.

[57] C. Ruiz-Samblás, A. González-Casado, L. Cuadros-Rodríguez, F.P.R. García, Application of selected ion monitoring to the analysis of triacylglycerols in olive oil by high temperature-gas chromatography/mass spectrometry, Talanta 82 (2010) 255-260.

[58] P. Marěs, High temperature capillary gas liquid chromatography of triacylglycerols and other intact lipids, Prog. Lipid Res. 27 (1988) 107-133.

[59] S. Indelicato, D. Bongiorno, R. Pitonzo, V. Di Stefano, V. Calabrese, S. Indelicato, G. Avellone, Triacylglycerols in edible oils: Determination, characterization, quantitation, chemometric approach and evaluation of adulterations, J. Chromatogr. A 1515 (2017) 1-16.

[60] P. Laakso, Mass spectrometry of triacylglycerols, Eur. J. Lipid Sci. Technol. 104 (2002) 43-49.

[61] M. Barber, T.O. Merren, W. Kelly, The mass spectrometry of large molecules I. The triglycerides of straight chain fatty acids, Tetrahedron Lett. 5 (1964) 1063-1067.

[62] P. Kalo, A. Kemppinen, Mass spectrometric identification of triacylglycerols of enzymatically modified butterfat separated on a polarizable phenylmethylsilicone column, J. Am. Oil Chem. Soc. 70 (1993) 1209-1217.

[63] W.M. Lauer, A.J. Aasen, G. Graff, R.T. Holman, Mass spectrometry of triglycerides: I. Structural effects, Lipids 5 (1970) 861-868.

[64] H. Kallio, P. Laakso, R. Huopalahti, R.R. Linko, P. Oksman, Analysis of butter fat triacylglycerols by supercritical fluid chromatography/electron impact mass spectrometry, Anal. Chem. 61 (1989) 698-700.

[65] M. Holčapek, M. Lísa, P. Jandera, N. Kabátová, Quantitation of triacylglycerols in plant oils using HPLC with APCI-MS, evaporative light-scattering, and UV detection, J. Sep. Sci. 28 (2005) 1315-1333.

[66] L. Fauconnot, J. Hau, J.M. Aeschlimann, L.B. Fay, F. Dionisi, Quantitative analysis of triacylglycerol regioisomers in fats and oils using reversed-phase high-performance liquid chromatography and atmospheric pressure chemical ionization mass spectrometry, Rapid Commun. Mass Spectrom. 18 (2004) 218-224.

[67] A. Jakab, I. Jablonkai, E. Forgács, Quantification of the ratio of positional isomer dilinoleoyl-oleoyl glycerols in vegetable oils, Rapid Commun. Mass Spectrom. 17 (2003) 2295-2302.

[68] W.W. Christie, Separation of molecular species of triacylglycerols by high-performance liquid chromatography with a silver ion column, J. Chromatogr. A 454 (1988) 273-284.

[69] M. Holčapek, H. Dvořáková, M. Lísa, A.J. Girón, P. Sandra, J. Cvačka, Regioisomeric analysis of triacylglycerols using silver-ion liquid chromatography-atmospheric pressure chemical ionization mass spectrometry: Comparison of five different mass analyzers, J. Chromatogr. A 1217 (2010) 8186-8194.

[70] M. Lísa, H. Velínská, M. Holčapek, Regioisomeric characterization of triacylglycerols using silver-ion HPLC/MS and randomization synthesis of standards, Anal. Chem. 81 (2009) 3903-3910.

[71] F. Santinelli, P. Damiani, W.W. Christie, The triacylglycerol structure of olive oil determined by silver ion high-performance liquid chromatography in combination with stereospecific analysis, J. Am. Oil Chem. Soc. 69 (1992) 552-556.

[72] T.L. Chester, Capillary supercritical-fluid chromatography with flame-ionization detection: reduction of detection artifacts and extension of detectable molecular weight range, J. Chromatogr. A 299 (1984) 424-431.

[73] P. Sandra, A. Medvedovici, Y. Zhao, F. David, Characterization of triglycerides in vegetable oils by silver-ion packed-column supercritical fluid chromatography coupled to mass spectroscopy with atmospheric pressure chemical ionization and coordination ion spray, J. Chromatogr. A 974 (2002) 231-241.

[74] J.W. Lee, T. Uchikata, A. Matsubara, T. Nakamura, E. Fukusaki, T. Bamba, Application of supercritical fluid chromatography/mass spectrometry to lipid profiling of soybean, J. Biosci. Bioeng. 113 (2012) 262-268.

[75] J.W. Lee, T. Nagai, N. Gotoh, E. Fukusaki, T. Bamba, Profiling of regioisomeric triacylglycerols in edible oils by supercritical fluid chromatography/tandem mass spectrometry, J. Chromatogr. B: Anal. Technol. Biomed. Life Sci. 966 (2014) 193-199.

[76] J.F. Cavalli, X. Fernandez, L. Lizzani-Cuvelier, A.M. Loiseau, Comparison of static headspace, headspace solid phase microextraction, headspace sorptive extraction, and direct thermal desorption techniques on chemical composition of French olive oils, J. Agric. Food Chem. 51 (2003) 7709-7716.

[77] A.M. Giuffrè, M. Capocasale, R. Macrì, M. Caracciolo, C. Zappia, M. Poiana, Volatile profiles of extra virgin olive oil, olive pomace oil, soybean oil and palm oil in different heating conditions, LWT--Food Sci. Technol. 117 (2020) 108631.

[78] D. Tura, P.D. Prenzler, D.R. Bedgood Jr, M. Antolovich, K. Robards, Varietal and processing effects on the volatile profile of Australian olive oils, Food Chem. 84 (2004) 341-349.

[79] I. Kosma, A. Badeka, K. Vatavali, S. Kontakos, M. Kontominas, Differentiation of Greek extra virgin olive oils according to cultivar based on volatile compound analysis and fatty acid composition, Eur. J. Lipid Sci. Technol. 118 (2016) 849-861.

[80] E. Pouliarekou, A. Badeka, M. Tasioula-Margari, S. Kontakos, F. Longobardi, M.G. Kontominas, Characterization and classification of Western Greek olive oils according to cultivar and geographical origin based on volatile compounds, J. Chromatogr. A 1218 (2011) 7534-7542.

[81] Q. Zhou, S. Liu, Y. Liu, H. Song, Comparative analysis of volatiles of 15 brands of extra-virgin olive oils using solid-phase micro-extraction and solvent-assisted flavor evaporation, Molecules 24 (2019) 1512.

[82] M. Sarolic, M. Gugic, C.I.G. Tuberoso, I. Jerkovic, M. Suste, Z. Marijanovic, P.M. Kus, Volatile profile, phytochemicals and antioxidant activity of virgin olive oils from croatian autochthonous varieties masnjaca and krvavica in comparison with italian variety leccino, Molecules 19 (2014) 881-895.

[83] L. Cecchi, M. Migliorini, E. Giambanelli, A. Rossetti, A. Cane, F. Melani, N. Mulinacci, Headspace solid-phase microextraction-gas chromatography-mass spectrometry quantification of the volatile profile of more than 1200 virgin olive oils for supporting the panel test in their classification: comparison of different chemometric approaches, J. Agric. Food Chem. 67 (2019) 9112-9120.

[84] F. Magagna, L. Valverde-Som, C. Ruíz-Samblás, L. Cuadros-Rodríguez, S.E. Reichenbach, C. Bicchi, C. Cordero, Combined untargeted and targeted fingerprinting with comprehensive two-dimensional chromatography for volatiles and ripening indicators in olive oil, Anal. Chim. Acta 936 (2016) 245-258.

[85] O. Baccouri, A. Bendini, L. Cerretani, M. Guerfel, B. Baccouri, G. Lercker, M. Zarrouk, D. Daoud Ben Miled, Comparative study on volatile compounds from Tunisian and Sicilian monovarietal virgin olive oils, Food Chem. 111 (2008) 322-328.

[86] Z. Zhang, J. Pawliszyn, Headspace solid-phase microextraction, Anal. Chem. 65 (1993) 1843-1852.

[87] S.-T. Chin, P.J. Marriott, Multidimensional gas chromatography beyond simple volatiles separation, Chem. Commun. 50 (2014) 8819-8833.

[88] P.J. Marriott, S.-T. Chin, B. Maikhunthod, H.-G. Schmarr, S. Bieri, Multidimensional gas chromatography, TrAC, Trends Anal. Chem. 34 (2012) 1-21.

[89] M. Herrero, E. Ibáñez, A. Cifuentes, J. Bernal, Multidimensional chromatography in food analysis, J. Chromatogr. A 1216 (2009) 7110-7129.

[90] D.R. Deans, A new technique for heart cutting in gas chromatography, Chromatographia 1 (1968) 18-22.

[91] B.M. Gordon, C.E. Rix, M.F. Borgerding, Comparison of state-of-the-art column switching techniques in high resolution gas chromatography, J. Chromatogr. Sci. 23 (1985) 1-10.

[92] D.R. Deans, I. Scott, Gas chromatographic columns with adjustable separation characteristics, Anal. Chem. 45 (1973) 1137-1141.

[93] K.A. Goode, In-situ fractionation-A simple technique for analysis complex mixtures using a routine-gas chromatograph, Chromatographia 10 (1977) 521-528.

[94] K.A. Krock, C.L. Wilkins, Recent advances in multidimensional gas chromatography, TrAC, Trends Anal. Chem. 13 (1994) 13-17.

[95] K.A. Krock, C.L. Wilkins, Quantitative aspects of a valve-based, multi-stage multidimensional gas chromatography-infrared spectroscopy-mass spectrometry system, J. Chromatogr. A 678 (1994) 265-277.

[96] K.A. Krock, C.L. Wilkins, Qualitative analysis of contaminated environmental extracts by multidimensional gas chromatography with infrared and mass spectral detection (MDGC-IR-MS), J. Chromatogr. A 726 (1996) 167-178.

[97] N. Ragunathan, K.A. Krock, C.L. Wilkins, Multidimensional gas chromatography with parallel cryogenic traps, Anal. Chem. 65 (1993) 1012-1016.

[98] P.M. Owens, D.W. Loehle, B.S. Scott, R.S. Gonzalez, Parallel column gas chromatography, J. Microcolumn Sep. 7 (1995) 551-566.

[99] W. Bertsch, Two-dimensional gas chromatography. Concepts, instrumentation, and applications - Part 1: Fundamentals, conventional two-dimensional gas chromatography, selected applications, J. High Resolut. Chromatogr. 22 (1999) 647-665.

[100] G. Schomburg, F. Weeke, F. Müller, M. Oreans, Multidimensional gas chromatography (MDC) in capillary columns using double oven instruments and a newly designed coupling piece for monitoring detection after pre-separation, Chromatographia 16 (1982) 87-91.

[101] J.C. Giddings, Two-dimensional separations: concept and promise, Anal. Chem. 56 (1984) 1258A-1270A.

[102] Z. Liu, J.B. Phillips, Comprehensive two-dimensional gas chromatography using an on-column thermal modulator interface, J. Chromatogr. Sci. 29 (1991) 227-231.

[103] W. Bertsch, Methods in high resolution gas chromatography. Two ‐ dimensional techniques, J. High Resolut. Chromatogr. 1 (1978) 85-90.

[104] J. Dallüge, J. Beens, U.A.T. Brinkman, Comprehensive two-dimensional gas chromatography: A powerful and versatile analytical tool, J. Chromatogr. A 1000 (2003) 69-108.

[105] P.Q. Tranchida, G. Purcaro, P. Dugo, L. Mondello, G. Purcaro, Modulators for comprehensive two-dimensional gas chromatography, TrAC, Trends Anal. Chem. 30 (2011) 1437-1461.

[106] J.B. Phillips, R.B. Gaines, J. Blomberg, F.W.M. Van Der Wielen, J.M. Dimandja, V. Green, J. Granger, D. Patterson, L. Racovalis, H.J. De Geus, J. De Boer, P. Haglund, J. Lipsky, V. Sinha, E.B. Ledford Jr, A robust thermal modulator for comprehensive two-dimensional gas chromatography, J. High Resolut. Chromatogr. 22 (1999) 3-10.

[107] R.M. Kinghorn, P.J. Marriott, P.A. Dawes, Design and implementation of comprehensive gas chromatography with cryogenic modulation, J. High Resolut. Chromatogr. 23 (2000) 245-252.

[108] P.A. Bueno Jr, J.V. Seeley, Flow-switching device for comprehensive two-dimensional gas chromatography, J. Chromatogr. A 1027 (2004) 3-10.

[109] M. Edwards, A. Mostafa, T. Górecki, Modulation in comprehensive two-dimensional gas chromatography: 20 years of innovation, Anal. Bioanal. Chem. 401 (2011) 2335-2349.

[110] M. Pursch, K. Sun, B. Winniford, H. Cortes, A. Weber, T. McCabe, J. Luong, Modulation techniques and applications in comprehensive two-dimensional gas chromatography (GCxGC), Anal. Bioanal. Chem. 373 (2002) 356-367.

[111] G. Semard, M. Adahchour, J. Focant, Chapter 2 Basic instrumentation for GC×GC, In: L. Ramos (Ed.), Comprehensive Analytical Chemistry, Elsevier Science & Technology, UK, 2009, pp. 15-48.

[112] T. Górecki, J. Harynuk, O. Panić, The evolution of comprehensive two-dimensional gas chromatography (GC x GC), J. Sep. Sci. 27 (2004) 359-379.

[113] P.J. Marriott, T. Massil, H. Hügel, Molecular structure retention relationships in comprehensive two-dimensional gas chromatography, J. Sep. Sci. 27 (2004) 1273-1284.

[114] F.J.M. Novaes, C. Kulsing, H.R. Bizzo, F.R. de Aquino Neto, C.M. Rezende, P.J. Marriott, Analysis of underivatised low volatility compounds by comprehensive two-dimensional gas chromatography with a short primary column, J. Chromatogr. A 1536 (2018) 75-81.

[115] H.G. Janssen, S. De Koning, U.A.T. Brinkman, On-line LC-GC and comprehensive two-dimensional LCxGC-ToF MS for the analysis of complex samples, Anal. Bioanal. Chem. 378 (2004) 1944-1947.

[116] H.G. Janssen, W. Boers, H. Steenbergen, R. Horsten, E. Flöter, Comprehensive two-dimensional liquid chromatography X gas chromatography: Evaluation of the applicability for the analysis of edible oils and fats, J. Chromatogr. A 1000 (2003) 385-400.

[117] S. de Koning, H.G. Janssen, M. van Deursen, U.A.T. Brinkman, Automated on-line comprehensive two-dimensional LC x GC and LC x GC - ToF MS: Instrument design and application to edible oil and fat analysis, J. Sep. Sci. 27 (2004) 397-409.

[118] J. Hu, F. Wei, X.Y. Dong, X. Lv, M.L. Jiang, G.M. Li, H. Chen, Characterization and quantification of triacylglycerols in peanut oil by off-line comprehensive two-dimensional liquid chromatography coupled with atmospheric pressure chemical ionization mass spectrometry, J. Sep. Sci. 36 (2013) 288-300.

[119] M. Beccaria, R. Costa, G. Sullini, E. Grasso, F. Cacciola, P. Dugo, L. Mondello, Determination of the triacylglycerol fraction in fish oil by comprehensive liquid chromatography techniques with the support of gas chromatography and mass spectrometry data, Anal. Bioanal. Chem. 407 (2015) 5211-5225.

[120] G. Purcaro, C. Cordero, E. Liberto, C. Bicchi, L.S. Conte, Toward a definition of blueprint of virgin olive oil by comprehensive two-dimensional gas chromatography, J. Chromatogr. A 1334 (2014) 101-111.

[121] L.T. Vaz-Freire, M.D.R.G. da Silva, A.M.C. Freitas, Comprehensive two-dimensional gas chromatography for fingerprint pattern recognition in olive oils produced by two different techniques in Portuguese olive varieties Galega Vulgar, Cobrançosa e Carrasquenha, Anal. Chim. Acta 633 (2009) 263-270.

[122] F. Stilo, E. Liberto, S.E. Reichenbach, Q. Tao, C. Bicchi, C. Cordero, Untargeted and targeted fingerprinting of extra virgin olive oil volatiles by comprehensive two-dimensional

gas chromatography with mass spectrometry: challenges in long-term studies, J. Agric. Food Chem. 67 (2019) 5289-5302.

Chapter 2

Methodology

Contents

The present Chapter describes the methodologies used in the studies included in the thesis. It summarises and gathers together the experimental approaches that were presented in the papers included in each of the separate Chapters (3-6). Note that in some cases more details can be found in the specific Chapter than in this section, however in some instances it expands on the methods that cannot be discussed in full detail in the written publications.

2.1. Samples and reference standards

2.1.1. Samples

In the studies included in the thesis, oil samples were analysed for their FA, TAG and VOC content. One of the oil samples analysed was sapucainha oil (*Carpotroche brasiliensis*), which was obtained from Brazil. The fruits of *Carpotroche brasiliensis* Endl. (Flacourtiaceae) were collected from Serra do Caparaó, Minas Gerais, in 2017 and a voucher sample was deposited at the Herbarium of Museu Nacional/UFRJ under SISGEN registration number A67B2CB. The FA and TAG content of the oil sample was analysed using GC–EIMS.

Extra virgin olive oil (EVOO) was used as a sample to develop a H/C MDGC method for the separation and identification of TAG components. The EVOO samples were obtained from a local supermarket and from Modern Olives (Lara, Victoria, Australia). For the study on differentiation of EVOO varieties based on the analysis of VOCs and FAs, samples were obtained from a commercial Australian producer (Victoria, Australia). The EVOO samples were seven single varieties that includes Hojiblanca, Coratina, Arbequina, Koroneiki, Frantoio, Picual, and Barnea, and three mixed EVOO samples (Medium, Mild and Robust flavours). Samples were obtained from both 2018 and 2019 production. The mixed samples are sold as commercial blends, reproducibly blended year-to-year largely based on sensory evaluation such that signature products are perceived to be equivalent. Oils were sealed in amber bottles during storage and transportation. In-house mixes were prepared from 2019 single variety

EVOO samples to investigate changes of FAs composition upon varying the ratio of EVOO varieties. The mixed variety samples were also evaluated for VOC composition, but since statistical analysis was not able to clearly differentiate these, the in-house mixes were not investigated for VOC. The commercial mixes derive from single EVOO varieties; Medium flavour (Barnea and Picual), Mild flavour (Arbequina and Barnea) and Robust flavour (Barnea, Coratina and Koroneiki). The company prepares these products from single varieties in a ratio unknown to the investigators.

2.1.2. Reference standards

TAG standards of tripalmitin (PPP) and tristearin (SSS) (both from Sigma Chemical Co., USA; and also from Nu-Chek Prep, Inc., Elysian, MN); triolein (OOO) and trilinolein (LLL) (from Nu-Chek Prep, Inc., Elysian, MN); 1,2-palmitin-3-stearin (PPS), 1,2-stearin-3-palmitin (SSP), 1,2-palmitin-3-olein (PPO), 1-2-olein-3-palmitin (OOP), 1,2- linolein-3-palmitin (LLP), 1,2-olein-3-linolein (OOL) and 1,2-olein-3-archidin (OOA) (from Larodan Fine Chemicals AB, Sweden) were used for identification of TAGs in EVOO as well as for demonstrating H/C MDGC−MS method. Where P = palmitic (C16:0), S = stearic (C18:0), O = oleic (C18:1n–9), L = linoleic (C18:2n–6) and A = arachidic (C20:0) FA respectively. The sequences of the letters are used for convenience and do not necessarily indicate the position of the acyl group on the glycerol moiety. For TAGs analysis, glyceryl triheptadecanoate (C17:0/C17:0/C17:0) (Sigma Chemical Co., USA) was used as internal standard (IS) for monitoring retention time shifts and variations in detector response from analysis to analysis. Methyl nonadecanoate (C19:0 FAME, Supelco) and 4-methyl-2-pentanol (TCI, Tokyo, Japan) were used as IS for FAME and VOC analysis respectively. An authentic standard mixture of FAMEs (Supelco 37-component FAMEs mix) was used for identification of EVOO FAMEs through retention time correlation.

2.2. FA derivatisation

Two different approaches of FA acid derivatisation methods to FA methyl ester (FAME) were used. Transesterification with methanolic sodium hydroxide followed by esterification of free FA by boron trifluoride in methanol was used for sapucainha oil sample, whereas transesterification by methanolic potassium hydroxide was used for EVOO samples. Since EVOO are known to contain less amount of free FAs, transesterification is considered sufficient for derivatisation.

2.2.1. Sapucainha oil FA derivatisation

The derivatisation of FA and TAG content of sapucainha oil to FAMEs was made according to a procedure developed by Joseph and Ackman, which has been adapted and used by many researchers [1]. A 0.10 g mass of sapucainha oil was weighed into a test tube followed by addition of 4 mL of 0.5 mol/L of methanolic sodium hydroxide. The test tube was heated in a boiling water bath (100 °C) approximately for 8 min until a transparent solution was obtained. After cooling 3 mL of 12% boron trifluoride in methanol was added and the test tube was heated again in the water bath (100 °C) for 3 min. Then, after cooling 4 mL of saturated NaCl solution was added with agitation followed by addition of 4 mL of hexane and the test tube was vigorously agitated. Then it was left to rest to allow for phase separation. The upper layer of the reaction product (1 μL) was injected into GC–MS using split injection of 10:1.

2.2.2. Extra virgin olive oil FA derivatisation

The derivatisation of EVOO samples to FAME was prepared according to European Union commission regulation (EEC) No 2568/91. 0.10 g of EVOO sample was weighed in a 5 mL screw top vial. Hexane (2 mL) was added and mixed. Methanolic potassium hydroxide (0.2 mL, 2 N) was added, the vial vigorously shaken for about 30 s and left to stratify until the upper

hexane layer become clear; a 400 µL aliquot of this layer was transferred into a GC vial. Internal standard methyl nonadecanoate (C19:0 FAME) IS (100 µL, 10.0 g/L in hexane) was added into the vial prior to injection. After mixing 1 µL of the sample was injected into the GC instrument in split injection of 50:1, with FID detection.

2.3. Head space solid phase microextraction (HS SPME) of VOCs

The HS SPME extraction of VOCs from EVOO varieties was conducted as follows: IS solution was prepared by adding 1 µL of 4-methyl-2-pentanol (TCI, Tokyo, Japan) into each EVOO variety (5.0 g) in a vial, as a diluent for the IS, and vortex mixed. Separate solutions were prepared for each variety of EVOO sample, and also a separate solution for each replicate of the same EVOO sample to serve as a better evaluation of the method reproducibility. A 0.050 g portion of this IS mix was transferred into a 20 mL SPME vial followed by addition of 5.0 g of the same variety of EVOO sample. The vial was crimp sealed and homogenised using vortex mixing. The sample headspace was extracted using a 50/30 µm divinylbenzene/carboxen©/polydimethylsiloxane fibre (Supelco, Bellefonte, PA) at 60 °C for 60 min for equilibrium extraction prior to GC injection. Preparation, extraction and analysis of each sample was performed in triplicate. For retention index (I) calculation, a standard alkane mixture (C7–C22, Sigma-Aldrich) prepared by mixing 7 µL of C7-C8, 15 µL of C9-C12 and 20 µL of C13-C22, (all from 10000 mg/L in hexane stock solutions) was extracted at 60 °C for 5 min using the same SPME fibre. This approach avoided column overloading.

2.4. Instrumentation

2.4.1. Sapucainha oil FAME analysis

For sapucainha oil FAME analysis a PerkinElmer gas chromatographic instrument (Clarus 680) coupled to a model Clarus SQ 8T mass spectrometer was used (PerkinElmer,

Brandon Park, VIC, Australia). The column employed for the analysis was an Elite-5ms (30 m × 0.25 mm internal diameter (I.D.) × 0.25 µm film thickness (d_f), PerkinElmer). The oven temperature (T) was programmed with initial T of 70 °C (2 min hold), increased at 15 °C/min to 190 °C, then increased at 3 °C/min to 301 °C. The GC inlet T was set at 280 °C. Helium was used as carrier gas with 1 mL/min flow. The MS mass scan range was from 40 to 500 *m/z*, with 70 eV ionisation energy.

2.4.2. Extra virgin olive oil FAME analysis

The instrument used for FAME analysis in EVOO was an Agilent 7890A GC (Mulgrave, Australia) equipped with FID and autosampler, and installed with a SUPELCOWAX10 (30 m × 0.20 mm I.D. × 0.20 µm d_f, Supelco) column. The oven T was programmed from 180 ℃ (held 1 min), then ramped at 5 ℃/min to 250 ℃ (held 8 min). Inlet and detector T were both held at 250 ℃ and split injection (50:1) was used. The carrier gas was hydrogen (99.999% purity) at constant flow of 1 mL/min. GC–MS analysis (using the instrument described under Section 2.4.3 below) of the FAME was carried out for MS identification purposes. Results were expressed as relative percentage of each FA based on FID area ratio of the FA peak to IS, without considering mass response factor.

2.4.3. Analysis of VOCs in extra virgin olive oil

For VOCs analysis in EVOO an Agilent 7890A GC equipped with an Agilent 7000 MS (Mulgrave, Australia), installed with a DB-5 (30 m × 0.25 mm I.D. × 0.25 µm d_f, Agilent) column was used. Helium (99.999% purity) was used as carrier gas (flow rate 1.2 mL/min). The GC oven was programmed as follows: initial oven T 40 °C (held 3 min), ramped at 5 °C/min to 200 °C, then ramped at 15 °C/min to 250 °C (held 2 min). The GC inlet T was 250 °C. The SPME fibre was inserted into the GC manually and the analysis started immediately, with split injection of 20:1. The MS source and transfer line T were 250 °C. The MS was

operated in full scan mode from 50 to 500 mass units. The same GC–MS method was used for alkane analysis for retention index (*I*) determination.

2.4.4. Analysis of FAs and TAGs in sapucainha oil

For GC separation and MS analysis of free FAs and TAGs in sapucainha oil a Bruker GC (SCION 456 GC) coupled to a triple quadrupole MS (TQD) (Bruker, Preston, VIC, Australia) was used, with an Rtx-65 column (17.5 m × 0.25 mm I.D. × 0.1 µm d_f, Restek) installed. The column was chosen based on its relatively high T limit (370 °C) and its mid-polarity phase that can separate TAGs to a certain degree based on their carbon number and degree of unsaturation. The oven T program started at 60 °C, was increased by 15 °C/min to 315 °C, and then by 1 °C/min to 340 °C (held for 28 min). The GC inlet T was set at 300 °C. The MS was operated in full scan mode from *m/z* 50 to 1000, and after initial testing, 90 eV ionisation energy (IE) and 80 µA filament current were chosen. The IE was optimised by varying the energy from 50 to 130 eV in 20 eV steps, with the energy giving highest molecular ion abundance considered to be the best condition, and applied for further analysis. Other factors were kept constant while varying the IE. For the free FA and TAG analysis, a 0.5%v/v solution of sapucainha oil in hexane was prepared and 1 µL of the solution was injected into the GC–MS in split injection mode (10:1).

2.5. MDGC analysis of TAGs

2.5.1. H/C MDGC analysis of olive oil TAGs

A H/C MDGC method for improved separation of TAGs in olive oil was developed using a gas chromatographic instrument (7890A, Agilent Technologies, Mulgrave, Australia) equipped with dual FID. The GC was also equipped with an Agilent DS which has one inlet and two outlet column channels plus two inlet channels to control the switching flow. Two sets of columns, composed of non-polar/mid-polar columns, with relatively short lengths were

selected for use due to their high T limits (up to 370 °C). The use of columns with relatively short lengths was to elute TAGs at lowest T possible. Column set I: ^{1}D SLB-5ms (15 m × 0.25 mm I.D. × 0.25 µm d_f); ^{2}D Rtx-65 (11.5 m × 0.25 mm I.D × 0.1 µm d_f); restrictor – deactivated fused silica (DFS, 1.75 m × 0.15 mm I.D.). Column set II: ^{1}D HP-5 (10 m × 0.32 mm I.D. × 0.25 µm d_f); ^{2}D Rtx-65 (11 m × 0.25 mm I.D. × 0.1 µm d_f); restrictor – DFS (1.45 m × 0.15 mm I.D.). Column set I was used for investigation of flow rate effects on the chromatographic result and target H/C analysis while column set II was used for comprehensive H/C analysis.

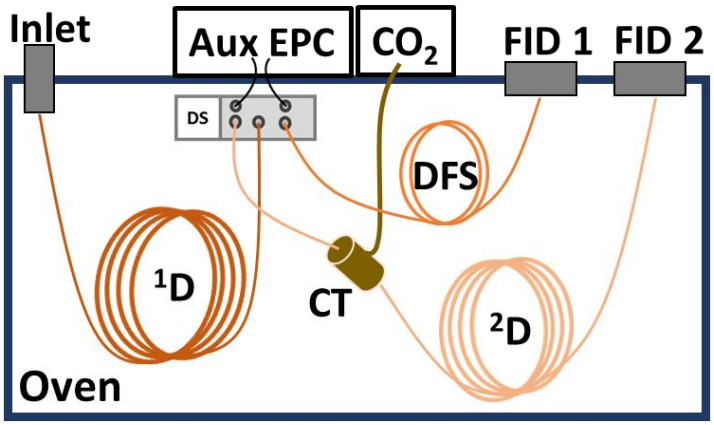

Figure 2.1. Configuration of the H/C MDGC system. AUX EPC: pneumatic auxiliary port with electronic pressure control; DS: Deans switch; ^{1}D: ^{1}D column; ^{2}D: ^{2}D column; CT: cryotrap; CO_2: compressed liquid carbon dioxide supply; FID: flame ionisation detector; DFS: deactivated fused-silica capillary tubing.

For the H/C MDGC experiment the instrument configuration shown in **Figure 2.1.** comprising the following elements was used: (1) ^{1}D column connected between the GC inlet and the DS inlet; (2) ^{2}D column connected between one of the DS outlets and FID 2; and (3) a short restrictor column connected between the other DS outlet and FID 1. The ^{2}D column passes through a cryofocusing trap (CT) near the column inlet (approximately 10-20 cm from the inlet). Liquid CO_2 was provided as an on-demand flow to CT, which expands as a coolant gas to trap TAGs sampled or H/C from the ^{1}D column to the ^{2}D column. CO_2 was supplied to the

CT at least two min prior to the first H/C event, with target regions from ^{1}D effluent selected based on retention times detected at FID 1. The H/C regions of TAGs remain trapped at CT until all TAGs were eluted from the ^{1}D column. The CT CO_2 supply was stopped in order to release TAGs to the ^{2}D column, which can be at the prevailing oven T, or the oven can be cooled before the CO_2 supply is terminated.

The following oven T program was found to be suitable for the H/C MDGC experiment: from different ^{1}D start T (80 °C or 250 °C), the T was ramped up to 340 °C (15 °C/min), held for 25 min until all TAGs elute from the ^{1}D column, and then cooled (at -60 °C/min) to the ^{2}D start T (80 °C or 250 °C), 0.5 min hold for system equilibration. The use of oven starting T of 250 °C was to decrease the total analysis time required without significant compromise in resolution of the TAG components. Heart-cut sampling is conducted at required times. This is referred to as the 1st T program. The trapped components were then released from the CT, and a 2nd T program was applied by ramping up the oven T again to 340 °C (15 °C/min) and then held until the TAGs eluted from the ^{2}D column. The inlet and detector T were set at 300 and 350 °C, respectively.

Constant flow mode was used throughout the experiment in both columns, with two constant flow programs used. The flow for the ^{1}D separation (1st flow program) elutes TAGs from the ^{1}D column during the 1st T program, while the flow for the ^{2}D separation (2nd flow program) provides separation of TAGs on the ^{2}D column during the 2nd T program. Thus, the ^{1}D and ^{2}D column flows in each program are different, with the overall flow for the ^{2}D separation preferably lower than that for ^{1}D. The 1st flow program provided a preliminary separation on the ^{1}D column. The DS flow was balanced in order to avoid carrier flow (and solute leakage) to the ^{2}D column while the DS valve was in the off position; all flow is directed from the ^{1}D column flow to the restrictor (no heart-cutting). The DS flow provides H/C to the ^{2}D column and CT for target regions as required during the 1st T program. The 1st flow program

was changed to the 2nd flow program prior to the release of cryotrapped solutes and commencement of the 2nd T program. The flow was adjusted to provide better separation of TAGs on the ^{2}D column. Different ^{2}D carrier gas flow rates were investigated to choose the final suitable flow rate before conducting olive oil TAGs separation. In summary, the TAG regions were sampled from the ^{1}D column, cryotrapped, the ^{2}D flow adjusted, and then separated on the ^{2}D column using the appropriate ^{2}D T program.

2.5.2. Comprehensive H/C MDGC analysis of olive oil TAGs

In order to reveal the number of TAGs co-eluted in ^{1}D TAG peaks it may require to perform H/C sampling across each target peak to ^{2}D for possible improved separation. This requires a high number of analyses to be carried out to reveal the co-elution in every ^{1}D TAG peaks. To reduce the total analysis time a comprehensive sequential heart cutting method of ^{1}D TAG peaks covering the target TAG region was made using column set II (see Section 2.5.1). The sampling time for each H/C was 6 s. The comprehensive sequential H/C approach was performed in such a way that first the TAG region was divided into three equal regions, and each narrow sampled region was H/C and trapped together in the CT, according to the following. For each region, narrow H/Cs were taken; the first H/C from region 1 was combined with the first H/C of region 2, and likewise for region 3. The combined H/C were then analysed on the ^{2}D column. For the second injection, each H/C was incremented so that the second H/C from region 1, 2 and 3 were collected in the CT, then analysed. This continues until all regions were sampled by the narrow H/C process. This is conducted with the expectation that the early, middle and later sampled zones will not lead to overlap of the components from each region on the ^{2}D column, but with improved resolution for each zone. In each analytical separation, an additional H/C comprising the IS (6 s) was also H/C and cryotrapped at the start of the ^{2}D

column. The purpose of the IS was to correct retention time shifts in the ^{2}D column in the sequential runs.

2.5.3. H/C MDGC−MS analysis of olive oil TAGs

A H/C MDGC−MS method for separation and identification of olive oil TAGs was developed using a gas chromatograph (Agilent Technologies, 7890A) equipped with a mass spectrometry detector (MSD) (Agilent Technologies, 5975C inert XL MSD with Triple-Axis Detector) and FID. The GC was equipped with an Agilent Capillary Flow Technology DS which has similar configuration and function as explained in Section 2.5.1. Also, a similar instrument configuration and H/C MDGC experimental procedure was used, except the use of MS as the ^{2}D detector instead of FID, different ^{2}D column and restrictor column dimensions, and suitable flow programs used in the new configuration. The employed columns for the new configuration were: ^{1}D; SLB-5ms (15 m × 0.25 mm I.D. × 0.25 μm d_f), ^{2}D; Rtx-65 (9 m × 0.25 mm I.D. × 0.1 μm d_f) and restrictor – deactivated fused-silica (DFS, 1.72 m × 0.18 mm I.D.). The flow program used in this experiment is different from the previous procedure due to the difference in column dimensions and the use of MS as the ^{2}D detector. The purpose of this experiment was to develop a similar H/C MDGC method with one described in Section 2.5.1 with the use of MS as the ^{2}D detector for the identification of separated TAG components.

To increase the detectability of minor TAG peaks multiple injections, with repeated sampling to ^{2}D and preconcentration by trapping in the CT, was carried out. This experiment was conducted after noticing a lower detectability of minor TAG peaks in MS detection as compared to FID detection.

2.5.4. Method validation for H/C MDGC−MS analysis of TAGs

Retention times and peak area repeatability using MS on the ^{2}D column were determined using a mixture of six standard TAGs (PPO, OOP, LLP, OOL, OOA and IS; 100 ppm each). The standard mixture was injected five times to determine repeatability. Repeatability was determined in two different ways: (1) by 'heart-cutting' fractions of the peaks in 6 s H/C windows, and recording their ^{2}D retention times and peak areas, and (2) by 'heart-cutting' the whole peak of the TAGs from ^{1}D to ^{2}D and again recording ^{2}D retentions and peak areas. The repeatability for both retention times and area ratios (peak area of standard TAG/peak area of IS) were reported as relative standard deviations of the repeated injections.

The LOD of standard TAGs using MS on the ^{2}D was determined through sampling of the whole peak regions from ^{1}D to ^{2}D. Five standard TAGs (PPO, OOP, LLP, OOL and OOA) were used to demonstrate the method. The LOD was determined based on the graphical method, where the standard TAGs were analysed at three levels of concentrations (25, 50 and 100 mg/L) with six repeat measurements for each level. The injections were made with split ratio of 10:1. The standard deviation for repeat measurements and LOD were calculated based on linear dependence that correlates the calculated standard deviations and respective concentrations ($SD = f(C)$ and $LOD = 3 \cdot SD_o$) [2].

2.6. Data processing and analysis

2.6.1. FAMEs and TAGs identification

The identification of sapucainha oil FAMEs was made based on NIST database library and mass spectrum information; note that sapucainha oil mainly contain cyclic FAs for which standards are not readily available. However, the identification of FAMEs derived from EVOO was made by retention time correlation with an authentic standard mixture (Supelco 37-

component FAMEs mix) and using NIST database library and mass spectrum information. Identification of possible TAGs in sapucainha oil was manually performed. Identification of co-eluting TAG within a peak cluster was made by searching regions of the peak for mass spectra which contained higher signal of the molecular ion ($M^{+\bullet}$) of the TAG of interest with minimum interference from signals of other TAG. Identification was based on characteristic fragment ions formed by EI ionisation of the TAG component. The fragment ions used for identification of the TAG molecules were $[M–RCO_2]^+$, $[RCO+128]^+$ and $[RCO+74]^+$ corresponding to the fatty acyl residues on glycerol, and RCO^+ fatty acyl residue, where R = the aliphatic hydrocarbon chain. Identification of TAG components in EVOO analysis was made based on interpretation of characteristic fragment ions listed above, and comparison of second dimension retention time (^2t_R) and mass spectra of the peaks of interest with standard TAG analysis.

2.6.2. Differentiation of extra virgin olive oil varieties

For differentiation of EVOO varieties and mixed EVOO samples based on the analysis of VOCs and FAs composition, data analysis was performed using principal component analysis (PCA). PCA results were calculated using Minitab 16 (Minitab Inc.). Data for PCA were peak area ratios of the compound *vs* the IS. Scores and loadings plots of the first two components were reported. Since an aliquot of the oil was taken and directly processed for FA composition, these data correspond to the quantitative composition of FA in the EVOO.

For VOCs analysis average values of analyte amount from triplicate sample preparations were calculated *vs* the IS response area for the total ion chromatogram peak, and relative abundance results or normalised data with respect to the internal standard were reported. Since SPME sampling was used, these values do not directly reflect the composition of VOC compounds in the oils, nor account for factors such as equilibrium extraction

differences between compounds and the fibres. The values essentially only reflect the analyte composition as sorbed on the fibre, and may only be a qualitative measure of the VOCs in the EVOO head space at the given SPME extraction conditions using the specified fibre. Establishing equilibrium between EVOO and vial headspace, and then between headspace and SPME fibre can vary substantially between chemical classes, and homologues within chemical classes, plus for different fibre compositions. Some literature studies report concentrations of VOCs expressed as mg/kg of EVOO relative to IS assuming a 'response factor' equal to 1 [3-5]. Since the relative magnitude of the response may vary significantly (and sometimes, very significantly) for different VOCs due to SPME sampling parameters resulting from the aforementioned factors, it is appropriate to base interpretation on relative abundance values for reproducibly prepared samples. In the absence of data for individually calibrated compounds, the study included in the thesis reported area ratios for analytes *vs* the IS. This is expected to allow valid comparison of sample-to-sample relative amounts.

2.7. References

[1] C.A. Ballus, A.D. Meinhart, F.A. de Souza Campos Jr, L.F.d.O. da Silva, A.F. de Oliveira, H.T. Godoy, A quantitative study on the phenolic compound, tocopherol and fatty acid contents of monovarietal virgin olive oils produced in the southeast region of Brazil, Food Res. Int. 62 (2014) 74-83.

[2] P. Konieczka, J. Namieśnik, Method validation, in: C.H. Lochmüller (Ed.), Quality assurance and quality control in the analytical chemical laboratory: a practical approach, CRC Press Taylor & Francis Group, Boca Raton, London, New York, 2009, p. 131.

[3] I. Lukić, S. Carlin, I. Horvat, U. Vrhovsek, Combined targeted and untargeted profiling of volatile aroma compounds with comprehensive two-dimensional gas chromatography for differentiation of virgin olive oils according to variety and geographical origin, Food Chem. 270 (2019) 403-414.

[4] Q. Zhou, S. Liu, Y. Liu, H. Song, Comparative analysis of volatiles of 15 brands of extra-virgin olive oils using solid-phase micro-extraction and solvent-assisted flavor evaporation, Molecules 24 (2019) 1512.

[5] I. Kosma, A. Badeka, K. Vatavali, S. Kontakos, M. Kontominas, Differentiation of Greek extra virgin olive oils according to cultivar based on volatile compound analysis and fatty acid composition, Eur. J. Lipid Sci. Technol. 118 (2016) 849-861.

Chapter 3

Gas chromatography–mass spectrometry of sapucainha oil (*Carpotroche brasiliensis*) triacylglycerols comprising straight chain and cyclic fatty acids

Habtewold D. Waktola[1], Chadin Kulsing[1,2], Yada Nolvachai[1], Claudia M. Rezende[3], Humberto R. Bizzo[4], Philip J. Marriott[1]

[1] Australian Centre for Research on Separation Science, School of Chemistry, Monash University, Wellington Road, Clayton, VIC 3800, Australia

[2] Chromatographic Separation and Flavor Chemistry Research Unit and Centre of Molecular Sensory Science, Department of Chemistry, Faculty of Science, Chulalongkorn University, Pathumwan, Bangkok 10330, Thailand

[3] Instituto de Química, Universidade Federal do Rio de Janeiro, Avenida Athos da Silveira Ramos, Rio de Janeiro, RJ 21941-895, Brazil

[4] Embrapa Agroindústria de Alimentos, Avenida das Américas, Rio de Janeiro, RJ 23020-470, Brazil

Published in Analytical and Bioanalytical Chemistry (2019) 411:1479–1489. doi.org/10.1007/s00216-019-01579-7

Contents

3.1. Chapter overview

This chapter details GC−MS of sapucainha oil (*Carpotroche brasiliensis*) TAGs. Sapucainha oil, which may be used to treat leprosy, comprises straight chain and interestingly has a reasonably high proportion of cyclic FAs, and TAGs. TAGs are often analysed using HTGC where separation is based on their CN and degree of unsaturation on mid-polar and polar columns. TAGs with the same CN and similar degree of unsaturation often co-elute and therefore achieving adequate separation is challenging. Peak identification may be based on use of standard TAG elution data, or interpretation of their mass spectra, using GC–MS. In many cases, both standard TAG and mass spectrum library information are not readily available, which is the case of sapucainha oil TAGs. In these instances, identification can be performed based on diagnostic fragment ions in the mass spectrum, generated through loss of, or from, fatty acid residue(s) comprising the TAG molecules.

The FA and TAG content of the sapucainha oil was analysed using GC–electron ionisation (EI)MS. Prior to the TAGs identification, and in order to maximise the ion information arising from MS stage, the effect of ionisation energy (IE; 50, 70, 90, 110 and 130 eV) on molecular ion abundance was studied and 90 eV was considered the best ionisation condition for mass fingerprinting of the TAG. However, different literatures reported the use of lower energy (<70 eV) and lower source temperature generate mass spectra with a higher relative abundance of ions at higher *m/z* values during the analysis of variety of different molecules such as alkanes, FAMEs, vitamin E, squalene, linear alcohol and pesticides [1-3]. Unlike for lower mass compounds commonly there were no studies that compares different ionisation energy used to analyse higher mass molecules including sapucainha oil TAGs.

FA analysis was performed after derivatisation to FAME using methanolic sodium hydroxide and boron trifluoride in methanol. For free FA and TAG analysis, the oil sample was dissolved in hexane and injected into a short, high-temperature column of Rtx-65 (17.5 m

× 0.25 mm I.D. × 0.1 μm d_f; a 35% dimethyl, 65% diphenyl polysiloxane phase), for GC–MS analysis. Free FA and FAME were tentatively identified based on mass spectrum information of their molecular and fragment ions, as well as library matching. Overlapping TAG peaks were deconvoluted based on mass fingerprint data. The FA composition was utilised to predict possible TAG identities. FA residues of TAG were identified based on characteristic fragment ions, such as $[M–RCO_2]^+$, $[RCO+128]^+$, $[RCO+74]^+$ and RCO^+ where R is the aliphatic hydrocarbon chain.

FAME analysis showed that the cyclic FA hydnocarpic (36.1%), chaulmoogric (26.5%) and gorlic (23.6%) acids were the major components. The cyclic FAs have a terminal cyclopentenyl ring in their structure (see Section 3.3 Supporting information). In addition, straight chain FA such as palmitic, palmitoleic, stearic, oleic and linoleic acids were detected. Palmitic, oleic, hydnocarpic, chaulmoogric and gorlic acids were also detected as free FA in the oil sample. Palmitoleic and linoleic acids were not reported before. Six groups of TAG peaks were eluted from GC at temperatures ≥330 °C. After deconvolution and mass spectrum analysis, each TAG peak group was revealed to comprise 2 to 5 co-eluted TAG molecules; >18 TAG were identified. These TAG consisted of a mix of both cyclic and straight chain FA, but were mostly derived from cyclic FA.

The absence of both authentic standards and MS spectrum library data for TAG derived from cyclopentenyl FA, and overlapped spectra confounded the identification. Nevertheless, a first account of identification of TAG derived from cyclopentenyl FA and derived from mixed cyclopentenyl and straight chain FA was conducted. Resolution of overlapped TAGs in GC analysis of oil samples may be improved through application of higher dimensionality. Thus, the subsequent study outlined in Chapter 4 is dedicated for multidimensional GC for improved separation of TAGs in olive oil.

3.2. Article

Analytical and Bioanalytical Chemistry (2019) 411:1479–1489
https://doi.org/10.1007/s00216-019-01579-7

RESEARCH PAPER

Gas chromatography–mass spectrometry of sapucainha oil (*Carpotroche brasiliensis*) triacylglycerols comprising straight chain and cyclic fatty acids

Habtewold D. Waktola[1] · Chadin Kulsing[1,2] · Yada Nolvachai[1] · Claudia M. Rezende[3] · Humberto R. Bizzo[4] · Philip J. Marriott[1]

Received: 11 October 2018 / Revised: 16 December 2018 / Accepted: 4 January 2019 / Published online: 22 January 2019

Abstract
Sapucainha oil, which may be used to treat leprosy, comprises straight chain and cyclic fatty acids (FA), and triacylglycerols (TAG). The FA and TAG content of the oil sample was analysed using gas chromatography–electron ionisation mass spectrometry (GC–EIMS). FA analysis was performed after derivatisation to fatty acid methyl esters (FAME). For free FA and TAG analysis, the oil sample was dissolved in hexane and injected into a short, high-temperature column, for GC with MS analysis. Free FA and FAME were tentatively identified based on mass spectrum information of their molecular and fragment ions, as well as library matching. Overlapping TAG peaks were deconvoluted based on mass fingerprint data. The FA composition was utilised to predict possible TAG identities. FA residues of TAG were identified based on characteristic fragment ions, such as $[M–RCO_2]^+$, $[RCO+128]^+$, $[RCO+74]^+$ and RCO^+ where R is the aliphatic hydrocarbon chain. FAME analysis showed that the cyclic FA hydnocarpic (36.1%), chaulmoogric (26.5%) and gorlic (23.6%) acids were the major components. In addition, straight chain FA such as palmitic, palmitoleic, stearic, oleic and linoleic acids were detected. Palmitic, oleic, hydnocarpic, chaulmoogric and gorlic acids were also detected as free FA in the oil sample. Six groups of TAG peaks were eluted from GC at temperatures ≥330 °C. After deconvolution and mass spectrum analysis, each TAG peak group was revealed to comprise 2 to 5 co-eluted TAG molecules; >18 TAG were identified. These TAG consisted of a mix of both cyclic and straight chain FA, but were mostly derived from cyclic FA.

Keywords Sapucainha oil · Triacylglycerols · Cyclic fatty acids · High-temperature GC · Mass spectrometry

Electronic supplementary material The online version of this article (https://doi.org/10.1007/s00216-019-01579-7) contains supplementary material, which is available to authorized users.

✉ Philip J. Marriott
philip.marriott@monash.edu

[1] Australian Centre for Research on Separation Science, School of Chemistry, Monash University, Wellington Road, Clayton, VIC 3800, Australia

[2] Chromatographic Separation and Flavor Chemistry Research Unit and Center of Molecular Sensory Science, Department of Chemistry, Faculty of Science, Chulalongkorn University, Pathumwan, Bangkok 10330, Thailand

[3] Instituto de Química, Universidade Federal do Rio de Janeiro, Avenida Athos da Silveira Ramos, Rio de Janeiro, RJ 21941-895, Brazil

[4] Embrapa Agroindústria de Alimentos, Avenida das Américas, Rio de Janeiro, RJ 23020-470, Brazil

Introduction

Cyclic fatty acids (FA) occur in plants, especially in certain seed oils, and microorganisms. They belong to two families. The first family includes cyclopentenyl FA and the second family includes the cyclopropene and cyclopropane FA. The major cyclopentenyl FA are gorlic (C18:2cyc), chaulmoogric (C18:1cyc) and hydnocarpic (C16:1cyc) acids. They are found in seed oils of *Hydnocarpus* species and other genera of the Flacourtiaceae family [1]. One example is sapucainha (*Carpotroche brasiliensis* Endl.) oil which was used for the treatment of leprosy before the development of sulpha drugs. Cole and Cardoso [2] reported that sapucainha oil also contained straight chain FA such as palmitic and oleic acids. The seed oil of a closely related plant species of the same family was also reported to contain myristic (C14:0) and linoleic acids (C18:2) [3]. Analysis of FA by these authors was performed using crystallisation, fractional distillation,

paper chromatography as well as other chemical and physical characterisation methods. A gas chromatography–mass spectrometry (GC–MS) study of sapucainha oil acid fraction by Oliveira et al. [4] showed the presence of FA ranging from C_{12} to C_{20} and many more unidentified components.

The triacylglycerol (TAG) composition of chaulmoogra oils, obtained from seeds of plant species belonging to the family Flacourtiaceae, was reported by Shukla and Spener [5]; HPLC was used to separate the TAG peaks, with collection, derivatisation and further analysis by GC for elucidation according to their corresponding methyl esters. Although the study estimated and reported the presence of TAG that consisted of cyclic and straight chain FA, the effective analysis of TAG derived from cyclic FA remains a challenge.

TAG from different oil sources are often analysed using high temperature GC (HTGC) [6], where they usually separate based on their carbon number (CN) and degree of unsaturation on mid-polar and polar columns. Separation of TAG with the same CN and similar degree of unsaturation is incomplete since they often co-elute, and may require improved separation such as multidimensional GC (MDGC). Recent studies have shown improvement in separation of co-eluted TAG through the application of GC×GC [7] and 'heart-cut' MDGC [8] for coffee and olive oils respectively.

Peak identification may be based on use of standard TAG elution data, or interpretation of their mass spectra, using GC–MS. In many cases, both standard TAG and mass spectrum library information are not readily available. In these instances, identification can be performed based on diagnostic fragment ions in the mass spectrum, generated through loss of, or from, fatty acid residue(s) comprising the TAG molecules [9]. GC–MS with electron ionisation (EI) of TAG allows structural elucidation by analysing molecular and fragment ions produced by using 70 eV standard ionisation energy. Useful fragment ions for characterising molecular species of TAG include $[M–18]^+$, $[M–RCO_2]^+$, $[M–RCO_2H]^+$, $[M–RCO_2CH_2]^+$, $[RCO+128]^+$, $[RCO+74]^+$ and RCO^+, where R is the aliphatic hydrocarbon chain [10]. $[M–RCO_2]^+$ and RCO^+ were reported as the most abundant ions used for identification of TAG [11, 12]. However, relatively low abundance $M^{+\bullet}$ and $[M–18]^+$ ions is a drawback in analysis of EIMS, and hinders direct determination of molecular masses of the TAG from MS data [11].

In this study, GC–MS was applied to analysis of the straight chain and cyclic FA content of sapucainha oil after derivatisation to FAME. Further analysis of underivatised samples was conducted to identify free FA and TAG components based on mass spectrum information of their molecular and fragment ions. Effects of ionisation energy on abundance of molecular ions of TAG compounds were also investigated, and suitable conditions were selected for analysis of the underivatised samples. TAG profiles were correlated with the FAME profiles to deduce suspected FA residues in TAG.

Materials and methods

Instrumentation

FAME analysis

A PerkinElmer gas chromatographic instrument (Clarus 680) coupled to a model Clarus SQ 8T mass spectrometer was used (PerkinElmer, Brandon Park, VIC, Australia). The column employed for the analysis was an Elite-5MS (30 m × 0.25 mm internal diameter (I.D.) × 0.25 μm film thickness (d_f)). The oven temperature was programmed with initial setting of 70 °C (2 min hold), increased at 15 °C/min to 190 °C, then increased at 3 °C/min to 301 °C. The GC inlet temperature was set at 280 °C. Helium was used as carrier gas with 1 mL/min flow. The MS scan range was from 40 to 500 *m/z*, with 70 eV ionisation energy.

FA and TAG analysis

A Bruker GC (SCION 456 GC) coupled to a triple quadrupole MS (TQD) (Bruker, Preston, VIC, Australia) was used to directly analyse the sapucainha oil sample. An Rtx-65 column (Restek, Bellefonte, PA; 17.5 m × 0.25 mm I.D. × 0.1 μm d_f; a 35% dimethyl, 65% diphenyl polysiloxane phase) was installed for GC separation and MS analysis of FA and TAG. The oven temperature program started at 60 °C, was increased by 15 °C/min to 315 °C, and then by 1 °C/min to 340 °C (held for 28 min). The GC inlet temperature was set at 300 °C. The MS was operated in full scan mode from *m/z* 50 to 1000, and after initial testing, 90 eV ionisation energy (IE) and 80 μA filament current were chosen. The IE was optimised by varying the energy from 50 to 130 eV in 20 eV steps, with the energy giving highest molecular ion abundance considered to be the best condition, and applied for further analysis. Other factors were kept constant while varying the IE.

Samples

Sapucainha oil was obtained from Brazil. The fruits of *Carpotroche brasiliensis* Endl. (Flacourtiaceae) were collected from Serra do Caparaó, Minas Gerais, in 2017 and a voucher sample was deposited at the Herbarium of Museu Nacional/UFRJ under SISGEN registration number A67B2CB. Derivatisation of FA and TAG to FAME was made according to a procedure developed by Joseph and Ackman, which has been adapted and used by many researchers [13].

Transesterification with methanolic sodium hydroxide was followed by esterification of free FA by boron trifluoride in methanol. This reaction product (1 μL) was injected into GC–MS using a 10:1 split injection. For free FA and TAG analysis, a 0.5% *v/v* solution of sapucainha oil in hexane was prepared and 1 μL of the solution was injected into the GC–MS in split injection mode (10:1). Triplicate analyses of FA and TAG were performed under different MS conditions.

Data processing and analysis

The NIST database library was used to identify FAME. Bruker MSWS data review was used to obtain total ion chromatograms (TICs) and mass spectra of the oil sample components. The identification of possible TAG for each peak was manually performed. Identification of co-eluting TAG within a peak cluster was made by searching regions of the peak for mass spectra which contained higher signal of the molecular ion ($M^{+\bullet}$) of the TAG of interest with minimum interference from signals of other TAG.

The following abbreviations were used to represent the respective fatty acids: P, palmitic acid (C16:0); Po, palmitoleic acid (C16:1); H, hydnocarpic acid (C16:1cyc); S, stearic acid (C18:0); O, oleic acid (C18:1); L, linoleic acid (C18:2); C, chaulmoogric (C18:1cyc) acid and G, gorlic acid (C18:2cyc). H, C and G have a terminal cyclopentenyl moiety and thus the suffix 'cyc' is added to their abbreviations. The TAG are represented by a combination of three letters of the fatty acids from which they are derived, e.g. HHH represents a TAG with 3 hydnocarpic chains. The sequences of the letters are used for convenience and are not necessarily related to the position of the acyl group on the glycerol moiety.

The fragment ions used for identification of TAG molecules were $[M–RCO_2]^+$, $[RCO+128]^+$ and $[RCO+74]^+$ corresponding to the fatty acyl residues on glycerol, and RCO^+ fatty acyl residue, where R = the aliphatic hydrocarbon chain. For example, when a TAG molecule formed from the three cyclic FA (C, G and H) such as CGH with molecular mass of 848 g mol^{-1} is fragmented, it results in $[M–RCO_2]^+$ residues of $[CG]^+$, $[GH]^+$ or $[CH]^+$ through the losses of H, C and G acyl moieties, respectively. The $[CG]^+$, $[GH]^+$ and $[CH]^+$ residues correspond to *m/z* 597, *m/z* 569 and *m/z* 571 respectively. The $[RCO+128]^+$ and $[RCO+74]^+$ and RCO^+ residues, formed for instance from H, correspond to *m/z* values of 363, 309 and 235, respectively.

Results and discussion

FAME analysis

Sapucainha oil contains free FA and TAG. The analysis of its total FA content requires esterification of the free FA and transesterification of the FA functionalities comprising the TAG to FAME. The injection of the FAME from the derivatised oil sample resulted in 8 MS identified FA or mixtures of FAME, and some unidentified peaks (Fig. 1). The major FA are cyclic, being H (36.1%), C (26.5%) and G (23.6%) (Table 1). In addition to the 3 cyclic FA, 5 straight chain FA were identified, of which 2 apparently have not been reported before. Cole and Cardoso [2], who separated the sapucainha oil FA after multiple chemical treatments and fractional distillation, reported only five FA with the cyclic FA H (45.0%), C (24.4%) and G (15.4%) in the highest amount. The presence of Po, S and L were not reported. Oliveira et al. [4] reported the presence of more cyclic FA, which includes aleprylic (C12:1cyc), alepric (C14:1cyc), hormelic (C20:1cyc) and oncobic (C20:2cyc) FA. These FA were not detected in this study which might be attributed to the difference in the oil fraction extracted from the plant seed analysed. However, they did not report the presence of Po and L. These two FA and S were detected as minor compounds in this study.

Here, it is important to note the elution order of the FAME (Table 1). For straight chain FAME with the same number of carbons, the increasing order of elution on non-polar columns, such as Elite-5MS used here, is based on their decreasing order of polarity corresponding to fewer double bonds (i.e. saturated FAME elute latest). This trend was also observed among the cyclic FA; G (C18:2cyc) methyl ester eluted before C (C18:1cyc) methyl ester. However, FAME of cyclic FA were eluted after straight chain FA with the same number of carbons. For example, methyl esters of H (C16:1cyc) eluted after both Po (C16:1) and P (C16:0). The same was true for C18 FA methyl esters; both G (C18:2cyc) and C (C18:1cyc) eluted after S (C18:0), which eluted after L (C18:2) and O (C18:1). C18:1 elutes 1.67 min before C18:1cyc. This indicates that the terminal cyclopent-2-enyl moiety plays a role

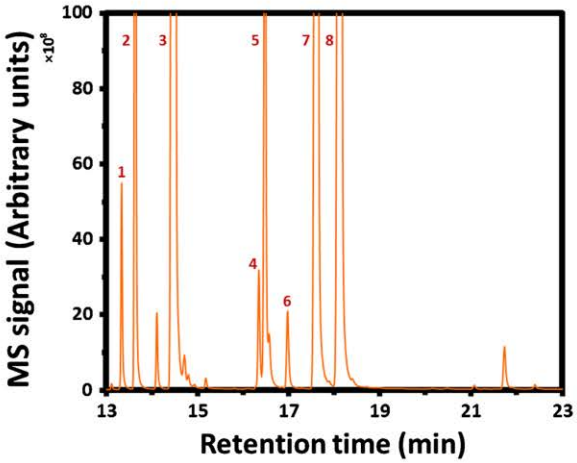

Fig. 1 Chromatograms of FAME of sapucainha oil FA, plus unidentified peaks. Peak numbers correspond to the FAME in Table 1. Major FAME are shown off-scale to better indicate the minor components

Table 1 Cyclic and straight chain FAME identified from transesterified sapucainha oil sample

Peak no.	t_R (min)	FAME	M. F.	Area (%)
1	13.34	Palmitoleic acid (C16:1) methyl ester	$C_{17}H_{32}O_2$	1.10
2	13.64	Palmitic acid (C16:0) methyl ester	$C_{17}H_{34}O_2$	6.32
3	14.50	Hydnocarpic acid (C16:1cyc) methyl ester	$C_{17}H_{30}O_2$	36.09
4	16.34	Linoleic acid (C18:2) methyl ester	$C_{19}H_{34}O_2$	0.71
5	16.48	Oleic acid (C18:1) methyl ester	$C_{19}H_{36}O_2$	4.98
6	16.96	Stearic acid (C18:0) methyl ester	$C_{19}H_{38}O_2$	0.66
7	17.64	Gorlic acid (C18:2cyc) methyl ester	$C_{19}H_{32}O_2$	23.62
8	18.15	Chaulmoogric acid (C18:1cyc) methyl ester	$C_{19}H_{34}O_2$	26.51

t_R retention time, *M. F.* molecular formula

governing their later elution order. This might indicate stronger interaction of the cyclopentenyl moiety with the stationary phase than the methylene chain of the straight chain fatty acids. The cyclic FA structures are presented in Fig. S3, Electronic Supplementary Material (ESM).

Ionisation energy

Analysis of the sapucainha oil sample with GC–MS showed a number of peaks that may correspond to FA, DAG and TAG. Prior to their identification, the effect of ionisation energy (IE; 50, 70, 90, 110 and 130 eV) on molecular ion abundance was studied to select an effective energy for further analysis. The molecular ($M^{+\bullet}$) ions corresponding to some FA (straight chain and cyclic) and TAG molecules were chosen to investigate the effect of IE on their relative abundance. The selected $M^{+\bullet}$ ions obtained for different IE were extracted from the TIC chromatograms and their areas were obtained by integration. For each molecular ion, peak areas from two repeats were averaged. To improve data presentation, the areas were normalised by dividing by the smallest area obtained from the different IE levels for that specific mass, plotted versus eV. Figure 2a shows the effect of IE on $M^{+\bullet}$ abundance of two straight chain FA, P (*m/z* 256) and O (*m/z* 282), and two cyclic FA, H (*m/z* 252) and G (*m/z* 278). Rather than the IE of 70 eV usually used in the MS analysis and for MS library data, the IE of 90 eV resulted in higher relative abundance of $M^{+\bullet}$ of the FA, except for O, which was higher at 70 eV. For P $M^{+\bullet}$ abundance was only slightly higher at 90 eV than at 70 eV compared to the cyclic FA, H and G, where 90 eV gave clearly higher abundance of $M^{+\bullet}$. A similar study was conducted for TAG $M^{+\bullet}$ abundance. TAG with mixed straight chain and cyclic FA residues as well as TAG with different mass (low to high $M^{+\bullet}$) were selected to study the effect of IE on $M^{+\bullet}$ abundance. Similar to the effect on cyclic FA, 90 eV gave the highest abundance of $M^{+\bullet}$ of TAG molecules than all other IE (Fig. 2b). The same effect was observed for TAG derived from mixed FA, derived only from cyclic FA, and TAG with different $M^{+\bullet}$ masses. Since TAG derived entirely from straight chain FA were not detected in the sample, it is not possible to confirm that the effect of IE is due to the cyclic FA residue. Since this study objective was to increase the detection of $M^{+\bullet}$

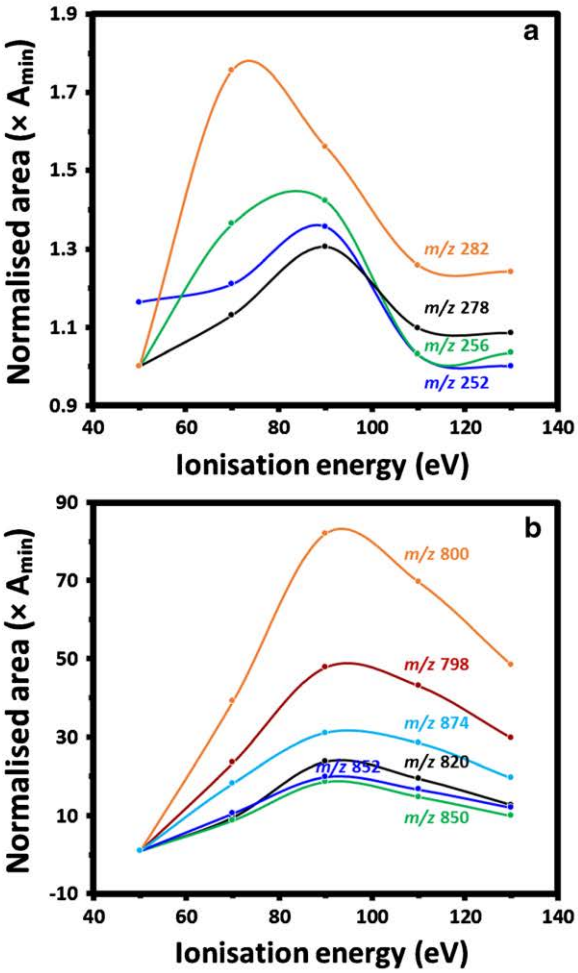

Fig. 2 Plots of molecular ion abundance versus ionisation energy (IE) for **a** free FA, **b** TAG. Where *m/z* 252, *m/z* 256, *m/z* 278 and *m/z* 282 correspond to H, P, G and O respectively, and *m/z* 798, *m/z* 800, *m/z* 820, *m/z* 850, *m/z* 852 and *m/z* 874 correspond to PHH, PPoH, GHH, CCH, OCH and CGG respectively. Mass values are rounded down to unit values for convenience

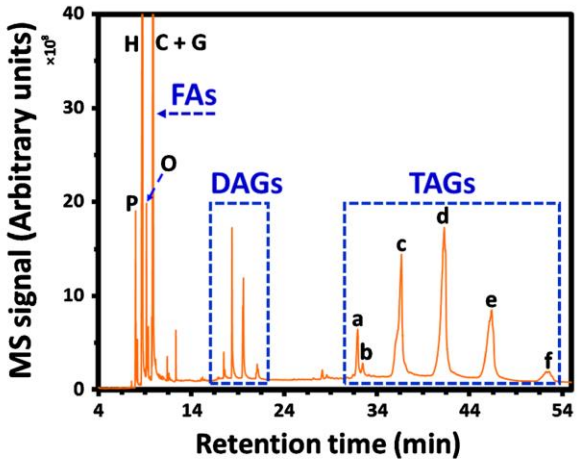

Fig. 3 GC–MS total ion chromatogram of sapucainha oil showing FA (P, H, O, C and G), DAG and TAG components

of the TAG to aid structural elucidation, 90 eV was considered the best ionisation condition for mass fingerprinting of the TAG.

Identification of FA and TAG

The FA and TAG found in the oil sample were separated on the high temperature mid-polarity column (Fig. 3; this is shown as Fig. S1 in ESM). Between the FA and TAG peaks were various unidentified peaks and peaks which may correspond to diacylglycerols (DAG). They were not the focus in this study. For the peaks that may correspond to DAG, it was possible to see fragments that correspond to RCO^+ and $[RCO+74]^+$ which indicated the FA residues present. The fragments correspond to both cyclic and straight chain FA, with that corresponding to the cyclic FA being abundant. However, the $M^{+\bullet}$ which was used to identify the DAG molecular masses and thus confirm the acyl residues present, were not readily detected or clearly identified. Therefore, the subsequent discussions focus only on the identification of FA and TAG.

Identification of free FA

The library matching and MS information of molecular ions and fragment ions of the FA peaks indicated the presence of free FA of P, H, O, C and G. Molecular ion mass and mass fragment ions were used to identify the free FA. Figure 4a shows the mass spectrum of hydnocarpic acid (H). The prominent ions were *m/z* 67, *m/z* 82 and *m/z* 95. The *m/z* 67 base peak is characteristic for cyclopentenyl FA, formed due to cleavage of the terminal cyclopent-2-enyl moiety. The *m/z* 82 ion was formed due to β-cleavage to the ring (*m/z* 81 = $C_5H_7CH_2^+$) with transfer of one hydrogen atom from the chain. These fragment ions were similar to the fragments described for methyl hydnocarpate by Christie *et. al.* [14].

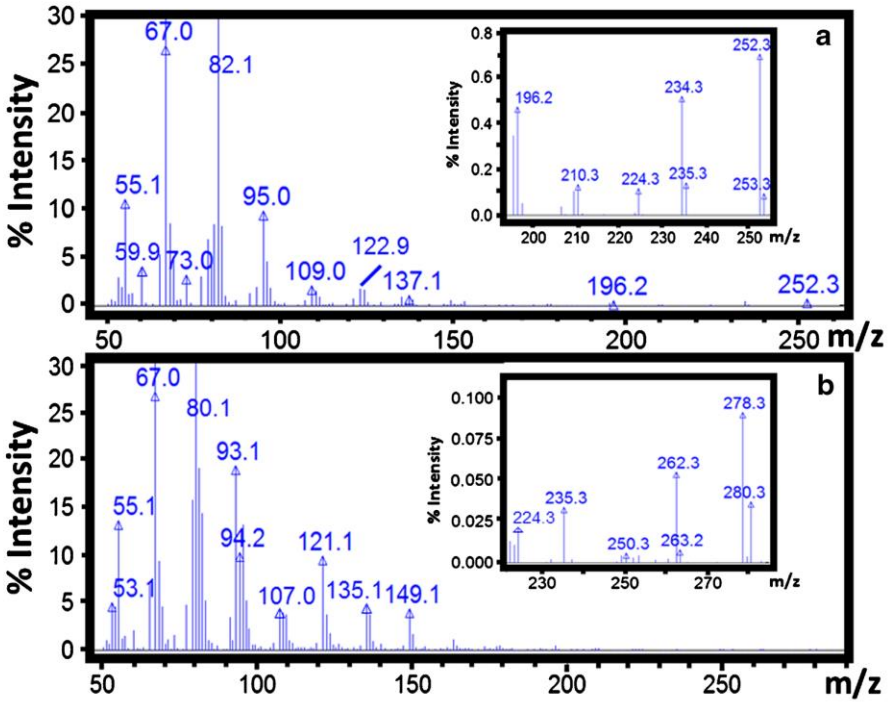

Fig. 4 Mass spectra of **a** hydnocarpic acid ($M^{+\bullet}$ = 252.3) and **b** gorlic acid ($M^{+\bullet}$ = 278.3) detected in sapucainha oil

The structure of the main fragments formed from the cyclic FA and their FAME are shown in Fig. S3 (see ESM). In methyl hydnocarpate spectra, *m/z* 185, formed after cleavage β to the cyclopentene ring, and *m/z* 153 (CH_2 = $CH(CH_2)_7CO^+$), formed from *m/z* 185 after loss of the methoxyl group and possible transfer of a hydrogen atom, were also characteristic peaks. The analogous ion fragment of hydnocarpic acid (*m/z* 171), formed after cleavage β to the cyclopentene ring, was minor. The *m/z* 153, which might be formed from *m/z* 171 after loss of H_2O, was also present but with a low abundance.

The *m/z* 95 ion was formed possibly through cleavage of the alkyl cyclopentenyl group ($C_5H_7(CH_2)_2^+$). Fragment ions which might also be formed in the same manner through cleavage of a series of alkyl cyclopentenyl groups, though detected in lower intensity. These are *m/z* 109, *m/z* 123 and *m/z* 137 formed through cleavage of ($C_5H_7(CH_2)_n^+$), $n = 3$, 4 and 5 respectively, from the hydnocarpic acid. The molecular ion, $M^{+\bullet}$ (*m/z* 252), and other masses such as $[M–18]^+$ (*m/z* 234), $[M–28]^+$ (*m/z* 224), $[M–43]^+$ (*m/z* 209) and $[M–56]^+$ (*m/z* 196) that resulted from cleavage in the aliphatic chain, were also detected. The McLafferty rearrangement ion of *m/z* 60 was also an intense peak.

The other two cyclopentenyl FA (C and G) closely eluted. They were identified by choosing elution times (i.e. away from the overlapped peak maximum) for each component where the interference from the ion masses of the other FA was at minimum. The MS of chaulmoogric acid (Fig. S4, ESM) is very similar to that of hydnocarpic acid.

The MS for gorlic acid (Fig. 4b) was dominated by hydrocarbon fragments compared to hydnocarpic acid. This was in agreement with the methyl gorlate described by Christie et al. [14]. The base peak was *m/z* 67, as for hydnocarpic acid. The other prominent ions detected were *m/z* 80, *m/z* 93, *m/z* 107, *m/z* 121, *m/z* 135 and *m/z* 149. As described by Christie et al., *m/z* 80 was due to formation of dihydrofulvene ion (C_5H_6 = CH_2^+); other ions were due to formation of a series of alkyl dihydrofulvene ions. The possible structures suggested were $C_5H_6 = CH(CH_2)_n^+$ and $C_5H_6 = CH(CH_2)_nH^+$. *m/z* 93, *m/z* 107, *m/z* 121, *m/z* 135 and *m/z* 149 were formed where *n* is equal to 1–4 respectively with possible structures of $C_5H_6 = CH(CH_2)_n^+$. *m/z* 94 and *m/z* 108 were formed when *n* is equal to 1 and 2 respectively with possible structure of $C_5H_6 = CH(CH_2)_nH^+$. *m/z* 163 and *m/z* 178 were also assumed to be formed the same way, and were detected as smaller peaks. The alkyl dihydrofulvene ions such as *m/z* 121, *m/z* 135 and *m/z* 149 were detected also in hydnocarpic acid spectra but in very low intensities. The mechanism by which these fragments were formed was unclear. The $M^{+\bullet}$, $[M–18]^+$, $[M–28]^+$, $[M–43]^+$ and $[M–56]^+$ ions were detected as smaller signals for gorlic acid.

Identification of TAG

Six peaks that correspond to TAG molecules were eluted at higher temperature (Fig. 3, a–f). The TAG possibly comprise 8 different FA residues, as identified in FAME analysis of the whole oil sample, esterified with glycerol. From 8 FA, many possible TAG could arise for any combination of three of these FA with glycerol.

Being derived from C_{16} (P, Po and H) and C_{18} (S, O, L, C and G) FA, the TAG peaks could assume total CNs of 48, 50, 52 and 54, formed from 3 C_{16}, 2 C_{16} and 1 C_{18}, 1 C_{16} and 2 C_{18}, and 3 C_{18} FA, respectively. TAG molecules are known to elute according to increasing order of CN and also the degree of unsaturation within the fatty acyl residues (or their boiling point and polarity) on polar and mid-polarity columns. On the Rtx-65 column employed, it is expected that peak a could correspond to a 48 CN TAG, whereas peak f should correspond to a 54 CN TAG. By inference, peaks b–e could correspond to TAG with 50 or 52 CN. The cyclopentenyl cyclic FA structure should also affect the elution order.

Given the 8 FA detected in the oil sample, the possible combinations of FA that form the TAG would be numerous. But the high abundance of the cyclic FA indicates that the TAG mainly comprise H, G and C. Po, L and S were detected in minor amounts, thus TAG derived from these components are expected to be of minor abundance. This was evident from the detection of *m/z* 67 as the base peak in mass spectra corresponding to the TAG (Fig. S5, ESM), and also with the detection at lower mass of hydrocarbon fragment ions that were similar to ions in the spectrum of the free FA. The ions were alkyl cyclopentenyl groups, dihydrofulvene and alkyl dihydrofulvene, which were described earlier. The peaks corresponded to ions of mass *m/z* 80, 81, 93, 95, 107, 109, 121, 135 and 149 (ESM Fig. S5).

The TAG identification was performed based on their mass fingerprints. The $M^{+\bullet}$ ions detected for the TAG peaks were used to determine the molar mass of the TAG. Two or more molecular ions were therefore detected for TAG peaks that co-eluted. Relative intensities of different $M^{+\bullet}$ over a co-eluted peak differ with retention time, so identification of a specific TAG comprising the peak was made at the retention time where its molecular ion was most abundant. FA residues of the TAG molecule were identified based on characteristic fragment ions, such as $[M–RCO_2]^+$, $[RCO+128]^+$, $[RCO+74]^+$ and RCO^+. $[M–RCO_2]^+$ was formed due to loss of an acyloxy group. For TAG derived from mixed FA residues, an ion corresponding to the loss of each acyloxy group in the molecule was observed, an important ion for structural elucidation. $[RCO+128]^+$ and $[RCO+74]^+$, which are characteristic fragment ions specific to the FA group attached to the glycerol skeleton, were used to determine the FA residue. Additionally, $[RCO]^+$ was also used to confirm each fatty acid present in the TAG molecule. In this study, $[M–RCO]^+$, which was formed

after cleavage of an acyl group, was detected for all possible TAG suggested, and was used as an additional identification fragment ion.

Manual deconvolution was performed for each peak and the result is summarised in Table 2. Figure 5 (which is the same as Fig. S2 in ESM) shows extracted ion chromatograms for the molecular ions that correspond to TAG molecules, numbered and reported as in Table 2. It shows the proposed number of TAG that co-eluted within each broad peak depicted in Fig. 3. Thus each TAG peak in Fig. 3 was suspected to comprise 2–5 co-eluted TAG molecules. From Table 2, 18 possible TAG molecules were proposed (2 could not be ascribed to a TAG). Most of the TAG were derived from the cyclic FA; H, C and G. This result agrees with their abundance described earlier. The H FA contributed to 13 TAG where at least as one of the three FA residues was H; C and G also contributed to a significant number of TAG molecules. A number of TAG were derived from both straight chain and cyclic FA. The only FA not detected as a component of the TAG molecules was S, which was the least abundant (0.66% peak area) FA detected in the FAME result of the whole oil sample.

The detailed deconvolution process of each unresolved TAG peak and the assignment of a possible TAG molecule to the specific molecular ion identified is described below, taking peak e in Fig. 3 as an example. Detailed interpretation and analysis for the rest of the peaks is provided in ESM (Section S1. Identification of TAG), which includes Figs. S6–S10.

In peak e (Fig. 3), four $M^{+\bullet}$ with *m/z* 852.5, *m/z* 850.6, *m/z* 848.6 and *m/z* 846.8 were proposed (Fig. 5). These $M^{+\bullet}$ possibly correspond to TAG with CN = 52 (derived from 1 C_{16} and 2 C_{18} FA). The *m/z* values of $M^{+\bullet}$ of the four TAG showed a 2 mass unit decrease from the highest mass to the lowest mass, suggested to be related to a change in unsaturation. In general, the extracted ion peaks also show an increase in retention times from higher to lower mass (Fig. 5). This is in agreement with the fact that TAG with an increased number of double bonds elute later than TAG with the same CN but fewer double bonds, on mid-polar and polar columns.

The TAG with $M^{+\bullet}$ of *m/z* 850.6, *m/z* 848.6 and *m/z* 846.8 were considered to be TAG derived from combination of the three cyclic FA, gorlic acid G (18:2), chaulmoogric acid C (18:1) and hydnocarpic acid H (16:1) (see peaks 13, 14 and 15, Table 2). This is based on the fragment ions obtained at the retention times used to identify the TAG, as discussed below. The approach to their identification will be discussed first, followed by the identification of TAG with *m/z* 852.5.

The mass spectrum at the retention time of the TAG corresponding to $M^{+\bullet}$ = *m/z* 850.6 is shown in Fig. 6a. The $[M\text{-}RCO_2]^+$ ions with *m/z* 571 and 599, which correspond to $[CH]^+$ and $[CC]^+$ respectively, were detected in high abundance. This is indicative of a TAG comprising CCH. The $[RCO+74]^+$ ions with *m/z* 309 and 337, corresponding to H and C respectively, were very prominent peaks in the mass spectrum in Fig. 6a2. The ions corresponding to $[RCO+28]^+$ for both fatty acids were also abundant, with *m/z* 363 and 391 for H and C respectively. The ions corresponding to RCO^+, with *m/z* 235 and 263 for H and C respectively, were also prominent peaks. Moreover, the $[M–RCO]^+$ ions with *m/z* 615 and 587 were detected after cleavage of the acyl group corresponding H and C respectively. Thus, the fragment ions were all strongly suggestive of the presence of a TAG of CCH.

The TAG corresponding to *m/z* 848.6 is 2 u less than the mass of CCH. It elutes later than the *m/z* 850.6 peak. At its indicated retention time (46.3 min), $[M–RCO_2]^+$ ions detected in abundance were *m/z* 569, 571 and 597 (Fig. 6b1). These fragment ions were due to $[GH]^+$, $[CH]^+$ and $[GC]^+$ respectively, which were possibly derived from the parent molecule GCH. The *m/z* 571 due to $[CH]^+$ was common to both CCH and GCH, and thus appeared in high abundance due to overlap of the two TAG. The $[RCO+74]^+$, $[RCO+128]^+$ and RCO^+ fragment ions that correspond to H, G and C were also detected (Table 2 and Fig. 6b2). Thus, the $M^{+\bullet}$ and the fragment ions strongly suggested that the *m/z* 848.6 ion corresponds to GCH.

For the TAG corresponding to $M^{+\bullet}$ of *m/z* 846.8 (t_R = 46.4 min), the $[M–RCO_2]^+$ ions detected were *m/z* 569 and 595 (Fig. 6c1), which were due to $[GH]^+$ and $[GG]^+$ derived from GGH. The $[RCO+74]^+$, $[RCO+28]^+$ and RCO^+ fragment ions, corresponding to H and G, used for identification were clear in the mass spectrum (Table 2 and Fig. 6c2) showing these two FA are components of the TAG molecule. The $[M–RCO]^+$ ions were also detected, and this indicated *m/z* 846.8 corresponds to GGH.

The other TAG that co-eluted with the above three TAG corresponded to $M^{+\bullet}$ of *m/z* 852.5. Its mass is higher by 2 u than the $M^{+\bullet}$ for CCH (*m/z* 850.6). Thus the TAG with *m/z* 852.5 might have two FA acyl residues in common with CCH, suggesting that the different FA residue will have one less double bond or may be a straight chain FA with the same CN as its analogue FA residue on CCH. Accordingly from the $[RCO+74]^+$ and $[RCO+128]^+$ ions with *m/z* 339 and 393 respectively, this corresponds to detection of O, i.e. C chaulmoogric (C18:1cyc) replaced by O oleic (C18:1), straight chain group. This was indicative of the presence of OCH. The detection of *m/z* 573 and *m/z* 601 corresponding to $[OH]^+$ and $[OC]^+$, respectively, further strengthen the suggestion for the presence of OCH (Table 2 and Fig. 6d1 and d2). Note that the peak for *m/z* 852.5 was less intense (Fig. 5) and its spectrum was dominated by the fragment ions from CCH.

It is also worth noting the elution order of the TAG on the Rtx-65 column. In general, the elution of the TAG followed an increase in carbon number (CN), where groups of TAG with the same CN closely eluted. Within a group of the same CN, there were small differences in their retention times, noted for

Table 2 Molecular ions and fragment ions and their molar mass values for the deconvoluted peaks detected in Fig. 5, with the possible corresponding TAG identifications

Peak no.	$M^{+\bullet}$	t_R (min)	FA residue	$[M-RCO_2]^+$	$[RCO+128]^+$	$[RCO+74]^+$	RCO^+	$[M-RCO]^+$	Possible TAG
1	798.8	31.8	H	547.7	363.4	309.3	235.3	563.2	PHH
			P	543.7	367.5	313.4	239.3	559.6	
2	800.1	31.8	H	549.8	363.4	309.4	235.3	565	PPoH
			Po	547.7	365.3	311.4	237.4	563.6	
			P	545.7	367.4	313.4	239.3	561.6	
3	798	32.4	H	547.6	363.4	309.4	235.3	563.6	PoPoH
			Po	545.6	365.4	311.4	237.3	561.7	
4	796.6	32.4	H	545.6	363.4	309.4	235.3	561.8	PoHH
			Po	543.6	365.6	311.4	237.4	559.6	
5	826.7	36.0	H	575.8	363.4	309.4	235.3	591.2	LPH/CPH
			P	571.7	367.4	313.4	239.3	587.6	
			L	547.6	391.4	337.4	263.3	563.6	
6	828.9	35.9							n.i.
7	794.8	36.5	H	543.6	363.4	309.4	235.3	559.6	HHH
8	824.9	36.5							n.i.
9	824.0	41.2	H	573.7	363.4	309.4	235.3	590	OHH/LPoH
			Po	571.7	365.4	311.4	237.3	587.6	
			L	545.7	391.3	337.4	263.3	561.5	
			O	543.6	393.1	339.4	265.3	559.6	
10	822.7	41.2	H	571.7	363.4	309.4	235.3	587.6	CHH
			C	543.6	391.5	337.4	263.3	559.5	
11	820.7	41.3	H	569.6	363.4	309.4	235.3	585.7	GHH
			G	543.5	389.4	335.4	261.3	559.5	
12	852.3	46.0	H	601.8	363.4	309.3	235.2	617.4	OCH
			C	573.1	391.4	337.4	263.3	589.7	
			O	571.6	393.2	339.4	265.4	587.8	
13	850.6	46.0	H	599.7	363.4	309.4	235.3	615.6	CCH
			C	571.7	391.4	337.4	263.3	587.6	
14	848.6	46.3	H	597.6	363.4	309.4	235.3	613.5	CGH
			G	571.7	389.4	335.4	261.3	588	
			C	569.6	391.4	337.4	263.3	585.6	
15	846.8	46.4	H	595.5	363.4	309.3	235.3	611.5	GGH
			G	569.6	389.4	335.4	261.3	585.6	
16	880.5	51.7	C	601.8	391.3	337.4	263.3	617.4	OCC
			O	599.3	393.2	339.3	265.3	615.2	
17	878.9	51.7	G	601.9	389.2	335.5	261.4	617.2	CCC/OCG
			C	599.8	391.3	337.5	263.4	615.5	
			O	597.7	393.1	339.4	265.4	613.5	
18	876.6	52.1	G	599.8	389.3	335.3	261.3	615	CCG
			C	597.7	391.3	337.4	263.4	613.2	
19	874.5	52.5	G	597.7	389.2	335.4	261.4	613.9	CGG
			C	595.6	391.3	337.4	263.3	611.7	
20	872.6	52.8	G	595.9	389.3	335.4	261.3	610.9	GGG

n.i. not identified, *P* palmitic acid, *Po* palmitoleic acid, *H* hydnocarpic acid, *L* linoleic acid, *C* chaulmoogric acid, *O* oleic acid, *G* gorlic acid

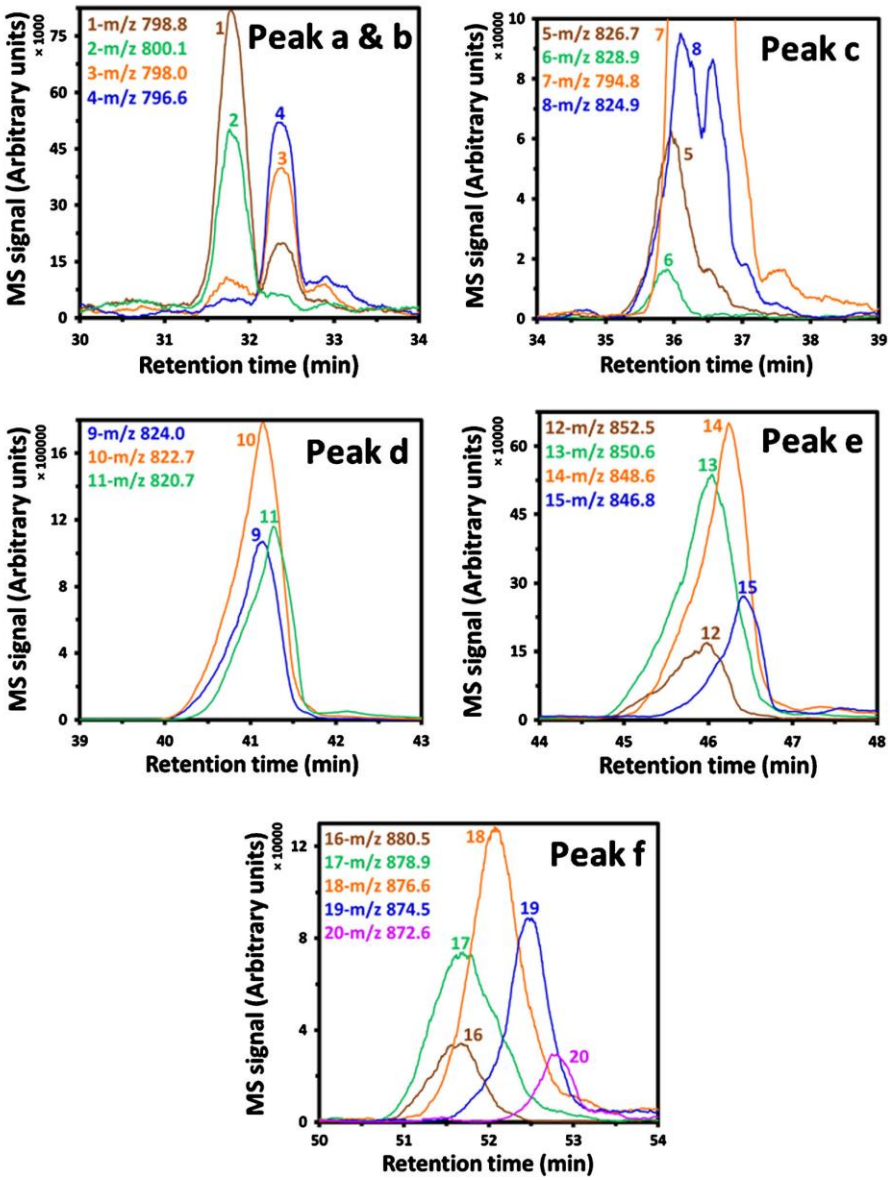

Fig. 5 Extracted ion chromatograms (EIC) of molecular ions of the possible TAG described in Table 2, detected in peaks **a**–**f** in Fig. 3

the molecular ion extracted chromatogram (Fig. 5 and Table 2). This indicates that TAG with the same CN eluted based on their increasing number of total double bonds (DB). Consider for example peak f, where 5 TAG with the same CN closely eluted. The first two TAG (OCC and CCC), having the same total DB, eluted at the same retention time whereas the retention time order of the other three TAG were according to their increasing total DB after the first two TAG.

Elution order of TAG on GC columns depends on carbon number and degree of unsaturation, and has been well investigated. The effect of other structural features on the elution order of TAG, such as branching, cyclic moieties and hydroxyl and epoxy groups, is still unclear. Saturated, unsaturated, straight chain and cyclic FA dominate in sapucainha oil. The TAG elution order depends on the structural nature of the FA residues. In the "FAME analysis" section, it was indicated that the elution time, on a non-polar column, of the methyl ester of cyclic FA, was significantly different from its straight chain analogue. However, the elution behaviour of TAG containing cyclopentenyl FA and straight chain FA with equal number of carbon and DB appeared the same. TAG such as PHH and PPoH, PoPoH and PoHH, and OCH and CCH eluted at the

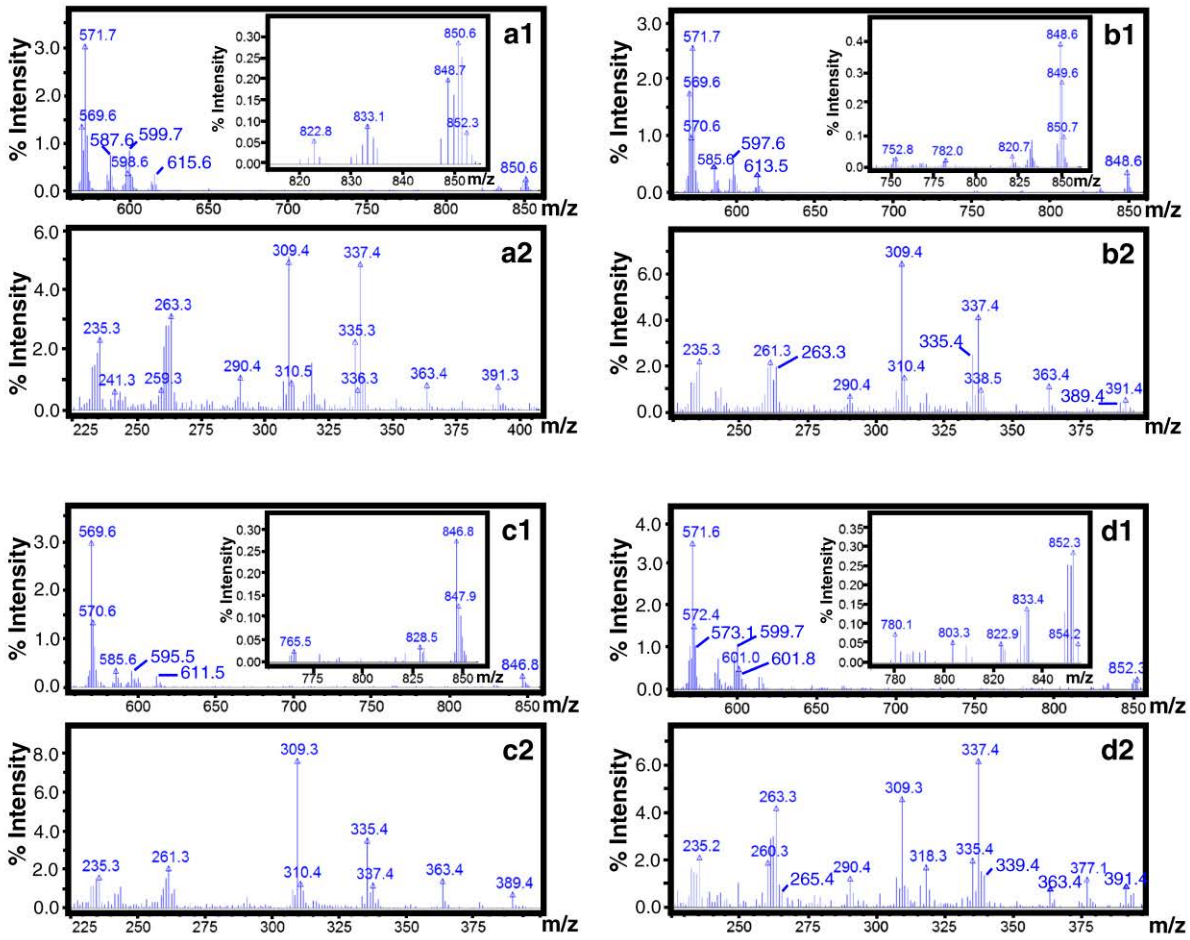

Fig. 6 Mass spectra of TAG identified in peak **e**. Where a, b, c and d correspond to *m/z* 850, *m/z* 848, *m/z* 846 and *m/z* 852 TAG, and 1 refers to the mass range that include $M^{+\bullet}$, $[M–RCO_2]^+$ and $[M–RCO]^+$ ions, and 2 refers to the mass range that include RCO^+, $[RCO+74]^+$ and $[RCO+128]^+$ ions respectively

same retention time (Fig. 5 and Table 2). The only exception to this trend was HHH, which eluted far later than PoPoH. Similar chromatographic behaviour was noted in HPLC analysis of TAG containing cyclopentenyl FA using a reversed-phase column, where HHH was eluted earlier than PHH [5].

Conclusion

The free fatty acid and triacylglycerol composition of sapucainha oil was determined using direct injection into GC–EIMS. The total FA composition was determined after conversion to FAME, which revealed 3 cyclic (H, G and C; with one unsaturated bond in the ring) and 5 straight chain (P, Po, L, O and S; saturated and unsaturated) FA as the higher abundance species. The cyclic FA were the most abundant; 2 of the straight chain FA (Po and L) have not been reported before. The information on FA composition together with MS fingerprinting was used to identify the possible TAG that existed in the oil sample.

Molecular ions ($M^{+\bullet}$) were used to determine the molar masses of the FA and the TAG. The low abundance $M^{+\bullet}$ ion was enhanced in selected FA (straight chain and cyclic) and TAG (containing at least one cyclic FA residue) molecules by investigating different ionisation energies. For the cyclic FA and TAG, a higher ionisation energy of 90 eV resulted in higher abundance $M^{+\bullet}$.

The GC–MS analysis of the oil sample displayed groups of FA, DAG and TAG in increasing retention time. FA components were readily identified by MS library matching. DAG were not identified in this study. TAG components were proposed based on mass fingerprinting. The TAG appeared as six unresolved GC peaks, which were then deconvoluted into individual TAG peaks. Manual deconvolution revealed each

peak to comprise 2 to 5 overlapping TAG molecules, revealing at least 18 TAG molecules. Overlapped TAG peaks were identified based on $M^{+\bullet}$ and characteristic fragment ions, such as $[M–RCO_2]^+$, $[RCO+128]^+$, $[RCO+74]^+$ and RCO^+. Based on these ions the FA residues of specific TAG were determined and the possible TAG suggested. The absence of both authentic standards and MS spectral library data for TAG derived from cyclopentenyl FA, and overlapped spectra confounded the identification. Nevertheless, a first account of identification of TAG derived from cyclopentenyl FA and derived from mixed cyclopentenyl and straight chain FA was conducted. Conducting further study employing higher separation dimensionality with mass spectrometry to obtain improved resolution, without requiring deconvolution, will be of interest.

Acknowledgements HDW acknowledges provision of MGS and DIPRS Scholarships from Monash University. This work was conducted under support from the Australian Research Council and PerkinElmer through ARC Linkage Grant LP150100465. We are grateful for the support from the Brazil funding agencies Coordenação de Aperfeiçoamento de Pessoal de Nível Superior (CAPES), Conselho Nacional de Desenvolvimento Científico e Tecnológico (CNPq) and Fundação Carlos Chagas Filho de Amparo à Pesquisa do Estado do Rio de Janeiro (FAPERJ).

Compliance with ethical standards

Conflict of interest The authors declare no conflict of interest.

Publisher's note Springer Nature remains neutral with regard to jurisdictional claims in published maps and institutional affiliations.

References

1. Sebedio JL, Grandgirard A. Cyclic fatty acids: natural sources, formation during heat treatment, synthesis and biological properties. Prog Lipid Res. 1989;28(4):303–36.
2. Cole HI, Cardoso HT. Analysis of chaulmoogra oils. I. *Carpotroche brasiliensis* (Sapucainha) oil. J Am Chem Soc. 1938;60(3):614–7.
3. Sengupta A, Gupta JK, Dutta J, Ghosh A. The component fatty acids of chaulmoogra oil. J Sci Food Agric. 1973;24(6):669–74.
4. Oliveira AS, Lima JA, Rezende CM, Pinto AC. Cyclopentenyl acids from sapucainha oil (*Carpotroche brasiliensis* Endl, Flacourtiaceae): the first antileprotic used in Brazil. Quim Nova. 2009;32(1):139–45.
5. Shukla VKS, Spener F. High-performance liquid chromatography of triglycerides of Flacourtiaceae seed oils containing cyclopentenyl fatty acids (chaulmoogric oils). J Chromatogr A. 1985;348:441–6.
6. Ruiz-Samblás C, González-Casado A, Cuadros-Rodríguez L. Triacylglycerols determination by high-temperature gas chromatography in the analysis of vegetable oils and foods: a review of the past 10 years. Crit Rev Food Sci Nutr. 2015;55(11):1618–31.
7. Novaes FJM, Kulsing C, Bizzo HR, de Aquino Neto FR, Rezende CM, Marriott PJ. Analysis of underivatised low volatility compounds by comprehensive two-dimensional gas chromatography with a short primary column. J Chromatogr A. 2018;1536:75–81.
8. Waktola HD, Kulsing C, Nolvachai Y, Marriott PJ. High temperature multidimensional gas chromatographic approach for improved separation of triacylglycerols in olive oil. J Chromatogr A. 2018;1549:77–84.
9. Moldoveanu SC, Chang Y. Dual analysis of triglycerides from certain common lipids and seed extracts. J Agric Food Chem. 2011;59(6):2137–47.
10. Kalo P, Kemppinen A. Mass spectrometric identification of triacylglycerols of enzymatically modified butterfat separated on a polarizable phenylmethylsilicone column. J Am Oil Chem Soc. 1993;70(12):1209–17.
11. Laakso P. Mass spectrometry of triacylglycerols. Eur J Lipid Sci Technol. 2002;104(1):43–9.
12. Kemppinen A, Kalo P. Quantification of triacylglycerols in butterfat by gas chromatography-electron impact mass spectrometry using molar correction factors for [M-RCOO]+ ions. J Chromatogr A. 2006;1134(1–2):260–83.
13. Ballus CA, Meinhart AD, de Souza Campos FA Jr, da Silva LFO, de Oliveira AF, Godoy HT. A quantitative study on the phenolic compound, tocopherol and fatty acid contents of monovarietal virgin olive oils produced in the southeast region of Brazil. Food Res Int. 2014;62:74–83.
14. Christie WW, Rebello D, Holman RT. Mass spectrometry of derivatives of cyclopentenyl fatty acids. Lipids. 1969;4(3):229–31.

3.3. Supporting information

Gas chromatography–mass spectrometry of sapucainha oil (*Carpotroche brasiliensis*) triacylglycerols comprising straight chain and cyclic fatty acids

Habtewold D. Waktola, Chadin Kulsing, Yada Nolvachai, Claudia M. Rezende, Humberto R. Bizzo, Philip J. Marriott

Analytical and Bioanalytical Chemistry

Contents

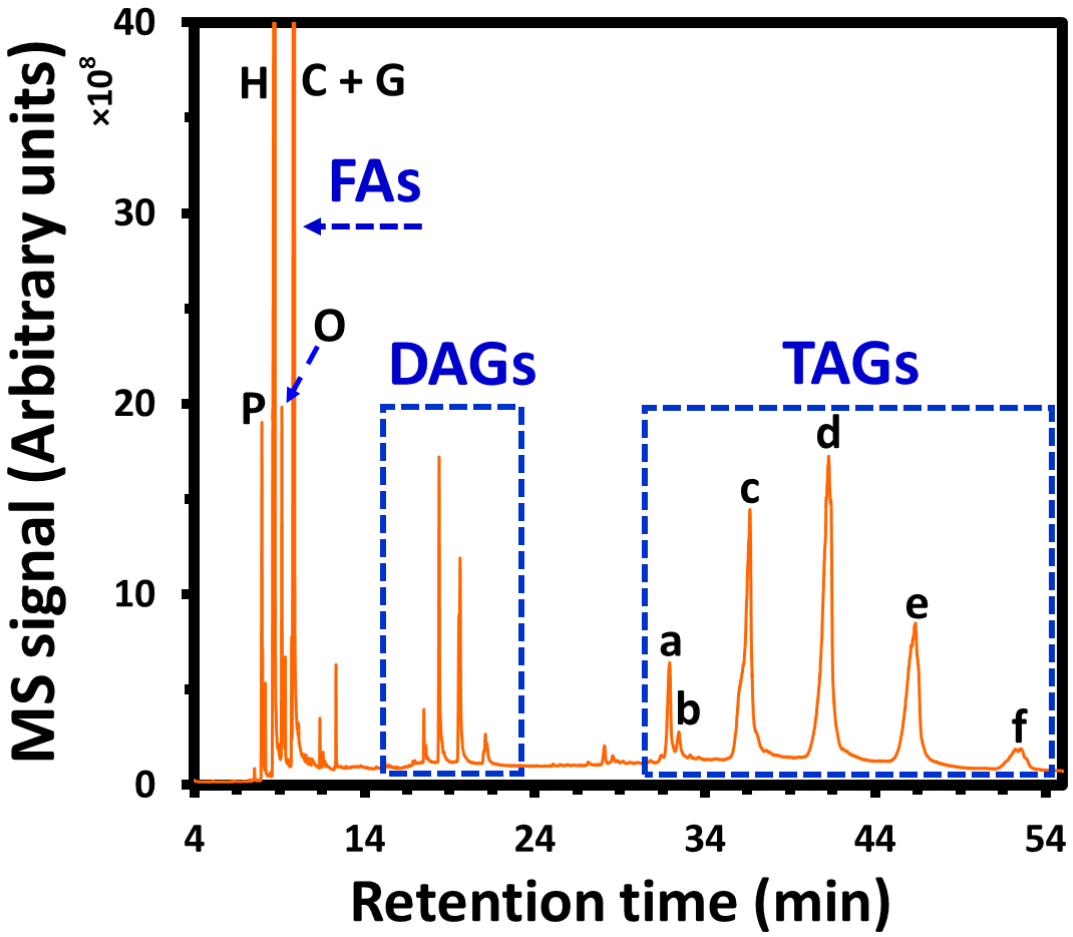

Fig. S1 GC–MS total ion chromatogram of sapucainha oil showing FA (P, H, O, C and G), DAG and TAG components. (this is the same as Fig. 3 in the main text)

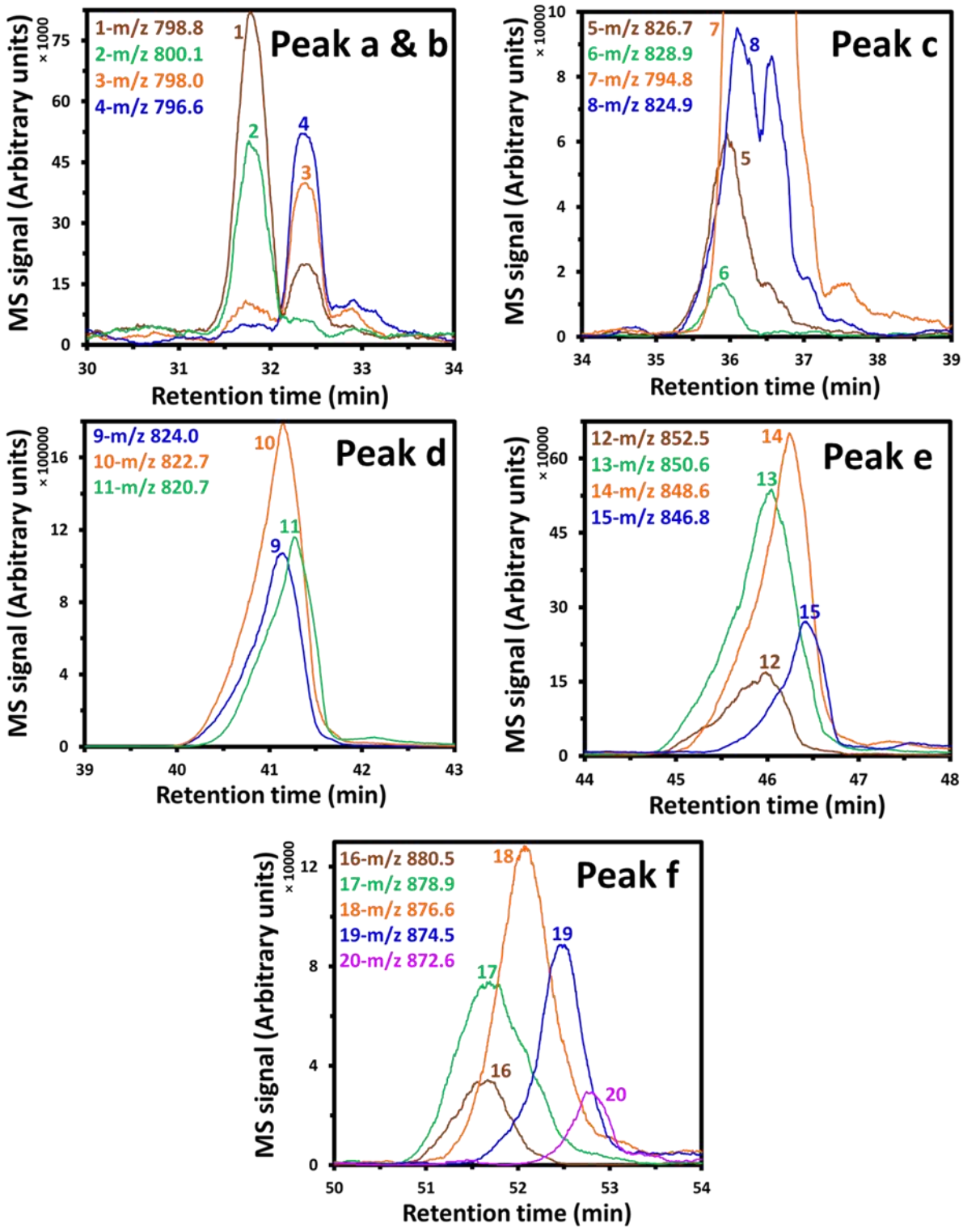

Fig. S2 Extracted ion chromatograms (EICs) of molecular ions of the possible TAGs described in Table 2, detected in peaks **a-f** in Fig. S1. (this is the same as Fig. 5 in the main text)

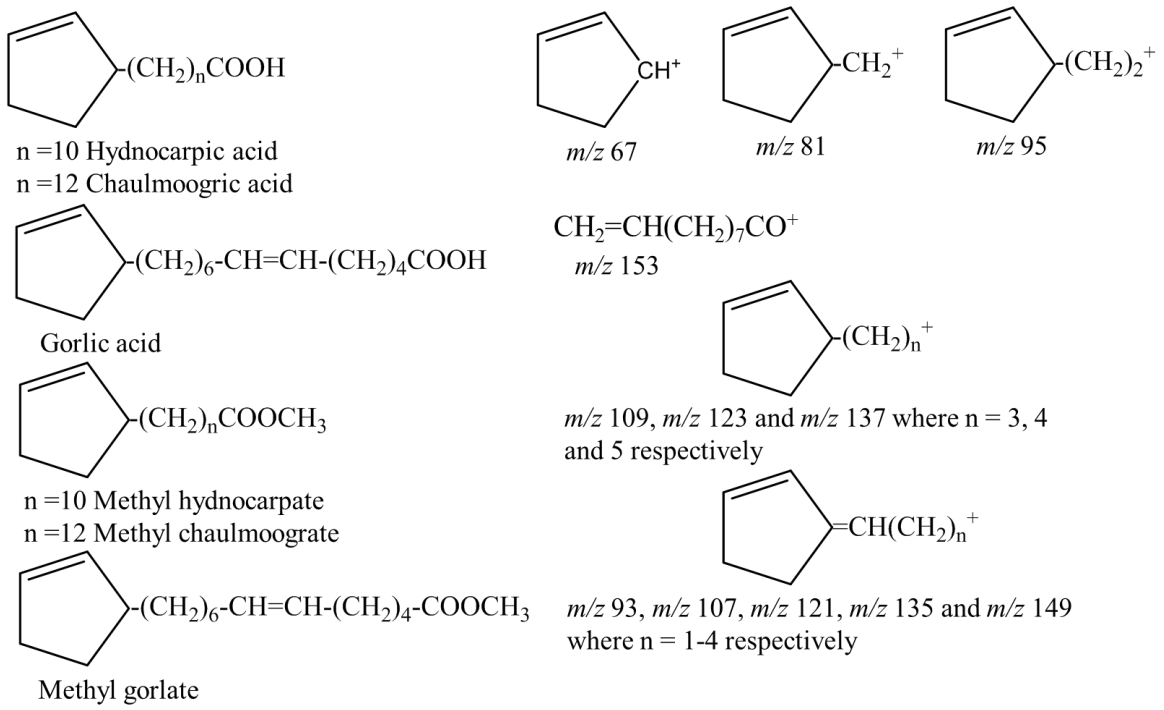

Fig. S3 Chemical structure of sapucainha oil cyclopentenyl FAs, FAMEs and the main fragments used for their identification.

The mass spectra for chaulmoogric acid (Fig. S4) was similar with that of hydnocarpic acid (Fig. 4). The prominent fragment ions were *m/z* 67, *m/z* 82 and *m/z* 95. Fragments formed through cleavage of alkyl cyclopentenyl groups such as *m/z* 109 and *m/z* 123 were also detected. Note that the McLafferty rearrangement ion of *m/z* 60 was also prominent.

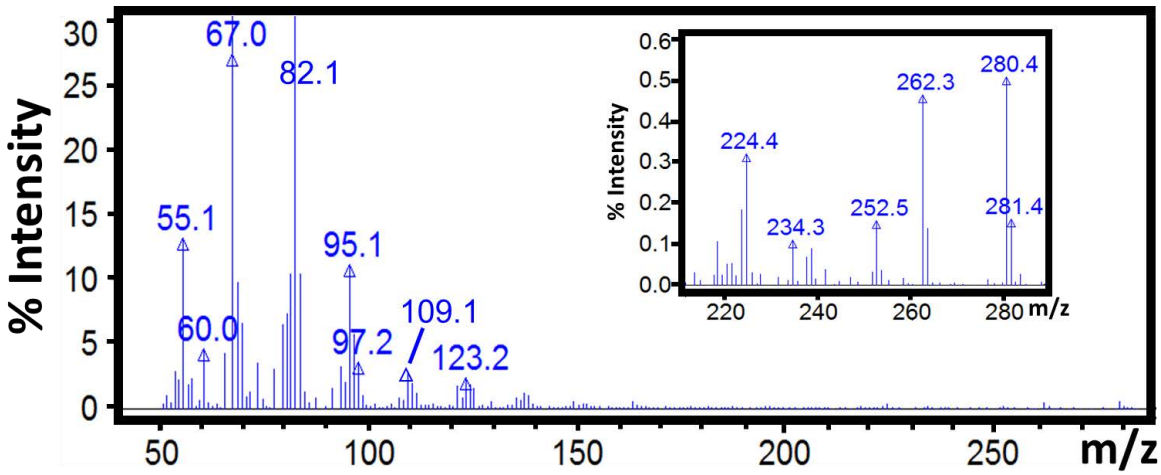

Fig. S4 Mass spectrum of chaulmoogric acid.

The mass spectra of the TAGs have shown that *m/z* 67 was the base peak (Fig. S5), which is formed after cleavage of the cyclopentenyl ring from the cyclopentenyl FAs. Other characteristic fragment ions such as alkyl cyclopentenyl, dihydrofulvene and alkyl dihydrofulvene were also detected.

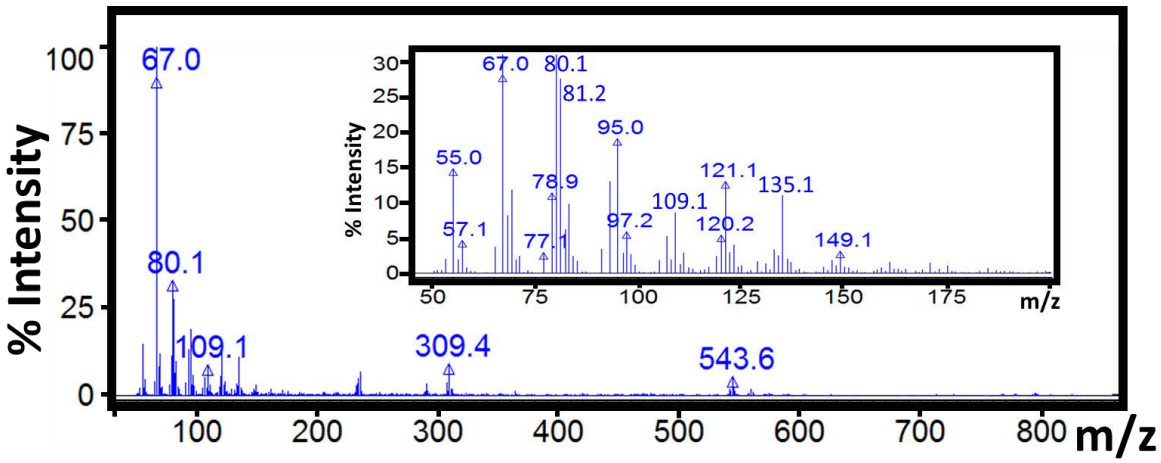

Fig. S5 Mass spectrum of TAG derived from cyclopentenyl FAs showing the characteristic base peak, *m/z* 67, and the alkyl cyclopentenyl, dihydrofulvene and alkyl dihydrofulvene fragment ions that occur at lower mass range.

Section S1. Identification of TAGs

In peak **a** two $M^{+\bullet}$, with *m/z* 798.8 and *m/z* 800.1, were detected and the peaks for their extracted mass are shown in Fig. S2. Based on the $M^{+\bullet}$ masses and the fragment ions both masses possibly belong to TAGs with CN of 48 (derived from 3 C16:0). The three C16:0 fatty acids that were identified through FAMEs analysis were H (C16:0cyc), P (C16:0) and Po (C16:1). The $[M - RCO_2]^+$ fragment ions detected, at the retention times the TAGs were identified, were *m/z* 543, *m/z* 545, *m/z* 547 and *m/z* 549, which correspond to $[HH]^+$, $[PoH]^+$, $[PH]^+/[PoPo]^+$ and $[PPo]^+$ respectively. The *m/z* 547, which corresponds to $[PH]^+/[PoPo]^+$, was the most abundant ion (Fig. S6). This might indicate both $[PH]^+$ and $[PoPo]^+$ exists, where each fragment ion belongs to one of the two TAGs that co-eluted in peak **a**, or possibly the two TAGs have either of $[PH]^+$ or $[PoPo]^+$ in common. A further look at $[RCO+74]^+$ fragment ions

has shown abundant ions of *m/z* 309 and *m/z* 313, which corresponds to H and P respectively. A minor peak of *m/z* 311 which correspond to Po was also detected. In addition $[RCO+128]^+$ fragment ions, *m/z* 363 and 367, corresponding to H and P respectively were the abundant ions. The RCO^+ fragments corresponding to H and P, which are *m/z* 235 and *m/z* 239 respectively, were also abundant. The *m/z* 237 corresponding to Po was very low in abundance. These were highly suggestive for the existence of $[PH]^+$ as a common fragment for both TAGs. With this information the TAGs with *m/z* 798.8 and *m/z* 800.1 were possibly related to PHH and PPoH respectively, given their molecular masses. Other TAGs that could match the *m/z* 798.8, such as PoPoH, and the *m/z* 800.1, such as PoPoPo, were ruled out, because fragment ions that are related to Po were less abundant.

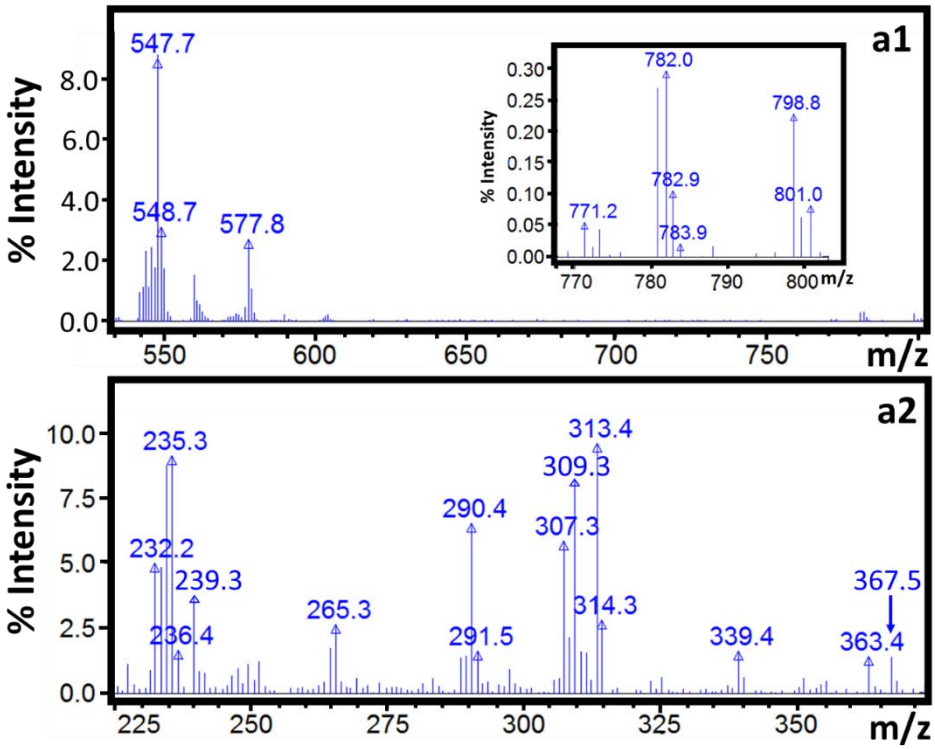

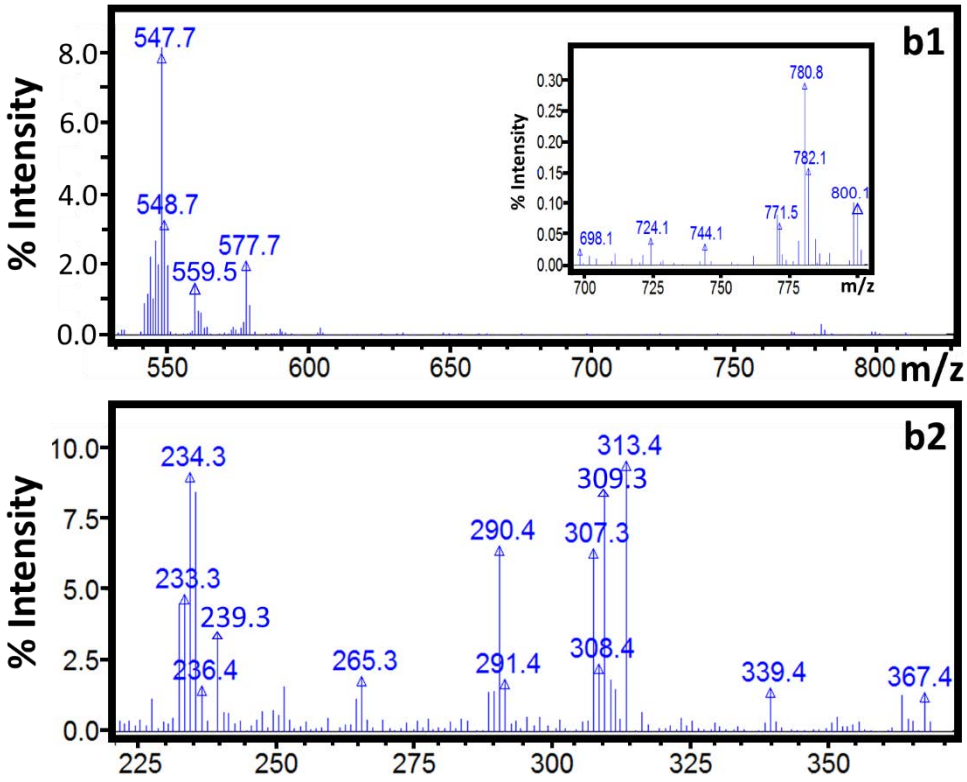

Fig. S6. Mass spectra of TAGs identified in peak **a**. Where a and b correspond to *m/z* 798 and *m/z* 800, and 1 refers to the mass range that include $M^{+\bullet}$, $[M\text{-}RCO_2]^+$ and $[M\text{-}RCO]^+$ ions, and 2 refers to the mass range that include RCO^+, $[RCO+74]^+$ and $[RCO+128]^+$ ions respectively.

Peak **b** was composed of M^+ with *m/z* 798.0 and *m/z* 796.6 (Fig. S2). The TAGs in this peak were also considered to be derived from C_{16} fatty acids. The $[M–RCO_2]^+$ fragment ions detected were with *m/z* 543, *m/z* 545 and *m/z* 547, which correspond to $[HH]^+$, $[PoH]^+$ and $[PH]^+/[PoPo]^+$ respectively (Table 2). The *m/z* 545 was more abundant than the other two fragment ions (Fig. S7). As discussed above *m/z* 798.0 may correspond to PHH or PoPoH. The $[RCO+74]^+$ fragment ion indicated that *m/z* 311, which corresponds to Po, was more abundant than *m/z* 313, which corresponds to P. The same was true for RCO^+ fragment ions. The $[RCO+128]^+$ fragment ion for Po, which is *m/z* 365, was detected with more abundance whereas *m/z* 367, which corresponds to P, was not detected (Fig. S7a2). Thus, the TAG with *m/z* 798.0 in peak **b** was likely related to PoPoH. The other TAG which eluted with this TAG was with *m/z* 796.6. This mass is less only by *m/z* 2 from PoPoH. This can possibly happen if one Po is substituted by H, i.e. the TAG could be PoHH. The $[M–RCO_2]^+$ fragment ions with

m/z 543.6, which corresponds to $[HH]^+$; *m/z* 545, which corresponds to $[PoH]^+$; and *m/z* 547.6, which corresponds to $[PoPo]^+$, were all detected in peak **b**, which indicated that the two TAGs, PoPoH and PoHH possibly co-eluted.

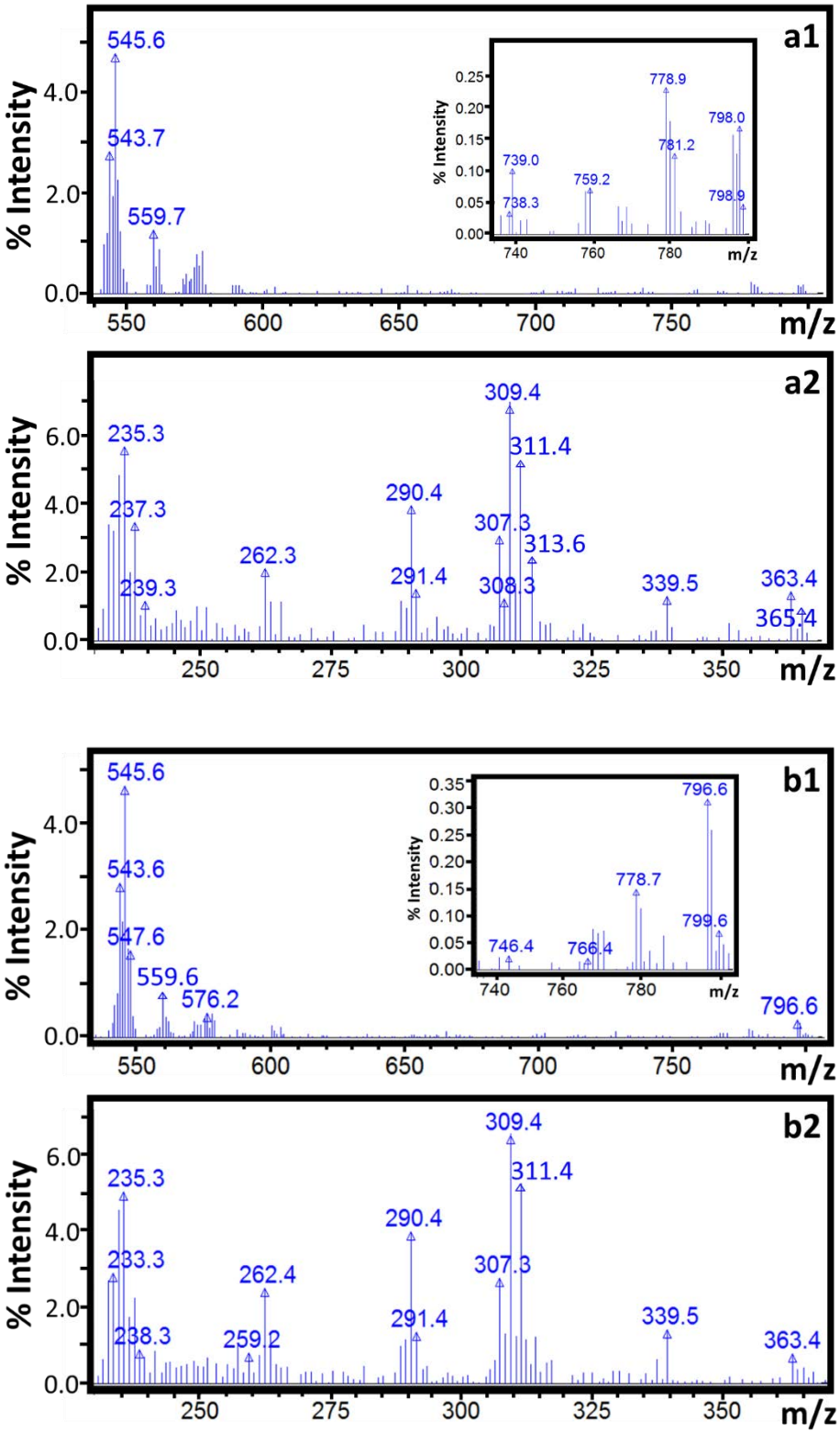

Fig. S7 Mass spectra of TAGs identified in peak **b**. Where a and b correspond to *m/z* 798 and *m/z* 796, and 1 refers to the mass range that include $M^{+\bullet}$, $[M\text{-}RCO_2]^+$ and $[M\text{-}RCO]^+$ ions, and 2 refers to the mass range that include RCO^+, $[RCO+74]^+$ and $[RCO+128]^+$ ions respectively.

Peak **c** was composed of four $M^{+\bullet}$ with *m/z* 794.8, *m/z* 824.9, *m/z* 826.7 and *m/z* 828.9 (Fig. S2). These masses could possibly related to TAGs derived from 2 C_{16} and 1 C_{18} fatty acids, except *m/z* 794.8, which could be derived from three C_{16}. From these M^+ ions, only TAGs corresponding to *m/z* 794.8 and *m/z* 826.7 were identified.

A $M^{+\bullet}$ with *m/z* 794.8 of large peak area, which cover up all the TAG peaks described under peak **c**, was detected (Fig. S2). The $[M–RCO_2]^+$ fragment ions with *m/z* 543, which corresponds to $[HH]^+$, was an abundant peak (Fig. S8a1). The *m/z* 794.8 could only be related to a TAG with minimum mass that can be derived from the lowest mass detected fatty acid in the sample, which was H. Thus, the TAG was possibly HHH. The $[RCO+74]^+$, $[RCO+128]^+$ and RCO^+ fragment ions corresponding to H were more abundant and clearly standing at this retention (Table 2 and Fig. S8a2). The $[M–RCO]^+$ fragment ion with *m/z* 559 was also detected.

At the retention time *m/z* 826.7 identified, $[M–RCO_2]^+$ fragment ions of *m/z* 547 and *m/z* 575 were detected as prominent ions (Fig. S8). The *m/z* 547 could correspond to $[PH]^+$/$[PoPo]^+$. The $[RCO+74]^+$ fragment ions detected shown that *m/z* 309 and *m/z* 313, which corresponds to H and P respectively, were the most abundant ions compared to the very low abundance of *m/z* 311 for Po. The same was true for $[RCO+128]^+$ and RCO^+ fragment ions corresponding to the three fatty acids (Table 2 and Fig. S8b2). Thus, $[PH]^+$ was possibly the fragment with *m/z* 547 that was formed at this retention time. Then the possible C_{18} fatty acid that could match with $[PH]^+$ to form a TAG with mass of 826 is therefore L/C. Thus, the TAG could be LPH/CPH. The $[RCO+74]^+$ and $[RCO+128]^+$ fragment ions corresponding to L/C, which were *m/z* 337 and *m/z* 391, were apparent (Fig. S8b2). The $[M–RCO_2]^+$ fragment ions with *m/z* 575 and *m/z* 571, which corresponds to $[LP]^+$/$[CP]^+$ and $[LH]^+$/$[CH]^+$ respectively, were also detected (Table 2 and Fig. S8b1). Thus, the TAG could be LPH or CPH, or possibly both existed but co-eluted.

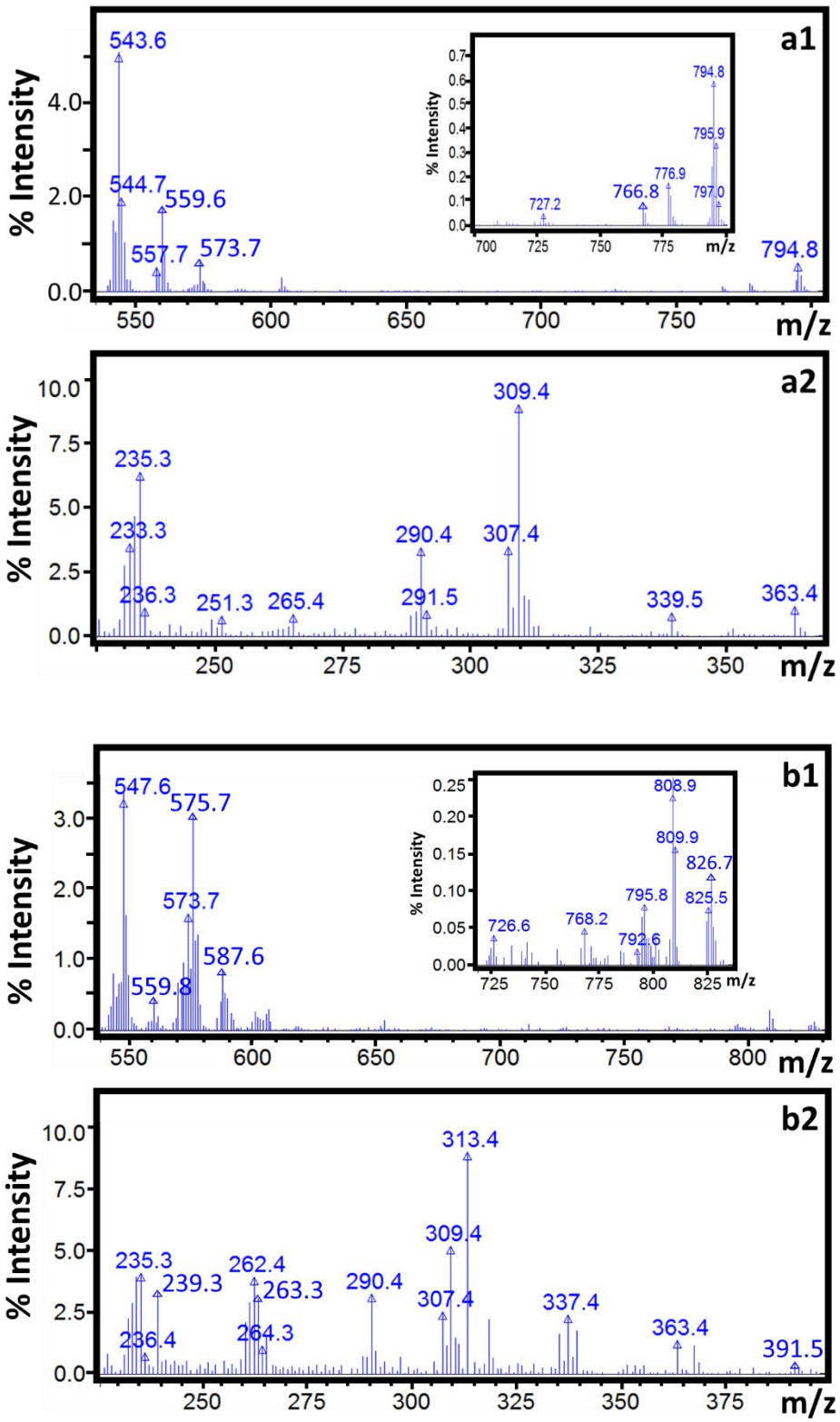

Fig. S8 Mass spectra of TAGs identified in peak **c**. Where a and b correspond to *m/z* 794.8 *and m/z* 826.7, and 1 refers to the mass range that include $M^{+\bullet}$, $[M\text{-}RCO_2]^+$ and $[M\text{-}RCO]^+$ ions, and 2 refers to the mass range that include RCO^+, $[RCO+74]^+$ and $[RCO+128]^+$ ions respectively.

As shown in Fig. S2, in peak **d** three $M^{+\bullet}$ (*m/z* 824.0, *m/z* 822.7 and *m/z* 820.7) were proposed. These *m/z* values possibly correspond to TAGs with CN = 50 (derived from 2 C_{16} and 1 C_{18} FA) with saturated and/or unsaturated bonds.

At the retention time the TAG with *m/z* 822.7 identified the mass spectrum has shown $[M - RCO_2]^+$ fragment ions with *m/z* 543 and *m/z* 571 with high abundance (Fig. S9a1). The *m/z* 543 corresponds to $[HH]^+$ whereas *m/z* 571 may correspond to $[CH]^+$ or $[LH]^+$, since C and L have the same mass. H is the only detected FA with lower molecular weight (252 g/mol) that could give $[M–RCO_2]^+$ residue with *m/z* 543. The assumption that one of the FA residue was P or Po, as in $[PH]^+$ or $[PoH]^+$, could give a residue with 4 or 2 mass units higher than the *m/z* 543. Then a TAG with $M^{+\bullet}$ *m/z* 822.7 could give $[HH]^+$ residue only after loss of an acyloxy group with *m/z* of 279, which could only correspond to C or L. Mass spectra in Fig. S9a2 shows additional fragment ions that were used for identification. The $[RCO+74]^+$ fragment ions for corresponding fatty acyl groups were related to H, *m/z* 309, and C or L, *m/z* 337. Note that the fragment with *m/z* 309, which corresponds to H, was highly abundant. The $[RCO+128]^+$ fragment ions with *m/z* 363 and *m/z* 391, which correspond to H and; C or L respectively, were also detected. The corresponding RCO^+ masses, *m/z* 235 for H and *m/z* 263 for C or L, were also the abundant ions. The $[M\text{-}RCO]^+$ with *m/z* 587 and *m/z* 559, after cleavage of acyl groups corresponding to H and C respectively, were also detected. Thus, the possible TAG(s) that correspond to the *m/z* 822.7 could be either CHH or LHH, or both. Given the fact that the peak related to the TAG was intense and the fraction of L in the oil sample was very low (0.71% peak area of the total FAs detected) it was highly possible that the TAG with *m/z* 822.7 correspond to CHH than LHH. It should also be noted that the possibility for the presence and co-elution of both TAGs could not be ruled out.

For the TAG molecule corresponding to $M^{+\bullet}$ of *m/z* 820.7 the mass spectra were shown in Fig. S9b. The fragment ions used for identification were described in Table 2. The [M–

$RCO_2]^+$ fragment ions with *m/z* 543 and *m/z* 569, which correspond to $[HH]^+$ and $[GH]^+$, respectively, were detected. H and G, with C_{16} and C_{18} respectively, are the FAs with the lowest molecular masses that could give $[M–RCO_2]^+$ residue of *m/z* 569. The $[RCO+74]^+$, $[RCO+128]^+$ and RCO^+ fragment ions, corresponding to H and G, used for identification were detected, which indicated the presence of H and G. The $[M\text{-}RCO]^+$ fragment ions were also additional ions that were detected. Note that $[HH]^+$ and other fragment ions corresponding to H could come from the CHH that was suggested earlier. But a TAG with *m/z* 820.7 could only give $[GH]^+$, with *m/z* 569, after loss of an acyloxy group that correspond to H. Thus, the TAG with *m/z* 820.7 was suggestive of the presence of GHH having in common $[HH]^+$ residue with CHH.

TAG with $M^{+\bullet}$ of *m/z* 824.0 was identified in peak **d** in addition to the two TAGs described above. The $[M–RCO_2]^+$ fragment ions, *m/z* 545 and *m/z* 573, which were not related to both CHH and GHH were detected. In addition $[RCO+128]^+$ and $[RCO+74]^+$ fragment ions that correspond to O and Po were also detected (Fig. S9 and Table 2). This indicates that *m/z* 545 may correspond to $[PoH]^+$ whereas *m/z* 573 may correspond to $[OH]^+$ or $[LPo]^+/[CPo]^+$. The TAG that corresponds to *m/z* 824 was OHH or LPoH/CPoH. Note that L and C have the same mass and fragments related to C were generated from the co-eluting CHH. While it is difficult to distinguish between LPoH and CPoH the fact that L is detected in minor amount in the oil sample gives more probability for CPoH to exist. Thus, the molecular and fragment ions information indicated the possibility of that two TAGs, OHH and CPoH, with the same molecular mass eluted at the same retention time.

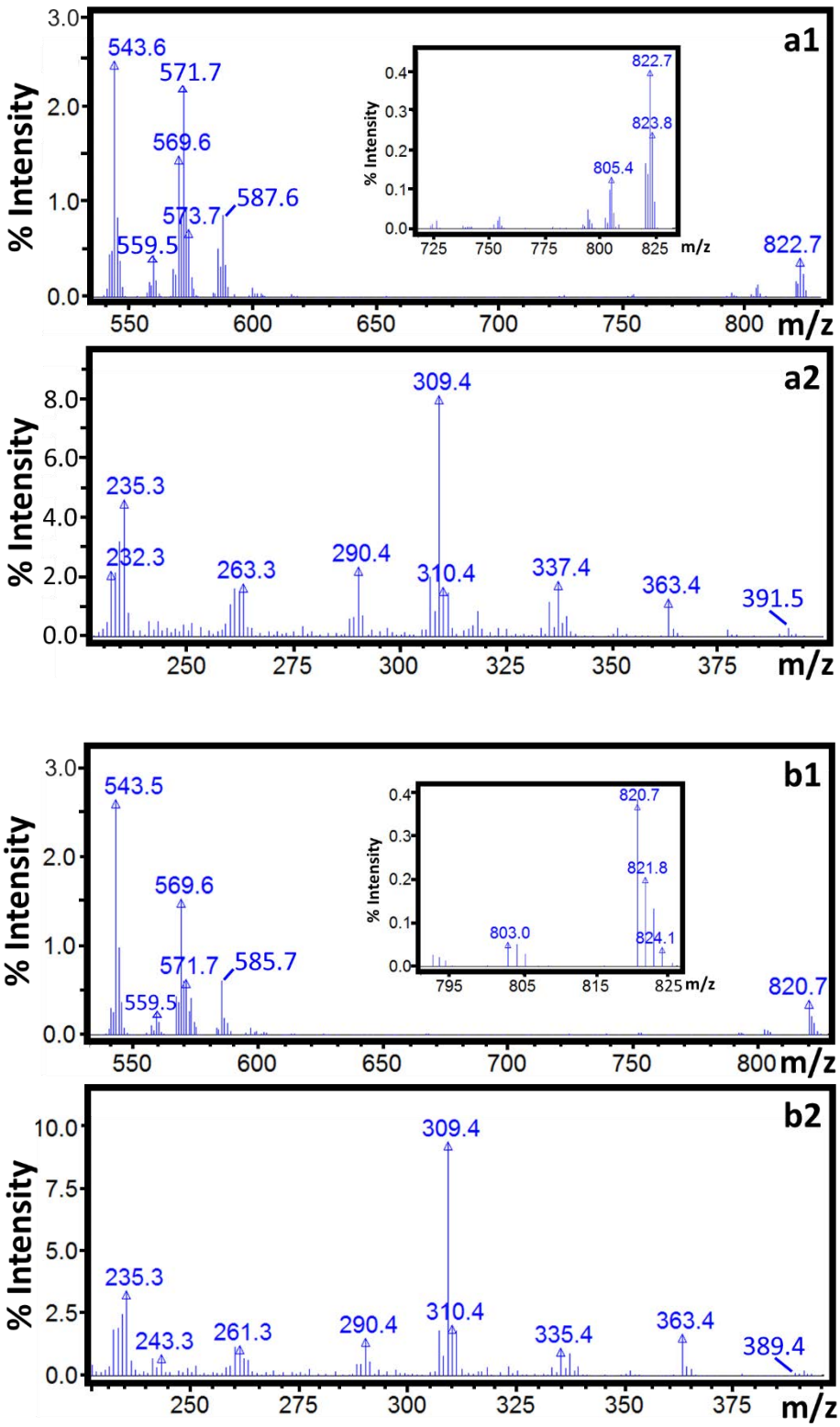
a1
% Intensity
m/z
543.6
571.7
569.6
587.6
573.7
559.5
822.7
822.7
823.8
805.4
a2
309.4
235.3
232.3
263.3
290.4
310.4
337.4
363.4
391.5
b1
543.5
569.6
571.7
585.7
559.5
820.7
820.7
821.8
803.0
824.1
b2
309.4
235.3
243.3
261.3
290.4
310.4
335.4
363.4
389.4

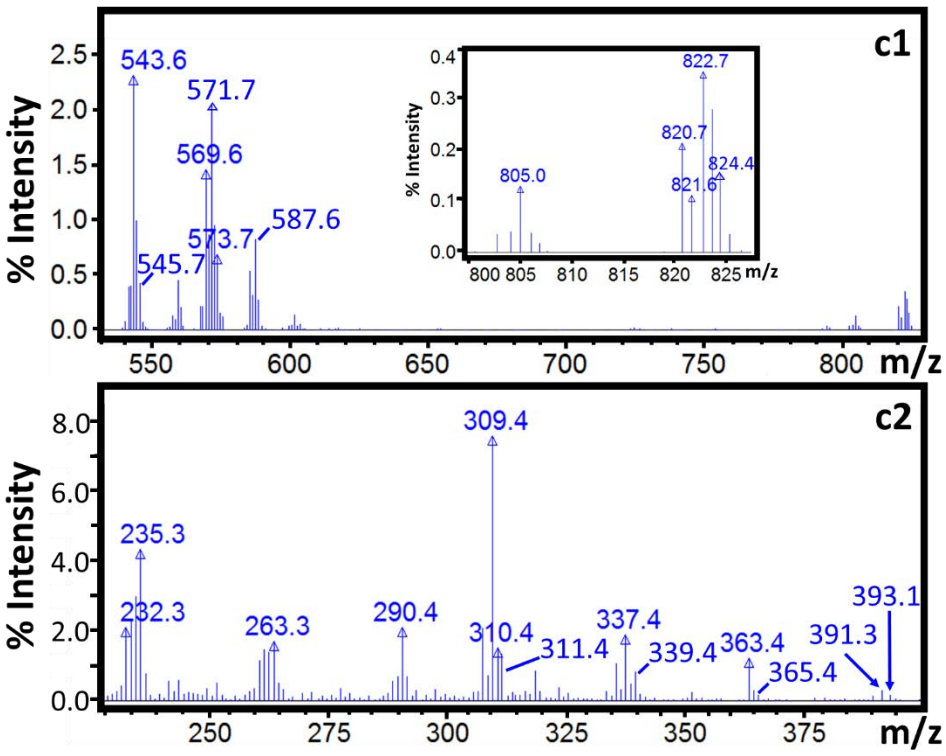

Fig. S9 Mass spectra of TAGs identified in peak d. Where a, b and c correspond to *m/z* 822, *m/z* 820 and *m/z* 824 TAGs, and 1 refers to the mass range that include $M^{+\bullet}$, $[M\text{-}RCO_2]^+$ and $[M\text{-}RCO]^+$ ions, and 2 refers to the mass range that include RCO^+, $[RCO+74]^+$ and $[RCO+128]^+$ ions respectively.

Peak **f** was composed of five TAG components (Fig. S2). Based on the molecular ions detected all TAGs in this group could be derived from 3 C_{18} FAs. The TAGs were with $M^{+\bullet}$ of *m/z* 880.9, *m/z* 878.6, *m/z* 876.6, *m/z* 874.5 and *m/z* 872.6, eluted in increasing retention time with the first two having the same retention (Table 2). For simplicity reason their identification will be discussed from the last to first eluting TAGs.

At the retention time TAG corresponding to *m/z* 872.6 identified, *m/z* 595 corresponding to $[GG]^+$ and; $[RCO+128]^+$, $[RCO+74]^+$ and RCO^+ fragment ions with *m/z* 335, *m/z* 389 and *m/z* 261 respectively, corresponding to G were detected (Fig. S10a). The *m/z* 595 and *m/z* 335 were very abundant ionss. The fragment ions as well as the fact that only 3 G molecules can give the *m/z* 872.6 suggests that the TAG was GGG.

The $M^{+\bullet}$ with *m/z* 874.5 is only 2 mass unit higher than the mass for GGG. Thus, it is possible to assume that the TAG that corresponds to *m/z* 874.5 could differ only by one FA acyl group from GGG. The FA could then be C or L. The $[RCO+74]^+$ fragment ion detected at this retention time was also in agreement with this assumption. A *m/z* 597, which corresponds to $[CG]^+$/ $[LG]^+$ was detected with high intensity (Fig. S10b1). The $[RCO+74]^+$ and $[RCO+128]^+$ fragment ions corresponding to both C and G were also detected in abundance (Table 2 and Fig. S10b2). Thus, the TAG with *m/z* 874.5 possibly correspond to CGG. LGG was not considered here given the low abundance of L in the oil sample.

The TAG with *m/z* 876.6, which is 2 mass units higher than *m/z* 874.5, was identified. The $[M–RCO_2]^+$ fragment ion with *m/z* 599 and *m/z* 597, which correspond to $[CC]^+$ and $[CG]^+$ were detected (Fig. S10c1). The $[RCO+74]^+$, $[RCO+128]^+$ and RCO^+ fragment ions corresponding to G and C were also detected (Table 2 and Fig. S10c2). All the characteristic peaks were clearly observed and strongly suggested that *m/z* 876.6 corresponds to CCG.

The TAGs with *m/z* 878.6 and *m/z* 880.9 were eluted before other TAGs detected in peak **f** (Fig. S2). At the retention time where *m/z* 878.6 was identified $[M–RCO_2]^+$ fragment ions with *m/z* 597, *m/z* 599 and *m/z* 601, which correspond to $[CG]^+$, $[CC]^+$ and $[CO]^+$, were detected (Fig. S10d1). Then the TAG could be CCC or OCG. The $[RCO+74]^+$ corresponding to O, C and G were all detected with peak corresponding to C being the most intense (Fig. S10d2). The $M^{+\bullet}$ with *m/z* 880.9 has 2 mass units higher than the $M^{+\bullet}$ with *m/z* 878.6. At the retention time it was identified $[M–RCO_2]^+$ fragment ions with *m/z* 599 and *m/z* 601, which correspond to $[CC]^+$ and $[CO]^+$, were detected (Fig. S10e1). This was suggestive for the presence of OCC. The $[RCO+74]^+$ corresponding to O was also detected (Fig. 10e2). The peaks for *m/z* 878.6 and *m/z* 880.9 have the same retention time (Fig. S2 and Table 2). This indicate that the *m/z* 878.9 was more likely correspond to CCC than to OCG. This is because CCC and OCC have the same ECN value and thus could co-elute.

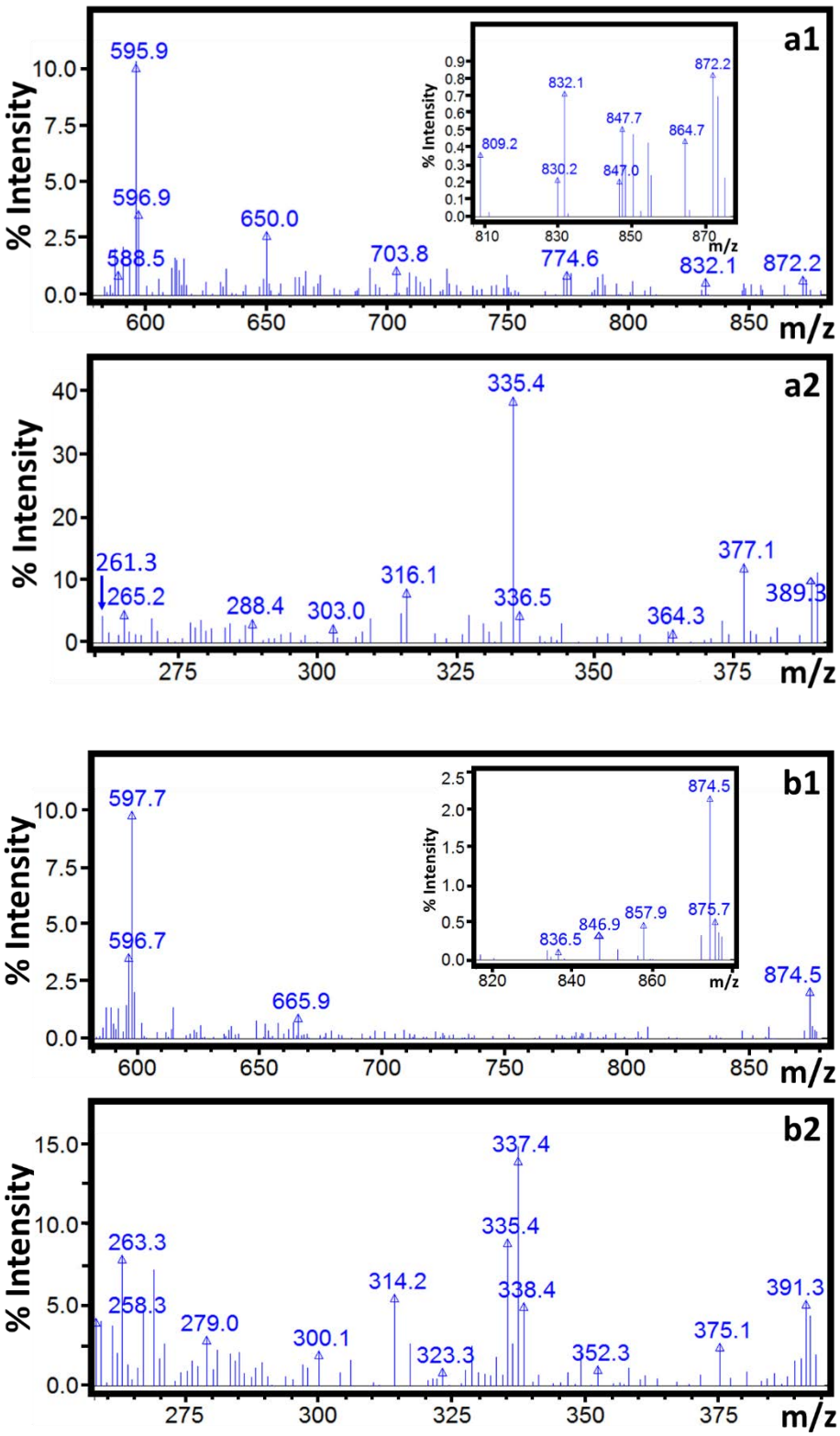
a1
595.9
596.9
650.0
588.5
703.8
774.6
832.1
872.2
809.2
830.2
847.0
847.7
832.1
864.7
872.2
% Intensity
m/z
a2
335.4
261.3
265.2
288.4
303.0
316.1
336.5
364.3
377.1
389.3
b1
597.7
596.7
665.9
874.5
836.5
846.9
857.9
875.7
b2
337.4
335.4
263.3
258.3
279.0
300.1
314.2
323.3
338.4
352.3
375.1
391.3

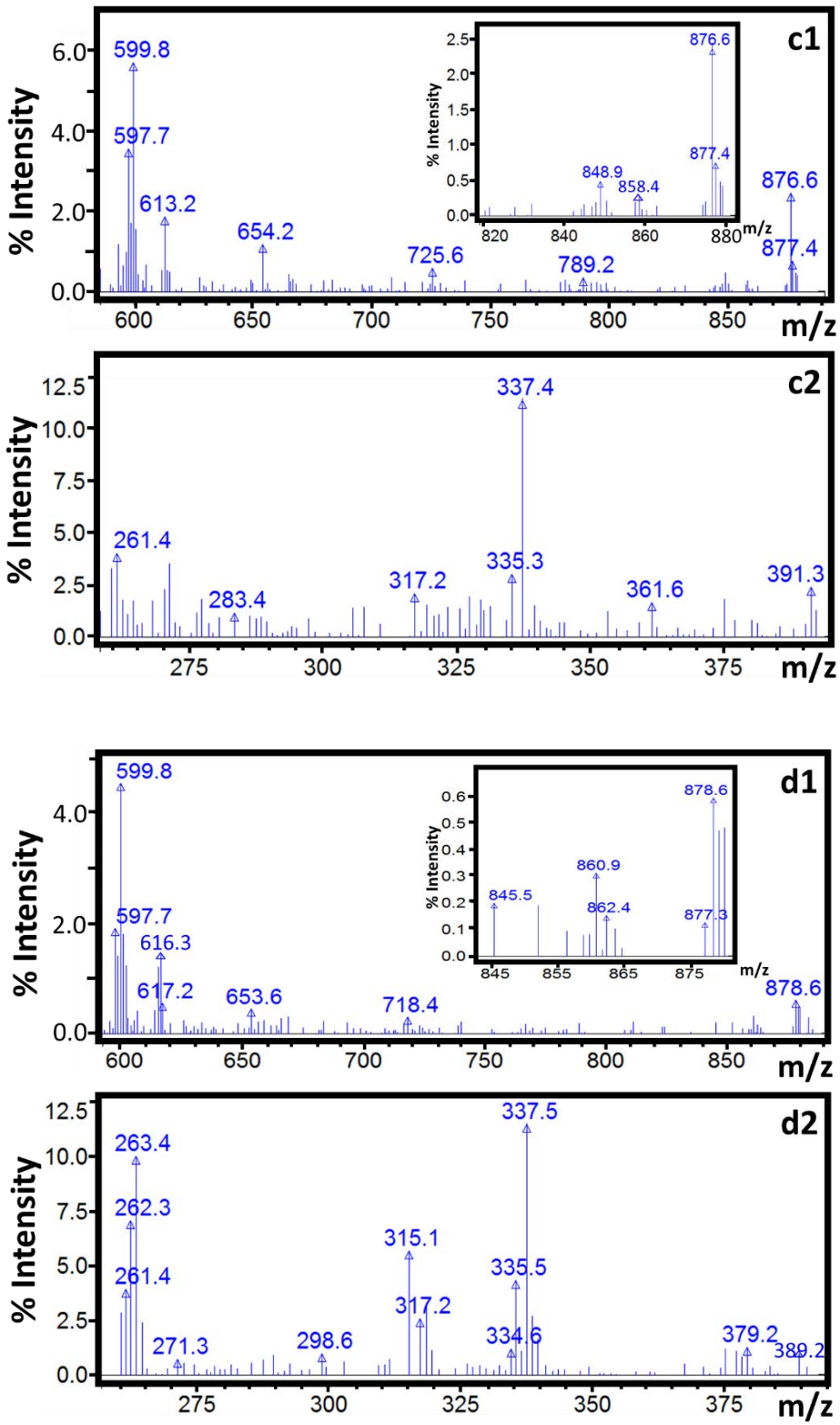
c1
% Intensity
m/z
599.8
597.7
613.2
654.2
725.6
789.2
876.6
877.4
848.9
858.4
c2
337.4
261.4
335.3
317.2
283.4
361.6
391.3
d1
599.8
597.7
616.3
617.2
653.6
718.4
878.6
860.9
845.5
862.4
877.3
d2
337.5
263.4
262.3
315.1
261.4
335.5
317.2
271.3
298.6
334.6
379.2
389.2

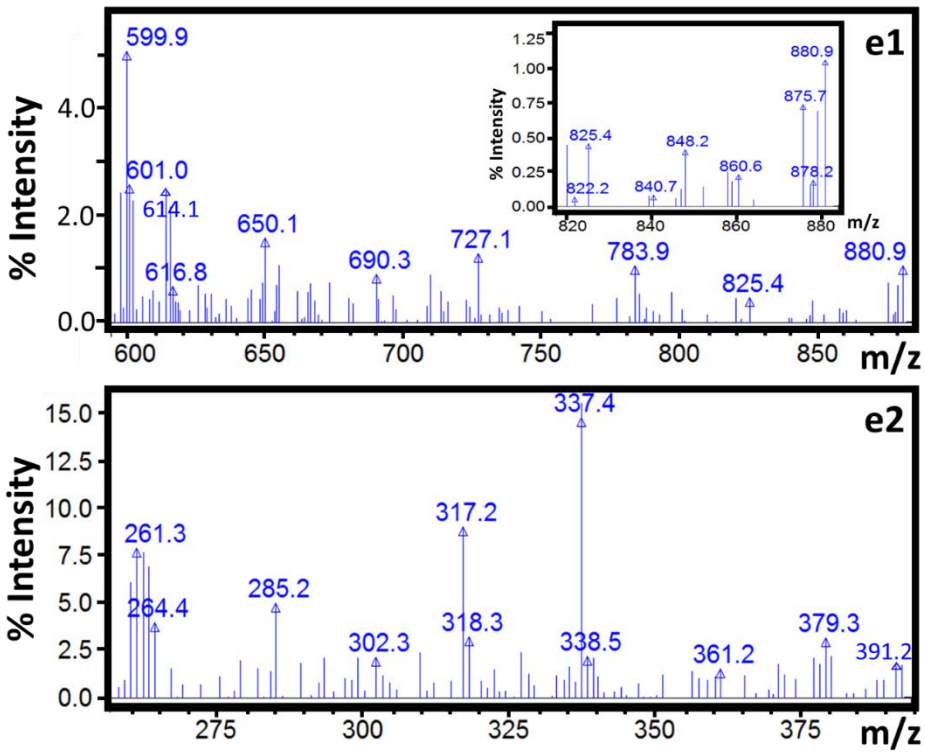

Fig. S10 Mass spectra of TAGs identified in peak **f**. Where a, b, c, d and e correspond to 872.2, *m/z* 874.5, *m/z* 876.6, *m/z* 878.6 and *m/z* 880.9, and 1 refers to the mass range that include $M^{+\bullet}$, $[M\text{-}RCO2]^+$ and $[M\text{-}RCO]^+$ ions, and 2 refers to the mass range that include RCO^+, $[RCO+74]^+$ and $[RCO+128]^+$ ions respectively.

3.4. References

[1] M.S. Alam, C. Stark, R.M. Harrison, Using Variable Ionization Energy Time-of-Flight Mass Spectrometry with Comprehensive GC×GC to Identify Isomeric Species, Anal. Chem. 88 (2016) 4211-4220.

[2] M. Beccaria, F.A. Franchina, M. Nasir, T. Mellors, J.E. Hill, G. Purcaro, Investigation of mycobacteria fatty acid profile using different ionization energies in GC–MS, Anal. Bioanal. Chem. 410 (2018) 7987-7996.

[3] P.Q. Tranchida, I. Aloisi, B. Giocastro, M. Zoccali, L. Mondello, Comprehensive two-dimensional gas chromatography-mass spectrometry using milder electron ionization conditions: A preliminary evaluation, J. Chromatogr. A 1589 (2019) 134-140.

Chapter 4

High temperature multidimensional gas chromatographic approach for improved separation of triacylglycerols in olive oil

Habtewold D. Waktola[a], Chadin Kulsing[a,b], Yada Nolvachai[a], Philip J. Marriott[a]

[a] Australian Centre for Research on Separation Science, School of Chemistry, Monash University, Wellington Road, Clayton, VIC 3800, Australia

[b] Department of Chemistry, Faculty of Science, Chulalongkorn University, 254 Phyathai Road, Patumwan, Bangkok 10330, Thailand

Published in Journal of Chromatography A, 1549 (2018) 77–84.
doi.org/10.1016/j.chroma.2018.03.037

Contents

4.1. Chapter overview

As discussed in Chapter 3 TAGs often co-elute based on their CN and degree of unsaturation in the usual 1D GC. The same co-elution problem exists also in 1D liquid chromatography. Similar to the overlap of FAs in 1D GC, inadequate separation of TAGs in 1D has led to the proposal to use of 2D chromatographic separation in this study. While 2D separation is becoming a separation technique of choice by using HPLC, less attention has been paid to TAG analysis using MDGC. Thus, the present Chapter focuses on the development of MDGC technique for TAG separation in olive oil.

Heart-cut (H/C) MDGC methods under suitable flow and high T program conditions were developed to separate olive oil TAGs. A SLB-5MS (15 m × 0.25 mm I.D. × 0.25 µm d_f) and Rtx-65 (11.5 m × 0.25 mm I.D. × 0.1 µm d_f) were selected as ^{1}D and ^{2}D columns respectively, both with high T limits (up to 370 °C). Stationary phase choice and use for ^{1}D and ^{2}D was not separately studied because of the availability of limited number of columns with high T limit phases compared to the high elution T of TAGs (mostly >300 °C). The use of a non-polar column as ^{1}D and mid-polar column as ^{2}D was for the same reasoning as the MDGC of FAMEs, non-polar ^{1}D gives a benefit of sampling TAGs with the same CN as a group, and resolving them on the mid-polar ^{2}D based on their degree of unsaturation.

The ^{1}D separation displayed three major groups of peaks in an area ratio of approximately 5:33:62 (of increasing retention), using FID. Four groups of minor peaks, with 2 of them located between the major peaks, were also detected. The H/C fractions of the minor peaks, and sub-sampled regions across the major peaks eluting from the ^{1}D outlet, were cryotrapped at the ^{2}D inlet. The function of cryotrapping is to reduce the dispersion of the peak fraction that is transferred from the ^{1}D column. The trapped TAGs then underwent T programmed ^{2}D separation. For this step, either analysis on the ^{2}D column can be at the prevailing oven T, or the oven can be cooled, the H/C cryotrapping turned off, and the oven re-

programmed in order to achieve better separation. Each of the 'H/C' zones generally gave 2–5 – and in some cases more – separated peaks of TAGs on the ^{2}D column, under suitable flow condition and phase polarity that resulted in improved separation. Six sub-sampled H/Cs from various regions of the individual peaks from the ^{1}D column were simultaneously trapped and released to ^{2}D, resulting in apparently more than 22 individual TAG peaks. According to their different retention times, different TAGs were revealed within each of the 3 major groups, using H/C sub-sampling.

A comprehensive analysis with a sampling strategy that covers most of the ^{1}D peaks was conducted to reveal the presence of more TAG components in the olive oil sample. In order to enhance loading capability to improve detection of minor TAGs, and to reduce overall analysis time for the ^{1}D separation a wide bore non-polar ^{1}D column (HP-5; 10 m × 0.32 mm I.D. × 0.25 µm d_f) with a relatively short length was used instead of the previously employed relatively narrow bore SLB-5MS (0.25 mm I.D.) column. The strategy yielded about 29 total TAGs separated that are present in the olive oil. This is a significant increase in the number of TAGs detected in olive oil compared to the 15 TAGs detected using 1D GC and Rtx-65 column (the 1D chromatogram is presented in Section 4.3 as supporting information).

The tandem column strategy was able to resolve more components than that usually observed on a single column. The system was also found to be sufficiently stable to allow extended sampling for multiple H/C required for comprehensive H/C analysis of the TAG groups. Compared to a GC×GC report for the separation of TAGs, which has shown difficulty in separation within the TAG group in an extracted coffee bean mainly due to the limitation of the short ^{2}D column, the H/C MDGC, where a longer ^{2}D column with adjustable flow and T program applied, offered an alternative approach. The method can be applied in a straightforward manner to analysis of more complex samples such as fish oil. Since TAG fingerprinting can be used for determination of types of vegetable oil, and for authenticity and

quality control purpose, it is important to identify separated TAG components. This led to the development of H/C MDGC−MS method for the separation and identification of olive oil TAGs, which is the focus of Chapter 5.

4.2. Article

Journal of Chromatography A, 1549 (2018) 77–84

Contents lists available at ScienceDirect

Journal of Chromatography A

journal homepage: www.elsevier.com/locate/chroma

High temperature multidimensional gas chromatographic approach for improved separation of triacylglycerols in olive oil

Habtewold D. Waktola[a], Chadin Kulsing[a,b], Yada Nolvachai[a], Philip J. Marriott[a,*]

[a] Australian Centre for Research on Separation Science, School of Chemistry, Monash University, Wellington Road, Clayton, VIC 3800, Australia
[b] Department of Chemistry, Faculty of Science, Chulalongkorn University, 254 Phyathai Road, Patumwan, Bangkok 10330, Thailand

ARTICLE INFO

Article history:
Received 9 November 2017
Received in revised form 6 March 2018
Accepted 17 March 2018
Available online 19 March 2018

Keywords:
Triacylglycerols
Olive oil
Heart-cut multidimensional GC
Comprehensive sampling

ABSTRACT

Heart-cut multidimensional gas chromatographic (H/C MDGC) methods under suitable flow and high temperature (T) program conditions were developed to separate olive oil triacylglycerols (TAGs). Different column sets were selected for further evaluation, each with relatively short non-polar first dimension (^{1}D) and mid-polar second dimension (^{2}D) columns of high T limits (350 °C). The ^{1}D separation displayed three major groups of peaks in an area ratio of approximately 5:33:62 (of increasing retention), using flame ionisation detection (FID). Four groups of minor peaks, with 2 of them located between the major peaks, were also detected. The H/C fractions of the minor peaks, and sub-sampled regions across the major peaks eluting from the ^{1}D outlet, were cryotrapped at the ^{2}D inlet. The trapped TAGs then underwent temperature programmed ^{2}D separation. Each of the 'H/C' zones generally gave 2–5 – and in some cases more – separated peaks of TAGs on the ^{2}D column, under suitable flow condition and phase polarity that resulted in improved separation. Six sub-sampled H/Cs from various regions of the individual peaks from the ^{1}D column were simultaneously trapped and released to ^{2}D, resulting in apparently more than 22 individual TAG peaks. According to their different retention times, different TAGs were revealed within each of the 3 major groups, using H/C sub-sampling. A comprehensive sampling strategy that covers most of the ^{1}D peaks further revealed the presence of more TAGs in the olive oil sample. This tandem column strategy was able to resolve more components than that usually observed on a single column.

1. Introduction

Triacylglycerols (TAGs) are the main constituents of vegetable oils and animal fats, arising from esterification of the three hydroxyl groups of glycerol. Based on the number of fatty acids present and the specificity of the enzyme involved in the synthesis of the particular fat or oil, a large number of different TAGs with a variety of functional groups and chemical structures can be found [1,2].

Analysis of TAGs in lipids gives information on the original composition of components in the lipid sample and may be preferential to studying fatty acid composition [3]. Their structures are important in terms of nutritional, biochemical and technological aspects [4]. The number of TAGs that can be detected in a given oil sample is dependent on the degree of separation achieved, and the mode of detection used [5]. Structurally, most TAGs differ according to the number of carbons, the degree of unsaturation, and variation of positions, of each acyl group on the glycerol backbone. This makes their separation as well as identification somewhat difficult. TAGs may be analysed by different methods; analytical techniques mainly employed in the analysis of TAGs in oils are high performance liquid chromatography (HPLC), capillary gas chromatography (CGC), supercritical fluid chromatography (SFC) and thin layer chromatography (TLC) [2,6,7]. More commonly employed techniques are HPLC [5,8,9] and high temperature GC (HTGC) [10–12] coupled to mass spectrometry (MS), using different modes of operation.

In reversed-phase HPLC (RP-HPLC), elution of TAGs follows the increase in their equivalent carbon number (ECN) [4,6]. Equivalent carbon number is defined as ECN = CN – (2 × DB), where CN is the number of carbon atoms and DB is the number of double bond(s) in the fatty acyl chains. TAGs with the same ECN value, called critical pairs, such as oleoyl-linoleoyl-linolenoyl-glycerol (OLLn) and palmitoyl-linoleoyl-linolenoyl-glycerol (PLLn), co-elute. These critical TAG pairs can be separated if they differ in their theoretical carbon number (TCN), on columns with smaller particle size (3 or 5 μm). TCN is an analogue of ECN calculated for unsaturated TAGs from CN and retention factor (k) relationship of the saturated TAGs and used to predict the separation of critical pairs. However, TAGs

* Corresponding author.
E-mail address: philip.marriott@monash.edu (P.J. Marriott).

https://doi.org/10.1016/j.chroma.2018.03.037
0021-9673/

with the same unsaturation and carbon number, such as linoleoyl-linoleoyl-linoleoyl-glycerol (LLL) and OLLn, still have a tendency to co-elute [6]. Moreover, the separation and identification of regioisomers and enantiomers of TAGs are other challenges [4,13].

In CGC, TAGs are eluted mainly in order of increasing molecular mass on non-polar stationary phases whereas on medium polarity and polar stationary phases, which are commonly employed in HTGC analysis of TAGs, elution occurs according to both molecular mass and degree of unsaturation in the fatty acyl groups on the TAG molecules [14]. On medium polarity and polar columns, retention times of TAGs with the same chain length of fatty acyl group but different degree of unsaturation increase with increasing numbers of double bonds.

Although from the above discussion TAG elution seems to follow a predictable order, detection and identification of TAGs in samples is difficult. This may be because oil and fat samples contain varying concentration and numbers of TAGs than present in the TAG standard mixture used to represent the sample in method development [10]. In HPLC, a single column packed with silver-ion-modified octyl and sulfonic co-bonded silica (mixed mode separation) demonstrated an improved selectivity for TAGs separation with rapid analysis time [15]. However, the inadequacy of one dimensional (1D) chromatographic separation for the detection and identification of TAGs in complex samples has led to the use of two dimensional (2D) chromatographic separations. Beccaria et al. reported the identification of more than 250 TAGs in menhaden oil sample using off-line comprehensive 2D HPLC [16]. While 2D separation is becoming a separation technique of choice by using HPLC, less attention has been paid to TAG analysis using multidimensional GC (MDGC).

MDGC conventionally employs two columns providing different selectivity, although alternative use of a single column with thermal sensitivity is also possible [17]. It is superior in terms of enhanced separation and peak capacity as well as improved detection limit, *e.g.* as a result of the cryogenic refocusing effect [18] which has been previously applied in the area of food analysis [19]. Analysis of TAGs in an extracted coffee bean sample by comprehensive two dimensional GC (GC × GC) has been recently reported [20] showing difficulty in separation within the TAG group. This is due to the limitation of the short ^{2}D column applied in GC × GC, as well as the high T elution of compounds resulting in insufficient separation. Development of heart-cut multidimensional GC (H/C MDGC), where a longer ^{2}D column with adjustable flow and T program can be applied, offers an alternative approach. In MDGC separation can be improved by manipulation of gas flows in each column and more than one H/C can be cryotrapped to reduce the number of analyses for ^{1}D target region analysis [21].

Olive oil is prone to adulteration. Separation and detection of its TAG components can assist with authentication of the oil. Reports from different studies indicate that 39 TAGs, existing in concentrations ranging from <1% to >50%, have been identified in olive oil. The TAGs are largely derived from eight different fatty acids [6]. In this study, olive oil was selected as a sample to develop a H/C MDGC method. Effects of chromatographic conditions such as stationary phases, column geometries, T programs and flow rates on the separation performance (analysis time and resolution) were investigated. A suitable condition was further applied to perform comprehensive multiple H/C MDGC of TAGs.

2. Experimental

2.1. H/C MDGC analysis

A gas chromatographic instrument (7890A, Agilent Technologies, Mulgrave, Australia) equipped with dual flame ionisation detectors (FID) was used for this experiment. The GC was also equipped with an Agilent Deans Switch (DS) which has one inlet, and two further outlet column channels plus two inlet channels to control the switching flow. Two sets of columns with relatively short lengths were used for TAGs separation. An Rtx-65 column, which is a mid-polar phase, was used either as ^{1}D or ^{2}D column in each set with the other column comprising a non-polar phase. Column set I: ^{1}D SLB-5MS (15 m × 0.25 mm × 0.25 μm); ^{2}D Rtx-65 (11.5 m × 0.25 mm × 0.1 μm); restrictor – deactivated fused-silica (DFS, 1.75 m × 0.15 mm). Column set II: ^{1}D HP-5 (10 m × 0.32 mm × 0.25 μm); ^{2}D Rtx-65 (11 m × 0.25 mm × 0.1 μm); restrictor – DFS (1.45 m × 0.15 mm). A speciality Rtx-65TG phase suited to triglycerides is a higher T version of the Rtx-65 phase, though was not used here.

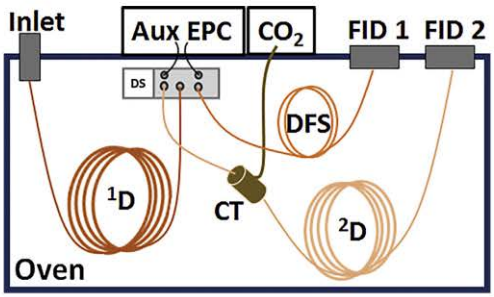

Fig. 1. Configuration of the H/C MDGC system. AUX EPC: pneumatic auxiliary port with electronic pressure control; DS: Deans switch; ^{1}D: ^{1}D column; ^{2}D: ^{2}D column; CT: cryotrap; CO_2: compressed liquid carbon dioxide supply; FID: flame ionisation detector; DFS: deactivated fused- silica capillary tubing.

As shown in Fig. 1 the applied H/C MDGC configuration comprise the following elements: (1) ^{1}D column connected between the GC inlet and the DS inlet; (2) ^{2}D column connected between one of the DS outlets and FID 2; and (3) a short restrictor column connected between the other DS outlet and FID 1. The ^{2}D column passes through a cryofocusing trap (CT) near the column inlet. Liquid CO_2 was provided as an on-demand flow to CT, which expands as a coolant gas to trap TAGs sampled or heart-cut from the ^{1}D column to the ^{2}D column. CO_2 was supplied to the CT at least 2 min prior to the first H/C event, with target regions from ^{1}D effluent selected based on retention times detected at FID 1. The H/C regions of TAGs remain trapped at CT until all TAGs were eluted from the ^{1}D column. The CT CO_2 supply was stopped in order to release TAGs to the ^{2}D column, which can be at the prevailing oven T, or the oven can be cooled before the CO_2 supply is terminated.

The oven T program used was as follows: from different ^{1}D start T (80 °C or 250 °C), the T was ramped up to 340 °C (15 °C/min), held for 25 min until all TAGs elute from the ^{1}D column, and then cooled down (at 60 °C/min) to the ^{2}D start T (80 °C or 250 °C; 0.5 min hold). Heart-cut sampling is conducted at required times. This is referred to as the first T program. The trapped components were then released from the CT, and a second T program was applied by ramping up the oven T again to 340 °C (15 °C/min) and then held until the TAGs eluted from the ^{2}D column. The inlet and detector T were set at 300 and 350 °C, respectively.

Constant flow mode was used throughout the experiment in both columns, with two constant flow programs used. The flow for the ^{1}D separation (1st flow program) elutes TAGs from the ^{1}D column during the 1st T program, while the flow for the ^{2}D separation (2nd flow program) provides separation of TAGs on the ^{2}D column during the 2nd T program. Thus the ^{1}D and ^{2}D column flows in each program are different, as summarised in Table 1, with the overall flow for the ^{2}D separation preferably lower than that for ^{1}D. The 1st flow program provided a preliminary separation on the ^{1}D column.

Table 1
Flow programs applied for separation on column set I.

Experimental conditions	Flow program for ^{1}D separation (mL/min)		Flow program for ^{2}D separation (mL/min)	
	^{1}D column	^{2}D column	^{1}D column	^{2}D column
Condition 1	2.0	4.4	0.2	0.4
Condition 2	2.0	4.4	0.3	0.6
Condition 3	2.0	4.4	0.6	1.0
Condition 4	2.0	4.4	0.6	1.4
Condition 5	2.0	4.4	0.8	2.0
Condition 6	2.0	4.4	1.5	3.2

The DS flow was balanced in order to avoid carrier flow (and solute leakage) to the ^{2}D column while the DS valve was in the off position; all flow is directed from the ^{1}D column flow to the restrictor (no heart-cutting). The DS flow provides H/C to the ^{2}D column and CT for target regions as required during the 1st T program. The 1st flow program was changed to the 2nd flow program prior to the release of cryotrapped solutes and commencement of the 2nd T program. The flow was adjusted to provide better separation of TAGs on the ^{2}D column. In summary, the TAG regions were sampled from the ^{1}D column, cryotrapped, the ^{2}D flow adjusted, and then separated on the ^{2}D column using the appropriate ^{2}D T program.

2.2. Sample and standards

Extra virgin olive oil (Spain) was bought from a local supermarket and used as a sample to develop the method. The sample was prepared by dissolving the oil in hexane to result in a 0.5% v/v solution. The sample (1 μL) was injected into the GC with a 10:1 split ratio. TAG standards of tripalmitin (PPP), tristearin (SSS) (both from Sigma Chemical Co., USA), 1,2-palmitin-3-stearin (PPS) and 1,2-stearin-3-palmitin (SSP) (both from Larodan Fine Chemicals AB, Sweden) were used as indicative TAGs present in olive oil, where P = saturated C_{16} and S = saturated C_{18}. Glyceryl triheptadecanoate (C17:0/C17:0/C17:0) (Sigma Chemical Co., USA) was used as internal standard.

3. Result and discussion

Fig. 1 is a schematic diagram showing the instrumentation used in this experiment. Mid-polar – non-polar and non-polar – mid-polar column sets were initially applied, and revealed greater benefit of the non-polar – mid-polar column set for ^{2}D separation (results not shown). As discussed above, on non-polar columns TAGs elute mainly according to their increasing molecular mass or more appropriately carbon number (CN). Which means the contribution from variation in degree of unsaturation to the separation is relatively small, thus on a non-polar column TAGs with the same CN appear as a single peak or as a closely eluting cluster of peaks. On the other hand on polar and mid-polar columns TAGs are further resolved based on their degree of unsaturation. Thus, using a non-polar column as ^{1}D gives a benefit of sampling TAGs with the same CN as a group, and resolving them on ^{2}D based on their degree of unsaturation. This strategy has a similarity with a non-polar – polar column set used for the MDGC separation of fatty acid methyl esters with the same CN according to their degree of unsaturation [22]. Other ^{2}D column phases that exhibit even better resolution of unsaturated isomers tend to have limited thermal stability, and so were determined to be not suited for high temperature operation. As a result, the remainder of this study focuses on two column sets; set I: ^{1}D non-polar and ^{2}D mid-polar (both 0.25 mm I.D.) for investigation of flow rate effects on the chromatographic result and target H/C analysis, and set II: ^{1}D non-polar (0.32 mm I.D.) and ^{2}D mid-polar (0.25 mm I.D.) for comprehensive H/C analysis.

3.1. 1DGC experiment using column set I with the DS 'off'

Olive oil sample at 0.5% v/v was injected to the GC. Three major and four minor peaks of TAGs were obtained on the ^{1}D column (Fig. 2). The three major peaks in increasing t_R (**2**, **4** and **6**) have a 5:33:62 area ratio. Four peaks (**1**, **3**, **5** and **7**) were of minor abundance. On the ^{1}D non-polar column, SLB-5MS, the TAGs eluted in an increasing order of CN [23]. The injection of four standard TAGs mixture of PPP, PPS, SSP and SSS with CN of 48, 50, 52 and 54 respectively confirms this order of elution. It also demonstrated that three major peaks and one of the minor peaks in the sample are groups of TAGs with the same CN to the corresponding standard TAGs. Note that an aim of this work at this stage is not to identify the TAG components present in the sample, but rather to develop a method to achieve better separation on the ^{2}D column.

The result in Fig. 2 established an acceptable ^{1}D result, and was chosen throughout the remaining analyses to develop ^{2}D separation strategies. Thus, H/C of the minor peaks, and sub-sampling across the major peaks, to the ^{2}D column were conducted using the various procedures in the Experimental section. Based on experiments that sampled different zones across each of the major peaks, different numbers (**2**–**5**) of separated TAG peaks were resolved on the ^{2}D column. The three later-eluting minor peaks (peaks **3**, **5** and **7**) each were subsequently separated into two TAG peaks. This is demonstrated in detail in Section 3.3. The extent of resolution of the peaks on the ^{2}D column was found to be dependent on column gas flow rate.

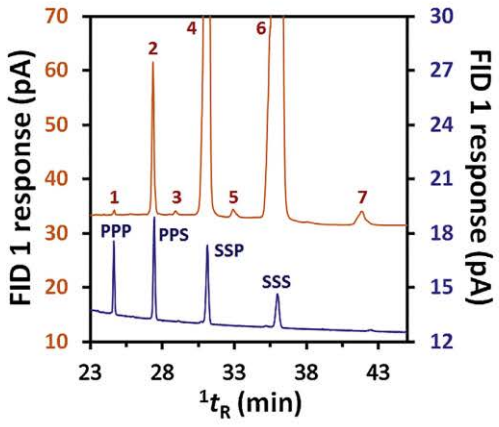

Fig. 2. Overlaid GC–FID 1 chromatograms of olive oil TAGs (upper trace) and standard TAGs (lower trace) on the ^{1}D non-polar column (0.25 mm I.D.). The oven temperature program commenced at 80 °C, was increased to 340 °C (15 °C/min), then held for 25 min. Isothermal conditions commenced at 17.3 min, so all TAGs eluted during the isothermal hold region. The ^{1}D and ^{2}D column flows were 2 and 4.4 mL/min, respectively.

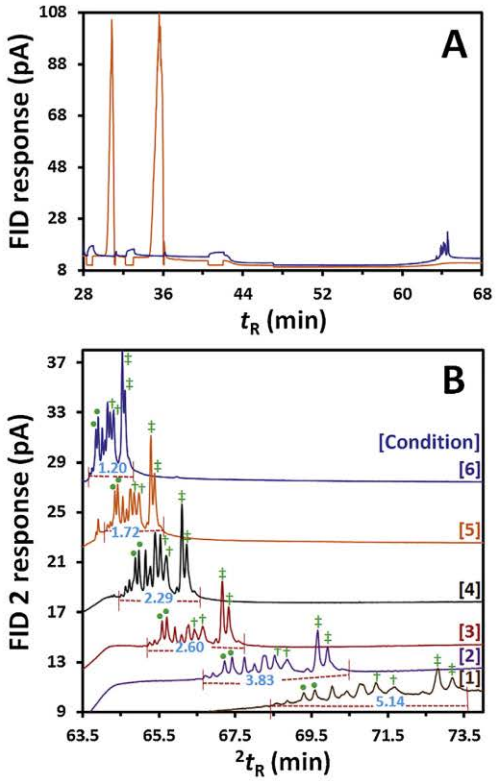

Fig. 3. (A) GC–FID chromatograms of TAGs on column set I showing various H/C or sampled regions from the ^{1}D non-polar column (0.25 mm I.D.) (orange, FID 1) and separated TAGs on the ^{2}D column (blue, FID 2); t_R represents ^1t_R or ^2t_R for FID 1 and FID 2 respectively. (B) Separation of TAG peaks on the ^{2}D column at different gas flow rates, detected by FID 2 using the experimental conditions 1–6 as shown in Table 1. The target fractions were trapped at the ^{2}D inlet until all TAGs eluted from the ^{1}D column. The T program was initially the same as that in Fig. 2 then the oven was cooled to 80 °C (60 °C/min). The CT CO_2 flow was stopped, then the oven T increased again to 340 °C (15 °C/min), and held until all TAGs eluted from the ^{2}D column. (For interpretation of the references to colour in this figure legend, the reader is referred to the web version of this article.)

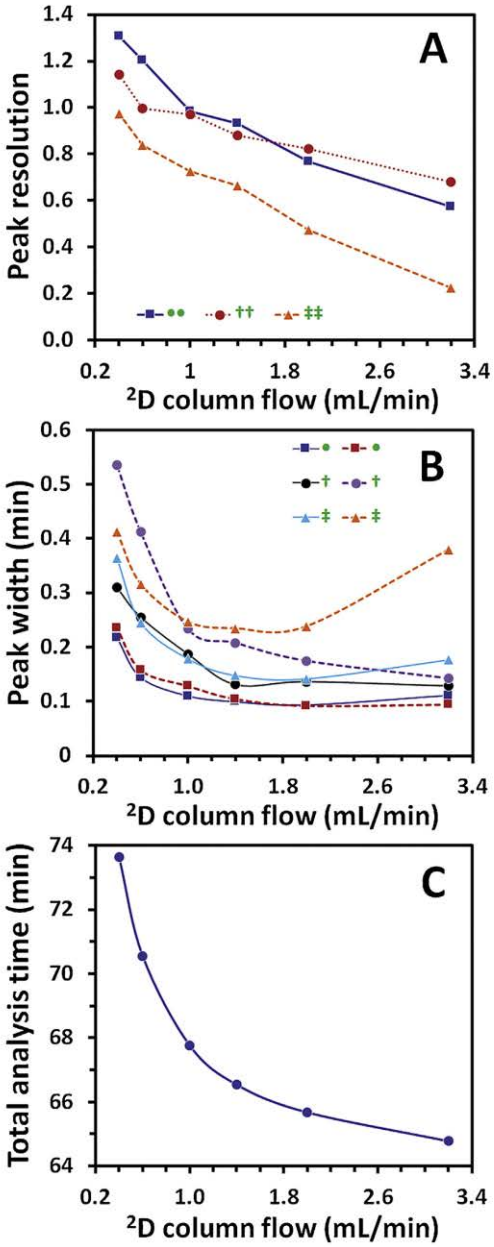

Fig. 4. Graphs showing (A) change in peak resolution with ^{2}D column flow rate calculated using peak pairs as marked by ●, †, and ‡ in Fig. 3B; (B) peak width with ^{2}D column flow rate for peaks as marked in Fig. 3B, peak width for 1st and 2nd peaks of the same mark are represented by solid line and dashed line curves respectively; and (C) total analysis time at different flow rate on ^{2}D column, obtained from each chromatogram in Fig. 3B.

3.2. Column flow optimisation

Generally constant flow mode carrier gas was used for both ^{1}D and ^{2}D columns to effect separation. Two flow programs were used for each run; the first program was used to provide effective separation of groups of TAGs on the ^{1}D column, without necessarily trying to maximise resolution within the groups; the second flow program was then chosen so as to separate TAGs on the ^{2}D column, via H/C transfer and trapping at the inlet of the ^{2}D column. Effective operation of H/C analysis using a DS device requires use of a ^{2}D column flow significantly higher than the ^{1}D column flow in order to use flow to switch the direction of carrier gas. The ^{2}D column flow velocity will likely be higher than an optimum flow in ^{2}D. The 2nd flow program was applied here in order to reduce ^{2}D column flow (to a more optimal setting) subsequent to the H/C event, changing to the 2nd flow program just before the trapped TAG molecules were released to the ^{2}D column and the 2nd T program commenced. The 1st flow program was 2 mL/min on the ^{1}D column, and 4.4 mL/min on the ^{2}D column; the latter flow did not affect the quality of ^{2}D separation, since this was only used prior to the start of ^{2}D separation. The subsequent 2nd flow program in the ^{2}D column was lower than that during the first step, and was adjusted to give better separation of TAGs on the ^{2}D column.

Sub-samples taken across the two major peaks (**4** & **6**) and H/C of each of the three latter minor peaks (**3, 5** & **7**) were transferred and simultaneously trapped at the ^{2}D column inlet, and then released at different ^{2}D carrier gas flow rates to study the effect of flow rate

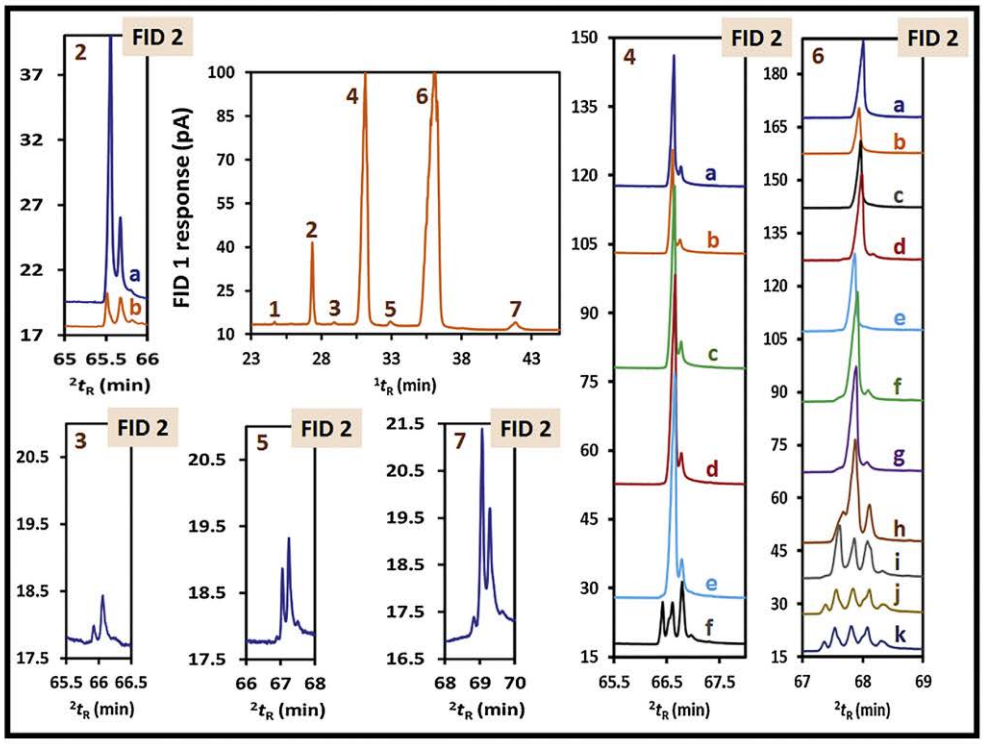

Fig. 5. Chromatograms showing the TAG peaks (peaks 2–7) separated in the ^{1}D non-polar column (0.25 mm I.D.), which were H/C according to different sampling strategies across each peak, trapped, then further separated on the ^{2}D mid-polarity column and detected by FID 2 using flow condition 2 (see Table 1). Column set I and the same T program as used in Fig. 3. a-k correspond to H/C zones from the front to rear part of the respective peaks.

on ^{2}D column separation (Fig. 3); the ^{2}D column flow was varied from 3.2 to 0.4 mL/min (Fig. 3B).

The resolutions of some of the adjacent peaks shown as marked at the top (●, †, ‡) were calculated (Fig. 4A). Peak resolution increased, with more peaks closer to being baseline separated, as the flow decreased. The values range from 0.22 to 1.31, for poorly resolved peaks at 3.2 mL/min to almost baseline resolved peaks at 0.4 mL/min respectively. Simultaneously, the peak height decreased and peak width increased significantly as the flow rate became lower. Peak widths were measured according to changes in ^{2}D column flow rate (Fig. 4B). In general, the peak width was about constant or marginally increased as flow rate decreased from 3.2 mL/min to 1 mL/min (except for one of the peaks labelled ‡, where an overlapping peak increased the apparent peak width at 3.2 mL/min), then increased somewhat more rapidly with a flow rate <1 mL/min. Whilst the peak width increased rapidly at lower flow rate, as expected, this corresponded to an increased resolution. In general the increase in elution range of the TAGs was greater than the increase in their peak widths (Fig. 3B) – leading to greater resolution, somewhat following the efficiency expected from a van Deemter relationship. While the reduction in flow rate increases peak resolution, it also reduces the detectability of minor TAGs, attributed to broader and smaller peaks, as evidenced at a flow rate of <0.4 mL/min. A flow rate a little higher than 0.4 mL/min (e.g. 0.6 mL/min) on the ^{2}D column is considered sufficient for improved resolution with acceptable detection of minor TAGs with column set I. On the other hand, such a low flow rate requires longer analysis time. Retention time increased by nearly 9 min when the flow rate decreased from 3.2 to 0.4 mL/min (Fig. 4C). Compared to the gain in peak resolution, which is a 2–5 fold increase as flow rate decreased, the increase in analysis time might be considered less significant or relevant. However, there should be a compromise between the level of separation needed and the time of analysis that the analyst affords.

3.3. Target H/C analysis of different regions of the main peaks

Regions across the peaks from the ^{1}D run (Fig. 5) were sampled and separated on the ^{2}D column using flow condition 2 (Table 1), to observe the number of TAG components that can be further separated within the individual ^{1}D peaks. The two bigger ^{1}D peaks (**4** and **6**) were H/C using 6 s H/C windows, while peak **2** was sampled using two 12 s H/C to the ^{2}D column. The minor peaks (**1**, **3**, **5** and **7**) were each sampled as one discrete H/C. The two major peaks (**4** and **6**) generated a greater number of clearly separated TAG peaks (on the ^{2}D mid-polarity column) than any of the other ^{1}D peaks. The number of resolved components depended on the sampled H/C region of the major peak. H/C samples from the front and the middle parts gave only 1 or 2 separated peaks on the ^{2}D column (see **a**–**e** and **a**–**g** chromatograms of major peaks (**4**) and (**6**) respectively in Fig. 5) whereas samples from the rear parts of the two peaks resulted in up to 5 TAG peaks (see **f** and **h**–**k** chromatograms for peaks (**4**) and (**6**) respectively), with peak **6** giving the greatest number of separated TAGs (**j** and **k**). While there is no doubt that the peaks generated from one H/C sampling represent different separated TAG molecules, that had been overlapped in the ^{1}D separation, it is not possible from this experiment to confirm whether the peaks from different sampling zones that happen to have the same ^2t_R represent different TAG molecules. The minor peaks and the major peak (**2**) each generated only two clearly sep-

arated larger TAG peaks (plus some trace peaks), for example see **a** and **b** for the major peak (**2**) in Fig. 5.

The regions of the three major peaks, that generate a greater number of separated TAG peaks, and the full regions of the latter three minor groups of peaks were all sampled and trapped in the one cryotrap event, and then all released simultaneously and further separated on the ^{2}D column (Fig. 6). This was performed in order to demonstrate the total number of TAGs that can be resolved in a single run. A total number of 23 TAG peaks were observed on the ^{2}D column (Fig. 6C). As indicated above, separation on the ^{2}D column was relatively good at the lower flow rate of 0.6 mL/min, with acceptable response height (Fig. 6B). The ^{1}D and ^{2}D retention time of the separated TAGs are given in Table S1. From Fig. 6C, complete TAG separation in olive oil will be difficult. While it is relatively easy to separate standard TAG mixtures with few components, and also of TAGs that are prepared with similar concentration, achieving adequate separation of olive oil TAGs and especially of minor TAGs that might overlap major components on the ^{2}D column is not easily accomplished. In previous investigation using GC–MS with an Rtx-65 column (30 m × 0.32 mm I.D. × 0.1 μm), Ruiz-Samblás et al. [10] were able to separate only 8 TAG peaks, with some incomplete separations, in an olive oil sample compared to the separation of a fourteen component TAG standard mixture used to simulate olive oil. The number of TAGs found in trace amounts in olive oil could also exacerbate this separation problem if the separation system has inadequate peak capacity. When used as a ^{1}D column, Rtx-65 (11.5 m × 0.25 mm I.D. × 0.1 μm) displayed 15 separated TAG peaks (Fig. S1) compared to the 23 TAG peaks separated by this column when used as a ^{2}D column. Andrikopoulos et al. [24] reported use of GC–FID to separate and identify 16 TAGs in olive oil using a single Rtx-65 column (30 m × 0.25 mm I.D. × 0.1 μm).

3.4. Comprehensive H/C experiment using column set II

A comprehensive sequential heart cutting method of ^{1}D TAG peaks covering the region between 14 to 24 min, for peaks **2**–**6** (Fig. 7A) was made using column set II. The selected ^{1}D column was a wide bore non-polar column with a relatively short length of 10 m. This was chosen in order to enhance loading capability to improve detection of minor TAGs, and to reduce overall analysis time for the ^{1}D separation. A 1st flow program of 4 and 8.4 mL/min for ^{1}D and ^{2}D columns respectively was used to separate TAGs on the ^{1}D column, while a 2nd flow program of 0.1 and 0.5 mL/min on ^{1}D and ^{2}D columns respectively was used to separate TAGs on the ^{2}D column. Glyceryl triheptadecanoate was used as an internal standard (IS) to correct retention time shifts (which were observed to be within ± 3.2 s in this study) in the ^{2}D column in the sequential runs. The IS positions for the ^{1}D GC analysis with the DS 'off', and ^{2}D result are shown in Fig. 7A and B, respectively. The sampling time for each H/C was 6 s. The comprehensive sequential H/C approach was performed in such a way that first the region between 14 to 24 min was divided into three equal regions. Then the sampling of each sub-region was made within the same run starting from the lower retention time and moving to the higher retention time. The sampled TAGs from all three regions were trapped together in the cryotrap and simultaneously released for separation on the ^{2}D column. For example, H/C samples from 14.0–14.1 min, 17.3–17.4 min and 20.6–20.7 min were analysed in the first analysis and then 14.1–14.2 min, 17.4–17.5 min and 20.7–20.8 min were analysed in the second analysis, and so on until the whole region from 14 to 24 min was covered. This strategy was used so as to reduce the total time, and with the expectation that the early, middle and latter sampled zones will not lead to overlap of the components from each region, but with improved resolution for each zone. In each analytical separation, an additional H/C comprising the IS (16.5–16.6 min) was also H/C and cryotrapped at the start of the ^{2}D column. This strategy decreased the number of runs that needed to be performed in order to cover the whole region using sequential H/Cs of 6 s, with 33 separate injections made. The three regions that were sampled together should have a clear difference in their retention time on the ^{2}D column so that peak assignment to the respective H/C region on the ^{1}D is not difficult (Fig. 7B).

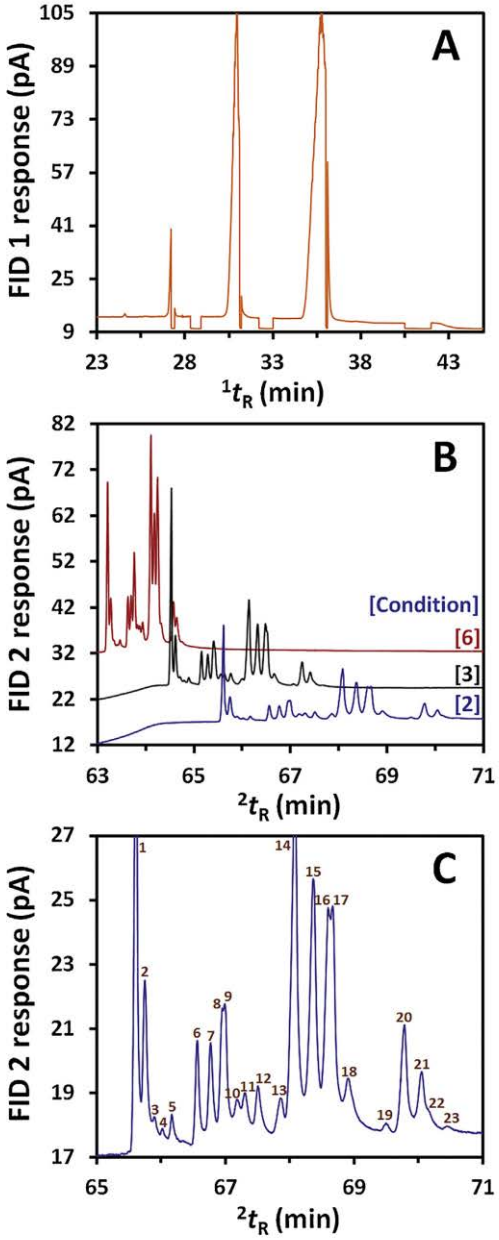

Fig. 6. GC–FID chromatogram showing (A) sub-sampled regions of the major TAG peaks and H/C of the minor peaks of the ^{1}D eluent, which were trapped in one cryotrap event and released for ^{2}D separation; (B) separated TAGs on a ^{2}D mid-polarity column at flow rates of 3.2 mL/min, 1 mL/min and 0.6 mL/min using flow conditions 6, 3 and 2 respectively (see details in Table 1); and (C) number of separated TAGs on the ^{2}D column, at flow rate of 0.6 mL/min (see details of the flow condition 2 in Table 1) using column set I and the same temperature program as that in Fig. 3.

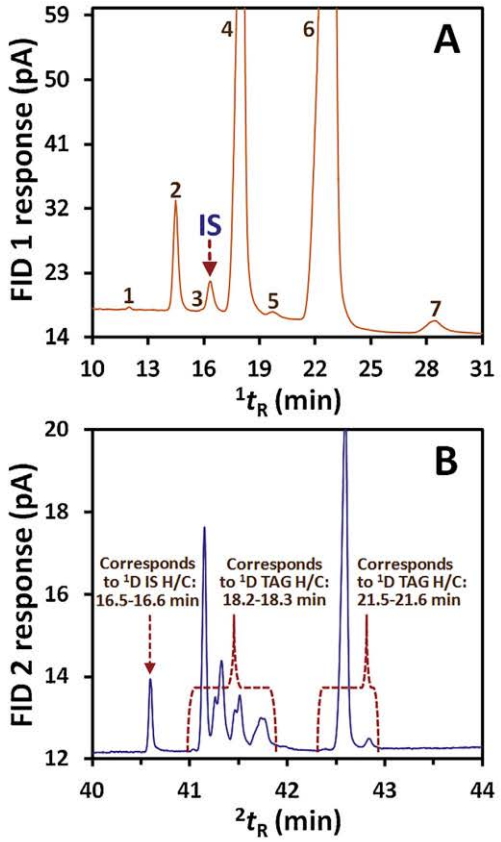

Fig. 7. (A) GC–FID 1 chromatogram of olive oil TAGs plus glyceryl triheptadecanoate IS on the ^{1}D non-polar column (0.32 mm I.D.) using column set II. The ^{1}D and ^{2}D column flows were 4 and 8.4 mL/min, respectively, with the same T program as that in Fig. 2 except with an initial T of 250 °C, and (B) GC–FID 2 of olive oil TAGs and the IS on the ^{2}D column using flow condition of 0.1 mL/min and 0.5 mL/min on ^{1}D and ^{2}D respectively, column set II and the same temperature program as that in Fig. 3 except that the initial temperature was set to 250 °C (held for 0.5 min). For analysis in (B), the sampled regions of ^{1}D were from 14.9–15.0 min, 18.2–18.3 min and 21.5–21.6 min for olive oil TAGs, plus from 16.5–16.6 min for IS. The 14-9 –15.0 H/C gave no TAG peaks.

Fig. 8 shows the 2D plot of the TAGs that are separated using column set II, which is a reconstructed plot using the full multi-injection comprehensive strategy. As shown earlier, each TAG peak on the ^{1}D column gave ≥2 separated TAG peaks on the ^{2}D column. The three major peaks generated the largest number of separated TAGs, with each generating ≥5 peaks. Since FID detection is used, peaks with similar ^2t_R are considered the same compound even though they might be sampled from different 6 s regions across a given ^{1}D peak. Without MS data, this cannot be tested. Accordingly, 5 of the 7 TAG peaks (peaks **2**–**6**) obtained from ^{1}D separation resulted in ≥26 TAGs for the ^{2}D analysis. Considering the TAG from peak **1**, which was described earlier in Section 3.1 as a TAG with 48 CN, and TAGs from peak **7**, which was separated into two TAG peaks (Section 3.3), this strategy yields about 29 total TAGs separated in this study. Using Rtx-65 (0.25 mm) as a single column only 15 TAG peaks were separated (Fig. S1). The number of TAG peaks generated by this comprehensive H/C method might be further improved, *e.g.* by hyphenation with mass spectrometry with additional capability to perform peak deconvolution, total molar mass assessment, and spectrum interpretation for fatty acid residue identification.

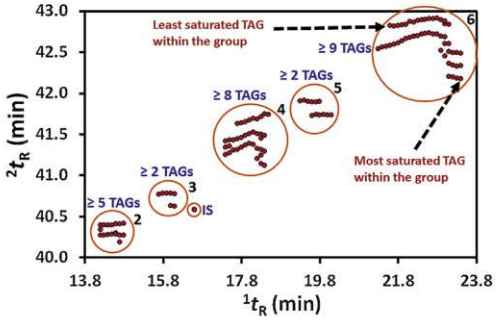

Fig. 8. Two dimensional plot showing number of separated TAGs using column set II. The flow condition was 4 and 8.4 mL/min on ^{1}D and ^{2}D respectively for the ^{1}D separation, and 0.1 and 0.5 mL/min on ^{1}D and ^{2}D respectively for the ^{2}D separation. The same T program as in Fig. 3 was applied except the initial T was set to 250 °C, with 0.5 min hold before the 2nd T ramp.

TAGs are expected to elute on ^{1}D non-polar and ^{2}D mid-polarity columns according to increasing carbon number in the first instance. They also elute based on their degree of unsaturation, with either shorter retention or greater retention on the ^{1}D (non-polar) and ^{2}D (mid-polarity) columns with increased unsaturation, respectively, within the same carbon number. This gives the possibility to label the TAG peak degree of unsaturation, within a group of peaks in this separation. Within each group of the same carbon number, the most saturated TAGs are those with higher ^1t_R and lower ^2t_R and the most unsaturated ones are those with the opposite t_R trend (Fig. 8).

Olive oil is known to contain mainly TAGs with CN of 50 (with two C_{16} and one C_{18} acyl groups), 52 (with one C_{16} and two C_{18} acyl groups), and 54 (with three C_{18} acyl groups), and they elute in increasing order of retention times with total CN on both polar and non-polar columns [10,14,23]. Thus, it is possible to label the main TAG groups (**2**, **4** and **6**) in Fig. 8 with total CN of 50, 52 and 54. But it is not clear whether the two smaller groups (**3** and **5**) belong to the main groups having different number of double bonds, or are groups with different total CN (possibly with odd CN). Peak **7** (not covered in the comprehensive study) with much higher ^1t_R may correspond to TAGs with higher CN, such as those with 56 CN (with two C_{18} and one C_{20} acyl groups) [6].

Where the TAG composition is known it could be possible to tentatively identify the separated TAGs within each group based on their elution behaviour on polar or mid-polarity columns. Olive oil TAGs composition reported in the literature are often dependent on the specific method of separation and detection used, for example oleoyl-oleoyl-linoleoyl (OOL) was reported at 9.8–16.7% using HPLC while it was not detected using CGC–FID [6]. It is also believed that the current method has revealed more TAGs than that previously reported in the literature. Thus, tentative identification of the separated TAGs based on literature results was not attempted in this study.

4. Conclusion

This study demonstrates method development of a H/C MDGC strategy under suitable flow and elevated T program conditions for analysis of TAG components in olive oil. The approaches involved use of independent flow and T programs for each dimension of separation. For the analytical ^{2}D separation, target H/C analysis generated higher resolution for TAG peaks by employing a reduced flow rate, which accompanied somewhat broader peaks and decreased sensitivity; this results in a compromise between separation quality and detectability of TAGs. Using the final devel-

oped condition, a comprehensive MDGC approach provided a significantly increased number of detected TAGs (≥29 peaks) compared to 1DGC (15 peaks). The system was found to be sufficiently stable to allow extended sampling for multiple H/C required for comprehensive H/C analysis of the TAG groups. The separation quality in this method is improved over the recently established GC×GC approach for TAG analysis [20], due to the use of a longer ^{2}D column, with effective flow control that improves efficiency, and T programs for the ^{2}D separation. By addition of an internal standard that is also H/C to the ^{2}D column which acts as a retention time marker and allows correction of retention data, a reliable comprehensive 2DGC result can be established, which should be possible to apply in a straightforward manner to analysis of more complex samples such as fish oil.

Acknowledgements

HDW acknowledges provision of MGS and DIPRS Scholarships from Monash University. This work was conducted under support from the Australian Research Council and PerkinElmer through ARC Linkage Grant LP150100465.

Appendix A. Supplementary data

Supplementary data associated with this article can be found, in the online version, at https://doi.org/10.1016/j.chroma.2018.03.037.

References

[1] F. Marini, Triacylglycerols: characterization and determination, in: Encyclopedia of Food and Health, Academic Press Oxford, 2016, pp. 345–350.
[2] M. Buchgraber, F. Ulberth, H. Emons, E. Anklam, Triacylglycerol profiling by using chromatographic techniques, Eur. J. Lipid Sci. Technol. 106 (2004) 621–648.
[3] P. Mareš, High temperature capillary gas liquid chromatography of triacylglycerols and other intact lipids, Prog. Lipid Res. 27 (1988) 107–133.
[4] T. Řezanka, K. Pádrová, K. Sigler, Regioisomeric and enantiomeric analysis of triacylglycerols, Anal. Biochem. 524 (2017) 3–12.
[5] K. Ben Arfa, M. de Person, D. Hmida, J. Bleton, S. Boukhchina, A. Tchapla, S. Héron, F. Moussa, UHPLC-APCI-MS profiling of triacylglycerols in vegetable oils—application to the analysis of four North African sesame seed varieties, Food Anal. Methods 10 (2017) 2827–2838.
[6] N.K. Andrikopoulos, Triglyceride species compositions of common edible vegetable oils and methods used for their identification and quantification, Food Rev. Int. 18 (2002) 71–102.
[7] V. Ruiz-Gutiérrez, L.J.R. Barron, Methods for the analysis of triacylglycerols, J. Chromatogr. B: Biomed. Sci. Appl. 671 (1995) 133–168.
[8] N. Hu, F. Wei, X. Lv, L. Wu, X.-Y. Dong, H. Chen, Profiling of triacylglycerols in plant oils by high-performance liquid chromatography–atmosphere pressure chemical ionization mass spectrometry using a novel mixed-mode column, J. Chromatogr. B 972 (2014) 65–72.
[9] M. Fasciotti, A.D. Pereira Netto, Optimization and application of methods of triacylglycerol evaluation for characterization of olive oil adulteration by soybean oil with HPLC–APCI-MS–MS, Talanta 81 (2010) 1116–1125.
[10] C. Ruiz-Samblás, A. González-Casado, L. Cuadros-Rodríguez, F.P.R. García, Application of selected ion monitoring to the analysis of triacylglycerols in olive oil by high temperature-gas chromatography/mass spectrometry, Talanta 82 (2010) 255–260.
[11] P.A. Sutton, S.J. Rowland, High temperature gas chromatography-time-of-flight-mass spectrometry (HTGC–ToF-MS) for high-boiling compounds, J. Chromatogr. A 1243 (2012) 69–80.
[12] C. Ruiz-Samblás, F. Marini, L. Cuadros-Rodríguez, A. González-Casado, Quantification of blending of olive oils and edible vegetable oils by triacylglycerol fingerprint gas chromatography and chemometric tools, J. Chromatogr. B: Anal. Technol. Biomed. Life Sci. 910 (2012) 71–77.
[13] N.K. Andrikopoulos, Chromatographic and spectroscopic methods in the analysis of triacylglycerol species and regiospecific isomers of oils and fats, Crit. Rev. Food Sci. Nutr. 42 (2002) 473–505.
[14] B.X. Mayer, E. Lorbeer, Triacylglycerol mixture for testing capillary columns for high-temperature gas chromatography, J. Chromatogr. A 758 (1997) 235–242.
[15] F. Wei, S.X. Ji, N. Hu, X. Lv, X.Y. Dong, Y.Q. Feng, H. Chen, Online profiling of triacylglycerols in plant oils by two-dimensional liquid chromatography using a single column coupled with atmospheric pressure chemical ionization mass spectrometry, J. Chromatogr. A 1312 (2013) 69–79.
[16] M. Beccaria, R. Costa, G. Sullini, E. Grasso, F. Cacciola, P. Dugo, L. Mondello, Determination of the triacylglycerol fraction in fish oil by comprehensive liquid chromatography techniques with the support of gas chromatography and mass spectrometry data, Anal. Bioanal. Chem. 407 (2015) 5211–5225.
[17] Y. Nolvachai, C. Kulsing, P.J. Marriott, Thermally sensitive behavior explanation for unusual orthogonality observed in comprehensive two-dimensional gas chromatography comprising a single ionic liquid stationary phase, Anal. Chem. 87 (2015) 538–544.
[18] P.J. Marriott, S.-T. Chin, B. Maikhunthod, H.-G. Schmarr, S. Bieri, Multidimensional gas chromatography, TrAC Trends Anal. Chem. 34 (2012) 1–21.
[19] Y. Nolvachai, C. Kulsing, P.J. Marriott, Multidimensional gas chromatography in food analysis, TrAC Trends Anal. Chem. 96 (2017) 124–137.
[20] F.J.M. Novaes, C. Kulsing, H.R. Bizzo, F.R. de Aquino Neto, C.M., Rezende, P.J. Marriott, Analysis of underivatised low volatility compounds by comprehensive two-dimensional gas chromatography with a short primary column, J. Chromatogr. A 1536 (2018) 75–81.
[21] P.Q. Tranchida, D. Sciarrone, P. Dugo, L. Mondello, Heart-cutting multidimensional gas chromatography: a review of recent evolution, applications, and future prospects, Anal. Chim. Acta 716 (2012) 66–75.
[22] A.X. Zeng, S.-T. Chin, P.J. Marriott, Integrated multidimensional and comprehensive 2D GC analysis of fatty acid methyl esters, J. Sep. Sci. 36 (2013) 878–885.
[23] E. Geeraert, P. Sandra, Capillary GC of triglycerides in fats and oils using a high temperature phenylmethylsilicone stationary phase, part I, J. High Resolut. Chromatogr. 8 (1985) 415–422.
[24] N.K. Andrikopoulos, I.G. Giannakis, V. Tzamtzis, Analysis of olive oil and seed oil triglycerides by capillary gas chromatography as a tool for the detection of the adulteration of olive oil, J. Chromatogr. Sci. 39 (2001) 137–145.

4.3. Supporting information

High temperature multidimensional gas chromatographic approach for improved separation of triacylglycerols in olive oil

Habtewold D. Waktola, Chadin Kulsing, Yada Nolvachai, Philip J. Marriott

Journal of Chromatography A

Contents

Table S1. First and second dimension retention times of TAG peaks in Figure 6C.

Peak number	$^{1}t_{R}$ (min)	$^{2}t_{R}$ (min)	Peak number	$^{1}t_{R}$ (min)	$^{2}t_{R}$ (min)
1	27.3	65.616	13	36.05	67.878
2	27.3	65.756	14	36.05	68.085
3	27.3	65.905	15	36.05	68.375
4	28.6	66.036	16	36.05	68.608
5	28.6	66.178	17	36.05	68.675
6	31.15	66.568	18	36.05	68.928
7	31.15	66.775	19	41.25	69.518
8	31.15	66.958	20	41.25	69.788
9	31.15	66.995	21	41.25	70.063
10	31.15	67.2	22	41.25	70.121
11	32.6	67.135	23	41.25	70.481
12	32.6	67.518			

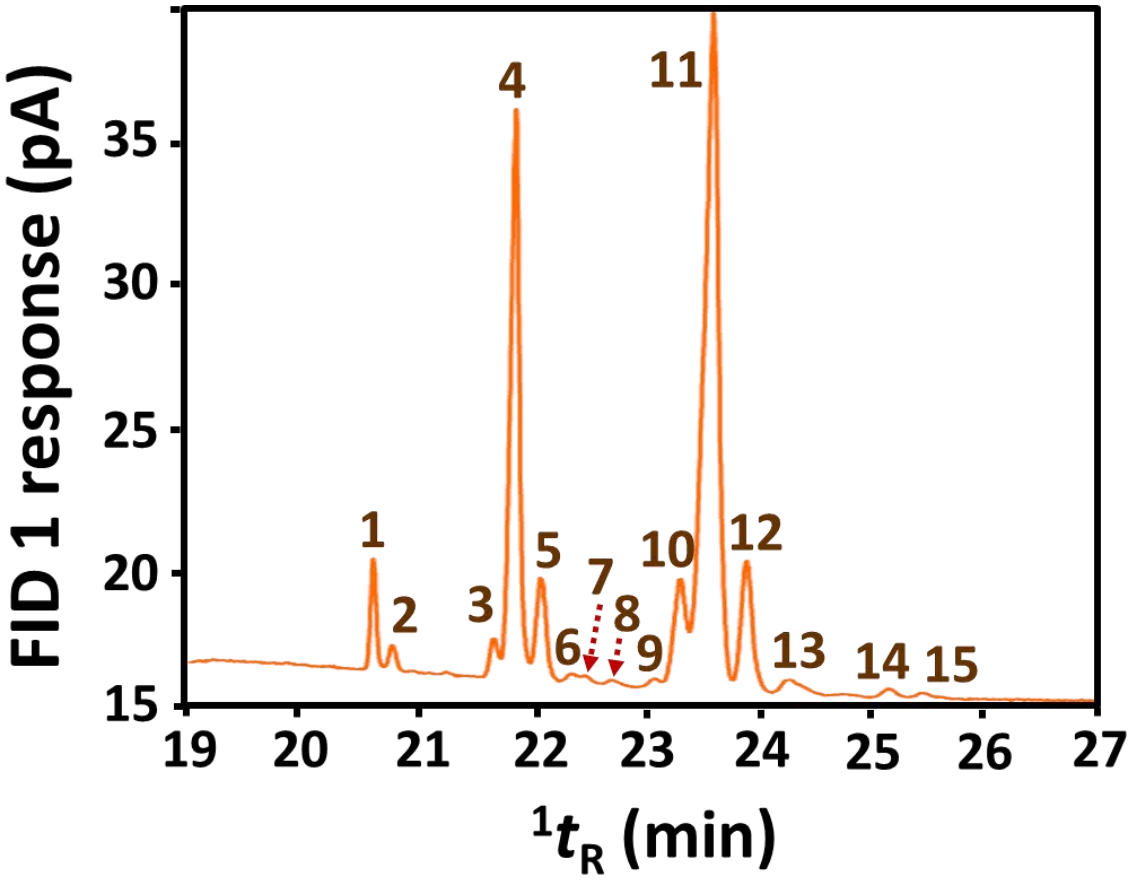

Fig. S1. GC-FID chromatogram of olive oil TAGs on the ^{1}D Rtx-65 column (0.25 mm I.D.). The oven temperature program commenced at 60 °C, was increased to 340 °C (15 °C/min), then held for 9 min. Isothermal conditions commence at 18.67 min, so all TAGs elute during the isothermal hold region. The ^{1}D column flow was 1.5 mL/min.

Chapter 5

Multidimensional gas chromatographic–mass spectrometric method for separation and identification of triacylglycerols in olive oil

Habtewold D. Waktola, Yada Nolvachai, Philip J. Marriott

Australian Centre for Research on Separation Science, School of Chemistry, Monash University, Wellington Road, Clayton, VIC 3800, Australia

Published in Journal of Chromatography A, 1629 (2020) 461474
doi.org/10.1016/j.chroma.2020.461474

Contents

5.1. Chapter overview

In Chapter 4, the study focus was to evaluate the likely separation of olive oil TAGs using H/C MDGC, which was demonstrated but apart from the use of a few selected standard, their identification was not investigated. Identification of TAG components in olive oil is crucial because TAG composition can be used to verify the authenticity or determine the adulteration of the oil. For instance, the IOC method for determination of extraneous oils in olive oil is based on the determination of TAG composition. However, the IOC method, being a 1D GC method, is limited to group type separation according to total CN of the TAGs and reports TAG content of olive oil as the percentage of TAGs with specific CN. Thus, the present Chapter builds on Chapter 4 with a focus on the MDGC separation with MS identification of olive oil TAGs.

A H/C MDGC–MS method for separation and identification of TAGs in EVOO was developed. A GC configuration, comprising a non-polar ^{1}D column (SLB-5MS; 15 m × 0.25 mm I.D. × 0.25 μm d_f) and mid-polarity ^{2}D column (Rtx-65; 9 m × 0.25 mm I.D. × 0.1 μm d_f), was employed. Standard TAGs were used to evaluate and demonstrate the H/C MDGC method, for identification of TAG components, and to validate the method. Glyceryl triheptadecanoate with fully saturated C17 substituents, was used as IS to account for any retention time shift which may occur, and variation in response from analysis to analysis. Various chromatographic conditions such as column flow and temperature program were evaluated.

The ^{1}D separation resulted in overlap of some standard TAG peaks, which were clearly separated into groups, largely based on CN. These overlapped ^{1}D regions of the standard TAGs were H/C to ^{2}D for further separation, and resulted in clearly distinguished individual TAG component peaks. The ^{1}D separation of olive oil TAGs displayed three major peaks and four minor peaks. The application of the H/C MDGC method to olive oil TAGs resulted in the separation of each sampled ^{1}D region into two or more TAG peaks. The MS detectability of

the minor TAG peaks was increased through use of multiple injection with repeated sampling to ^{2}D and preconcentration by trapping in the cryotrap (multiple injection directly into a cryotrap will be inappropriate) before releasing them to complete the ^{2}D separation. TAG components in olive oil resolved on the ^{2}D column were identified based on characteristic mass fragment ions such as $[M\text{-}RCO_2]^+$, $[RCO+128]^+$, $[RCO+74]^+$ and RCO^+ and comparison of their mass spectra with that of the standard TAGs. Sixteen olive oil TAGs were identified by MS after ^{2}D separation. The repeatability of the H/C method was evaluated in terms of retention time shift and area response in the ^{2}D and found to be <0.02% and <8% RSD respectively.

Thus, the MDGC–MS method demonstrated separation and identification of many olive oil TAG components; it was found to be sufficiently reproducible, although the sensitivity of the MS for detection of minor TAG components was reduced as compared to the FID (detailed in Chapter 4). The method can be applied to different complex samples such as fat and oil samples. This study can open a door for further study into high boiling point compounds using MDGC separation techniques.

5.2. Article

Journal of Chromatography A 1629 (2020) 461474

Contents lists available at ScienceDirect

Journal of Chromatography A

journal homepage: www.elsevier.com/locate/chroma

Multidimensional gas chromatographic–Mass spectrometric method for separation and identification of triacylglycerols in olive oil

Habtewold D. Waktola, Yada Nolvachai, Philip J. Marriott*

Australian Centre for Research on Separation Science, School of Chemistry, Monash University, Wellington Road, Clayton, VIC 3800, Australia

ARTICLE INFO

Article history:
Received 11 May 2020
Revised 10 July 2020
Accepted 10 August 2020
Available online xxx

Keywords:
Triacylglycerols
Olive oil
'Heart-cut' multidimensional gas chromatography
Mass spectrometry

ABSTRACT

A 'heart-cut' multidimensional gas chromatography–mass spectrometry (H/C MDGC–MS) method for separation and identification of triacylglycerols (TAGs) in extra virgin olive oil was developed. A GC configuration, comprising a non-polar first dimension (^{1}D) column (15 m length) and a mid-polarity second dimension (^{2}D) column (9 m length), was employed. Standard TAGs were used to test and demonstrate the H/C MDGC method, for identification of TAG components and to validate the method. Various chromatographic conditions such as column flow and temperature program were evaluated. The ^{1}D separation resulted in overlap of some standard TAG peaks. These overlapped ^{1}D regions of the standard TAGs were H/C to ^{2}D for further separation and resulted in clearly distinguished individual TAG component peaks. The ^{1}D separation of olive oil TAGs displayed three major peaks and four minor peaks. The application of the H/C MDGC method to olive oil TAGs resulted in the separation of each sampled ^{1}D region into two or more TAG peaks. TAG components in olive oil resolved on the ^{2}D column were identified based on characteristic mass fragment ions such as $[M–RCO_2]^+$, $[RCO+128]^+$, $[RCO+74]^+$ and RCO^+ and comparison of their mass spectra with that of the standard TAGs. Sixteen olive oil TAGs were identified by MS after ^{2}D separation. The repeatability of the H/C method was evaluated in terms of retention time shift and area response in the ^{2}D and found to be <0.02% and <8% RSD respectively.

1. Introduction

Triacylglycerols (TAGs) are the main components of edible oils and fats, which are an important component of the human diet. The TAG molecule comprises three fatty acid (FA) residues on a central glycerol molecule. The TAG composition of vegetable oils differ based on the FAs from which the TAGs were derived, and on the positions of the FA residues on the glycerol backbone. Thus, TAG fingerprinting can be used for determination of type of vegetable oil, and for authenticity or quality control purposes.

Given its expensive price, extra virgin olive oil (EVOO) is prone to adulteration through addition of cheaper vegetable oils such as hazelnut, soybean, sunflower and corn oils. Studies to verify the authenticity and adulteration of olive oil have focused on the determination of variation in the TAG composition of olive oil, which often is expressed as either the presence or increase in levels of TAG components that normally do not exist or are present in lower levels in olive oil [1–5]. According to the International Olive Council (IOC) method, the presence of extraneous oils in olive oil is determined based on the determination of TAG composition. The method is based on the fact that each type of oil has a characteristic TAG profile which depends on FA composition as well as on the biosynthesis rules [6]. A method for identification and quantification of adulteration of olive oil in terms of blending with other vegetable oils was developed using TAG fingerprinting and chemometric tools [7,8]. Detection of olive oil adulteration was also made by determination of FA composition [9]. Since a similar fatty acid composition does not necessarily indicate equivalence in TAG composition, the determination of the original component, i.e. TAGs, may be preferred to estimation of FA composition [10]. However, there is an IOC method that determines the coherence of olive oil TAG composition with its FA composition. The theoretical TAG composition is calculated from the FA composition, assuming random 1,3- and 2- distribution of FA in the TAG with only restriction of saturated FA on the 2-position, by a computer program. The program calculates several mathematical algorithms from theoretical and experimental TAG compositions, and compares the values with those contained in the database built from genuine olive oils [11].

The determination of TAGs in oil components depends critically on the method of separation and identification used. Various analytical techniques may be used to analyse TAGs in oil samples, which include liquid chromatography (LC), gas chromatography

* Corresponding author.
E-mail address: philip.marriott@monash.edu (P.J. Marriott).

https://doi.org/10.1016/j.chroma.2020.461474
0021-9673/

(GC), thin layer chromatography (TLC), nuclear magnetic resonance (NMR), Raman and infrared spectroscopy [12,13].

Gas chromatography is one of the techniques employed for determination of TAGs in vegetable oils. Since TAGs have relatively large mass with low vapour pressure, this requires use of high temperature GC (HTGC) [14]. HTGC–mass spectrometry (MS) has been used for separation and identification of TAG components in different fat and oil samples including olive oil [15,16], and for the TAG composition of sapucainha oil with direct analysis of TAG and also their component fatty acid methyl esters [17].

One dimensional GC (1D GC) is the usual GC technique applied for determination of TAGs, whereby TAGs analysis is largely limited to group type separation according to the number of double bonds or the total carbon number (CN) distribution of the TAGs, on relatively low polarity GC phases [18]. As a result the IOC recommends a GC method that reports TAG content of olive oil as the percentage of TAGs with specific CN [6]. Similarly, an IOC method that uses HPLC to determine TAG composition in olive oil reports several TAG components that co-elute as unresolved peaks [11]. A HT multidimensional GC (HTMDGC) method that employed dual flame ionisation detectors (FID) was developed for improved separation of TAGs in olive oil [19]. MDGC employs two columns with different selectivity connected sequentially with a device located between these columns offering an effective 'heart-cut' (H/C) or modulation process. In the study mentioned above, a H/C MDGC separation method was employed to reveal overlapping TAG components which otherwise could not be separated and detected using the usual 1D GC method.

In this study, a H/C MDGC–MS method for the separation and identification of TAGs was developed. Relatively short non-polar first dimension (^{1}D) and mid-polarity second dimension (^{2}D) columns were employed to separate TAGs. Standard TAGs mixture was used to develop the method, and it was then applied for the separation of olive oil TAGs.

2. Experimental

2.1. H/C MDGC analysis

A gas chromatograph (Agilent Technologies, 7890A) equipped with a mass spectrometry detector (MSD) (Agilent Technologies, 5975C inert XL MSD with Triple-Axis Detector), flame ionisation detector (FID) and split/splitless inlet was used in this study. The GC was equipped with an Agilent Capillary Flow Technology Deans switch (DS). The DS has one column inlet and two further outlet column channels. In addition, it has two inlet channels to control the switching flows. The employed columns were: ^{1}D; SLB-5ms (15 m × 0.25 mm × 0.25 μm), ^{2}D; Rtx-65 (9 m × 0.25 mm × 0.1 μm) and restrictor – deactivated fused-silica (DFS, 1.72 m × 0.18 mm).

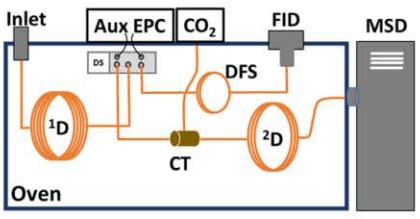

Fig. 1. Configuration of the H/C MDGC system. AUX EPC: pneumatic auxiliary port with electronic pressure control; DS: Deans switch; ^{1}D: ^{1}D column; ^{2}D: ^{2}D column; CT: cryotrap; CO_2: compressed liquid carbon dioxide supply; FID: flame ionisation detector; MSD: mass spectrometer detector; DFS: deactivated fused- silica capillary tubing.

The applied configuration for the H/C MDGC is shown in Fig. 1. This comprises: (1) ^{1}D column connected between the GC inlet and the DS inlet; (2) ^{2}D column connected between one of the DS outlets and the MSD; and (3) a short restrictor column connected between the other DS outlet and the FID. The ^{2}D column passes through a cryofocusing trap (CT) near the column inlet (approximately 10-20 cm from the inlet). Liquid CO_2 was provided as an on-demand flow to CT, which expands as a coolant gas to trap TAGs sampled or heart-cut from the ^{1}D column. CO_2 was supplied to the CT at least 2 min prior to the first H/C event, with target regions of ^{1}D effluent selected based on retention times detected at the FID. The H/C regions of TAGs remain trapped at CT until all TAGs were eluted from the ^{1}D column. The CT CO_2 supply was stopped in order to release TAGs to the ^{2}D column. For this, the oven was cooled to the starting temperature (T) before the CO_2 supply was terminated. Thus, two separate oven T programs were used; one to select the desired H/C regions, and the other to elute the target region(s) after cooling the oven. These are detailed below.

The overall oven T program used was as follows: using a ^{1}D start T of 250 °C, the T was ramped up to 340 °C (15 °C/min), held for 19 min until all TAGs elute from the ^{1}D column. Heart-cut sampling is conducted at the required times. This is referred to as the first T program. The T was then cooled (at -60 °C/min) to the ^{2}D start T of 250 °C; 0.5 min hold (system conditioning). The trapped components were then released by stopping the flow of liquid CO_2 to the CT, and a second T program was applied by ramping the oven T to 340 °C (15 °C/min) and then held until the TAGs eluted from the ^{2}D column. The inlet, FID, MSD transfer line and MSD source T were set at 300, 350, 320 and 250 °C, respectively. Helium was used as a carrier gas. The FID gas flows were hydrogen at 40 mL/min, air at 400 mL/min and nitrogen at 10 mL/min. The full scan mode MSD was over the range *m/z* 700 to 50, with electron ionisation (EI) at 70 eV. All injections in this study were made in the split ratio of 10:1.

Constant flow mode was used throughout the experiment in both columns, with two constant flow programs used. The flow for the ^{1}D separation (1st flow program) elutes TAGs from the ^{1}D column during the 1st T program, while the flow for the ^{2}D separation (2nd flow program) provides separation of TAGs on the ^{2}D column during the 2nd T program. Thus, the ^{1}D and ^{2}D column flows in each program are different. The 1st flow program used 2.1 mL/min and 3.7 mL/min on ^{1}D and ^{2}D, respectively, and the 2nd flow program used 0.1 mL/min and 0.8 mL/min on ^{1}D and ^{2}D, respectively. The initial pressures at the inlet of ^{1}D and ^{2}D were 34.5 psi and 20.5 psi respectively for the 1st flow program and 3.5 psi and 1.8 psi respectively for the 2nd flow program.

The overall flow for the ^{2}D separation of TAGs is preferably lower than that for ^{1}D. The 1st flow program provided a preliminary separation on the ^{1}D column. The DS flow was balanced in order to avoid carrier flow (and solute) leakage to the ^{2}D column while the DS valve was in the off position; all flow is directed from the ^{1}D column flow to the restrictor (no heart-cutting). The DS flow provides H/C to the ^{2}D column using CT cooling for target regions as required during the 1st T program. The 1st flow program was changed to the 2nd flow program prior to the release of cryotrapped solutes and commencement of the 2nd T program. The flow was adjusted to provide an appropriate separation of TAGs on the ^{2}D column. In summary, the TAG regions were sampled from the ^{1}D column, cryotrapped with the ^{2}D flow adjusted, and then separated on the ^{2}D column using the appropriate ^{2}D T program.

The instrument configuration and experimental procedure explained above is similar to the H/C MDGC work done in [19], except the use of MS as the ^{2}D detector instead of FID, different ^{2}D column and restrictor column dimensions, and suitable flow programs used in the new configuration. The basic idea in this study

was to develop a similar method to the previous method with the use of MS as a detector for identification of the TAGs after ^{2}D separation. In addition, method validation and detailed description of MS identification of TAGs in olive oil was conducted. Increase in the detectability of the minor TAG peaks through multiple injections, with repeat sampling to ^{2}D and preconcentration by trapping in the CT was also described. Key elements of the experimental procedures have been summarised here for reference of the reader.

2.2. Sample and standards

EVOO (Cobram Estate®) sample was obtained from Modern Olives (Lara, Victoria, Australia). The sample was dissolved in hexane to give a 0.5% v/v solution, and 1 μL of this solution was injected to the GC for analysis. TAG standards of tripalmitin (PPP), tristearin (SSS), triolein (OOO) and trilinolein (LLL) (from Nu-Chek Prep, Inc., Elysian, MN); and 1,2-palmitin-3-olein (PPO), 1,2-olein-3-linolein (OOL), 1-2-olein-3-palmitin (OOP), 1,2-linolein-3-palmitin (LLP) and 1,2-olein-3-archidin (OOA) (from Larodan AB, Solna, Sweden) were used as reference standard TAGs, where P = palmitic (C16:0), S = stearic (C18:0), O = oleic (C18:1n–9), L = linoleic (C18:2n–6), Ln = linolenic (C18:3n–3), A = arachidic (C20:0) FA respectively. Glyceryl triheptadecanoate (C17:0/C17:0/C17:0, MgMgMg) (Sigma Chemical Co., St. Louis, MO) was used as internal standard. The standard TAGs were dissolved in hexane to give 1000 ppm stock solutions from which lower concentrations were prepared as required. The sequences of the letters are used for convenience and do not necessarily indicate the position of the acyl group on the glycerol moiety.

3. Result and discussion

3.1. H/C MDGC–MS of standard TAGs

H/C MDGC–MS was used to separate TAGs using the GC configuration shown in Fig. 1. Suitable GC conditions such as temperature and gas flow for ^{1}D and ^{2}D separation were selected before performing the H/Cs following previous work using FID as a detector [19]. Ten standard TAGs including the internal standard (IS) were used to demonstrate the H/C MDGC protocol and to determine repeatability and limit of detection (LOD) of the method. The standard TAGs were selected to represent groups of TAGs with different CN and includes those that were reported to be components of olive oil. Glyceryl triheptadecanoate was used as IS to account for retention time shift and variation in response from analysis to analysis.

Fig. 2A shows the GC–FID chromatogram of the standard TAGs mix (each 200 ppm) on the ^{1}D column, directed through the DFS to the FID (Fig. 1). It can be observed that three of the TAG components (peak **5**, SSS, OOL, OOO; all are C18 FA) essentially co-eluted while LLL (peak **6**) partially overlapped with the peak of the three co-eluted TAGs. OOP and LLP (peaks **3** and **4;** also having the same CN) also partially overlapped. Many edible vegetable oils, including olive oil, contain a number of TAG components that have the same CN, which also exist in variable amounts [20]. This leads to most of the TAG components exhibiting some measure of co-elution with other TAG in conventional 1D GC separation of TAGs [15].

The ^{1}D peak comprising co-eluted TAGs (peak **5**) was H/C to the ^{2}D column for further separation (Fig. 2B), including the IS, following the procedure outlined in the experimental section. The TAGs were subsequently separated into individual TAG peaks on the ^{2}D column as shown by the MS result in Fig. 2C. Identifications of the TAG peaks after separation were made by comparison of mass spectra of the peaks of interest, by interpretation with the characteristic mass fragments obtained from the individual standard TAG analysis, as well as $^{2}t_{R}$ (Table 1). The three overlapping TAGs in ^{1}D

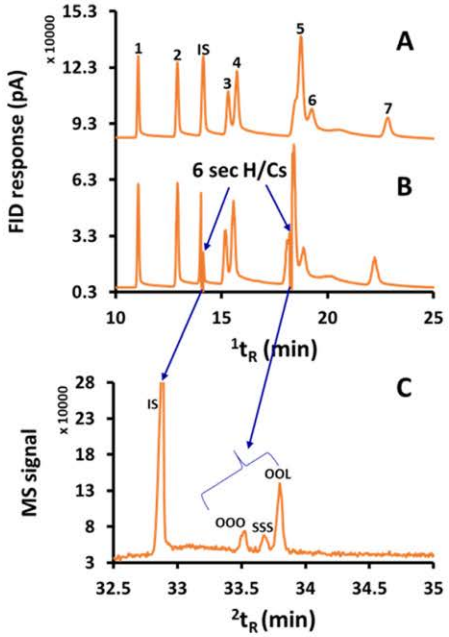

Fig. 2. (A) GC–FID chromatogram of standard TAGs mixture on ^{1}D column using the 1st T and 1st flow programs, no sampling was done; (B) same ^{1}D result as (A) but two peak zones were H/C sampled using a 6 s H/C window, with the sampled TAGs trapped by the CT at the inlet of the ^{2}D column; (C) MS signal of the standard TAGs that were H/C according to the operation in (B) and separated on the ^{2}D column after releasing them from the CT, using the 2nd T and 2nd flow programs. (1) PPP, (2) PPO, (IS) glycerol triheptadecanoate, (3) OOP, (4) LLP, (5) co-eluted SSS, OOO and OOL, (6) LLL (7) OOA.

(peak 5), SSS, OOO and OOL have $^{2}t_{R}$ of 33.56, 33.74 and 33.86 min respectively. Their mass spectra are shown in Fig. 3, with IS given in **Fig. S1**. The $[M–RCO_2]^+$, $[RCO+128]^+$, $[RCO+74]^+$ and RCO^+ mass fragment ions for SSS (Fig. 3A), which is a TAG derived from three stearic acids, have ions of *m/z* 607, 395, 341 and 267 respectively. The corresponding ions for OOO (Fig. 3B) were *m/z* 603, 393, 339 and 265 respectively. In contrast OOL (Fig. 3C) generated $[M–RCO_2]^+$ mass fragment ions with *m/z* 603 and 601, corresponding to $[OO]^+$ and $[OL]^+$ fragment ions respectively. It also generated $[RCO+128]^+$, $[RCO+74]^+$ and RCO^+ fragment ions with *m/z* 391, 337 and 263 respectively, corresponding to the L residue, in addition to these fragment ions corresponding to O (Table 1). The *m/z* 262 ion appeared more prominent than the RCO^+ *m/z* 263 for L, which could be due to the loss of a hydrogen atom from the RCO^+ fragment.

In a separate experiment, the standard TAGs mix was analysed with the DS on, which channels all ^{1}D TAG components to ^{2}D; the CT was off for this operation. All other experimental conditions were kept the same as for the H/C experiment used to separate the co-eluted TAGs discussed above. On ^{2}D the TAG peaks appeared similar to the ^{1}D peaks with co-elution of SSS, OOL and OOO. In this instance, the mass spectrum of the co-eluted TAGs peak shows an unresolved mixture of characteristic fragment ions of all the three TAGs (Fig. 3D).

3.2. Method validation

3.2.1. Repeatability

Retention times and peak area repeatability at MS on the ^{2}D column was determined using a mixture of six standard TAGs (100

Table 1
m/z values of fragment ions for standard TAGs with their respective ^{1}D and ^{2}D retention times.

						m/z of fragment ions			
$^{1}t_R$ (min)	$^{2}t_R$ (min)	TAG	CN:DB	$M^{+\bullet}$	FA residue	$[M–RCO_2]^+$	$[RCO+128]^+$	$[RCO+74]^+$	RCO^+
					P	551	367	313	239
11.2	32.21	PPP	48:0	806	P	551	367	313	239
					P	551	367	313	239
					P	577	367	313	239
13.1	32.69	PPO	50:1	832	P	577	367	313	239
					O	551	393	339	265
					Mg	579	381	327	253
14.3	32.87	MgMgMg (IS)	51:0	848	Mg	579	381	327	253
					Mg	579	381	327	253
					O	577	393	339	265
15.6	33.16	OOP	52:2	858	O	577	393	339	265
					P	603	367	313	239
					L	575	391	337	263
15.9	33.34	LLP	52:4	854	L	575	391	337	263
					P	599	367	313	239
					O	603	393	339	265
18.6	33.74	OOO	54:3	884	O	603	393	339	265
					O	603	393	339	265
					S	607	395	341	267
18.9	33.56	SSS	54:0	890	S	607	395	341	267
					S	607	395	341	267
					O	601	393	339	265
18.9	33.86	OOL	54:4	882	O	601	393	339	265
					L	603	391	337	263
					L	599	391	337	263
19.5	34.12	LLL	54:6	878	L	599	391	337	263
					L	599	391	337	263
					O	633	393	339	265
23.1	34.30	OOA	56:2	914	O	633	393	339	265
					A	603	423	369	295

CN – Carbon number, DB – Total number of double bonds, IS – Internal standard, P – Palmitic (C16:0), Mg – Margaric (C17:0), O – Oleic (C18:1), S – Stearic (C18:0), L – Linoleic (C18:2), A – Arachidic (C20:0)

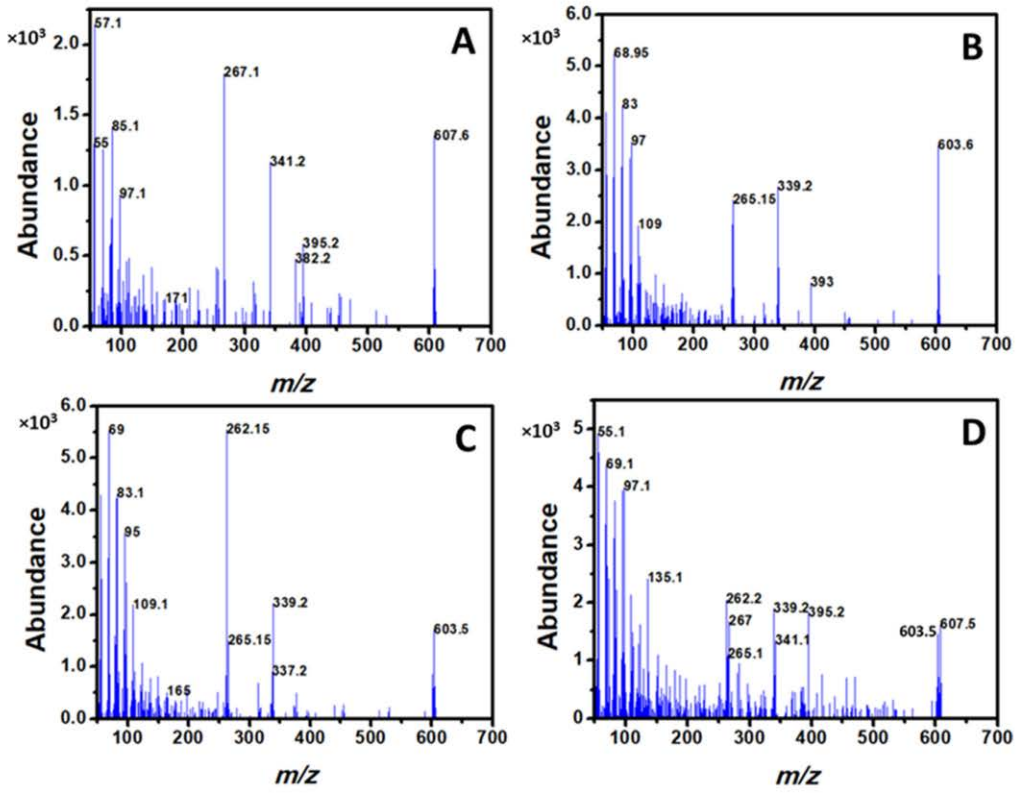

Fig. 3. Mass spectra of standard TAGs (A) SSS; (B) OOO; (C) OOL (D) co-eluted TAGs of SSS, OOL and OOO.

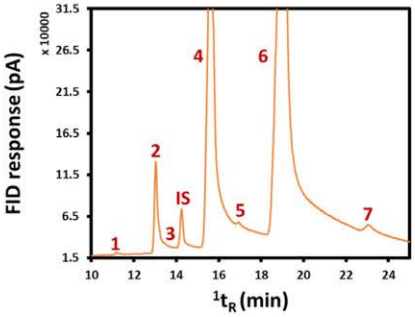

Fig. 4. GC–FID chromatogram of olive oil TAGs plus glyceryl triheptadecanoate (IS) on the ^{1}D column.

ppm each) including the IS. The standard mixture was injected five times to determine repeatability. Repeatability was determined in two different ways: (1) by 'heart-cutting' fractions of the peaks in 6 s H/C windows, and recording their ^{2}D retention times, and (2) by 'heart-cutting' the whole peak of the TAGs from ^{1}D to ^{2}D and again recording ^{2}D retentions. The 6 s H/Cs of each TAG peaks of ^{1}D, which were trapped together in the CT and released to ^{2}D, and their separated peaks on the ^{2}D are shown in the Supplementary Information (**Fig. S2**). The ^2t_R average reproducibility for the 6 s H/Cs approach was found to be 0.011% relative standard deviation (RSD) whereas it was 0.006% RSD for the approach where whole peaks were H/C (chromatogram for this result is not shown) (Supplementary Information **Table S1**). This shows the ^2t_R to be highly repeatable. Shellie *et al.* [21] conducted experiments to determine run-to-run retention time reproducibility in comprehensive two-dimensional gas chromatography using cryogenic modulation for different classes of compounds in essential oil and found an average variation of 0.74% RSD in ^2t_R.

Peak area repeatability for ^{2}D peaks were calculated for both operations as above, i.e. the 6 s H/Cs and the whole peak H/Cs to ^{2}D. RSD of the peak area ratios (peak area of standard TAG/peak area of IS) were calculated for all the five repeated injections. The peak area ratio RSD from 6 s H/Cs was between 1 and 8%% whereas for the whole peak H/Cs it was between 1 and 5%.

3.2.2. Limit of detection (LOD)

The LOD of standard TAGs at MS on the ^{2}D was determined through sampling of the whole peak regions from ^{1}D to ^{2}D. The LOD was determined based on the graphical method, where the standard TAGs were analysed at three levels of concentrations (25, 50 and 100 mg/L) with six repeat measurements for each level. The injections were made with split ratio of 10:1. The standard deviation for repeat measurements and LOD were calculated based on linear dependence that correlates the calculated standard deviations and respective concentrations [22]. To demonstrate the result of this method, five standard TAGs were used. These are generally in the range of 10-20 mg/L (**Table S2**).

3.3. H/C MDGC of olive oil and MS identification of TAG components

Injection of the 0.5% EVOO sample to the GC resulted in three major peaks (**2, 4** and **6**) and four minor peaks (**1, 3, 5** and **7**) of TAGs on the SLB-5 ms ^{1}D column (Fig. 4). The major peaks correspond to those TAGs with CN of 50, 52 and 54. This was confirmed based on the retention times of standard TAGs having similar CN to the TAGs detected in EVOO.

The separation of the EVOO TAGs was performed by 'heart-cutting' the ^{1}D peaks to the ^{2}D column. The separated TAGs were detected by MS and the TAGs were identified based on their mass

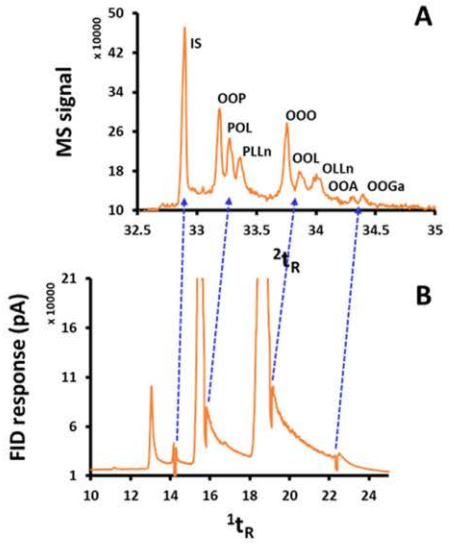

Fig. 5. (A) MS signal response of the olive oil TAGs separated on the ^{2}D column after their release from the CT, using the 2nd T and 2nd flow programs. (B) GC–FID chromatogram of olive oil TAGs on the ^{1}D column using the 1st T and 1st flow programs, showing the 6 s H/C sampled regions of the ^{1}D peaks, which were then trapped by the CT at the inlet of the ^{2}D column.

fragment ions and retention times. The approach here involved two different strategies: either H/C sampling across the 3 major peaks were performed with a 6 s window, or the whole peak was sampled for minor peaks. To reduce the total number of analyses required to cover the whole regions of TAG peaks, multiple and sequential H/Cs were performed as reported elsewhere [19]. Thus the ^{1}D TAGs peak region was divided into 3 equal regions, and each region was H/C and trapped together in the CT, according to the following. For each region, narrow H/Cs were taken; the first H/C from region 1 was combined with the first H/C of region 2, and likewise for region 3. The combined H/C were then analysed on the ^{2}D column. For the second injection, each H/C was incremented so that the second H/C from region 1, 2 and 3 were collected in the CT, then analysed. This continues until all regions were sampled by the narrow H/C process. On the ^{2}D column the sampled TAGs from the major peaks (**2, 4** and **6**) were each separated into 2 or more peaks (Fig. 5). The minor peaks (**1, 3** and **5**) except peak **7**, the latter which was separated into 2 peaks, were not detected by the MS after sampling the whole peaks to the ^{2}D. This may indicate the reduced sensitivity of the MS for detection of the minor TAG components as compared to the FID [19]. Thus, to increase the detectability of these minor TAG peaks multiple injections, with repeat sampling to ^{2}D and preconcentration by trapping in the CT was made, until sufficient amounts to be detectable by MS was collected, before closing the CO_2 supply to release the contents from the CT to complete the ^{2}D separation.

Peak **2** was resolved into three peaks which were identified to be PPO, PPoO and PPL. The $[M–RCO_2]^+$, $[RCO+128]^+$, $[RCO+74]^+$ and RCO^+ mass fragment ions corresponding to the separated TAGs were used for identification. The $[M–RCO_2]^+$ ions with *m/z* 551 and 577 corresponding to $[PP]^+$ and $[PO]^+$ were detected for the PPO peak. In addition the $[RCO+128]^+$, $[RCO+74]^+$ and RCO^+ fragment ions corresponding to O, which were *m/z* 393, 339 and 265, respectively, and the corresponding fragment ions for P, which were *m/z* 367, 313 and 239, respectively, were detected as confirmatory ions for the TAG PPO (Table 2). This was also in agreement with

Table 2
m/z values of fragment ions used for identification of olive oil TAGs with their respective ^{1}D and ^{2}D retention times.

$^{1}t_R$ (min)	$^{2}t_R$ (min)	TAG	CN:DB	M^+	FA residue	*m/z* of fragment ions			
						$[M–RCO_2]^+$	$[RCO+128]^+$	$[RCO+74]^+$	RCO^+
					Po	551	365	311	237
10.9	32.21	PPPo	48:1	804	P	549	367	313	239
					P	549	367	313	239
					P	577	367	313	239
13.1	32.71	PPO	50:1	832	P	577	367	313	239
					O	551	393	339	265
					P	575	367	313	239
13.1	32.82	PPoO	50:2	830	Po	577	365	311	237
					O	549	393	339	265
					P	575	367	313	239
13.1	32.78	PPL	50:2	830	P	575	367	313	239
					L	551	391	337	263
					P	591	367	313	239
13.8	32.64	PMgO	51:1	846	Mg	n.d.	381	327	253
					O	565	393	339	265
					P	n.d.	367	313	239
13.8	32.69	PHO	51:2	844	H	577	379	325	251
					O	563	393	339	265
					Mg	579	381	327	253
14.3	32.89	MgMgMg (IS)	51:0	848	Mg	579	381	327	253
					Mg	579	381	327	253
					O	577	393	339	265
15.6	33.17	OOP	52:2	858	O	577	393	339	265
					P	603	367	313	239
					P	601	367	313	239
15.6	33.29	POL	52:3	856	O	575	393	339	265
					L	577	391	337	263
					P	597	367	313	239
15.6	33.36	PLLn	52:5	852	L	573	391	337	263
					Ln	575	389	335	261
					Mg	603	381	327	253
16.5	33.10	MgOO	53:2	872	O	591	393	339	265
					O	591	393	339	265
					H	603	379	325	251
16.5	33.15	HOO	53:3	870	O	589	393	339	265
					O	589	393	339	265
					O	601	393	339	265
19.0	33.87	OOL	54:4	882	O	601	393	339	265
					L	603	391	337	263
					O	597	393	339	265
19.0	34.01	OLLn	54:6	878	L	599	391	337	263
					Ln	601	389	335	261
					O	603	393	339	265
19.0	33.73	OOO	54:3	884	O	603	393	339	265
					O	603	393	339	265
					O	633	393	339	265
23.1	34.45	OOA	56:2	914	O	633	393	339	265
					A	603	423	369	295
					O	631	393	339	265
23.1	34.52	OOGa	56:3	912	O	631	393	339	265
					Ga	603	421	367	293

CN – Carbon number, DB – Total number of double bonds, IS – Internal standard, P – Palmitic (C16:0), Po – Palmitoleic (C16:1), H – Heptadecenoic (C17:1), Mg – Margaric (C17:0), O – Oleic (C18:1), L – Linoleic (C18:2), Ln –Linolenic (C18:3), A – Arachidic (C20:0), Ga – Gadoleic (C20:1), n.d. – not detected
Note that $^{1}t_R$ indicates only the retention time at which 'heart-cut' sampling was done and not necessarily the retention times of the TAGs.

the standard TAG analysed. For the peak identified as PPoO, the $[M–RCO_2]^+$ fragment ions with *m/z* 549, 575 and 577, corresponding to $[PPo]^+$, $[PoO]^+$ and $[PO]^+$ respectively, were detected. The $[RCO+128]^+$, $[RCO+74]^+$ and RCO^+ fragment ions corresponding to each fatty acid residue were also detected (Table 2). Similarly, the characteristic fragment ions were detected for the peak corresponding to PPL.

Peak **4** obtained from ^{1}D separation comprised at least 3 co-eluted peaks of TAGs, which were OOP, POL and PLLn with corresponding $^{2}t_R$ of 33.17, 33.29 and 33.36 min, respectively. For the peak identified as OOP, the $[M–RCO_2]^+$ ions with *m/z* 577 and 603 were indicative of the presence of $[OP]^+$ and $[OO]^+$ mass fragments. The $[RCO+128]^+$, $[RCO+74]^+$ and RCO^+ fragment ions corresponding to both O and P were also detected (Table 2). In addition, its $^{2}t_R$ (33.17 min) and the mass spectra were similar to the standard TAG OOP. The $[M–RCO_2]^+$ fragment ions with *m/z* 575, 577 and 601 corresponding to $[PL]^+$, $[PO]^+$, and $[OL]^+$ respectively were detected for the peak identified as POL. The characteristic fragment ions for respective fatty acid residues were also detected (Table 2). Similarly for the peak identified as PLLn, the $[M–RCO_2]^+$ fragment ions *m/z* 573, 575 and 597 were detected. Additionally, the detection of characteristic fragment ions corresponding to P, L and Ln were confirmatory for the detection of PLLn. The discussion on the identification of co-eluted TAGs in peak **6** and peak **7** is presented in the Supplementary Information. The identified TAGs are presented in Table 2.

In a separate experiment detailed above, the complete minor peaks (**1, 3** and **5**) were sampled collectively and preconcentrated

by trapping in the CT after up to 5 replicate injections, before releasing them to ^{2}D for separation. This increased MS detectability of the minor TAGs. Accordingly, peak **1** was detected and identified to be PPPo. The $[M–RCO_2]^+$ ions of *m/z* 549 and 551 corresponding to $[PPo]^+$ and $[PP]^+$, indicating the presence of PPPo. The $[RCO+128]^+$, $[RCO+74]^+$ and RCO^+ fragment ions corresponding to P and Po were also confirmed that peak **1** corresponds to PPPo (Table 2).

Peak **3** was separated into two peaks with $^{2}t_R$ of 32.64 and 32.69 min. The 32.64 min peak with $[M–RCO_2]^+$ ions of *m/z* 565 and 591, corresponding to $[PMg]^+$ and $[MgO]^+$ respectively, were detected, but not *m/z* 577, which corresponds to $[PO]^+$. Similarly the 32.69 min peak gave $[M–RCO_2]^+$ ions with *m/z* of 563 and 577 corresponding to $[PH]^+$, $[PO]^+$ respectively, but not *m/z* 589 which corresponds to $[HO]^+$. The $[M–RCO_2]^+$ fragment ions detected suggested the presence of PMgO and PHO, where Mg = Margaric (heptadecanoic acid, C17:0) and H = heptadecenoic acid (C17:1). In addition the $[RCO+128]^+$, $[RCO+74]^+$ and RCO^+ fragment ions, corresponding to P, Mg, H and O, were detected (Table 2). The two TAGs contained Mg and H. The presence of these two FAs in olive oil in trace amounts was reported elsewhere [23]. The discussion on the identification of co-eluted TAGs in peak **5** is presented in Supplementary Information and the identified TAGs are listed in Table 2.

Importantly, the analysis time for the TAG components is noted. The total analysis time which includes the 1st T program (25 min), oven cooling period (1.5 min), oven stabilisation time (0.5 min) and the 2nd T program (8 min) was 35 min. Only 8 min was required to elute the TAGs from ^{2}D after the TAGs were released from the CT and the 2nd T program commenced. The time window for elution of the TAGs were 12 and 2 min for ^{1}D and ^{2}D respectively (Table 1 & 2). The use of shorter columns and high oven start T (250 °C) as well as fast ramping (15 °C/min) lead to fast analysis time. Minor TAGs required multiple injections to preconcentrate the trace peaks, so this involved longer total analysis time, but the fast overall turn-around also reduced the duration of this study.

4. Conclusions

Single capillary column (1D) separation of TAG components presents difficulties due to overlap of peaks for many samples. This is because the TAGs may have the same CN but differ for instance, only in the number or position of double bonds on their FA residues. However, the MDGC method offers a solution to this by increased resolution of TAGs. This study demonstrates the separation of overlapping TAG peaks using a H/C MDGC method. By using relatively short ^{1}D and ^{2}D columns, and through application of GC conditions designed to reduce time but still achieve resolution, TAG peaks that overlap on the ^{1}D column were sampled and further separated on the ^{2}D column. Identification of TAG components was accomplished using MS detection. Standard TAGs were initially used to demonstrate the H/C MDGC–MS method for identification of olive oil TAGs. Separated olive oil TAG peaks were identified according to the analysis of their mass spectra fingerprints. Characteristic mass fragment ions such as $[M–RCO_2]^+$, $[RCO+128]^+$, $[RCO+74]^+$ and RCO^+ were used to identify TAG components. Overlapped TAG peaks were separated and identified both in a standard TAGs mixture as well as in olive oil using the method developed. The technique can be applied to different complex samples such as fat and oil samples.

Declaration of Competing Interest

The authors declare that they have no known competing financial interests or personal relationships that could have appeared to influence the work reported in this paper.

CRediT authorship contribution statement

Habtewold D. Waktola: Methodology, Validation, Investigation, Writing - original draft, Visualization. **Yada Nolvachai:** Methodology, Resources, Writing - review & editing, Visualization. **Philip J. Marriott:** Conceptualization, Methodology, Resources, Supervision, Funding acquisition.

Acknowledgements

HDW acknowledges provision of MGS and DIPRS Scholarships from Monash University. This work was conducted under support from the Australian Research Council and PerkinElmer through ARC Linkage Grant LP150100465.

Supplementary materials

Supplementary material associated with this article can be found, in the online version, at doi:10.1016/j.chroma.2020.461474.

References

[1] E.N. Frankel, Chemistry of extra virgin olive oil: adulteration, oxidative stability, and antioxidants, J. Agric. Food Chem. 58 (2010) 5991–6006.
[2] N.R. Antoniosi Filho, E. Carrilho, F.M. Lanças, Fast quantitative analysis of soybean oil in olive oil by high-temperature capillary gas chromatography, J. Am. Oil Chem. Soc. 70 (1993) 1051–1053.
[3] R.R. Catharino, R. Haddad, L.G. Cabrini, I.B.S. Cunha, A.C.H.F. Sawaya, M.N. Eberlin, Characterization of vegetable oils by electrospray ionization mass spectrometry fingerprinting: classification, quality, adulteration, and aging, Anal. Chem. 77 (2005) 7429–7433.
[4] J. Parcerisa, I. Casals, J. Boatella, R. Codony, M. Rafecas, Analysis of olive and hazelnut oil mixtures by high-performance liquid chromatography-atmospheric pressure chemical ionisation mass spectrometry of triacylglycerols and gas-liquid chromatography of non-saponifiable compounds (tocopherols and sterols), J. Chromatogr. A 881 (2000) 149–158.
[5] N.K. Andrikopoulos, I.G. Giannakis, V. Tzamtzis, Analysis of olive oil and seed oil triglycerides by capillary gas chromatography as a tool for the detection of the adulteration of olive oil, J. Chromatogr. Sci. 39 (2001) 137–145.
[6] International Olive Council, Determination of composition of triacylglycerols and composition and content of di-acylglycerols by capillary gas chromatography, in vegetable oils, Decision DEC-11/101-V/2013, Method COI/T.20/Doc. No 32/2013, 2013.
[7] C. Ruiz-Samblás, F. Marini, L. Cuadros-Rodríguez, A. González-Casado, Quantification of blending of olive oils and edible vegetable oils by triacylglycerol fingerprint gas chromatography and chemometric tools, J. Chromatogr. B 910 (2012) 71–77.
[8] M. Fasciotti, A.D. Pereira Netto, Optimization and application of methods of triacylglycerol evaluation for characterization of olive oil adulteration by soybean oil with HPLC–APCI-MS–MS, Talanta 81 (2010) 1116–1125.
[9] Y. Yang, M.D. Ferro, I. Cavaco, Y. Liang, Detection and identification of extra virgin olive oil adulteration by GC-MS combined with chemometrics, J. Agric. Food Chem. 61 (2013) 3693–3702.
[10] S.C. Moldoveanu, Y. Chang, Dual analysis of triglycerides from certain common lipids and seed extracts, J. Agric. Food Chem. 59 (2011) 2137–2147.
[11] International Olive Council, Evaluation of the coherence of TAG composition with the fatty acid composition, Decision DEC-III.1/107-VI/2018, Method COI/T.20/DOC. NO 25/REV. 2 – 2018, 2018.
[12] S. Indelicato, D. Bongiorno, R. Pitonzo, V. Di Stefano, V. Calabrese, S. Indelicato, G. Avellone, Triacylglycerols in edible oils: determination, characterization, quantitation, chemometric approach and evaluation of adulterations, J. Chromatogr. A 1515 (2017) 1–16.
[13] M. Buchgraber, F. Ulberth, H. Emons, E. Anklam, Triacylglycerol profiling by using chromatographic techniques, Eur. J. Lipid Sci. Technol. 106 (2004) 621–648.
[14] P.A. Sutton, S.J. Rowland, High temperature gas chromatography–time-of-flight-mass spectrometry (HTGC–ToF-MS) for high-boiling compounds, J. Chromatogr. A 1243 (2012) 69–80.
[15] C. Ruiz-Samblás, A. González-Casado, L. Cuadros-Rodríguez, F.P.R. García, Application of selected ion monitoring to the analysis of triacylglycerols in olive oil by high temperature-gas chromatography/mass spectrometry, Talanta 82 (2010) 255–260.
[16] C. Ruiz-Samblás, A. González-Casado, L. Cuadros-Rodríguez, Triacylglycerols determination by high-temperature gas chromatography in the analysis of vegetable oils and foods: a review of the past 10 years, Crit. Rev. Food Sci. Nutr. 55 (2015) 1618–1631.
[17] H.D. Waktola, C. Kulsing, Y. Nolvachai, C.M. Rezende, H.R. Bizzo, P.J. Marriott, Gas chromatography–mass spectrometry of sapucainha oil (Carpotroche brasiliensis) triacylglycerols comprising straight chain and cyclic fatty acids, Anal. Bioanal. Chem. 411 (2019) 1479–1489.

[18] S. De Koning, H.G. Janssen, U.A.T. Brinkman, Characterization of triacylglycerides from edible oils and fats using single and multidimensional techniques, LC GC Eur. 19 (2006) 590–600.
[19] H.D. Waktola, C. Kulsing, Y. Nolvachai, P.J. Marriott, High temperature multidimensional gas chromatographic approach for improved separation of triacylglycerols in olive oil, J. Chromatogr. A 1549 (2018) 77–84.
[20] N.K. Andrikopoulos, Triglyceride species compositions of common edible vegetable oils and methods used for their identification and quantification, Food Rev. Int. 18 (2002) 71–102.
[21] R.A. Shellie, L.-L. Xie, P.J. Marriott, Retention time reproducibility in comprehensive two-dimensional gas chromatography using cryogenic modulation: an intralaboratory study, J. Chromatogr. A 968 (2002) 161–170.
[22] P. Konieczka, J. Namieśnik, Method validation, in: C.H. Lochmüller (Ed.), Quality Assurance and Quality Control in the Analytical Chemical Laboratory: A Practical Approach, CRC Press Taylor & Francis Group, Boca Raton, London, New York, 2009, p. 131.
[23] T.H. Borges, J.A. Pereira, C. Cabrera-Vique, L. Lara, A.F. Oliveira, I. Seiquer, Characterization of Arbequina virgin olive oils produced in different regions of Brazil and Spain: physicochemical properties, oxidative stability and fatty acid profile, Food Chem. 215 (2017) 454–462.

5.3. Supporting information

Multidimensional gas chromatographic–mass spectrometric method for separation and identification of triacylglycerols in olive oil

Habtewold D. Waktola, Yada Nolvachai, Philip J. Marriott

Journal of Chromatography A

Contents

Table S1. ^2t_R repeatability for standard TAG peaks (n = 5)

	6 s H/C approach			Whole peak H/C approach		
Peak number	Mean ^2t_R (min)	SD	RSD (%)	Mean ^2t_R (min)	SD	RSD (%)
1	32.718	0.003	0.0100	32.742	0.002	0.005
IS	32.898	0.003	0.008	32.928	0.002	0.006
2	33.184	0.004	0.011	33.219	0.002	0.005
3	33.363	0.004	0.011	33.404	0.001	0.004
4	33.865	0.003	0.009	33.932	0.003	0.009
5	34.294	0.007	0.019	34.368	0.003	0.009

Table S2. LOD for standard TAGs.

TAG	**LOD (mg/L)**
1,2-palmitin-3-olein (PPO)	17.2
1-2-olein-3-palmitin (OOP)	13.8
1,2-linolein-3-palmitin (LLP)	21.4
1,2-olein-3-linolein (OOL)	17.2
1,2-olein-3-archidin (OOA)	10.5

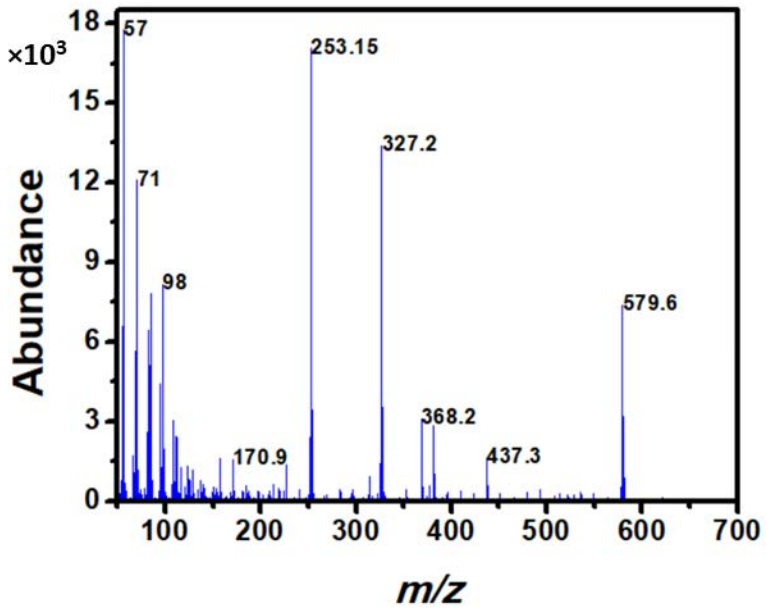

Fig. S1. Mass spectra of internal standard (IS) TAG: glycerol triheptadecanoate

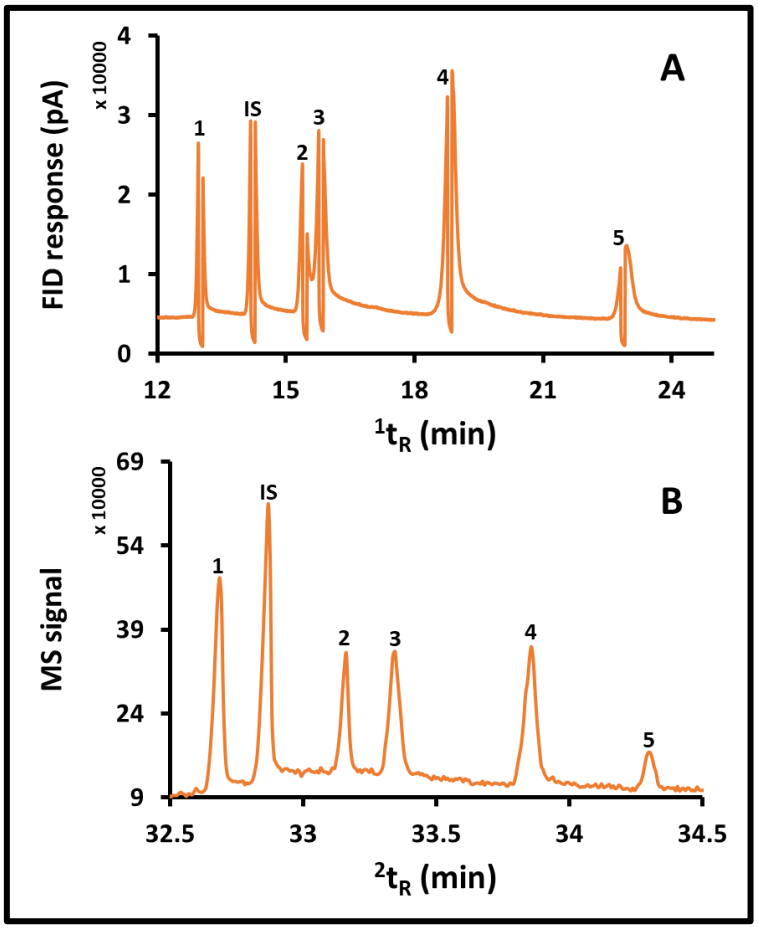

Fig. S2. (A) GC–FID chromatogram of separated standard TAGs mixture using 1st T and 1st flow programs on ^{1}D column showing the 6 s H/Cs across each peak, which were CT near the inlet of the ^{2}D column; (B) MS response of the TAGs after release from the CT and separated on ^{2}D column using the 2nd T and 2nd flow programs. (1) PPO (IS) glycerol triheptadecanoate (2) OOP (3) LLP (4) OOL (5) OOA.

MS identification of co-eluted TAG components in olive oil after H/C MDGC separation

Peak **6** was found to comprise co-eluted peaks of OOO, OOL and OLLn with corresponding ^2t_R of 33.73, 33.87 and 34.01 min, respectively. All the $[M–RCO_2]^+$, $[RCO+128]^+$, $[RCO+74]^+$ and RCO^+ fragment ions with *m/z* 603, 393, 339 and 265 respectively were detected for the peak identified as OOO. The $[M–RCO_2]^+$ fragment ions with *m/z* 601 and 603 corresponding to $[OL]^+$ and $[OO]^+$ were detected for the peak corresponding to OOL. The characteristic fragment ions for O and L were also detected. Similarly for the peak identified as OLLn the $[M-RCO_2]^+$ ions with *m/z* 597, 599 and 601corresponding to $[LLn]^+$, $[OLn]^+$ and

$[OL]^+$ were detected. In addition, the detection of characteristic fragment ions corresponding to O, L and Ln were evident for the OLLn presence (**Table 2**).

Peak **7** was separated into two TAG peaks in a separate run where the whole peak was sampled into ^{2}D. These two peaks corresponded to OOA and OOGa with corresponding ^2t_R of 34.45 and 34.52 min, respectively. The detection of $[M\text{-}RCO_2]^+$ ions with *m/z* 603 and 633 indicates presence of $[OO]^+$ and $[OA]^+$. Further the $[RCO+128]^+$, $[RCO+74]^+$ and RCO^+ fragment ions corresponding to O and A were also detected. In addition both ^1t_R and ^2t_R were found to be the same as for the standard TAG OOA. Similarly for OOGa the $[M–RCO_2]^+$ ions of *m/z* 603 and 631 corresponding to $[OO]^+$ and $[OGa]^+$ were detected. The $[RCO+128]^+$, $[RCO+74]^+$ and RCO^+ ions corresponding to both O and Ga were also detected (**Table 2**). This confirms the presence of OOA and OOGa as olive oil TAGs.

Peak **5** was separated into two peaks, identified to be MgOO and HOO with ^2t_R of 33.10 and 33.15 min respectively. The $[M–RCO_2]^+$ fragment ions with *m/z* of 591 and 603 corresponding to $[MgO]^+$ and $[OO]^+$ indicated MgOO. The detection of $[RCO+128]^+$, $[RCO+74]^+$ and RCO^+ ions corresponding to Mg and O also confirmed MgOO (**Table 2**). Similarly, characteristics fragment ions were detected for HOO, which confirmed its presence (**Table 2**).

Chapter 6

Extra virgin olive oil signature flavour mix differentiation based on analysis of volatile organic compounds and fatty acids

Habtewold D. Waktola[1], Yada Nolvachai[1], Claudia Guillaume[2], Bayden R. Wood[3], Philip J. Marriott[1]

[1]Australian Centre for Research on Separation Science, School of Chemistry, Monash University, Wellington Road, Clayton, VIC 3800, Australia

[2]Modern Olives, Lara, VIC 3212, Australia

[3]Centre for Biospectroscopy, School of Chemistry, Monash University, Wellington Road, Clayton, Melbourne, VIC 3800, Australia

The manuscript is not submitted to a journal but prepared in published paper format in order to generate a consistent presentation within the thesis.

Contents

6.1. Chapter overview

Extra virgin olive oil (EVOO) is composed of many chemical compounds that includes volatiles, FAs, TAGs, vitamins, and many more minor compounds. The analysis of these compounds in olive oil have significance in characterisation, differentiation, authentication and quality control purposes. In extending further the study conducted on olive oil from the preceding Chapters the present Chapter focuses on the differentiation of EVOO varieties based on the analysis of VOCs and FAs using GC techniques. VOCs can originate in the plant, and/or formed during oil processing and storage. They are responsible for the unique and characteristic flavour of the oil; the fruity and green aroma of EVOO is attributed to VOCs that are produced in an enzymatic pathway. The composition of VOCs as well as FAs in olive oil depends on many factors including varietal origin, agronomic factors, processing technology and storage parameters. Chemometric techniques assist in differentiation, classification and traceability of the oil samples.

The VOCs and FAs in seven single varieties (Hojiblanca, Coratina, Arbequina, Koroneiki, Frantoio, Picual, and Barnea) and three mixed samples of EVOO (Medium flavour, Mild flavour and Robust flavour) produced in 2018 and 2018/2019 respectively, were determined. The mixed samples are sold as commercial blends, reproducibly blended year-to-year largely based on sensory evaluation such that signature products are perceived to be equivalent.

For VOCs, HS SPME with GC–MS was used; IS was added to all samples. Major VOCs included hexanal, (*E*)-2-hexenal, (*Z*)-3-hexen-1-ol, (*E*)-2-hexen-1-ol, 1-hexanol, (*Z*)-3-hexenyl acetate, and hexyl acetate, though their varietal composition varied. (*E*)-2-Hexenal was the most abundant across most varieties. PCA poorly differentiated VOC profiles of the mixed samples.

In contrary to some literature studies that report concentrations of VOCs expressed as mg/kg of EVOO relative to IS assuming a 'response factor' equal to 1, the study in the present Chapter reports relative abundance of the VOCs as area ratio of analytes vs the IS. This is because the relative magnitude of the response may vary significantly for different VOCs. The equilibrium between EVOO and vial head space, and between head space and SPME fibre can vary substantially between chemical classes, and homologues within chemical classes, plus for different fibre compositions. Therefore, in the absence of data for individually calibrated compounds, it is appropriate to base interpretation on relative abundance values for reproducibly prepared samples.

The percentage FA (%FA) composition, determined by GC–FID of their methyl esters, showed 2018 varieties to have higher saturated FA and polyunsaturated FA content, compared to 2019 products; 2019 varieties had higher monounsaturated FA content. C18:1n–9 and C18:2n–6 abundances ranged from 67.9–73.8% and 4.9–11.1% respectively for 2018 products, and 68.1–77.4% and 3.1–10.3% respectively for 2019 products.

Since the company blends their signature Medium and Mild commercial products annually to have the same sensory profile, they may require different varieties and in different proportions each year. The mixing % was not known to the researchers prior to the study. Thus, in-house mixes were prepared from 2019 single variety EVOO samples to investigate changes of FAs composition upon varying the ratio of EVOO varieties. Through PCA interpretation, it was found that in-house mixes of EVOO varied linearly based on the percentage of their single variety EVOO, and were then compared with commercially prepared mixed variety samples; PCA clearly differentiated these EVOO according to percentage of single variety EVOO.

Based on the analysis of VOCs, single varieties were differentiated but not the mixed EVOO samples. This could be attributed to the fact that VOCs do not adequately reflect the flavour of the mixed EVOO varieties, where mixtures are prepared based on sensory

considerations. In addition, minor VOCs that may have high odour activity value (OAV) were not detected by the method used in the study. Analysis based on FAs more clearly differentiated among the varieties studied. Based on the PCA of the in-house EVOO mixes it is possible that the proportion of single varieties comprising the mixed sample oils could be reasonably well predicted.

6.2. Article

xx Journal xxx (2020) xxxxxx

Contents lists available at xxxx

xx Journal

journal homepage: www.xxxx.com/locate/xx

Extra virgin olive oil signature flavour mix differentiation based on analysis of volatile organic compounds and fatty acids

Habtewold D. Waktola[1], Yada Nolvachai[1], Claudia Guillaume[2], Bayden R. Wood[3], Philip J. Marriott[1]*

[1]Australian Centre for Research on Separation Science, School of Chemistry, Monash University, Wellington Road, Clayton, VIC 3800, Australia
[2]Modern Olives, Lara, VIC 3212, Australia
[3]Centre for Biospectroscopy, School of Chemistry, Monash University, Wellington Road, Clayton, Melbourne, VIC 3800, Australia

ARTICLEINFO

Keywords:
Extra virgin olive oil
Fatty acid
Gas chromatography
Solid phase microextraction
Volatile organic compound

ABSTRACT

Volatile organic compounds (VOCs) and fatty acids (FAs) in seven single varieties and three mixed samples of extra virgin olive oil (EVOO), produced in 2018 and 2018/2019 respectively, were determined. For VOCs, headspace solid-phase microextraction (HS SPME) with gas chromatography–mass spectrometry (GC–MS) was used; internal standard was added to all samples. Major VOCs included hexanal, (*E*)-2-hexenal, (*Z*)-3-hexen-1-ol, (*E*)-2-hexen-1-ol, 1-hexanol, (*Z*)-3-hexenyl acetate, and hexyl acetate, though their varietal composition varied. (*E*)-2-Hexenal was the most abundant across most varieties. Principal component analysis (PCA) poorly differentiated VOC profiles of the mixed samples. The percentage FA (%FA) composition, determined by GC–flame ionisation detector (FID) of their methyl esters, showed 2018 varieties to have higher saturated FA and polyunsaturated FA content, compared to 2019 products; 2019 varieties had higher monounsaturated FA content. C18:1n–9 and C18:2n–6 abundances ranged from 67.9–73.8% and 4.9–11.1% respectively for 2018 products, and 68.1–77.4% and 3.1–10.3% respectively for 2019 products. In-house mixes of EVOO varied linearly based on % of their single variety EVOO, and were compared with commercially prepared mixed samples. PCA clearly differentiated these EVOO according to percentage of single variety EVOO.

1. Introduction

Extra virgin olive oil (EVOO) is composed of many chemical classes including fatty acids (FAs), triacylglycerols, vitamins, volatiles, antioxidants, and oleocanthal. These are often used for characterisation, differentiation, classification and authentication of olive oil (Guissous, Le Dréau, Boulkhroune, Madani, & Artaud, 2018; Kosma, Badeka, Vatavali, Kontakos, & Kontominas, 2016; Lukić, Carlin, Horvat, & Vrhovsek, 2019; Portarena et al., 2019; Pouliarekou et al., 2011; Vaz-Freire, da Silva, & Freitas, 2009). The fruity and green aroma of EVOO is attributed to volatile organic compounds (VOCs), produced in an enzymatic pathway catalysed by lipoxygenase and hydroperoxide lyase enzymes (Angerosa et al., 2004). The concentration of VOCs in olive oil depends on many factors, including varietal origin, agronomic factors (geographical location, climatic conditions and harvest date), and processing technology and storage parameters (Amanpour, Kelebek, & Selli, 2019; Lukić et al., 2019; Oğraş, Kaban, & Kaya, 2018; Sanz, Belaj, Sánchez-Ortiz, & Pérez, 2018). The VOCs consist of complex mixtures of aldehydes, alcohols, ketones, esters, terpenes and other compounds (Zhou, Liu, Liu, & Song, 2019). Identification of VOCs is important for sensory, differentiation, classification, traceability and authentication of olive oil (Cajka et al., 2010; Damascelli & Palmisano, 2013; Kosma et al., 2016).

Headspace (HS) methods are popular techniques for analysis of VOCs in olive oil, such as purge-and-trap, and solid phase microextraction (HS SPME), combined with gas chromatography–mass spectrometry (GC–MS). Chemometric techniques assist in differentiation, classification and traceability of the oil samples; various methods based on analysis of volatiles have been developed (Cajka et al., 2010; Damascelli & Palmisano, 2013; Pouliarekou et al., 2011). Cajka et al. (Cajka et al., 2010) used fingerprinting with HS SPME followed by GC–MS to identify geographical origins of olive oil; chemometric tools were applied to develop models for recognition, prediction, and classification of olive oil. HS SPME with GC–MS of sesquiterpenes (e.g. α-muurolene and α-farnesene) was developed to differentiate between origins of olive oil and 'protected designation' of origin products from others (Damascelli & Palmisano, 2013).

Volatile and non-volatile compound analysis can support discrimination and tracing the variety of extra virgin olive oil with chemometrics, e.g. principal component analysis (PCA) (Guissous et al., 2018). FAs composition was found to be a better tool (improved correct prediction rate) than VOCs for differentiation of olive cultivars (Kosma et al., 2016); FA content of EVOO was influenced by environmental conditions such as altitude and temperature (Borges et al., 2017). Fatty acids are often determined as FA methyl esters (FAMEs) with GC coupled to flame ionisation detection (GC–FID), with identification based on retention time matching with an authentic standard mixture, or using effective chain length, with results expressed as percentage of total FAs (Borges et al., 2017

* Corresponding author.
E-mail address: philip.marriott@monash.edu

https://doi.org/10.1016/j.xx.2020.xxxxxx
Received x xx 2020; Received in revised form xx xx 2020; Accepted x xx 2020
Available online x xx 2020

; Guissous et al., 2018; Kosma et al., 2016). In this study analysis of VOCs and FAs in different varieties of EVOO were used to determine similarities and differences between varieties of olive oils, and some commercial blended signature oil mixtures.

2. Materials and method

2.1. Sample

Seven single varieties, Hojiblanca, Coratina, Arbequina, Koroneiki, Frantoio, Picual, and Barnea, and three mixed extra virgin olive oil (EVOO) samples from both 2018 and 2019 production were obtained from a large Australian producer (Victoria, Australia). The mixed samples are sold as commercial blends, reproducibly blended year-to-year largely based on sensory evaluation such that signature products are perceived to be equivalent. Oils were sealed in amber bottles during storage and transportation. VOCs were only investigated for 2018 produced EVOO samples (see later) whereas FAs composition was studied for 2018 and 2019 samples. In-house mixes were prepared from 2019 single variety EVOO samples (**Table 1**) to investigate changes of FAs composition upon varying the ratio of EVOO varieties. The commercial mixes derive from single EVOO varieties; Medium flavour (Barnea and Picual), Mild flavour (Arbequina and Barnea) and Robust flavour (Barnea, Coratina and Koroneiki). The company prepares these products from single varieties in a ratio unknown to the investigators.

Table 1
In-house EVOO mixes prepared from different single variety EVOO samples.

Varieties	Ratio
Arbequina:Barnea	1:4
Arbequina:Barnea	2:3
Arbequina:Barnea	3:2
Arbequina:Barnea	4:1
Barnea:Picual	1:4
Barnea:Picual	2:3
Barnea:Picual	3:2
Barnea:Picual	4:1
Barnea:Coratina:Koroneiki	2:3:5
Barnea:Coratina:Koroneiki	2:7:1

2.2. SPME extraction of volatile compounds

Internal standard (IS) solution was prepared by adding 1 µL of 4-methyl-2-pentanol (TCI, Tokyo, Japan) into each EVOO variety (5.0 g) in a vial, as a diluent for the IS, and vortex mixed. Separate solutions were prepared for each variety of EVOO sample. A 0.050 g portion of this IS mix was transferred into a 20 mL SPME vial followed by addition of 5.0 g of the same variety of EVOO sample. The vial was crimp sealed and homogenised using vortex mixing. The sample headspace was extracted using a 50/30 µm divinylbenzene/carboxen/polydimethylsiloxane fibre (Supelco, Bellefonte, PA) at 60 °C for 60 min for equilibrium extraction prior to GC injection (see below). Preparation, extraction and analysis of each sample was performed in triplicate. For retention index (*I*) calculation, a standard alkane mixture (C_7–C_{22}, Sigma-Aldrich) prepared by mixing 7 µL of C_7-C_8, 15 µL of C_9-C_{12} and 20 µL of C_{13}-C_{22}, (all from 10000 mg/L in hexane stock solutions) was extracted at 60 °C for 5 min using the same SPME fibre. This approach avoided column overloading.

2.3. GC–MS analysis of volatile compounds

An Agilent 7890A GC equipped with an Agilent 7000 MS (Mulgrave, Australia), installed with a DB-5 (30 m × 0.25 mm I.D. × 0.25 µm d_f, Agilent) column was used. Helium (99.999% purity) was used as carrier gas (flow rate 1.2 mL/min). The GC oven was programmed as follows: initial oven temperature 40 °C (held 3 min), ramped at 5 °C/min to 200 °C, then ramped at 15 °C/min to 250 °C (held 2 min). The GC inlet temperature was 250 °C. The SPME fibre was inserted into the GC manually and the analysis started immediately, with split injection of 20:1. The MS source and transfer line temperatures were 250 °C. The MS was operated in full scan mode from 50 to 500 mass units. The same GC–MS method was used for alkane analysis for retention index (*I*) determination.

Average values of analyte amount from triplicate sample preparations were calculated *vs* the IS response area. Relative abundance results are given in **Table 2**. Values do not directly reflect the composition of compounds in the oils, nor account for factors such as equilibrium extraction differences between compounds and the fibres. Establishing equilibrium between EVOO and vial headspace, and then between headspace and SPME fibre can vary substantially between chemical classes, and homologues within chemical classes, plus for different fibre compositions. Some literature studies report concentrations of VOCs expressed as mg/kg of EVOO relative to IS assuming a 'response factor' equal to 1 (Kosma et al., 2016; Lukić et al., 2019; Zhou et al., 2019). Since the relative magnitude of the response may vary significantly for different VOCs due to SPME sampling parameters resulting from the aforementioned factors, it is appropriate to base interpretation on relative abundance values for reproducibly prepared samples. In the absence of data for individually calibrated compounds, the present work will report area ratios for analytes *vs* the IS. This should allow valid comparison of sample-to-sample relative amounts. Data for peak area of the IS across EVOO analyses indicate adequate reproducibility (see Table 2 footnote for IS data).

2.4. Determination of FA composition

Fatty acid methyl esters (FAMEs) were prepared according to European Union commission regulation (EEC) No 2568/91. 0.10 g of olive oil sample was weighed in a 5 mL screw top vial. Hexane (2 mL) was added and mixed. Methanolic KOH (0.2 mL, 2 N) was added, the vial vigorously shaken for about 30 s and left to stratify until the upper hexane layer become clear; a 400 µL aliquot of this layer was transferred into a GC vial. Methyl nonadecanoate (C19:0 FAME) internal standard (100 µL, 10.0 g/L in hexane, C19:0 FAME, Supelco) was added into the vial prior to injection. An Agilent 7890A GC equipped with flame ionisation detector (FID) and autosampler, installed with a SUPELCOWAX10 (30 m × 0.20 mm I.D. × 0.20 µm df, Supelco) column was used. The oven temperature was programmed from 180 °C (held 1 min), then ramped at 5 °C/min to 250 °C (held 8 min). Inlet and detector temperature were both 250 °C and split injection (50:1) was used. The carrier gas was hydrogen (99.999% purity) at constant flow of 1 mL/min. FAMEs were identified by retention time correlation with an authentic standard mixture (Supelco 37-component FAMEs mix). Identification was confirmed using GC–MS mass spectrum information. Results were expressed as relative percentage of each FA based on FID area ratio of the FA peak to internal standard, without considering mass response factor. The IS area for each set of experiments is shown in footnotes to Tables 3-5.

2.5. Data Analysis

Principal component analysis (PCA) results were calculated using Minitab 16 (Minitab Inc.). The PCA was built with Eigenvalue decomposition algorithm. Data for PCA were peak area ratios of the compound *vs* the IS. Scores and loadings plots of the first two components were reported. Other calculations were performed using Microsoft Excel.

Table 2. Volatile organic compounds (VOCs) identified in EVOO varieties from 2018 products by SPME GC–MS analysis. Data in this Table are presented to 2 decimal places. In the text, 1 decimal place will be used.

Compound	t_R (min)	I_{Lit}[a]	I_{Exp}[a]	Average area ratio of VOCs to IS[b] ± SD, n=3									
				Hojiblanca	Coratina	Arbequina	Koroneiki	Frantoio	Picual	Barnea	Robust Flavour	Mild Flavour	Medium Flavour
Acetic acid, methyl ester	1.68		-	0.79±0.08	0.94±0.02	0.72±0.08	1.05±0.10	0.31±0.06	0.91±0.03	0.27±0.02	0.39±0.07	0.57±0.07	0.65±0.06
Acetic acid	2.00	600	603	n.d.	n.d.	0.62±0.03	n.d.	n.d.	1.12±0.23	n.d.	0.52±0.08	n.d.	n.d.
Ethyl acetate	2.10	613	613	n.d.	n.d.	0.60±0.04	0.60±0.06	0.73±0.10	0.91±0.09	n.d.	0.42±0.05	0.52±0.09	0.55±0.06
1-Penten-3-one	2.82	684	683	0.82±0.06	n.d.	n.d.	n.d.	n.d.	n.d.	n.d.	n.d.	n.d.	n.d.
3-Pentanone	2.98	700	699	0.47±0.06	0.57±0.04	0.23±0.03	0.54±0.03	0.27±0.05	0.55±0.02	n.d.	0.36±0.06	0.28±0.06	0.43±0.03
2-Penten-1-ol, (Z)-	4.50	768	771	0.28±0.03	n.d.	n.d.	n.d.	n.d.	0.25±0.04	n.d.	n.d.	n.d.	n.d.
3-Hexenal, (Z)-	5.12	800	799	2.33±0.19	n.d.	n.d.	n.d.	n.d.	n.d.	n.d.	n.d.	n.d.	n.d.
Heptane, 2,4-dimethyl-	5.14	803	800	n.d.	n.d.	0.21±0.00	0.25±0.01	0.39±0.07	0.33±0.01	n.d.	0.23±0.05	0.21±0.03	n.d.
Hexanal	5.18	804	801	4.16±0.34	2.03±0.01	1.17±0.10	1.22±0.08	2.73±0.55	0.93±0.02	1.63±0.03	1.64±0.30	0.98±0.10	1.78±0.05
2-Hexenal, (E)-	6.71	855	852	9.65±0.70	**34.96±1.81**	**15.82±0.83**	2.53±0.18	**21.91±3.99**	8.13±0.26	**72.62±2.09**	**31.39±5.35**	**12.82±2.02**	**27.48±0.97**
3-Hexen-1-ol, (Z)-	6.82	852	856	7.96±0.57	5.24±0.29	3.40±0.23	5.94±0.49	1.71±0.34	7.31±0.03	6.65±0.27	2.71±0.49	2.77±0.38	4.75±0.27
2-Hexen-1-ol, (E)-	7.16	869	867	0.38±0.06	7.93±0.48	3.30±0.17	0.50±0.02	3.57±0.67	1.97±0.07	4.51±0.18	3.38±0.58	2.68±0.38	3.68±0.16
1-Hexanol	7.28	868	871	4.59±0.43	8.24±0.46	4.21±0.26	1.93±0.11	4.35±0.86	2.48±0.03	4.08±0.23	4.57±0.84	3.43±0.53	4.77±0.23
Heptanal	8.25	902	902	n.d.	0.14±0.03	0.06±0.01	0.09±0.01	0.16±0.04	0.20±0.00	n.d.	0.09±0.02	0.06±0.01	0.12±0.01
3-Ethyl-1,5-octadiene	9.38	947	937	0.28±0.02	0.71±0.07	0.38±0.02	0.36±0.02	0.25±0.04	0.66±0.02	0.24±0.02	0.33±0.06	0.37±0.01	0.38±0.01
2-Heptenal, (E)-	10.04	951	957	n.d.	n.d.	n.d.	n.d.	0.35±0.06	n.d.	0.21±0.01	n.d.	n.d.	0.25±0.03
2(5H)-Furanone, 5-ethyl-	10.20	963	961	2.30±0.02	n.d.	n.d.	n.d.	n.d.	0.31±0.03	n.d.	n.d.	n.d.	n.d.
Octanal	11.57	1005	1003	n.d.	0.74±0.07	n.d.	0.23±0.02	0.60±0.10	0.47±0.03	0.16±0.01	0.40±0.06	0.14±0.01	0.43±0.03
3-Hexen-1-ol, acetate, (Z)-	11.65	1009	1006	**26.60±1.29**	2.05±0.18	1.85±0.22	**23.26±1.39**	0.40±0.05	9.76±0.77	2.46±0.08	0.81±0.10	1.68±0.20	2.78±0.10
Acetic acid, hexyl ester	11.88	1016	1013	4.85±0.24	0.42±0.04	0.36±0.04	3.24±0.23	0.30±0.04	0.75±006	0.37±0.02	0.37±0.05	0.33±0.03	0.50±0.01
trans-β-Ocimene	12.94	1049	1046	n.d.	n.d.	0.46±0.05	n.d.	n.d.	n.d.	0.35±0.03	0.83±0.11	0.46±0.03	1.34±0.08
Nonanal	14.79	1107	1104	0.23±0.00	1.88±0.28	0.45±0.03	0.67±0.01	1.55±0.22	1.28±0.12	0.98±0.12	0.97±0.11	0.42±0.03	1.46±0.15
Furan, 3-(4-methyl-3-pentenyl)-	15.05	1129	1113	1.51±0.01	0.42±0.03	0.60±0.09	1.35±0.03	0.38±0.05	0.22±0.02	0.25±0.04	0.37±0.03	0.57±0.06	0.57±0.05
Dodecene	17.80	1191	1204	1.18±0.03	0.59±0.13	0.44±0.09	7.05±0.18	0.28±0.03	**13.80±2.16**	0.52±0.09	1.78±0.18	0.52±0.03	4.39±0.53
α-Farnesene	25.76	1502	1504	n.d.	n.d.	n.d.	n.d.	n.d.	n.d.	0.16±0.01	0.17±0.02	0.14±0.02	0.26±0.04
Total Reported Analytes				17	15	18	17	18	20	16	20	19	19

[a] I_{Lit} – literature I value and I_{Exp} – experimental I value

[b] Average area ratio of VOCs detected in EVOO to the internal standard, 4-methyl-2-pentanol. n.d., not detected. IS t_R is 4.22±0.00 and area RSD of 13% (n=30, analysis made over a 3-day period).

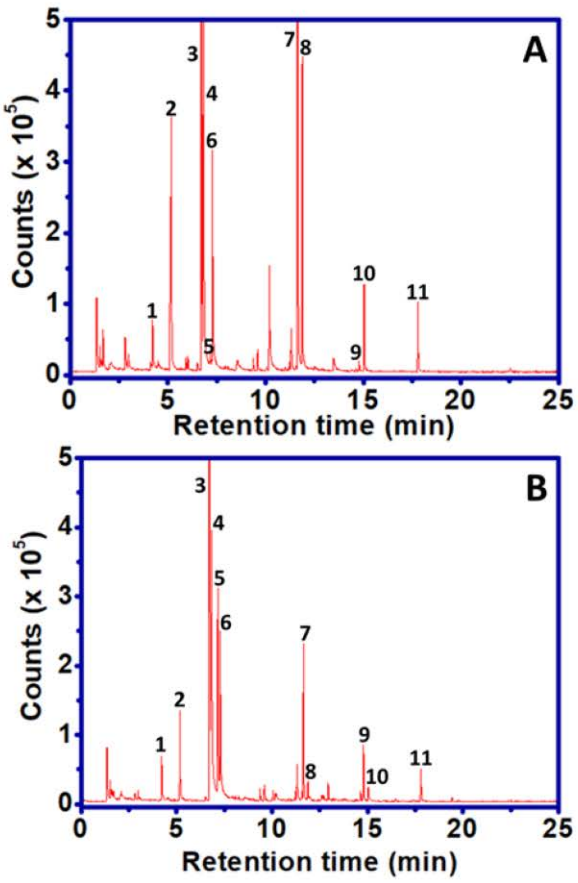

Fig. 1. GC–MS chromatogram of VOCs in EVOO varieties of (A) Hojiblanca and (B) Barnea, with some major peaks indicated. 1. 4-Methyl-2-pentanol (IS); 2. Hexanal; 3. (*E*)-2-Hexenal; 4. (*Z*)-3-Hexen-1-ol; 5. (*E*)-2-Hexen-1-ol; 6. 1-Hexanol; 7. (*Z*)-3-Hexen-1-ol, acetate; 8. Acetic acid, hexyl ester; 9. Nonanal; 10. Furan, 3-(4-methyl-3-pentenyl)-; 11. Dodecene.

3. Results and discussion

3.1. Analysis of volatile organic compounds (VOCs)

Seven single varieties (refer Section 2.1) and three mixed samples (Medium, Mild and Robust flavour) EVOO samples from 2018 products were analysed. Identification was based on the retention index (*I*, see Table 2) *vs* reference *I* data, and NIST11 MS library search match, and in absence of authentic standards is considered tentative.

Shown in Table 2, 25 of the most abundant VOCs were tentatively identified. Many minor components were noted, but only 25 major components will be further examined in this study. Not all components are obtained for each sample. **Fig. 1** shows the GC–MS chromatogram for two single variety EVOO samples (Hojiblanca, Barnea); major VOCs detected were labelled according to Table 2. GC–MS data of other EVOO varieties can be found in Supplementary Material **Fig. S1**. The VOCs detected in relatively high amounts were hexanal, (*E*)-2-hexenal, (*Z*)-3-hexen-1-ol, (*E*)-2-hexen-1-ol, 1-hexanol, (*Z*)-3-hexenyl acetate, hexyl acetate and dodecene. The major compound detected in most varieties was (*E*)-2-hexenal. The most abundant components are shown in bold. (*E*)-2-Hexenal was reported as a major compound in all Croatian EVOO samples (Lukić et al., 2019). An Australian study reported (*E*)-2-hexenal as the major compound in less than 50% of the oil samples analysed (Tura, Prenzler, Bedgood Jr, Antolovich, & Robards, 2004).

Compounds with five carbon atoms (C5), derived through the lipoxygenase (LOX) pathway, were detected, contributing bitter taste to the olive oil (Angerosa et al., 2004; Kalua et al., 2007). They include 1-penten-3-one, 3-pentanone and (*Z*)-2-penten-1-ol. 3-Pentanone was detected in all samples in a ratio range of 0.2±0.1–0.6±0.1 (Table 2), except in Barnea.

Compounds with six carbon atoms (C6) e.g. hexanal, were among the more abundant VOCs. They are responsible for the 'green' odour of olive oil and derive from LOX catalysed oxidation of linoleic and linolenic acids (Angerosa et al., 2004; Sarolic et al., 2014). (*E*)-2-Hexenal was the major compound in most of the varieties, in relative levels from 2.5±0.2 in Koroneiki to 72.62±2.1 in Barnea. C6 aldehydes were reported to arise from maturity stage and oxidation of olive oil (Angerosa, 2002; Pouliarekou et al., 2011). Hexanal was present in a ratio range of 0.9±0.1–4.2±0.3. (*Z*)-3-Hexenal was found only in Hojiblanca (2.3±0.2). Higher carbon number aldehydes such as heptanal, octanal and nonanal were also detected in most of the oil varieties (Table 2). 1-Hexanol was the major C6 alcohol compound detected, ranging from 1.9±0.1 in Koroneiki to 8.2±0.5 in Coratina. (*E*)-2-hexen-1-ol adds astringent bitter taste and 'green' odour to olive oil (Kosma et al., 2016).

Ester (*Z*)-3-hexenyl acetate was the most abundant VOCs in Hojiblanca (26.6±1.3) and Koroneiki (23.3±1.4%), and imparts sweet and pleasant flavours to olive oil (Baccouri et al., 2008; Kalua et al., 2007). Various hydrocarbons detected in EVOO included acetic acid, 2-4-dimethyl-heptane, 3-ethyl-1-5-octadiene, 5-ethyl-2(5H)-furanone, *trans*-β-ocimene and α-farnesene.

3.2. Principal component analysis (PCA) of VOCs

PCA multivariate analyses was applied to evaluate whether the VOC content of olive oil samples could be differentiated and classified into different groups. PCA employs principal components to represent the explained variance of the original data (Brereton, 2003), performed using responses of the 25 most abundant compounds (variables) of 30 EVOO samples (7 varieties plus 3 mixed products, $n = 3$). The PCA scores plot is shown in **Fig. 2**. (PC1 and PC2 represented 35.2% and 22.1% of the explained variance in the data set). Further PCA interpreta-

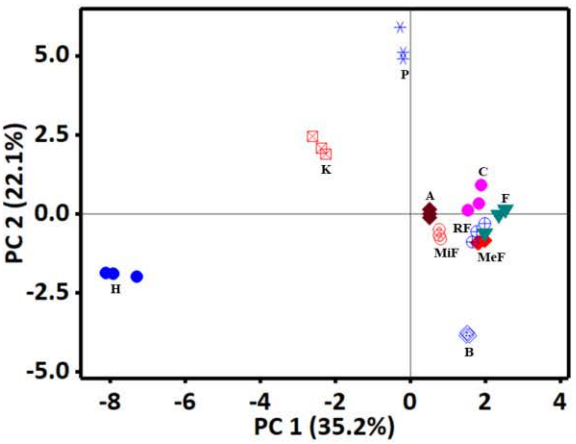

Fig. 2. Principal component analysis (PCA) score plot of 10 different EVOO varieties (n = 3) from 2018 products, based on 25 major VOCs composition. A: Arbequina; B: Barnea; C: Coratina; F; Frantoio; H: Hojiblanca; K: Koroneiki; P: Picual; MeF: Medium flavour; MiF: Mild flavour; and RF: Robust flavour.

Table 3
Percentage of FAs (%FA) composition of EVOO from 2018 products. (Data in this Table presented to two decimal places; in the manuscript text they will be presented to one decimal place).

FAME	%FA (Mean ± SD), n=3										
	Hojiblanca	Coratina	Arbequina	Koroneiki	Frantoio	Picual	Barnea	Mild Flavour	Robust Flavour	Medium Flavour	Average[#] (RSD)
C16:0	12.94±0.01	12.50±0.01	13.10±0.03	12.92±0.04	12.81±0.08	12.55±0.04	12.06±0.03	13.01±0.03	12.72±0.02	12.87±0.01	12.75 (2.41)
C16:1n–9	0.08±0.00	0.08±0.00	0.12±0.00	0.08±0.00	0.10±0.00	0.08±0.00	0.09±0.00	0.12±0.00	0.09±0.00	0.10±0.00	0.09 (17.54)
C16:1n–7	0.80±0.00	0.42±0.00	1.09±0.00	0.86±0.00	0.88±0.00	0.96±0.00	0.77±0.00	1.09±0.00	0.84±0.00	1.02±0.00	0.87 (22.48)
∑C16:1	0.88±0.00	0.50±0.00	1.21±0.00	0.94±0.00	0.98±0.00	1.04±0.00	0.86±0.00	1.22±0.00	0.92±0.00	1.12±0.00	0.97 (21.48)
C17:0	0.12±0.00	0.05±0.00	0.06±0.00	0.04±0.00	0.04±0.00	0.05±0.00	0.06±0.00	0.06±0.00	0.05±0.00	0.06±0.00	0.06 (40.76)
C17:1n–8	0.22±0.00	0.07±0.00	0.13±0.00	0.07±0.00	0.10±0.00	0.09±0.00	0.12±0.00	0.13±0.00	0.09±0.00	0.12±0.00	0.12 (38.44)
C18:0	2.36±0.01	2.26±0.01	2.04±0.00	2.42±0.01	2.24±0.02	2.98±0.03	2.22±0.01	2.02±0.01	2.44±0.01	2.52±0.00	2.35 (11.76)
C18:1n–9	71.78±0.05	73.52±0.08	69.73±0.06	73.37±0.05	67.92±0.21	73.81±0.03	71.59±0.07	69.79±0.03	69.23±0.16	69.02±0.04	70.98 (2.98)
C18:1n–7	3.12±0.02	2.60±0.05	3.84±0.03	3.27±0.01	3.44±0.37	3.28±0.01	3.23±0.05	3.82±0.03	3.18±0.11	3.55±0.03	3.33 (10.85)
∑C18:1	74.90±0.03	76.12±0.02	73.57±0.03	76.64±0.04	71.36±0.18	77.09±0.03	74.82±0.02	73.61±0.03	72.42±0.05	72.57±0.03	74.31 (2.59)
C18:2n–6	6.79±0.01	6.75±0.03	8.60±0.01	5.49±0.00	11.08±0.09	4.89±0.00	8.23±0.01	8.66±0.01	9.89±0.02	9.33±0.01	7.97 (24.61)
C18:3n–3	0.96±0.00	0.78±0.00	0.59±0.00	0.62±0.00	0.64±0.00	0.58±0.00	0.80±0.00	0.59±0.00	0.69±0.01	0.67±0.00	0.69 (17.65)
C20:0	0.39±0.01	0.42±0.00	0.33±0.00	0.41±0.00	0.35±0.00	0.38±0.00	0.40±0.00	0.33±0.00	0.37±0.01	0.36±0.01	0.37 (9.05)
C20:1n–9	0.29±0.01	0.41±0.00	0.27±0.00	0.30±0.00	0.29±0.00	0.23±0.00	0.28±0.00	0.27±0.01	0.29±0.01	0.26±0.01	0.29 (16.33)
C22:0	0.09±0.00	0.10±0.00	0.08±0.00	0.11±0.00	0.09±0.00	0.09±0.00	0.11±0.00	0.08±0.00	0.09±0.00	0.09±0.00	0.09 (11.29)
C24:0	0.05±0.00	0.04±0.00	0.03±0.00	0.04±0.00	0.03±0.00	0.03±0.00	0.04±0.00	0.03±0.00	0.03±0.00	0.03±0.00	0.04 (18.60)
∑SFA[a]	15.95	15.37	15.63	15.94	15.55	16.08	14.89	15.52	15.70	15.93	15.66 (2.26)
∑MUFA[a]	76.30	77.10	75.18	77.95	72.74	78.45	76.08	75.23	73.72	74.07	75.68 (2.45)
∑PUFA[a]	7.75	7.53	9.19	6.11	11.72	5.47	9.03	9.25	10.58	10.00	8.66 (22.57)

[a] ∑SFA consists of C16:0, C17:0, C18:0, C20:0, C22:0 and C24:0; ∑MUFA consists of C16:1n–9, C16:1n–7, C17:1n–8, C18:1n–9, C18:1n–7 and C20:1n–9; ∑PUFA consists of C18:2n–6 and C18:3n–3.
[#] Average is the reported %FA for the FAME across all varieties. Area RSD of IS (C19:0) = 4.1% (n = 30, analysis made over a 2-day period)

-tion but with a smaller number of compounds, e.g. by selecting VOCs with reported aroma activity, or omitting less abundant VOCs, did not result in better differentiation of the oil varieties.

Varieties clustered in the same region indicated they have similar VOCs profile. The three mixed samples Medium, Mild and Robust flavours, made by combining different single varieties (Section 2.1) were displayed somewhat in a geometrical average position between the single varieties from which they were composed, but all were located close together. Single varieties Arbequina, Coratina and Frantoio were also displayed in the same region, suggesting they have similar VOC composition with the mixed samples, in respect of PC1 and PC2. The volatile profiles of Hojiblanca, Koroneiki, Picual and Barnea, appeared to be very different to each other, and from the other varieties. Picual and Barnea were used to produce Medium flavour, which is located between these two varieties, but is still clustered in proximity to Robust and Mild flavour.

The mixed samples are blended from olive varieties to give a distinctive flavour, and to ensure a flavour profile consistent from year-to-year. Medium flavour has 'a combination of fresh, grassy notes, green banana, and tomatoes with moderate bitterness, pungency and creamy aftertaste'. Picual, the main variety of olive oil used to make the Medium flavour (see Section 3.4), has 'fruity punchiness and typical aromatic notes of tomato bush'. They possibly cluster in one region because: 1) all the mixed samples have the variety Barnea in common (although of different ratio), with similar VOCs profile, and/or 2) the mixed samples cluster in a 'favoured flavour' region comprising VOCs with desirable sensory attributes, though with some distinct flavour differences. There is no guarantee that the PCA selects for specific aroma compounds in the GC analyses, since sensory

Table 4
Percentage of FAs (%FA) composition of EVOO from 2019 products. (Data in this Table presented to two decimal places; in the manuscript text they will be presented to one decimal place).

FAME	%FA (Mean ± SD), n=3										
	Hojiblanca	Coratina	Arbequina	Koroneiki	Frantoio	Picual	Barnea	Mild Flavour	Robust Flavour	Medium Flavour	Average[#] (RSD)
C16:0	12.09±0.03	9.94±0.01	13.11±0.03	11.13±0.03	12.67±0.06	12.99±0.01	12.31±0.01	13.22±0.03	11.63±0.01	12.35±0.05	12.14 (8.37)
C16:1n–9	0.09±0.00	0.10±0.00	0.17±0.00	0.11±0.00	0.11±0.00	0.07±0.00	0.09±0.00	0.10±0.00	0.09±0.00	0.07±0.00	0.10 (27.65)
C16:1n–7	0.76±0.00	0.28±0.00	1.16±0.00	0.63±0.00	0.80±0.00	1.34±0.00	0.71±0.00	1.08±0.00	0.77±0.00	1.06±0.01	0.86 (35.41)
∑C16:1	0.85±0.00	0.38±0.00	1.32±0.00	0.74±0.00	0.91±0.00	1.41±0.00	0.80±0.00	1.19±0.00	0.86±0.00	1.13±0.01	0.96 (31.88)
C17:0	0.08±0.00	0.05±0.00	0.10±0.00	0.05±0.00	0.06±0.00	0.04±0.00	0.05±0.00	0.07±0.00	0.05±0.00	0.04±0.00	0.06 (31.86)
C17:1n–8	0.15±0.00	0.08±0.00	0.22±0.00	0.09±0.00	0.12±0.00	0.11±0.00	0.09±0.00	0.16±0.00	0.09±0.00	0.09±0.00	0.12 (37.31)
C18:0	2.32±0.01	2.11±0.01	1.64±0.00	2.29±0.00	1.84±0.01	1.95±0.01	2.38±0.00	2.35±0.01	2.69±0.01	2.60±0.00	2.22 (14.95)
C18:1n–9	73.75±0.03	77.38±0.04	68.10±0.13	75.51±0.02	70.79±0.18	74.90±0.05	70.42±0.00	70.63±0.06	74.87±0.06	74.87±0.05	73.12 (4.02)
C18:1n–7	3.18±0.01	2.23±0.03	3.90±0.15	3.05±0.01	3.16±0.29	3.98±0.03	3.27±0.00	3.65±0.07	3.12±0.06	3.53±0.01	3.31 (15.21)
∑C18:1	76.93±0.02	79.61±0.02	72.00±0.01	78.57±0.03	73.95±0.11	78.88±0.02	73.68±0.00	74.28±0.01	77.99±0.01	78.40±0.05	76.43 (3.52)
C18:2n–6	5.91±0.01	6.12±0.01	10.33±0.02	5.59±0.00	9.06±0.04	3.13±0.01	9.26±0.00	7.31±0.01	5.17±0.01	4.03±0.01	6.59 (35.74)
C18:3n–3	0.80±0.00	0.74±0.00	0.51±0.00	0.66±0.00	0.61±0.00	0.77±0.00	0.64±0.00	0.64±0.00	0.73±0.00	0.64±0.00	0.67 (12.64)
C20:0	0.41±0.00	0.39±0.00	0.34±0.01	0.42±0.01	0.34±0.00	0.33±0.00	0.37±0.00	0.37±0.01	0.38±0.01	0.35±0.00	0.37 (8.08)
C20:1n–9	0.31±0.00	0.44±0.00	0.30±0.00	0.32±0.00	0.31±0.00	0.27±0.00	0.29±0.00	0.27±0.01	0.29±0.00	0.25±0.00	0.30 (17.39)
C22:0	0.11±0.00	0.10±0.00	0.09±0.00	0.12±0.00	0.09±0.00	0.08±0.00	0.09±0.00	0.10±0.00	0.09±0.00	0.08±0.00	0.10 (12.31)
C24:0	0.04±0.00	0.04±0.00	0.03±0.00	0.04±0.00	0.04±0.00	0.04±0.00	0.03±0.00	0.04±0.00	0.04±0.00	0.03±0.00	0.04 (6.93)
∑SFA[a]	15.05	12.63	15.32	14.04	15.04	15.43	15.24	16.15	14.87	15.46	14.92 (6.47)
∑MUFA[a]	78.25	80.51	73.84	79.72	75.29	80.66	74.86	75.90	79.23	79.87	77.81(3.32)
∑PUFA[a]	6.71	6.86	10.84	6.24	9.67	3.90	9.90	7.95	5.89	4.68	7.26 (31.59)

[a] ∑SFA consists of C16:0, C17:0, C18:0, C20:0, C22:0 and C24:0; ∑MUFA consists of C16:1n–9, C16:1n–7, C17:1n–8, C18:1n–9, C18:1n–7 and C20:1n–9; ∑PUFA consists of C18:2n–6 and C18:3n–3.
[#] Average is the reported %FA for the FAME across all varieties. Area RSD of IS (C19:0) = 3.2% (n = 30, analysis made over a 2-day period)

analysis may also include less abundant compounds. Barnea is rich in (*E*)-2-hexenal, with an odour described as green, apple-like, bitter and fatty. Medium flavour combines Barnea and Picual; the latter having high abundance of (*Z*)-3-hexenyl acetate with an aroma described as green-banana, fruity, green and floral. (*Z*)-3-Hexenyl acetate was in high amounts in Koroneiki, used as a variety in Robust flavour. Both Picual and Koroneiki have relatively high amounts of sweet, fruity and floral hexyl acetate. Coratina, another component of Robust flavour, has high amounts of (*E*)-2-hexen-1-ol and 1-hexanol, with aromas of green, grassy, fruity, pungent and aromatic (Angerosa et al., 2004; Kalua et al., 2007). Why mixed samples are located close in the scores plot is unclear.

The mixed samples, and single varieties used to make mixed samples, were selected; other varieties (Hojiblanca and Frantoio) were removed from the data set and the PCA recalculated. **Fig. 3** shows the new scores plot and loadings plot. 1-Penten-3-one and (*Z*)-3-hexenal VOCs were removed, being detected only in Hojiblanca. The mixed samples are now better separated (Fig. 3A) and bracketed by the single varieties used in their preparation. The mixed varieties were located close to Barnea, a common variety for all mixed samples. The loadings plot (Fig. 3B) indicates that mainly α-farnesene and trans-β-ocimene characterise Barnea, Medium flavour, Mild flavour and Robust flavour. Coratina was associated with (*E*)-2-hexene-1-ol and nonanal, while hexyl acetate and (*Z*)-3-hexenyl acetate distinguish Koroneiki. Picual was distinguished by (*Z*)-3-hexenyl acetate and dodecene.

The alternative PCA procedure still fails to clearly differentiate the mixed samples, which is guided by the sensory flavour of the mixed samples. A study conducted on rapeseed oils reported that the results of volatile compound analysis differs from those of sensory analysis in oils comparison

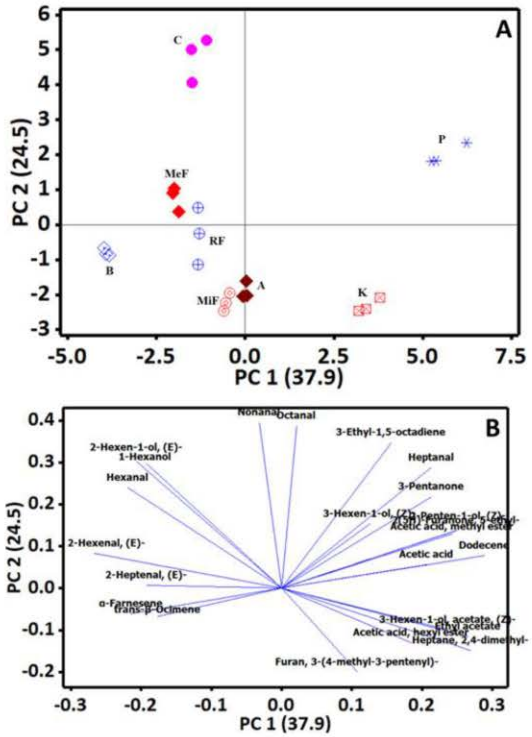

Fig. 3. Principal component analysis (PCA) (A) score plot and (B) loading plot of 8 different EVOO varieties (n = 3) from 2018 products, based on 23 major VOCs composition, by omitting 1-penten-3-one and (*Z*)-3-hexenal (which were only found in Hojiblanca, which was also removed). A: Arbequina; B: Barnea; C: Coratina; K: Koroneiki; P: Picual; MeF: Medium flavour; MiF: Mild flavour; and RF: Robust flavour.

(Gracka et al., 2017). Flavour is a result of combination of many chemicals including VOCs, for instance polyphenols lend pungency to the EVOO. It is possible that minor VOCs do not predominate in the PCA study though could have a pronounced role in differentiating mixed samples. Thus, clear differentiation of mixed EVOO samples was not achieved based on PCA of the VOCs.

3.3. *Analysis of fatty acid (FAs) composition*

The seven single varieties and three mixed samples of EVOO in both 2018 and 2019 were analysed for FAs composition. In-house mixed samples of EVOO were prepared (Table 1) from single varieties used to produce commercial samples, to investigate whether %FA composition can be used to predict the *v/v* composition of commercial mixtures. Thus, for example Arbequina and Barnea were mixed in ratios of 4:1, 3:2, 2:3, and 1:4 (Table 1). The compositions of 14 FAs found in EVOO were determined, expressed as mean percentage (%FA) (n = 3) of the total FA. Internal standard methyl nonadecanoate (C19:0 FAME) corrects for variation in retention times and to calculate %FA composition based on area ratio. Example GC–FID chromatograms of EVOO can be found in Supplementary Material **Fig. S2**. FAs were identified by comparing retention times with authentic FAME standards, confirmed by MS.

The %FA with standard deviations (SD) for different EVOO are shown in **Tables 3** and **4** for 2018 and 2019 products, respectively, with total amount of saturated (SFA), monounsaturated (MUFA), and polyunsaturated (PUFA) FAs reported. Major FAs detected were C16:0, C18:0, C18:1n–9, C18:1n–7 and C18:2n–6, with C18:1n–9 contributing to about 70% in all varieties. Minor abundance FAs were C16:1n–9, C16:1n–7, C17:0, C17:1n–8, C18:3n–3, C20:0, C20:1n–9, C22:0, and C24:0.

On average, 2018 products have higher SFA (15.7%, RSD = 2.3) and PUFA (8.7%, RSD = 22.6), compared to 2019 EVOO, which had 14.9% SFA (RSD = 6.5) and 7.3% PUFA (RSD = 31.6). The 2019 products have higher MUFA (77.8%, RSD = 3.3), mainly C18:1n–9, compared to 75.7% (RSD = 2.5) in 2018. However, there was more variation in FA composition between different varieties of EVOO. Among 2018 varieties Picual has the highest MUFA (78.5%) and the lowest PUFA (5.5%) whereas Frantoio contains the lowest MUFA (72.7%) and the highest PUFA (11.7%). Among 2019 varieties, Picual has the highest MUFA (80.7%) and the lowest PUFA (3.9%) content. Coratina had a high amount of MUFA (80.5%) with the lowest composition of SFA (12.6%). As expected, across all varieties there was more variation in the %FA composition for minor FAs than for major FAs – refer to the right hand column, Tables 3 and 4. For instance, for 2018, C17:0 gave RSD of 40.8%, and 31.8% for 2019. However, C18:2n–6 had reasonable abundance, but showed significant variability – RSDs of 24.6% and 35.7% for 2018 and 2019, respectively. Major MUFA (C18:1n–9) and major PUFA (C18:2n–6) ranged from 67.9–73.8% and 4.9–11.1% respectively for 2018, and 68.1–77.4% and 3.1–10.3% respectively for 2019 (Table 3 and 4). The maximum % of C18:1n–9 was detected in Coratina (73.5%), Koroneiki (73.4%) and Picual (73.8%) for 2018. In 2019, this was ≥73% in six varieties. The highest amount of C18:2n–6 was detected in Frantoio (11.1%, 2018) and Arbequina (10.3%, 2019), compared with Picual (4.9% and 3.1% respectively).

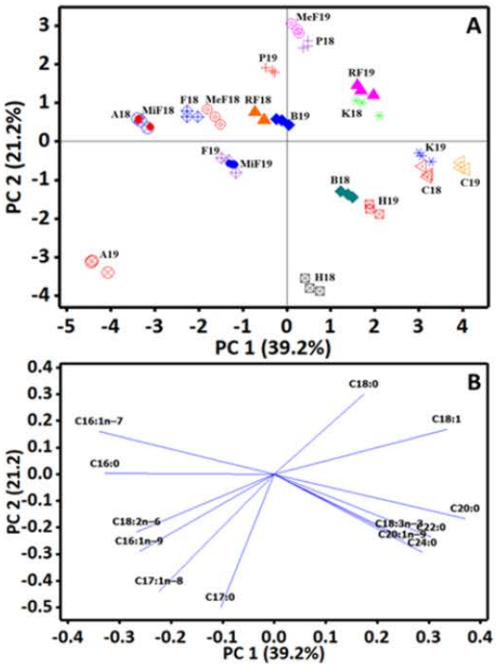

Fig. 4. Principal component analysis (PCA) (A) score plot and (B) loading plot of %FA composition for 2018 and 2019 EVOO products. The included EVOO varieties are A: Arbequina; B: Barnea; C: Coratina; F: Frantoio; H: Hojiblanca; P: Picual; K: Koroneiki; MeF: Medium flavour; MiF: Mild flavour; and RF: Robust flavour. The numbers 18 and 19 followed EVOO variety names represent 2018 and 2019 production year respectively.

Table 5
Percentage of FA (%FA) composition of in-house EVOO mixtures, prepared from 2019 products.

FAME	%FA (Mean ± SD)[a], n=3									
	A:B (1:4)	A:B (2:3)	A:B (3:2)	A:B (4:1)	B:P (1:4)	B:P (2:3)	B:P (3:2)	B:P (4:1)	B:C:K (2:3:5)	B:C:K (2:7:1)
C16:0	12.52±0.04	12.63±0.02	12.80±0.01	12.94±0.04	12.86±0.02	12.71±0.02	12.59±0.01	12.45±0.03	11.19±0.02	10.75±0.01
C16:1n–9	0.10±0.00	0.12±0.00	0.13±0.00	0.15±0.00	0.07±0.00	0.07±0.00	0.08±0.00	0.08±0.00	0.10±0.00	0.09±0.00
C16:1n–7	0.81±0.00	0.88±0.00	0.97±0.00	1.06±0.00	1.22±0.00	1.09±0.00	0.97±0.01	0.84±0.00	0.55±0.00	0.41±0.00
∑C16:1	0.91±0.01	1.00±0.00	1.10±0.00	1.20±0.00	1.29±0.00	1.17±0.00	1.05±0.01	0.93±0.00	0.64±0.00	0.51±0.00
C17:0	0.06±0.00	0.06±0.00	0.08±0.00	0.08±0.00	0.04±0.00	0.05±0.00	0.05±0.00	0.05±0.00	0.05±0.00	0.05±0.00
C17:1n–8	0.12±0.00	0.14±0.00	0.17±0.01	0.19±0.01	0.11±0.00	0.10±0.00	0.10±0.00	0.10±0.01	0.09±0.00	0.08±0.00
C18:0	2.18±0.01	2.06±0.01	1.92±0.00	1.79±0.00	2.02±0.01	2.10±0.02	2.18±0.02	2.26±0.00	2.19±0.01	2.11±0.02
C18:1n–9	69.86±0.09	69.42±0.07	69.10±0.14	68.67±0.08	74.04±0.06	73.18±0.11	72.31±0.08	71.44±0.18	72.51±0.06	73.04±0.06
C18:1n–7	3.50±0.13	3.64±0.05	3.61±0.12	3.73±0.11	3.84±0.06	3.70±0.08	3.47±0.09	3.32±0.13	5.50±0.04	5.36±0.03
∑C18:1	73.36±0.05	73.07±0.04	72.71±0.02	72.40±0.03	77.88±0.01	76.89±0.04	75.77±0.02	74.76±0.05	78.00±0.01	78.40±0.05
C18:2n–6	9.51±0.01	9.70±0.01	9.90±0.01	10.11±0.01	4.36±0.01	5.56±0.01	6.84±0.01	8.05±0.01	6.41±0.00	6.67±0.00
C18:3n–3	0.62±0.00	0.59±0.00	0.58±0.01	0.55±0.01	0.74±0.01	0.72±0.00	0.70±0.01	0.67±0.01	0.67±0.00	0.68±0.01
C20:0	0.34±0.00	0.35±0.01	0.34±0.01	0.33±0.00	0.32±0.01	0.33±0.00	0.34±0.00	0.35±0.00	0.36±0.01	0.33±0.01
C20:1n–9	0.27±0.00	0.27±0.01	0.28±0.01	0.28±0.01	0.26±0.00	0.26±0.01	0.27±0.00	0.27±0.01	0.30±0.00	0.34±0.00
C22:0	0.09±0.00	0.09±0.00	0.09±0.00	0.09±0.00	0.08±0.00	0.08±0.00	0.09±0.00	0.09±0.00	0.08±0.00	0.07±0.00
C24:0	0.03±0.00	0.03±0.00	0.03±0.00	0.03±0.00	0.04±0.00	0.03±0.00	0.04±0.00	0.04±0.00	0.02±0.00	0.02±0.00
∑SFA[b]	15.22	15.22	15.26	15.27	15.36	15.30	15.28	15.23	13.88	13.32
∑MUFA[b]	74.66	74.48	74.27	74.07	79.54	78.41	77.18	76.05	79.04	79.32
∑PUFA[b]	10.12	10.30	10.48	10.66	5.10	6.28	7.54	8.72	7.08	7.35

[a] The single varieties used were A: Arbequina; B: Barnea; C: Coratina; P: Picual; K: Koroneiki with the ratio shown in Table 1.
[b] ∑SFA consists of C16:0, C17:0, C18:0, C20:0, C22:0 and C24:0; ∑MUFA consists of C16:1n–9, C16:1n–7, C17:1n–8, C18:1n–9, C18:1n–7 and C20:1n–9; ∑PUFA consists of C18:2n–6 and C18:3n–3.
Area RSD of IS (C19:0) = 4.3% (n = 30, analysis made over a 2-day period)

Reportedly C18:1 increases, whereas C16:0 and C18:2 decrease, as fruit ripens. Ripening increases MUFAs and decreases total PUFAs (Fuentes de Mendoza et al., 2013); the ratio of unsaturated to SFAs composition varies depending on olive cultivar. FA composition also varies with processing (extraction) of olive oil from its fruit (Issaoui et al., 2009). Thus %FA may serve to distinguish olive oil variety.

Changes in %FA in in-house mixed samples depends on the mixing ratio of varieties (**Table 5**, 2019 products). For the mix Arbequina:Barnea, many %FA compositions, e.g. C16:0, C16:1n–9, C17:1n–8, C18:1n–7, C18:2n–6 and C20:1n–9 increased with increasing proportion of Arbequina, whereas %FA composition of C18:0, C18:1n–9 and C18:3n–3 decreased with increasing proportion of Arbequina, according to %FAs in the single varieties (Table 4). Similarly, for Barnea:Picual, C18:1n–9 and C18:3n–3 increased, but C18:2n–6 decreased with increasing proportion of Picual (Table 4 and 5).

3.4. Principal component analysis (PCA) of FAs

The PCA was calculated for 13 FAs in 60 samples (10 varieties of each 2018 and 2019 products, n = 3), shown in **Fig. 4A** with PC1 (39.2%) and PC2 (21.2%). Variety production year did not overlap; factors attributed to the FA differences were unclear. The greatest variation in FAs composition was for Arbequina and Coratina 2019 varieties. From the loadings plot (**Fig. 4B**), the upper right quadrant varieties Koroneiki and Picual (both 2018), Medium flavour and Robust flavour (both 2019) were distinguished by C18:0 and ΣC18:1. Varieties at the lower right quadrant Barnea and Coratina (both 2018), and Hojiblanca, Coratina and Koroneiki (all 2019) were correlated by C20:0 and C22:0, whereas Hojibanca (2018) was distinguished by C24:0. Arbequina (2019) and

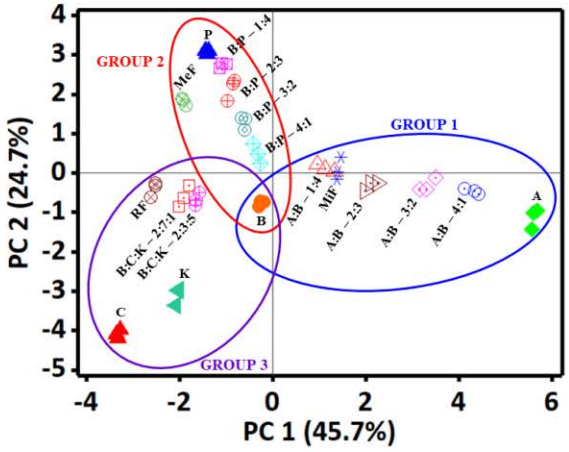

Fig. 5. Principal component analysis (PCA) score plot of %FAs composition for in-house mixed varieties. The included EVOO varieties are A: Arbequina; B: Barnea; C: Coratina; P: Picual; K: Koroneiki; MeF: Medium flavour; MiF: Mild flavour; RF: Robust flavour; A:B: Arbequina:Barnea in-house mix; B:P: Barnea:Picual in-house mix; and B:C:K: Barnea:Coratina:Koroneiki in-house mix, with the ratio of those in-house mix shown after the EVOO variety name.

Mild flavour (2019) in the lower left quadrant were distinguishable by C17:0 and C17:1n–8, but their 2018 varieties (upper left quadrant) were correlated by C16:0 and C16:1n–7. Even though the Medium, Mild and Robust flavour oils are blended to have the same flavour year-to-year, their positions on the PCA plot (FA compositions) do not overlap, presumably because blending is directed by sensory properties.

The PCA scores plot of in-house mixed samples (**Fig. 5**) and their pure single olive oil, comprising 13 FAs of 54 samples (18 samples, $n = 3$) gave PC1(45.7%) and PC2(24.7%) values. The in-house mixes are separated into clear groups (Groups 1, 2 and 3, Fig. 5) according to the single varieties used in their preparation, and the ratios of the different mixes. For Group 1, Arbequina:Barnea, the mixed oils were linearly distributed according to their *v/v* proportions, between the single variety oils. The loadings plot for the in-house mixed varieties is shown in Supplementary Material **Fig. S3**, with the FAs that most distinguished each group of in-house mixed samples. Group 1 (Mild) was correlated by C17:0 and C17:1n–8, Group 2 (Medium) and Group 3 (Robust) were distinguished by C18:0 and C18:1. These results were similar to the loadings plot of FA composition for the 2018 and 2019 samples, specifically Medium, Mild and Robust flavour (all 2019 samples), explained above (Fig. 4B).

The MiF variety located on the PCA close to A:B – 1:4 mix (Group 1), assumed to be prepared by mixing A:B at about 25% Barnea (the mixing ratio was not revealed to researchers). Similarly, B:P mix ratios (Group 2, Fig. 5) are linearly displayed between the B and P varieties according to *v/v* proportions. The MeF variety was located between B and P, but off the mixing ratio trend line. In Group 3, two mixes of B:C:K were prepared in ratios 2:3:5 and 2:7:1, from which the RF mix derives. The two mixes were displayed close to the RF variety. This suggests that based on the FAs composition, it is possible to predict the varietal composition of the signature oil products, if the authentic reference EVOO are available.

4. Conclusion

Analyses of VOCs and FAs display differences in composition among EVOO varieties. Based on PCA of VOCs, single varieties were differentiated while the mixed samples were not clearly differentiated. It is possible the VOCs that mainly contribute to PCA plots do not adequately reflect the aroma profile or flavour of the mixed EVOO varieties, where mixtures are prepared based on sensory considerations. There are other factors that could affect the VOCs profile, such as maturity index, that was not considered in this study. Analysis based on FAs comparison more clearly revealed differences among the varieties studied. PCA demonstrated differences in FAs composition between 2018 and 2019 varieties for reasons that are not apparent. The analysis of FAs in in-house mixes of single varieties clearly illustrate changes in FAs composition based on proportions of the single varieties in the mixes, suggesting the proportion of single varieties comprising the mixed sample oils could be reasonably well predicted.

Declarations of Conflict of Interest: Authors HDW, YN, BRW and PJM have no conflict of interest. CG is an employee of Modern Olives, and the results of this study on EVOO may be of relevance to the commercial interests of Modern Olives.

Acknowledgements

HDW acknowledges provision of MGS and DIPRS Scholarships from Monash University. This work was conducted under support from the Australian Research Council and PerkinElmer through ARC Linkage Grant LP150100465.

References

Amanpour, A., Kelebek, H., & Selli, S. (2019). Characterization of aroma, aroma-active compounds and fatty acids profiles of cv. Nizip Yaglik oils as affected by three maturity periods of olives. *Journal of the Science of Food and Agriculture, 99*(2), 726-740.

Angerosa, F. (2002). Influence of volatile compounds on virgin olive oil quality evaluated by analytical approaches and sensor panels. *European Journal of Lipid Science and Technology, 104*(9-10), 639-660.

Angerosa, F., Servili, M., Selvaggini, R., Taticchi, A., Esposto, S., & Montedoro, G. (2004). Volatile compounds in virgin olive oil: Occurrence and their relationship with the quality. *Journal of Chromatography A, 1054*(1-2), 17-31.

Baccouri, O., Bendini, A., Cerretani, L., Guerfel, M., Baccouri, B., Lercker, G., et al. (2008). Comparative study on volatile compounds from Tunisian and Sicilian monovarietal virgin olive oils. *Food Chemistry, 111*(2), 322-328.

Borges, T. H., Pereira, J. A., Cabrera-Vique, C., Lara, L., Oliveira, A. F., & Seiquer, I. (2017). Characterization of Arbequina virgin olive oils produced in different regions of Brazil and Spain: Physicochemical properties, oxidative stability and fatty acid profile. *Food Chemistry, 215*, 454-462.

Brereton, R. G. (2003). *Chemometrics: Data analysis for the laboratory and chemical plant*. England: John Wiley & Sons Ltd, (Chapter 4).

Cajka, T., Riddellova, K., Klimankova, E., Cerna, M., Pudil, F., & Hajslova, J. (2010). Traceability of olive oil based on volatiles pattern and multivariate analysis. *Food Chemistry, 121*(1), 282-289.

Damascelli, A., & Palmisano, F. (2013). Sesquiterpene fingerprinting by headspace SPME-GC-MS: preliminary study for a simple and powerful analytical tool for traceability of olive oils. *Food Analytical Methods, 6*(3), 900-905.

Fuentes de Mendoza, M., De Miguel Gordillo, C., Marín Expóxito, J., Sánchez Casas, J., Martínez Cano, M., Martín Vertedor, D., & Franco Baltasar, M. N. (2013). Chemical composition of virgin olive oils according to the ripening in olives. *Food Chemistry, 141*(3), 2575-2581.

Gracka, A., Raczyk, M., Hradecký, J., Hajslova, J., Jeziorski, S., Karlovits, G., et. al. (2017). Volatile compounds and other indicators of quality for cold-pressed rapeseed oils obtained from peeled, whole, flaked and roasted seeds. *European Journal of Lipid Science and Technology, 119*(10).

Guissous, M., Le Dréau, Y., Boulkhroune, H., Madani, T., & Artaud, J. (2018). Chemometric characterization of eight monovarietal algerian virgin olive oils. *Journal of the American Oil Chemists' Society, 95*(3), 267-281.

Issaoui, M., Dabbou, S., Brahmi, F., Hassine, K. B., Ellouze, M. H., & Hammami, M. (2009). Effect of extraction systems and cultivar on the quality of virgin olive oils. *International Journal of Food Science & Technology, 44*(9), 1713-1720.

Kalua, C. M., Allen, M. S., Bedgood Jr, D. R., Bishop, A. G., Prenzler, P. D., & Robards, K. (2007). Olive oil volatile compounds, flavour development and quality: A critical review. *Food Chemistry, 100*(1), 273-286.

Kosma, I., Badeka, A., Vatavali, K., Kontakos, S., & Kontominas, M. (2016). Differentiation of Greek extra virgin olive oils according to cultivar based on volatile compound analysis and fatty acid composition. *European Journal of Lipid Science and Technology, 118*(6), 849-861.

Lukić, I., Carlin, S., Horvat, I., & Vrhovsek, U. (2019). Combined targeted and untargeted profiling of volatile aroma compounds with comprehensive two-dimensional gas chromatography for differentiation of virgin olive oils according to variety and geographical origin. *Food Chemistry, 270*, 403-414.

Oğraş, Ş. Ş., Kaban, G., & Kaya, M. (2018). Volatile compounds of olive oils from different geographic regions in Turkey. *International Journal of Food Properties, 21*(1), 1833-1843.

Portarena, S., Anselmi, C., Zadra, C., Farinelli, D., Famiani, F., Baldacchini, C., & Brugnoli, E. (2019). Cultivar discrimination, fatty acid profile and carotenoid characterization of monovarietal olive oils by Raman spectroscopy at a single glance. *Food Control, 96*, 137-145.

Pouliarekou, E., Badeka, A., Tasioula-Margari, M., Kontakos, S., Longobardi, F., & Kontominas, M. G. (2011). Characterization and classification of Western Greek olive oils according to cultivar and geographical origin based on volatile compounds. *Journal of Chromatography A, 1218*(42), 7534-7542.

Sanz, C., Belaj, A., Sánchez-Ortiz, A., & Pérez, A. G. (2018). Natural variation of volatile compounds in virgin olive oil analyzed by HS-SPME/GC-MS-FID. *Separations, 5*(2), 24.

Sarolic, M., Gugic, M., Tuberoso, C. I. G., Jerkovic, I., Suste, M., Marijanovic, Z., & Kus, P. M. (2014). Volatile profile, phytochemicals and antioxidant activity of virgin olive oils from croatian autochthonous varieties masnjaca and krvavica in comparison with italian variety leccino. *Molecules, 19*(1), 881-895.

Tura, D., Prenzler, P. D., Bedgood Jr, D. R., Antolovich, M., & Robards, K. (2004). Varietal and processing effects on the volatile profile of Australian olive oils. *Food Chemistry, 84*(3), 341-349.

Vaz-Freire, L. T., da Silva, M. D. R. G., & Freitas, A. M. C. (2009). Comprehensive two-dimensional gas chromatography for fingerprint pattern recognition in olive oils produced by two different techniques in Portuguese olive varieties Galega Vulgar, Cobrançosa e Carrasquenha. *Analytica Chimica Acta, 633*(2), 263-270.

Zhou, Q., Liu, S., Liu, Y., & Song, H. (2019). Comparative analysis of volatiles of 15 brands of extra-virgin olive oils using solid-phase micro-extraction and solvent-assisted flavor evaporation. *Molecules, 24*(8), 1512.

6.3. Supporting information

Extra virgin olive oil signature flavour mix differentiation based on analysis of volatile organic compounds and fatty acids

Habtewold D. Waktola, Yada Nolvachai, Claudia Guillaume, Bayden R. Wood, Philip J. Marriott

Contents

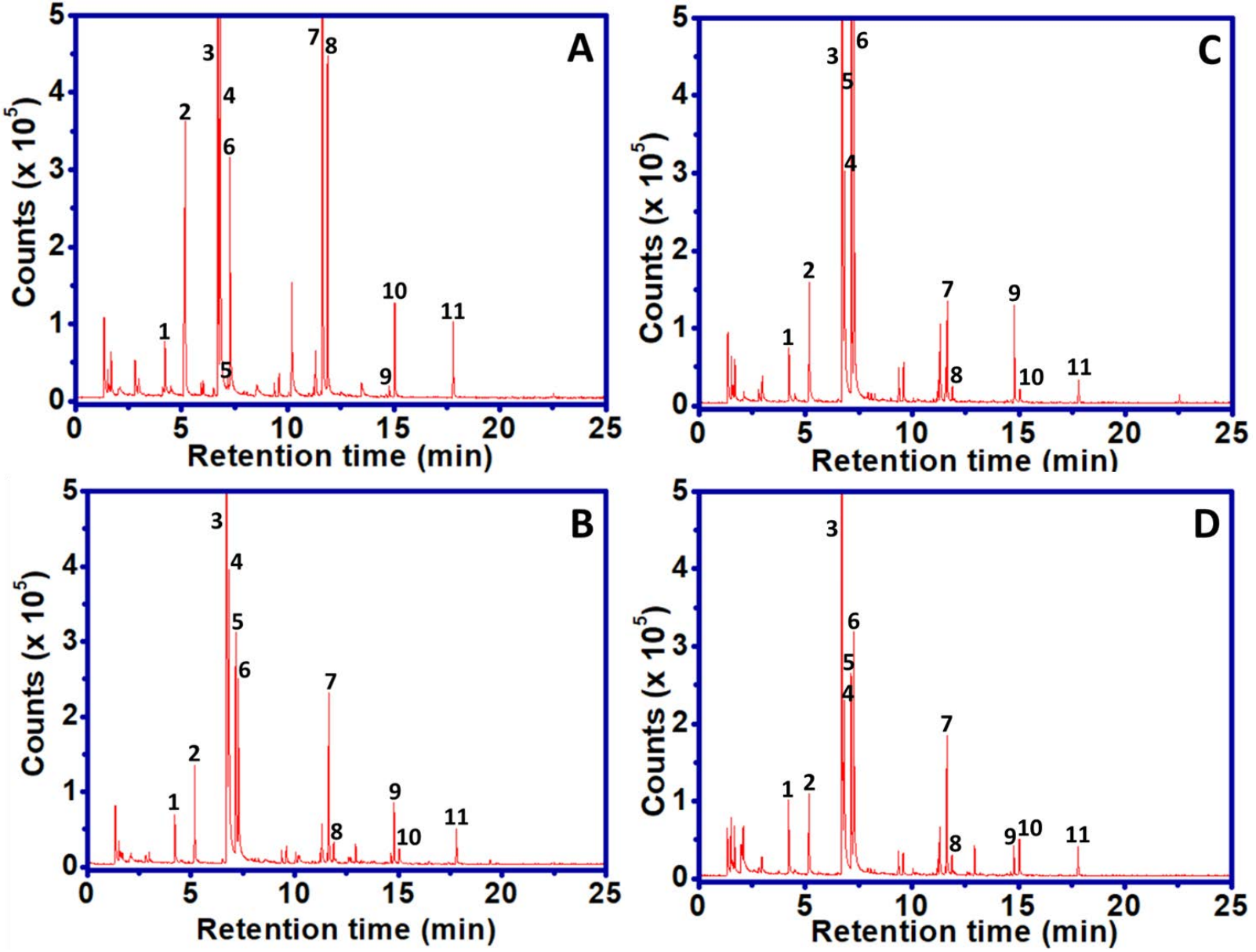
A
B
C
D
Counts (x 10^5)
Retention time (min)

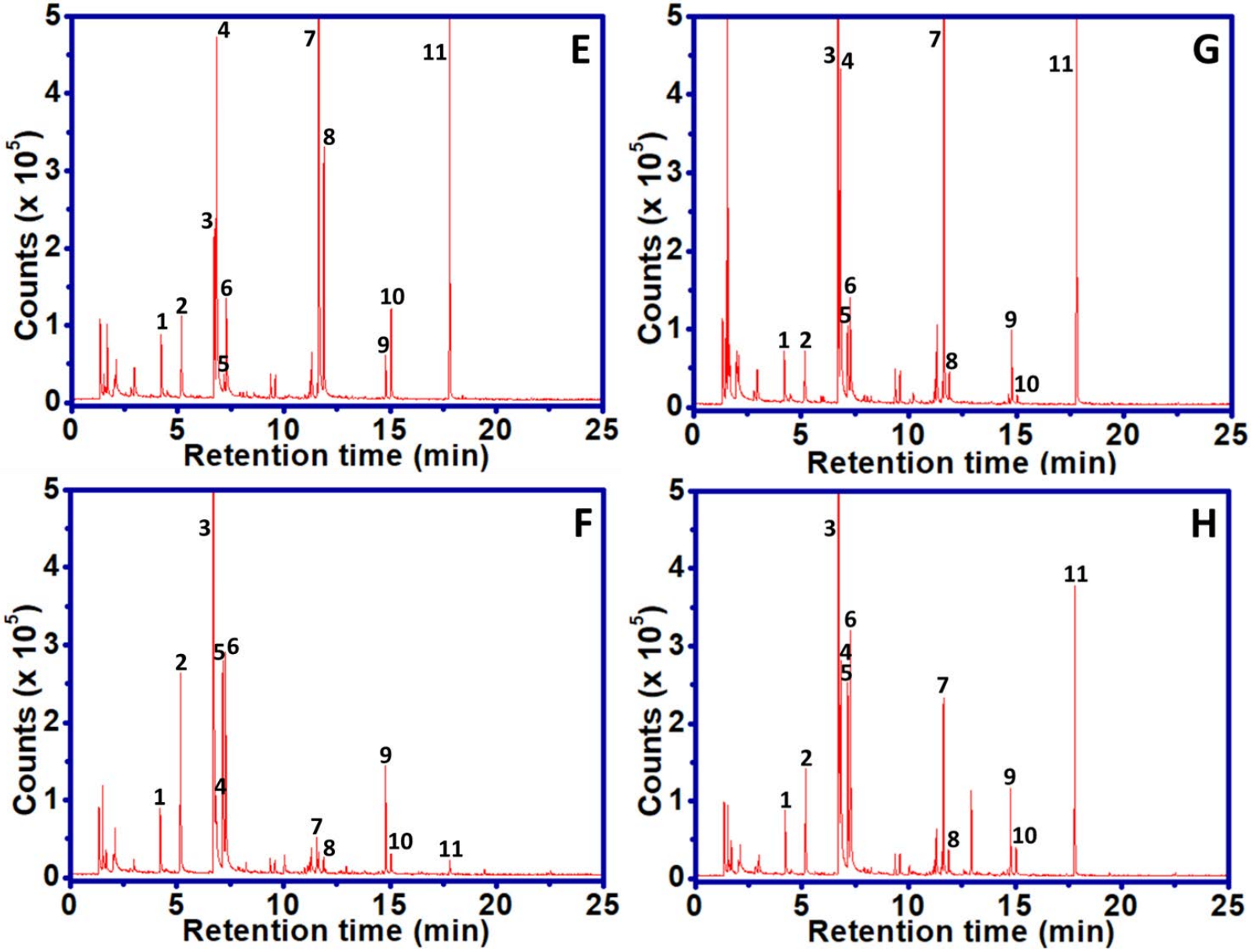
E
G
F
H
Counts (x 10^5)
Retention time (min)

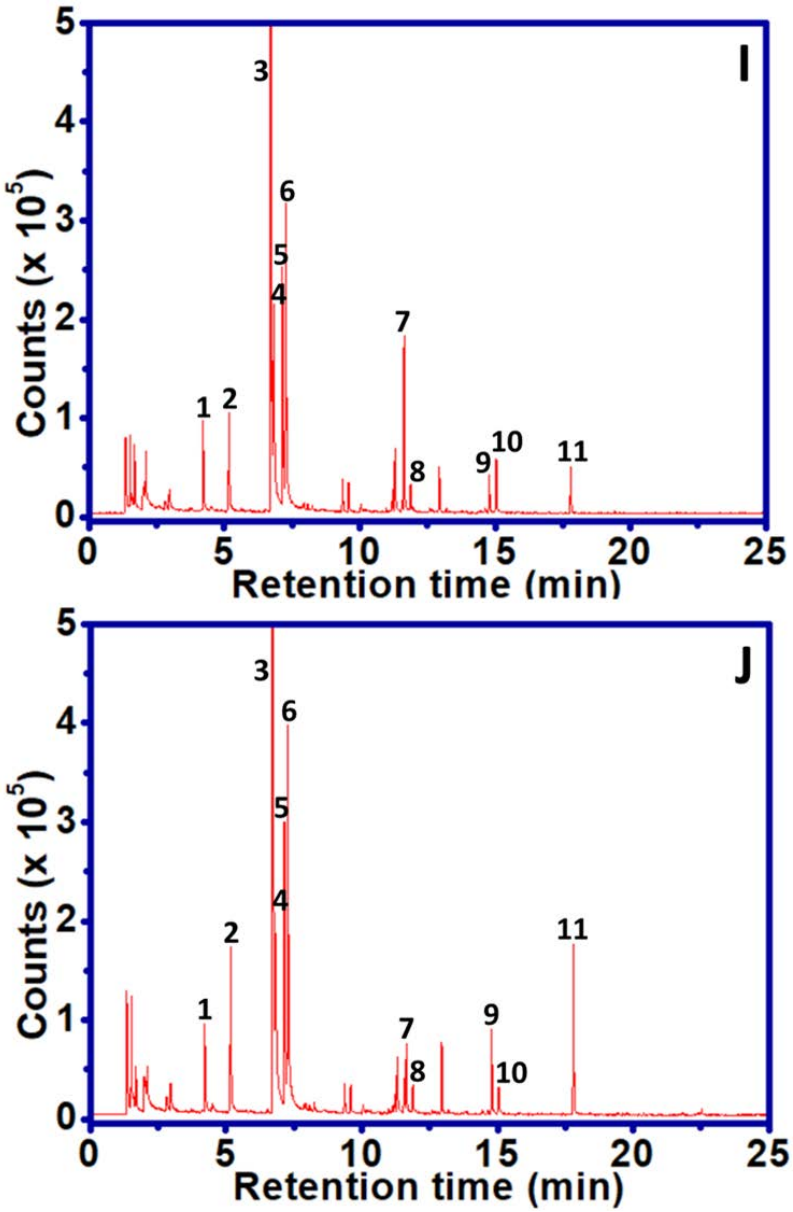

Fig. S1. GC–MS chromatogram of VCs in EVOO varieties (A) Hojiblanca (B) Barnea (C) Coratina (D) Arbequina (E) Koroneiki (F) Frantoio (G) Picual (H) Medium flavour (I) Mild flavour and (J) Robust flavor, with a number of the major peaks in the GC–MS trace indicated. **1**. 4-Methyl-2-pentanol (IS); **2**. Hexanal; **3**. (*E*)-2-Hexenal; **4**. (*Z*)-3-Hexen-1-ol; **5**. (*E*)-2-Hexen-1-ol; **6**. 1-Hexanol; **7**. (*Z*)-3-Hexen-1-ol, acetate; **8**. Acetic acid, hexyl ester; **9**. Nonanal; **10**. Furan, 3-(4-methyl-3-pentenyl)-; **11**. Dodecene.

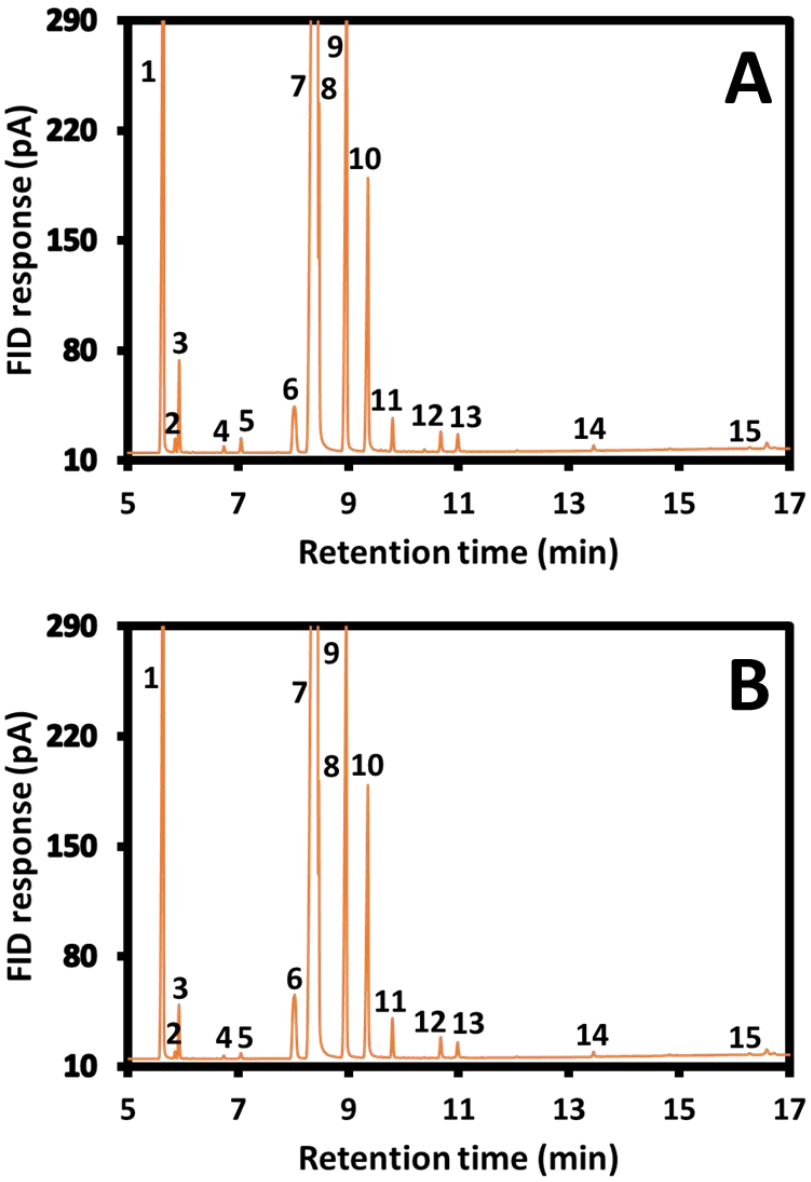

Fig. S2. Example GC–FID chromatogram of FAMEs derived from 2019 EVOO varieties of (A) Arbequina (B) Barnea, with peak numbers indicating FAMEs of: **1**. C16:0; **2**. C16:1n–9; **3**. C16:1n–7; **4**. C17:0; **5**. C17:1n–8; **6**. C18:0; **7**. C18:1n–9; **8**. C18:1n–7; **9**. C18:2n-6; **10**. C19:0 (internal standard); **11**. C18:3n-3; **12**. C20:0; **13**. C20:1n-9; **14**. C22:0 and **15**. C24:0.

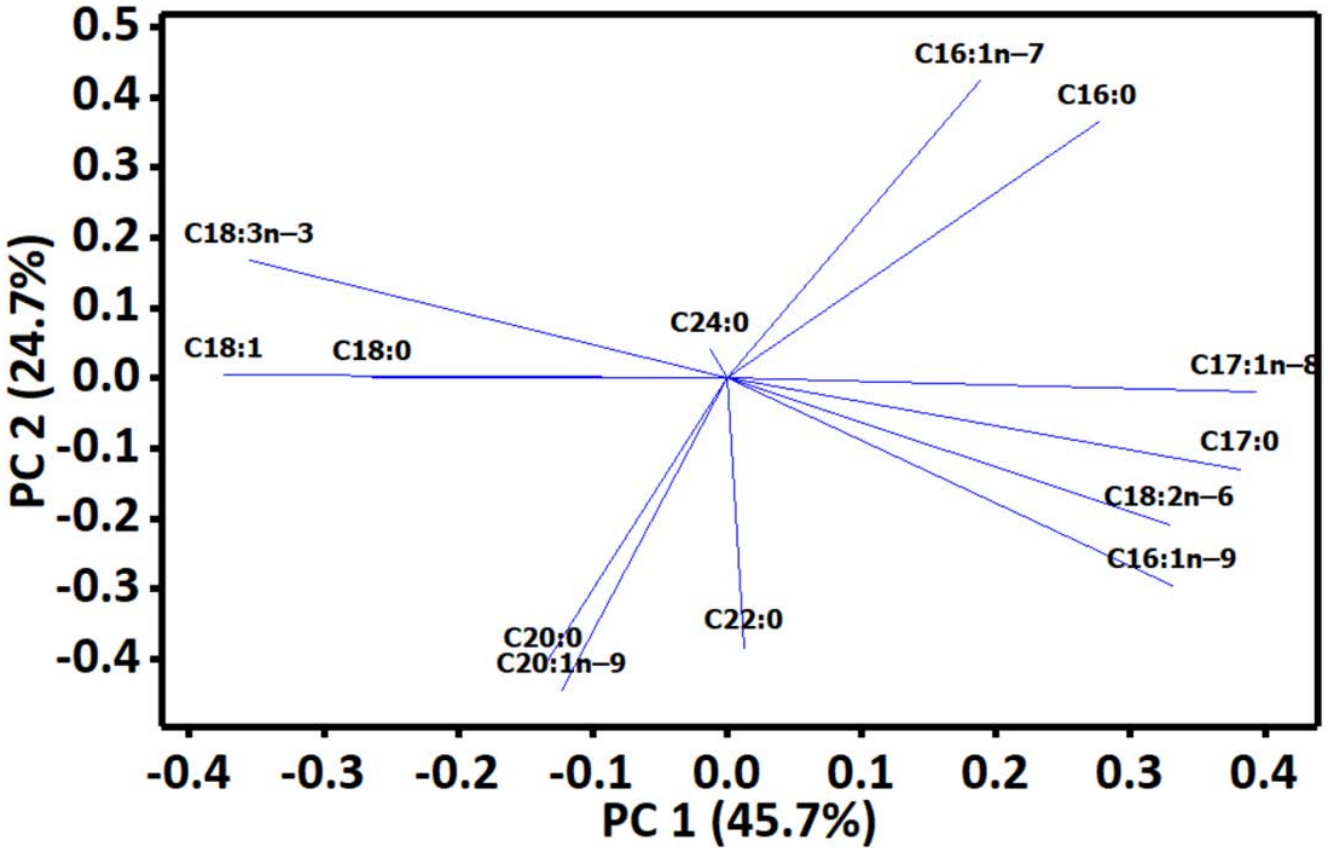

Fig. S3. Principal component (PCA) loading plot of %FAs composition for in-house mixed varieties. The included EVOO varieties are A: Arbequina; B: Barnea; C: Coratina; P: Picual; K: Koroneiki; MeF: Medium flavour; MiF: Mild flavour; RF: Robust flavour; A:B: Arbequina:Barnea in-house mix; B:P: Barnea:Picual in-house mix; and B:C:K: Barnea:Coratina:Koroneiki in-house mix (for the ratio of those in-house mixes see the score plot in **Fig. 4** and **Table 5)**.

Chapter 7

Conclusion and future directions

Contents

7.1. Conclusion

Natural oils such as plant oil and vegetable oil are characterised by a high proportion of lipids, mainly fatty acids (FAs) and triacylglycerols (TAGs). They also known to contain many minor compounds including volatile organic compounds (VOCs), sterols, waxes, fat soluble vitamins, carotenoids, chlorophylls, hydrocarbons, etc. The analysis of the chemical composition of oils, for instance in extra virgin olive oil (EVOO), can be used for the purpose of characterisation, differentiation, authentication and traceability as well as determination of the quality and purity of the oil. This is a major problem especially for EVOO, where adulteration with cheaper products is common. Different analytical techniques are used to analyse chemical compounds in oil samples. Gas chromatography (GC), both one dimensional (1D) and its multidimensional (MD) variant, is one of the commonly employed techniques to analyse oil samples. Literature on the analysis of FAs, TAGs and VOCs in oil samples, particularly in olive oil, using the GC techniques were reviewed and presented in Chapter 1 of the thesis. The Experimental Chapter (Chapters 3-6) outcomes are summarised in the subsequent paragraphs.

Analysis of TAGs in oil samples is important in terms of nutritional, biochemical and technological aspects. The separation of TAG molecular species is dependent on their structural differences; total carbon number (CN), degree of unsaturation, chemical variations on the acyl groups, and variations of acyl group position on the glycerol backbone. The presence of many TAG components with similar structure, e.g. TAGs with the same CN, in natural oils often leads to co-elution and make their separation challenging. In capillary GC the availability of limited number of columns with high temperature limit phase that matches the high elution temperature demands of TAGs (mostly >300 °C) makes their separation even more challenging. Nevertheless, GC–mass spectrometry (GC−MS) that utilise electron ionisation (EI) is the most widely used technique to analyse TAGs. Peak identification may be based on

use of standard TAG elution data, or interpretation of their mass spectra, using GC–MS. In many cases, both standard TAG and mass spectrum library information are not readily available.

Chapter 3. Demonstration of high temperature GC (HTGC) for sapucainha oil, which has been used as a leprosy treatment, for TAGs employed 1D GC, with MS. In these instances, identification can be performed based on diagnostic fragment ions in the mass spectrum, generated through loss of, or from, fatty acid residue (s) comprising the TAG molecules. The EI mass spectra of TAGs contains fragment ions, such as $[M–RCO_2]^+$, $[M–RCO_2H]^+$, $[M–RCO_2CH_2]^+$, $[RCO+128]^+$, $[RCO+74]^+$ and RCO^+, where R = aliphatic hydrocarbon chain, which are important for their structural elucidation and identification. Application of GC–EIMS for the separation and identification of sapucainha oil TAGs based on diagnostic fragment ions was necessitated by the absence of both standard TAGs and mass spectrum library information. Sapucainha oil comprises straight chain and cyclic FAs, and TAGs. Total FAs composition of the oil sample was determined and utilised to predict possible TAG identities, and overlapping TAG peaks were deconvoluted based on mass fingerprint data. Using GC separation only six groups of TAG peaks were detected. However, after deconvolution and mass spectrum analysis, each TAG peak group was revealed to comprise 2 to 5 co-eluted TAG molecules and as a result >18 TAGs were identified, with molecular masses that ranges from 794.8 to 880.5. Most of the identified TAGs were fully derived from cyclic FAs with few TAGs derived from mixed straight chain and cyclic FAs, which correlates with the FAME analysis that revealed >86% of sapucainha oil FAs were cyclic FAs. Thus, a first account of identification of TAG derived from cyclopentenyl FA and derived from mixed cyclopentenyl and straight chain FA was conducted in the absence of standard TAGs and mass spectrum library information. Although the study demonstrated the use of 1D GC–MS for the

identification of co-eluted peaks through manual peak deconvolution, the process is time consuming and there is a risk of misinterpretation of the mass spectral information.

Next, the incomplete separation of TAG molecular species in the usual 1D GC led to the development of multidimensional gas chromatography (MDGC) for their improved separation (**Chapter 4**). A 'heart-cut' (H/C) MDGC method under suitable flow and elevated temperature conditions was developed to analyse TAGs in olive oil. A relatively short non-polar first dimension (^{1}D) and mid-polar second dimension (^{2}D) columns with high temperature limits (up to 370 °C) were found to be useful for the TAGs separation. Only few TAG peaks were appeared on the ^{1}D: three major peaks and four minor peaks. The transfer of H/C fractions of the minor peaks, and sub-sampled regions across the major peaks eluting from the ^{1}D outlet to the ^{2}D generated higher resolution for TAG peaks. Sub-sampling certain regions was implemented as an approach to maximise resolution on the ^{2}D column. The method employed a reduced flow rate which was accompanied by somewhat broader but acceptably resolved peaks, and decreased sensitivity. This resulted in a compromise between separation quality and detectability of TAGs. Using a comprehensive MDGC approach provided a significantly increased number of detected TAGs (≥29 peaks) compared to 1D GC (15 peaks). The system was found to be sufficiently stable to allow extended sampling for multiple H/C required for comprehensive H/C analysis of the TAG groups.

In a further study (**Chapter 5**) a H/C MDGC–MS method for the separation and identification of TAGs in olive oil was developed. A similar column configuration to the preceding experimental Chapter was employed. Standard TAGs were used to test and demonstrate the H/C MDGC method for identification of TAG components and to validate the method. TAG components in olive oil resolved on the ^{2}D column were identified based on characteristic mass fragment ions such as $[M\text{-}RCO_2]^+$, $[RCO+128]^+$, $[RCO+74]^+$ and RCO^+ and comparison of their mass spectra with that of the standard TAGs. Sixteen olive oil TAGs

were identified by using MS after ^{2}D separation. The identified TAGs were derived from saturated and unsaturated FAs, and have molecular masses that ranges from 805.3 to 915.5. The repeatability of the H/C method was demonstrated in terms of retention time shift and area response in the ^{2}D. The method was found to have high repeatability of second dimension retention time ($^{2}t_{R}$) (RSD<0.2%) and area response (RSD<8%).

The analysis of chemical compositions of EVOO such as VOCs and FAs can be utilised for differentiation purposes. Thus, in **Chapter 6**, the differentiation of single varieties and mixed samples of EVOO was studied based on the analysis of VOCs and FAs composition. Headspace solid-phase microextraction with GC–MS was used to determine VOCs composition while GC−FID was employed for FAs analysis. Based on this study's results, single varieties of EVOO were found to be differentiated based on VOCs profile whereas mixed varieties were not clearly differentiated. This was a major impediment, since the signature mixed varieties are supposed to be produced according to a sensory-directed composition, consistent from year-to-year for one mix, and ideally should be different for the different signature mixes. It was thought that VOCs should distinguish the mixed varieties, but this was found to not be so. Since the preparation of mixed EVOO varieties are guided by sensory considerations the reason for VOCs to not adequately reflect the aroma profile or flavour of the mixed EVOO varieties is unknown. However, analysis based on FAs comparison more clearly revealed differences among the varieties studied. Principal component analysis (PCA) of FAs for in-house mixed varieties showed the changes in FAs composition based on the proportion of single varieties in the mixed EVOO varieties. This can be utilised to predict the proportion of single varieties comprising mixed EVOO varieties.

7.2. Future directions

Future research should focus on further improvements on TAGs separation through evaluation of different types of columns (such as those of higher selectivity, or based on novel chemistries, such as ionic liquids) but importantly to evaluate fast and potentially lower temperature methods (using short columns) of GC and configurations in H/C MDGC. Its application can also be extended to more complex lipid matrices such as fish oil. Application of comprehensive two-dimensional gas chromatography (GC×GC) to TAGs will be informative, but again will require columns of suitable thermal stability, and differences in selectivity. Complete profiling of triacylglycerol content of lipid matrices could be possible through coupling of the H/C MDGC method with liquid chromatography (LC) methods, with the LC stage preceding the GC stage. TAGs can be resolved based on their CN and degree of unsaturation using LC. TAGs having the same CN and similar degree of unsaturation co-elute. However, fractions of co-eluted TAGs in LC can be collected and further separated using the H/C MDGC method, where unresolved TAGs in the ^{1}D column are selectively transferred to ^{2}D column having different selectivity.

The laboratory has access to a prep-scale fractionation system for GC, to be finally commissioned in 2020. This offers considerable opportunity to fractionate FA and TAG as single compounds, which can then be characterised by spectroscopic methods. This will support accumulation of a suite of validated standards, that can then be used as primary standards in analytical GC for retention time matching. This will also allow the individual TAGs to be saponified to FA, for correlation of their FA composition.

The differentiation of the commercial EVOO mixed varieties based on VOCs can be further attempted by focusing on PCA of selected major VOCs, such as those having particular sensory attributes, plus minor VOCs that may have sensory attributes. Studying the prediction of varietal composition of in-house mixes can also be further extended by including more

varieties prepared at various ratios, especially those composed of more than two single varieties of EVOO, such as Robust flavour. Since other chemical classes also contribute to the flavour of EVOO, for instance polyphenols lend pungency to EVOO, and inclusion of more classes of compounds in addition to VOCs as differentiating compounds may give a better result. The use of sensory results from sensory panels participating in the EVOO signature flavour mix preparation, that can be obtained through collaboration with EVOO producers, in combination with chemical analysis may also improve the differentiation of the mixed EVOO samples.

Since olive oil chemical composition depends not only on the varietal difference but also on agronomic factors as well as processing and storage conditions of the oil, a comprehensive study that includes characterisation, differentiation and quality assessment of EVOO can be conducted by considering factors such as weather condition, olive fruits ripening stage, and the oil processing variables. Such study requires working closely with the EVOO industries, Boundary Bend Limited and Modern Olives in this particular case. This would benefit the industry in producing and maintaining the quality of their EVOO products. Moreover, the study on EVOO differentiation can be extended further through inclusion of more analytes, such as sterols, oleocanthal, etc. and by using multidimensional GC and FTIR techniques. The use of GC×GC in the analysis of VOCs is a better option in revealing minor components that could help in differentiating the EVOO varieties.